Understanding Vibration Transmitted to the Human Finger

A Thesis submitted to the University of Sheffield

for the degree of Doctor of Philosophy in the Faculty of Engineering

By

Almaky Almagirby

Department of Mechanical Engineering

The University of Sheffield

December 2016

Abstract

Prolonged exposure of the hand to tool-induced vibrations is associated with the occurrence of debilitating conditions such as vibration white finger. The primary aim of this work is to gain a better understanding of the effects of different aspects of exposure to finger transmitted vibration (FTV) related to operators using hand-held vibrating tools. To achieve this, firstly, a new method for measuring finger transmitted vibration was developed and assessed, including a tool vibration test rig and measurement protocol. The effect on FTV measurement of using a small accelerometer attached to the back of the finger was investigated using 2D finite element modelling. Comparisons were also made using a laser vibrometer. Analysis showed that the new test rig is capable of measuring FTV at frequencies ranging from 10 to 400 Hz, under different grip force levels, and that adding a small accelerometer mass (0.3 grams) did not significantly affect measurements.

A human participant study then carried out using the new rig. Various characteristic measurements were collected in tandem, including anthropometry, skin characterisation and behaviour under loading to investigate the effect of different factors on FTV. The results showed that FTV varied among individuals and the key finding was that exposure to vibration has a significant effect on finger temperature even for a short period of testing.

Anti-vibration (AV) glove materials were investigated using dynamic mechanical analysis (DMA) and tested using human participants. The results showed that the mechanical properties of AV materials change under real world industrial conditions such as excitation frequencies and temperature.

Finally, a new artificial test-bed was developed to replicate the transmitted vibration of the index finger. Studies were conducted on a range of 5 test-beds, to allow comparison with the human measurements, including indentation, vibration transmissibility and FE modelling. FE modelling showed that the distribution of dynamic strain was found to be highest in the vasculature region of the finger, indicating that this could be one of the contributing factors of VWF. One of the finger test-bed was selected as best replicating the mechanical properties of the real finger. The artificial test-bed provided better consistency than human participants, for testing parameters, such as grip force, and can be used in future for testing AV gloves with no need for human subjects.

Further investigations are suggested to be made to enhance the limitations of this project, including material analysis, testing protocol and finite element modelling.

Keywords:, hand-arm vibration syndromes, vibration white finger, FTV, transmissibility, resonance frequency, grip force, AV glove, finger mechanical properties, artificial finger, finite element modelling

Acknowledgment

I would like to start these acknowledgements by thanking Allah “God” the Merciful and Compassionate for the patience and knowledge he gave me throughout my PhD journey.

I would like to give my special thanks to my excellent PhD supervisors Dr Matt Carré and Dr Jem Rongong, not only for offering me the opportunity to pursue my Doctoral studies but also for their unlimited support, inspiration and encouragement throughout the past four years: without their guidance, the thesis would not have been accomplished.

I would also like to thank the many people who have contributed, encouraged, supported and helped me during my PhD, including Dr Raman Maiti for the help with the OCT scanner, Diyana Tasron for the help with the skin characteristic system and Jamie Booth for his technical support in equipment design; and all PhDs, RAs and staff members at the Mechanical Engineering Department for their kindest help in this project.

Also, I would like to express my greatest appreciation and respect to my brothers, Dr Ahmed Omaar, Dr Muftah Milad and Mr Suliman Amoud for their unconditional support, love, and care, as well as for being honest and dependable friends throughout my PhD long journey.

I would like to extend my gratitude and appreciation to my country for giving me this crucial opportunity to pursue my postgraduate studies overseas, and for supporting me financially throughout the years of studying in Britain.

Finally, my special gratitude and love to my father, who always supported me to continue my further studies and who I really wish was still alive to see this moment. May Allah “God” give him Peace and have Mercy on him. I would also like to thank my mother, brothers and sisters, to whom this thesis is dedicated, for their unconditional love and constant support through my life.

Table of contents

Abstract ..... **i**

Acknowledgment ..... **iii**

Table of contents ..... **iv**

List of Figures ..... **ix**

List of Tables ..... **xv**

Abbreviations ..... **xvii**

Chapter 1: Introduction **1**

1.1 Motivation of research 1

1.2 Aims and objectives 2

1.3 Structure of thesis 3

Chapter 2: Literature review **4**

2.1 Background to HAVS 4

2.1.1 Hand-arm vibration syndromes 4

2.1.2 Vibration-induced white finger 4

2.1.3 Prevalence of VWF 6

2.1.4 Causes of VWF 6

2.1.5 Vibration input induced white finger 7

2.2 Anatomy of the human hand 8

2.2.1 Structure of human skin 9

2.2.2 Bones 11

2.2.3 Finger joints 11

2.2.4 Blood 12

2.2.5 Human somatosensory system 13

2.2.6 Human mechanoreceptors 15

2.2.7 Human sensitivity to vibrations 17

2.3 Loading conditions for vibrating hand tools 18

2.3.1 Force applied by hand during use of tools 18

2.4 Existing technologies and protocols for HAVS research 21

2.4.1 ISO Standards 21

2.5 Previous research on VWF 32

2.5.1 In-vivo studies 32

2.5.2 In-silico modelling 38

2.5.3 Synthetic test-bed 40

2.6 Conclusion 41
Chapter 3: Development of vibration test rig 43
3.1 Introduction 43
3.2 Methodology 43
3.2.1 Vibration excitation system 44
3.2.2 Dynamic measurement system 48
3.2.3 Data acquiring system (DAQ) 50
3.2.4 Signal processing of the vibrations measurement 52
3.2.5 Transmissibility measurement 54
3.2.6 Calibration of the grip force system 57
3.2.7 Dynamic response of the entire system 59
3.3 Pilot studies 63
3.3.1 Vibration test rig evaluation under “no hands” condition 63
3.3.2 Grip force study 66
3.3.3 Investigation of the effects of an accelerometer mass on finger vibrations 68
3.4 Conclusion 80
Chapter 4: Human participant measurements 82
4.1 Introduction 82
4.2 Methodology 83
4.2.1 Participants and consent 83
4.2.2 Collection of measurement 83
4.2.3 Anthropometric measurements 85
4.2.4 Physical characteristics 90
4.2.5 Tactile sensitivity test 91
4.2.6 Skin characteristic measurement 94
4.2.7 Skin hydration 95
4.2.8 Skin temperature 95
4.2.9 Skin viscoelasticity 95
4.3 Indentation measurement 97
4.4 Finger transmitted vibration measurement 101
4.5 Results and discussions 102
4.5.1 Anthropometric measurements 102
4.5.2 Hand grip circumference 103
4.5.3 Hand and index finger grip strengths 103
4.5.4 Sensitivity test results 103
4.5.5 The effect of vibration testing on the finger temperature 104

4.5.6 Skin hydration results 106
4.5.7 Skin viscoelasticity results 107
4.5.8 Room temperature and humidity 108
4.5.9 Indentation and stiffness measurements 108
4.5.10 Transmissibility measurements 110
4.5.11 Statistical analysis – one-way ANOVA 117
4.5.12 Statistical analysis – correlation 118
4.5.13 Comparison of measured characteristics with other studies 120
4.5.14 Vibrations affect finger temperature 120
4.5.15 Parameters affect vibration behaviour 120
4.6 Conclusions 121
Chapter 5: Investigation of anti-vibration "AV" glove materials 122
5.1 Introduction 122
5.2 Material analysis 123
5.2.1 Methodology 123
5.2.2 Results from DMA of material specimens 125
5.3 Human subject testing 128
5.3.1 Methodology 128
5.3.2 Analysis of the transmissibility of gloves materials 130
5.3.3 The effect of grip force on the transmissibility of materials 132
5.4 Discussion 132
5.5 Conclusion 135
Chapter 6: Development of an artificial finger 136
6.1 Introduction 136
6.2 Anatomy of an index finger 137
6.3 Materials 139
6.4 Tensile testing 139
6.4.1 Methodology 139
6.4.2 Results and discussion 141
6.5 Dynamic mechanical analysis (DMA) 143
6.5.1 Material initially investigated 143
6.5.2 Selected materials 144
6.6 Results from DMA testing of materials 145
6.7 Design idea of an artificial finger 147
6.7.1 Initial prototype of an artificial finger 147
6.7.2 Development of an artificial model of finger 150

6.8 Measurements of static behaviour 152
6.9 Vibration measurement 158
6.10 Finite element model 165
6.11 Discussion 168
6.12 Conclusions 170
Chapter 7: Conclusions and future work 171
7.1 Conclusions 171
7.2 Contribution of the study 175
7.3 Future work 176
References 179
Appendixes 191
Appendix – A1: Ethics approval; vibration measurement 191
Appendix – A2: Ethics approval; Investigation on the properties of the skin 192
Appendix – A3: Participant consent 193
Appendix – A4: Measurement sheet used for the study 194
Appendix – B: All anthropometric data measured for all participants 195
Appendix – C: All data for hand and finger grip strength measured for all participants 196
Appendix – D: Stiffness measured at distal and proximal of the human finger at loading of 5 and 10 N for all participants 197
Appendix – E1: Peak transmissibility against peak frequency measured for all subjects 198
Appendix – E2: Mean grip forces against peak frequency measured for all subjects 199
Appendix – E3: Peak transmissibility against mean grip forces measured for all subjects 200
Appendix – F: One-way ANOVA between two groups (technicians and non-technicians) 201
Appendix – G: Pearson correlation for anthropometric measurements including hand and finger grip strength 203
Appendix – H: Pearson correlation anthropometric measurements including hand and finger grip strength with vibration measurements 204
Appendix – I: Strain sweep test obtained for Siliskin 10 silicone at two different manufacturing protocols 206
Appendix – J: Results obtained from temperature sweep test for the initial protocol used and over time 207
Appendix – K: Results obtained from temperature sweep test for the second protocol used and over time 208

Appendix – L: Stiffness measured for the five models of finger at loading of 5 and 10 N 209

Appendix – M: measurement of mean grip force, frequency and transmissibility peaks measured for all artificial models of finger.....210

List of Figures

Figure 2.1: The anatomy of the human finger 9

Figure 2.2: The structure of human skin 9

Figure 2.3: A typical synovial joint 11

Figure 2.4: Human finger joints 12

Figure 2.5: Myelin and nerve structure 14

Figure 2.6: Sensory receptors in human skin 15

Figure 2.7: The structure of Pacinian Corpuscles 16

Figure 2.8: Diagram of the three orthogonal directions, *x, y* and *z* and the frequency weighting curve (Wh) as outlined in ISO 5349-1 2001 23

Figure 2.9: Diagram of the palm adaptor used in ISO testing method 24

Figure 2.10: Diagram of how the palm adaptor is used when holding the handle during testing 25

Figure 2.11: The experimental set up of vibrating, controlling contact forces and measuring finger blood flow 32

Figure 2.12: A two-dimensional (2D) finite element model of a fingertip in contact with a flat surface reproduced from 39

Figure 2.13: The distributions of vibration magnitude (U, mm) across the tissues of the fingertip around the major resonance. (a) Normal vibration. (b) Shear vibration reproduced from 40

Figure 2.14: Sectional structure of the multi-layer artificial fingertip 41

Figure 3.1: Instrumentation set up showing the vibration generation and response measurement systems, as well as a grip force and temperature measurement and display system 44

Figure 3.2: Setup of the entire handle including its suspension method 45

Figure 3.3: Cross-sectional diagram of the instrumented end of the handle 45

Figure 3.4: a) Setup of the entire vibration test rig including vibration excitation system and vibration measuring system; b) Close-up view of the handle being held during a test; c) The standing upright posture maintained during all the vibration testing 46

Figure 3.5: 2D drawing showing the dimensions of the rigid base 48

Figure 3.6: The entire finger adaptor including the measuring accelerometer and strap 49

Figure 3.7: Front panel of the main LabView program showing vibration generation functions and display features used in this setup. 52

Figure 3.8: Diagram of signal processing of sequence and swept methods used 53

Figure 3.9: cross-sectional drawing showing transmissibility measurement when the finger adaptor method adaptor was used: a) transmissibility measured on the bare handle; b) transmissibility when the handle was being covered by glove material.....55

Figure 3.10: Cross-sectional drawing showing transmissibility measurement of finger ; a) transmissibility measured on bare handle; b) transmissibility through the bare finger; c) transmissibility through the finger when wearing a glove 56

Figure 3.11: Calibration of the grip force system showing the Mecmesin MDD stand and equipment used.....57

Figure 3.12: Force-volt relationship of the grip force system.....58

Figure 3.13: Set up for the hammer test.....59

Figure 3.14: Frequency response function FRF for the six positions along the handle when the stinger of 4 mm in diameter was used.....61

Figure 3.15: Frequency response function FRF for the six positions along the handle when the stinger of 4 mm in diameter was used and the right end was gripped by index finger and thumb 61

Figure 3.16: Initial stinger (4 mm) and the one being used (1.6 mm) with the vibration test rig 61

Figure 3.17: Frequency response function FRF for the six positions along the handle when the stinger of 1.6 mm in diameter was used.....62

Figure 3.18: Frequency response function FRF for the six positions along the handle when the stinger of 1.6 mm in diameter was used and the right end was gripped by index finger and thumb 62

Figure 3.19: Setup of the reference accelerometer (input) and measuring accelerometer (output).....64

Figure 3.20: Example set of raw data (sampling rate 10 kHz) measured by testing the vibration test rig including the excitation force, accelerations (input and output) and the grip force as well as room temperature. 65

Figure 3.21: PSD of grip force time history measured for the bare handle 66

Figure 3.22: Test setup showing the posture of gripping the bare handle and the close-up view of the right end 66

Figure 3.23: (a) Finger-thumb grip force used in this study (b) Palm-fingers grip force outlined in ISO 10819 1996, 2013 67

Figure 3.24: 2D finite element model of an index finger proximal in contact with an aluminium plate.....69

Figure 3.25: Transmissibility of measurement obtained from finite element model of the finger showing the effect of adding a small point mass (accelerometer mass) on the finger vibration response. 72

Figure 3.26: The set-up of transmissibility measurement: a) when measured using an accelerometer method; b) when a single axis laser vibrometer was being used 74

Figure 3.27: Transmissibility measurement through the human right index finger (proximal) when measured using a small accelerometer (0.3 grams) and laser vibrometer and transmissibility measured from the laser sensor investigating how the laser measurement can be affected by dynamic response of the entire vibration system. 75

Figure 3.28: Close-up view of the Dytran accelerometer attached to the back of the right index finger (proximal) after being aligned with the reference accelerometer connected to the handle. 76

Figure 3.29: Close-up view of the gloved hand: a) position of the accelerometer when wearing an AV glove; b) the gloved right hand gripping the handle. 76

Figure 3.30: Vibration transmissibility measured on the surface of the bare handle 78

Figure 3.31: Transmissibility measurement of both ungloved and gloved index finger under grip forces of 15, 30 and 50 N, for one subject with 5 repeats. 78

Figure 3.32: Power spectral density of grip force time history of both ungloved and gloved index finger under grip forces of 15, 30 and 50 N, for one subject with 5 repeats. 79

Figure 3.34: Transmissibility of the AV gloved test used in the study. 80

Figure 4.1: Order and category of measurements conducted in this study 84

Figure 4.2: Anthropometric dimensions for hand and index finger to be measured 85

Figure 4.3: Measuring the index finger length of a participant 86

Figure 4.4: Diameter measurement of the proximal segment of the index finger 87

Figure 4.5: Measurement of the right hand: a) Length of hand; b) Palm circumference; c) Wrist circumference 89

4.6: a) Method used for measuring hand grip circumference; b) A close-up view of thumb just touching the index finger 90

Figure 4.7: a) Hand grip strength measurement; b) Grip strength of the right index finger 91

Figure 4.8: Monofilament test kit used in the study. A-T represent the filaments from thinnest to thickest 92

Figure 4.9: Filament applied to the index distal finger (D) 92

Figure 4.10: Flowchart diagram for assessing finger sensitivity 93

Figure 4.11: Experimental set-up and equipment used for the skin characteristics testing 94

Figure 4.12: Measuring principal of the cutometer 96

Figure 4.13: Example of the cutometer deflection-time curve of human skin for mode one and measuring parameters as described by Cua et al. [128] 96

Figure 4.14: Experimental set-up of an indentation test rig used in the study 98

Figure 4.15: Calibration of displacement device used with the indentation test rig.....98

Figure 4.16: Close-up view of indentation test rig: a) When the curved proximal finger was tested and a finger supporter was attached; b) Measurement of the distal finger.....99

Figure 4.17: A sample of the measured and 4th order polynomial fitted indentation data 100

Figure 4.18: Sensitivity values measured for all participants.....104

Figure 4.19: Temperature drop after vibration exposure for all participants 105

Figure 4.20: Skin hydration measured at D and P of finger for all participants.....107

Figure 4.21: Indentation load-deflection measured at distal finger for all participants...109

Figure 4.22: Indentation load-deflection measured at proximal finger for all participants 109

Figure 4.23: Stiffness measured at distal and proximal finger for all participants, at indentation loads of 5 and 10 N 110

Figure 4.24: Transmissibility measured throughout the bare proximal (ungloved) right index finger under grip forces 15, 30 and 50 N, for all participants 112

Figure 4.25: Transmissibility measured throughout the gloved proximal of the right index finger under grip forces (15, 30 and 50 N), for all participants.....113

Figure 4.26: Transmissibility of the glove used in this study and under grip forces 15, 30 and 50 N for all participants 114

Figure 4.27: Mean transmissibility measurements of the bare (ungloved) and gloved finger and three grip forces (15, 30 and 50 N), for all participants 116

Figure 4.28: Mean transmissibility of the glove used in the study. 117

Figure 5.1: Material structures and dimensions of specimens used for DMA testing (in mm) 123

Figure 5.2: Optical microscope images (200 μm) of three glove materials used in the study 124

Figure 5.3: a) Viscoanalyser VA2000 machine; b) Sectional diagram of the chamber and specimens when using compression plates; c) Tension modes using clamps. 124

Figure 5.4: Young's modulus and loss factor against frequency for Material 1, Tg≈−23 °C 126

Figure 5.5: Young's modulus and loss factor against frequency for Material 2, Tg≈−30 °C 126

Figure 5.6: Young's modulus and loss factor against frequency for Material 3, Tg≈−41 °C 127

Figure 5.7: Testing setup showing: a) Finger mounting adapter; b) Material specimen and adapter alignment marked; c) Right end close-up (d) Posture of the handle being gripped. 129

Figure 5.8: Cross-sectional diagram of the right end of the handle during the test. 129

Figure 5.9: Transmissibility measurements against frequency for all participants when using Material 1 130

Figure 5.10: Transmissibility measurement against frequency for all participants when using Material 2 131

Figure 5.11: Transmissibility measurements against frequency for all participants when using Material 3 131

Figure 5.12: Transmissibility measurements against grip force for all participants, at frequency 125 Hz 132

Figure 5.13: Diagram of possible loading behaviour of material 2. 134

Figure 6.1: Anatomical diagram of the human index finger 137

Figure 6.2: Dimensions of specimens used in tensile test 140

Figure 6.3: Specimens of materials tested 140

Figure 6.4: Experimental set-up of tensile test rig used in the study. 141

Figure 6.5: Stress-strain relationship obtained from tested materials 142

Figure 6.6: Young's modulus and loss factors against dynamic strain and temperature of latex specimen 146

Figure 6.7: Young's modulus and loss factors against dynamic strain and temperature of silicone gel specimens 146

Figure 6.8: The stages of developing an artificial finger model 148

Figure 6.9: Optical Coherence Tomography system used and the processed image showing the detected outer and inner edges of latex layer 149

Figure 6.10: Final, adopted structure of the artificial model of the finger 150

Figure 6.11: Cross-sectional diagram of the finger model mounted on the test handle 150

Figure 6.12: Processed OCT images of outer layer (latex) of five artificial fingers 151

Figure 6.13: Image showing the final version of an artificial model of the finger 151

Figure 6.14: Artificial model of the finger being tested using a cutometer probe. 152

Figure 6.15: The experiment set-up for indentation measurement used for artificial fingers 152

Figure 6.16: Cross-sectional diagram of method used to estimate force-displacement behaviour of 2D FE model of finger 153

Figure 6.17: The load-displacement behaviour of five artificial finger models and the data obtained from the human right index proximal finger, as well as the FE models using human data and data from materials used in this study 156

Figure 6.18: The load-displacement behaviour of FE models using human data and data from material tested in this study and the five artificial finger models.....157

Figure 6.19: The experiment set up for transmissibility measurement: a) side view of the finger model being mounted on the test handle; b) front view of tested model and balancing model (initial version) mounted on the left end of the handle 158

Figure 6.20: Transmissibility measured at the bone (polypropylene) and outer layer (latex) of initial finger model 159

Figure 6.21: Transmissibility measured throughout artificial models of the finger (ungloved) and data obtained from ungloved human proximal right index finger under grip forces 15, 30 and 50 N 162

Figure 6.22: Transmissibility measured throughout the gloved artificial models of the finger and data obtained from gloved human proximal right index finger under grip forces 15, 30 and 50 N 163

Figure 6.23: Transmissibility of the glove used in this study and under grip forces 15, 30 and 50 N for artificial models of the finger and all human data 164

Figure 6.24: Transmissibility obtained from FE model of proximal finger under different grip levels 165

Figure 6.25: Mode shapes of the FE model showing the distribution of maximum strain at resonance frequency across the finger, for grip levels of 0.1, 0.2 and 0.3 N.166

Figure 6.26: Transmissibility measured from FE model using both human and tested material parameters and deflection of 6 mm towards the handle.....166

Figure 6.27: Mode shapes of FE models at resonance frequency and 400 Hz, during a deflection of 6 mm toward the handle: a) when human tissue parameters were applied; b) using parameters from tested materials.....167

List of Tables

Table 2.1: The stages of vibration-induced white finger 5

Table 2.2: Differences between the symptoms of vibration-induced white finger VWF and those of primary Raynaud's disease 5

Table 2.3: Prevalence rates of finger numbness and VWF among vibration-exposed worker groups from 1980-1988, by Bovenzi et al 6

Table 2.4: The affected factors for vibrations transmitted into hands 18

Table 2.5: The measured magnitudes by HSL on different vibrating tools in use at work .31

Table 2.6: Blood flow measurement of the effect of vibration in human finger. 33

Table 2.7: Summary of published studies with regards to the influence of vibration exposure on finger circulation 36

Table 3.1: Specifications of accelerometers used for measuring vibration 48

Table 3.2: The properties of the finger adaptor 49

Table 3.3: Descriptive statistics of the mean grip force measurement 67

Table 3.4: Material properties used in modelling 70

Table 3.5: Hyperelastic and viscoelastic parameters for the skin 70

Table 3.6: Hyperelastic and viscoelastic parameters for the subcutaneous tissue 70

Table 4.1: An example of the 4th order polynomial fitting used in this study 100

Table 4.2: An example of a method used for measuring a stiffness at a certain force. ...100

Table 4.3: Descriptive statistics of measured anthropometric dimensions 102

Table 4.4: Hand grip circumference as measured for all subjects 103

Table 4.5: Mean values of grip strength measured with hand and index finger 103

Table 4.6: Mean values of finger temperature at distal and proximal measured before and after exposure to vibration 105

Table 4.7: Mean values of finger temperature at distal and proximal measured before and after griping the test handle when the hand was gloved. 106

Table 4.8: Mean of finger hydration values measured at distal and proximal 106

Table 4.9: Mean of cutometer parameters (R values) measured at distal and proximal .107

Table 4.10: Mean values of temperature and humidity measured during all tests 108

Table 4.11: Descriptive statistics mean grip forces for all participants 115

Table 4.12: Mean resonance frequencies and amplitudes of mean transmissibility for all participants 116

Table 4.13: Pearson coefficients between R values and temperature drop at distal and proximal of the finger 119

Table 4.14: Correlation between the sensitivity at distal, middle and proximal with age120

Table 5.1: Characteristics of the specimens used in the study 123

Table 5.2: Characteristics of the human subjects used in the study.....128

Table 5.3: The effects of frequency and temperature on Young's modulus of tested materials 135

Table 6.1: Mechanical properties of finger anatomy and relevant skin properties measured at different regions, gathered from literature 138

Table 6.2: Candidate materials tested to replicate the finger layers.....139

Table 6.3: characteristics of material specimens used in the test 140

Table 6.4: Properties and dimensions of the specimens used in the study.....144

Table 6.5: Parameters used for testing the specimens of materials.....145

Table 6.6: Characteristics of initial model of the finger. 149

Table 6.7: Characteristics of all five models of the finger used in the study 151

Table 6.8: Cutometer parameters and OCT thickness of skin layer obtained for artificial models and the mean and SD measured at proximal segments of human participants 155

Table 6.9: Comparison of stiffness obtained from human testing and all five artificial models of finger.....158

Table 6.10: Mean grip forces measured for the finger models and human fingers with and without the glove, target grip forces of 15, 30 and 50 N 160

Abbreviations

HAVS	Hand-arm vibration syndromes
VWF	Vibration white finger
FTV	Finger transmitted vibration
AV	Anti-vibration
AF	Artificial finger
DAQ	Data acquisition system
DMA	Dynamic mechanical analysis
OCT	Optical coherence tomography
MRI	Magnetic resonance imaging
RTV	Room temperature vulcanizing
WC	Wrist circumference (mm)
PW	Palm circumference (mm)
Hand size	Hand size EN 420:2003 (inch)
L_{IF} , L_D, L_M, L_P	Length of index finger, distal, middle and proximal, respectively (mm)
D_D, P_D	Diameter of distal and proximal (mm)
IF_D	Average diameter D and P (mm)
IV_D, IV_P, IV_{IF}	Indicative volume of distal, proximal and full index finger, respectively (mm^3)
HGC	Hand grip circumference
HGS_Average	Hand grip strength average (N)
IFGS_Average	Index finger grip strength average (N)
R_i_D	R values at distal (*i* = 0-8)
R_i_P	R values at proximal (*i* = 0-8)
Hyd_D	Hydration at distal (au)
Hyd_P	Hydration at proximal (au)
au	Arbitrary units
STD_BV	Skin temp. at distal before vibration (˚C)
STP_BV	Skin temp. at proximal before vibration (˚C)
RT_BV	Room temp. before vibration (˚C)
RH_BV	Room humidity before vibration ()
STD_AV	Skin temp. distal after vibration (˚C)
STP_AV	Skin temp. proximal after vibration (˚C)
MGF	MGF Mean grip force (N) where G: represent the gloved case
RF	RF resonance frequency where G: represent the gloved case; GT: glove transmissibility; N : grip force
RP	RP Resonance Peak where G: represent the glove; GT: glove transmissibility; N : grip force
SP,D_5N	Stiffness at proximal and distal at 5 N, N/mm
SP,D_10N	Stiffness at proximal and distal at 10 N, N/mm
Sensitivity_D, M, P	Sensitivity at distal, middle and proximal of index finger
Tempdrop_D, P	Temp. drop at distal and proximal (˚C)

Chapter 1: Introduction

1.1 Motivation of research

Occupational exposure of the transmitted vibration into the hands and arms of workers may cause disorders in the vascular, neurological and musculoskeletal system. Also, this occupational exposure could affect workers' health and performance [1]. These complicated symptoms and disorders are known collectively as "hand-arm vibration syndrome" (HAVS), and can occur in workers who use vibrating tools. This syndrome is classified as an occupational illness [2, 3].

Vascular disorders are caused by prolonged exposure to vibration transmitted into workers' hands and arms [4]. This vascular disorder, called vibration-induced white finger (VWF), is the most common disease related to the use of vibrating hand-held tools [3, 5].

The first comprehensive investigation of VWF has been performed by doctor Alice Hamilton in 1918[6]. This has then motivated many researchers to study various aspects of VWF occurrence. Many researchers have indicated that the occurrence of VWF is linked to finger blood circulation[7]. The finger blood flow (FBF) was measured several times before and after exposure to vibration [8, 9]. These measurements showed that FBF was reduced during and after the end of each exposure to different magnitudes of vibration at various durations [7-10].

VWF occurs due to occupational and daily activities that involve prolonged exposure to segmental vibration[11]. This kind of vibration is transmitted to the human body through specific parts of the body, such as the hands and feet. The risk of HAVS can be reduced by decreasing the magnitude of the transmitted vibration into the operator's hands [11]. A significant relationship was found between the vibration exposure level and development of VWF stages among travertine (form of limestone) industry workers. When the subjected workers were divided into subgroups with respect to the vibration exposure time in hours, a study showed that prevalence of VWF increased with an increase in the exposure time [2]. The international standard ISO 5349:2 2001 reports the acceptable daily hand-arm exposure to vibration [12]. However, the aetiology of VWF is still incomplete and has not

yet been fully understood, therefore then this area of research is required further investigation in order to achieve a good understating of the causes of VWF.

1.2 Aims and objectives

The primary aim of this study is to gain a better understanding of the effects of different aspects of exposure to finger transmitted vibration (FTV) relevant to operators using hand-held vibrating tools. It is hoped that the results from the experiments and modelling carried out in this study will contribute towards an important understanding of the causes of VWF.

The objectives of this study are as follows:

- To identify and define the main issues related to hand-transmitted vibration from existing literature.
- To collect existing data on human finger including the mechanical properties and anatomical structure of the index finger that will be used to evaluate and validate experimental and in-silico models.
- To develop and evaluate a new methodology for assessing finger transmitted vibration including vibration test rig and measurement protocol.
- To develop a finite element model of the proximal finger system that will help to assess the measuring method and to validate physical finger models.
- To carry out various human participants measurements to study the effect of aspects of finger transmitted vibration in relation of VWF and to be used for validation of finger models.
- To develop and validate an artificial model of finger that will serve as an experimental test-bed for assessing finger transmitted vibration. This will replicate both loading and the vibration behaviours of the human finger system.
- To trial the artificial finger model and assess its ability to measure the effect of using anti-vibration gloves.

1.3 Structure of thesis

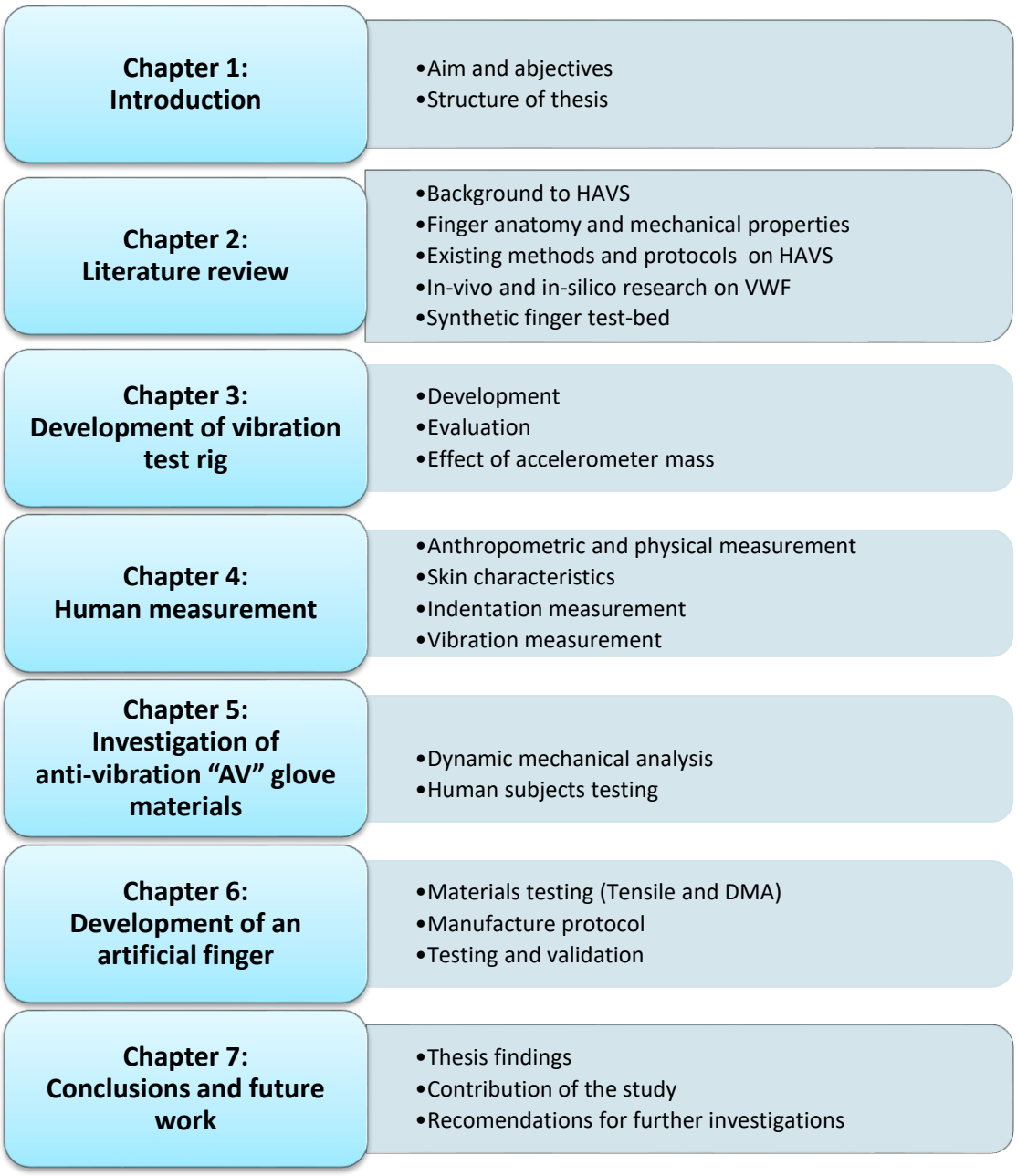

Chapter 2: Literature review

This chapter reviewed the detailed literature of the current knowldege regarding HAVS. Firstly, it reviewed the background to HAVS; secondly, the anatomy and mechanical properties of the human finger were also reviewed to study their effects on finger transmitted vibration. The existing technologies and standards for controlling HAVS are then presented, after which some previous research on VWF is reviewed, including in-vivo and in-silico studies. Finally, the literature attempts to introduce some studies on the use of synthetic materials that replicated the mechanical properties of the human fingertip.

2.1 Background to HAVS

2.1.1 Hand-arm vibration syndromes

Hand-arm vibration (HAVS) occurs in workers who use vibrating hand-held tools such as angle grinders, chain saws, pneumatic hammers, chipping hammers, concrete breakers, sanders, disc-cutters, and powered mowers. In the UK, these vibrating tools are used widely in the field of construction and manufacturing, and around 20,000 workers suffer from vibration white finger per year [13]. A study by Muzammili and Hasan claims that 34% of forestry workers who have used gasoline chain saws suffered from hand-arm vibration syndrome in the period between 1982 and 1986 [14].

The syndrome includes the following symptoms: weakness in muscles, muscle fatigue, arm and shoulder pains and vibration-induced white finger. Many researchers in this particular area are agreed that irritability, depression, sleeping problems and headaches should be included in the description of the syndrome.

2.1.2 Vibration-induced white finger

The occurrence of vibration white finger (VWF) and the rate of finger tissue degeneration has been related to several biodynamic and physical factors such as vibration characterisers of the handle, directions, duration, pattern of exposure, grip force and posture [15]. This syndrome is sometimes also technically called Raynaud's phenomenon of occupational origin, due to the similarity in the symptoms of VWF and those of Raynaud's syndrome at the early stages of the conditions, which are tingling and numbness

in fingers. Tables 2.1 and 2.2 indicate the stages of VWF and the differences between the symptoms of VWF and those of primary Raynaud's disease. These may not appear in a few days or even months of exposing hands to vibrations, and in workers with the complaint it can take years to appear. With continued use of vibrating handheld tools, the fingertip will blanch, particularly in cold conditions [3, 13, 16-18].

Table 2.1: The stages of vibration-induced white finger [11, 19].

Stages	Condition of digits	Interferences with work and social activities
0	No blanching of digits	No complaints
0T	Intermittent tingling	No interference with activities
0N	Intermittent numbness	No interference with activities
1	Blanching of one or more fingertips with or without tingling and numbness	No interference with activities
2	Blanching of one or more fingertips with numbness, usually occurring during winter	Slight interference with domestic and social activities
3	Extensive blanching. Frequent episodes in summer as well as winter	Definite interference at work, at home and with social activities. Restrictions on hobbies
4	Extensive blanching of most fingers	Occupation changed to stop further vibration exposure because of severity of signs and symptoms

Table 2.2: Differences between the symptoms of vibration-induced white finger VWF and those of primary Raynaud's disease [13]

VWF	Primary Raynaud's disease
Well demarcated localized blanching	Pallor tends to be diffuse, sometimes with unclear demarcation from surroundings
Blanching does not occur in toes	Blanching might occur in toes
Distribution correlates with the strongest vibration exposure	Symmetrical
Occurs in workers exposed to vibration	15% prevalence in women of child-bearing age Most common and 5% prevalence in men

Initially, the symptoms of VWF could be hand numbness and a tingling sense in the fingers and hands which may occur due to the vibration damage to the tips of fingers and also poor blood circulation. Whiteness of finger also occurs when the workers' hands become wet or cold. To re-warm the hands (so they become red in colour and the vessels become relaxed) may take at least 15 minutes [20]. This is due to the reactivation of an excess blood in the cutaneous vessels supplying the organ of body [21].

2.1.3 Prevalence of VWF

The prevalence of VWF was apparent in operators who used several types of rotatory tools and at a range between 20.9% and 35.5%, as shown as in

Table 2.3. In addition, it has been found that VWF occurred in 47% of 147 of workers who were employed at two foundries using chippers and grinders [21].

Table 2.3 shows the prevalence rates of numbness in finger and VWF among different groups of workers who use different types of vibrating tools.

Research has been carried out in Great Britain, Japan, Scandinavia and Canada, to study lumberjacks who operate chainsaws. The VWF prevalence in lumberjacks varied between the range of 30 and 80%. However, after anti-vibration tools were introduced, the VWF prevalence decreased in chainsaw users from 40% in 1972 to 7% in 1980 [21].

Table 2.3: Prevalence rates of finger numbness and VWF among vibration-exposed worker groups from 1980-1988, by Bovenzi et al. [21]

Work tool	Subjects in numbers	Finger numbness (%)	VWF (%)	Published Year
Shipyard caulkers	169	43.2	31.3	1980
Foundry operators	67	19.4	20.9	1985
Stone drillers/ chippers	76	40.8	35.5	1988
Engine workers	79	44.7	26.3	1988
Lumberjacks	66	40.9	28.8	1989

2.1.4 Causes of VWF

Even though the nature of vibration syndrome is well understood, the aetiology of VWF is still incomplete and has not yet been explained satisfactorily. The first hypothesis of vibration induced white finger by Lewis [22] indicated that VWF was caused by the damage

in the nerve endings which yielded excessive vasoconstriction during the exposing of the vessel when vessel walls were exposed to cold. Vasoconstriction is defined as a narrowing in blood vessels, which leads to increasing blood pressure. This theory was later extended not only to a vessel in cold conditions, but also to the loss of vasodilation, which is the opposite of vasoconstriction and is defined as the widening of the blood vessels as a result of the relaxation that has occurred in the muscular walls of the vessels [23]. A study carried out by Pyykko and Starck [23] on blood circulation measurements showed that an increase in peripheral resistance in finger circulation, which happened after the cold condition was applied, was found to be the main factor of vibration induced white finger. The cause of this increase is still unknown; however, it has been suggested that an excessive affinity of vasoactive substances for the efferent receptors exists [23].

Blood flow circulation is related to several aspects of vibration induced white finger, such as pressure difference and peripheral resistance. These have been defined mathematically as follows:

$$FBF \propto \Delta P_F \qquad \textbf{Equation 2.1}$$

where: FBF is finger blood flow and $\Delta P_{F,}$ the pressure difference in finger.

$$FBF \propto 1/R \qquad \textbf{Equation 2.2}$$

where: R is peripheral resistance as illustrated in the formula.

$$R = (8kl\mu)/r^4 \qquad \textbf{Equation 2.3}$$

Here: k is an individual constant, l is the length of capillary beds in mm, μ is the blood viscosity in centipoise, and r is the radius of the interior of the vessel in mm, also known as the lumen.[23]

2.1.5 Vibration input induced white finger

A study by Pattnaik et al. was carried out to model a small artery which was based on a changeable diameter, fluid-filled elastic tube; the motion equation was developed by considering the interaction between the artery wall, the fluid and soft tissue bed[4] as shown in Equation 2.4.

$$\int_0^{\pi}\left(P - K_{wf}W - j\omega r_w W\right)sin\,\theta R d\theta - \sigma 2h = \int_0^{\pi} -\phi\omega^2\ \rho_w hW sin\theta R d\theta \qquad \textbf{Equation 2.4}$$

where P is pressure amplitude; K_{wf} and r_w represent the spring and damping effects of the surrounding tissue and pulp; W is the displacement of the artery wall; $j = \sqrt{-1}$; R is the radius of the artery; σ is the stress of the wall; h is the thickness of the wall; ρ_w is the density of the wall material; and ϕ is a factor greater than 1, which takes into account the motion of the surrounding material.

As a result, spatial resonance in the artery only occurred when the vertical vibration entered the artery and induced a wave that travelled horizontally from the centre of the smallest diameter toward the largest one. The artery system developed shows a spatial resonance the same as that in the basilar membrane in the cochlea [4]. Moreover, the greatest response of the artery system to the vibration excitation was found at the same vibration frequency input point, regardless of the input excitation location. The important implication of the spatial resonance of the artery system to the HAVS is that the highest response of an artery system to a vibration excitation always occurs at the same point, determined by the input frequency independent of the input location. This may cause a high level of stress at this location, which may be a possible cause of vascular disorder leading to VWF. [4]

2.2 Anatomy of the human hand

The human hand is covered with two different types of skin: the palm side is called the volar aspect (glabrous skin) whereas the back side is referred to as dorsal aspect (hairy skin). These surfaces have much thicker skin than other places in the body [24]. Anatomy of the human finger is shown in Figure 2.1. The finger nail is made of a tough protective protein which is called keratin and covered on dorsal aspect of distal phalange of each finger. Fingers are constructed of ligaments which are a group of strong supportive tissues that connect bone to bone. The bones are attached to muscles in the forearm by tendons which control finger movement (there are no muscles in the finger itself) [25]. There are two types of tendons, flexor and extensor.

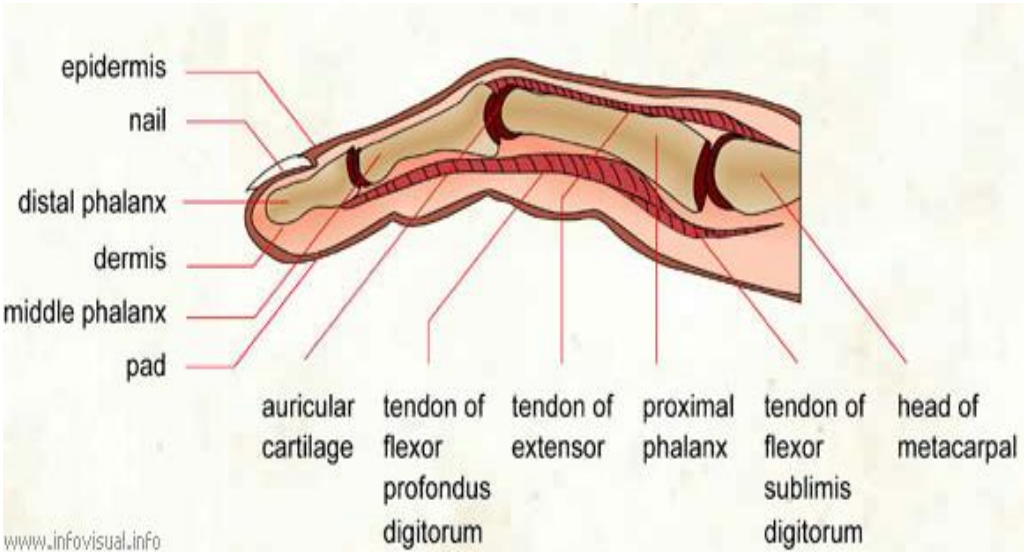

Figure 2.1: The anatomy of the human finger [26].

2.2.1 Structure of human skin

Human skin is the largest organ in the body, and it has a major role as the first protector of the human body against any exterior damage or inhospitable environment. It also plays a very important role in keeping the human body in a balanced and healthy condition, through its basic processes, which include sensation, thermal regulation, and absorption. Skin consists of two main layers: the epidermis and the dermis, as shown in Figure 2.2 .

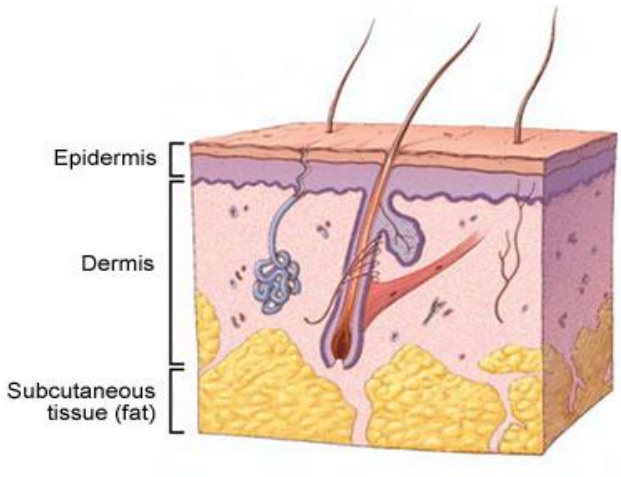

Figure 2.2: The structure of human skin [27].

The epidermis is the external layer which directly touches exterior surfaces. The epidermis has a varying thickness among different regions of the skin: the thinnest is on the eyelids at about 0.05 mm and the thickest is about 1.5 mm on soles of feet and palms [28]. In addition, the epidermis itself is categorised into five different layers (living layers), which are the stratum corneum, stratum lucidum, stratum granulosum, stratum spinosum and stratum basale [28-30]. The stratum corneum has a thickness range from 0.06 to 0.1 mm across most of the body regions. Both palms and soles of feet have the thickest stratum corneum. This thickness greatly helps in protecting these parts of the human body from daily interactions.

The dermis is the skin layer which is located directly under the epidermis. The dermis itself consists of two layers: the papillary layer (which is an interface between epidermis and dermis) and the reticular one, which is the lower layer of dermis. The dermis is about 7 times thicker than the epidermis, and its thickness also varies, depending on the region of the body, being between 0.3 mm on the eyelid and 3.0 mm on the back [28]. Many blood vessels and free-ending nerves are found in the dermis layer, which plays a role in feeding the epidermis.

Below the skin layer is the hypodermis, also known as subcutaneous fat tissues. As well as fatty tissues, it also contains blood vessels and nerves which feed the human skin [28].

Elastic properties of finger skin

Each of the skin's layers has a different elastic modulus (Young's modulus) and the elastic modulus of the skin is dependent on several factors such as age, gender and the region of the body. Young's modulus of human finger layers was assigned by Bowden et al. [31] for finite element modelling as follows: 1.36×10^5 Pa for the dermis and 3.4×10^4 Pa for the subcutaneous tissue. These values were based on an image-based technique. Magnetic Resonance Images (MRI) were taken before and during exposure to a compressional load (indentation test) to be used in tracking stress-strain fields in the human finger. The Poisson's ratio was assigned as 0.48 for each layer [31]. However, the mechanical properties of finger system have been found to vary among different studies, and this section will be extended in more details later in related chapters.

2.2.2 Bones

The bone in the human finger is called the phalanx bone. All human fingers are divided into three phalanx bones, except for the thumb, which has two phalanges. The phalanges are categorised in terms of their location (distal, middle and proximal). The dimension, shape and mechanical properties of human bones vary among humans and are dependent on several factors such as age, gender and the type of bone as well as its location.[32]. Bone is a hard material and it has similar stress-strain behaviour to that of many engineering materials [33]. Bowden et al [31], chose a Young's modulus (compression) for the phalanx bone as 1.5×10^9 Pa and Poisson's ratio as 0.48 to develop and validate finite element model of a finger that also used in many other finite element modelling studies[32, 34].

2.2.3 Finger joints

The joints in human fingers are classified as synovial joints, which consist of two hard ends of articular cartilage bone, a low friction material that can allow phalangeal bones to glide freely across each other (see Figure 2.3). The bone joints are joined by a fibrous capsule which is lined by the synovial membrane. The synovial fluid is secreted into the capsule by the synovial membrane, and it helps in lubricating the articular cartilage ends.

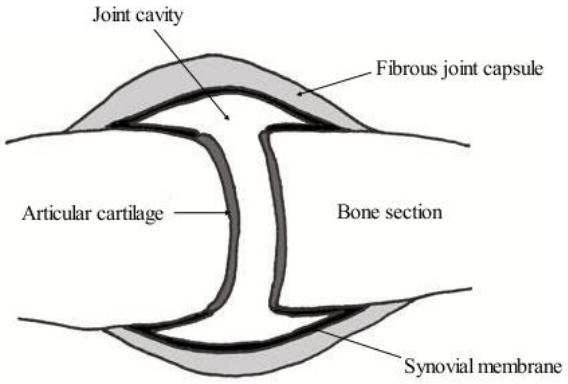

Figure 2.3: A typical synovial joint [35]

The joints in the finger are called interphalangeal joints and are categorised into three types: distal interphalangeal (DIP), proximal interphalangeal (PIP) and metacarpophalangeal (MCP) joints (see Figure 2.4). Both DIP and PIP have only two possible movements, which are flexion and very small extension. These two joints are

categorised as hinge joints. The MCP joint has large possible flexion movements, moderate adduction/ abduction and small possible movements after its straightness level with metacarpal bones [43].

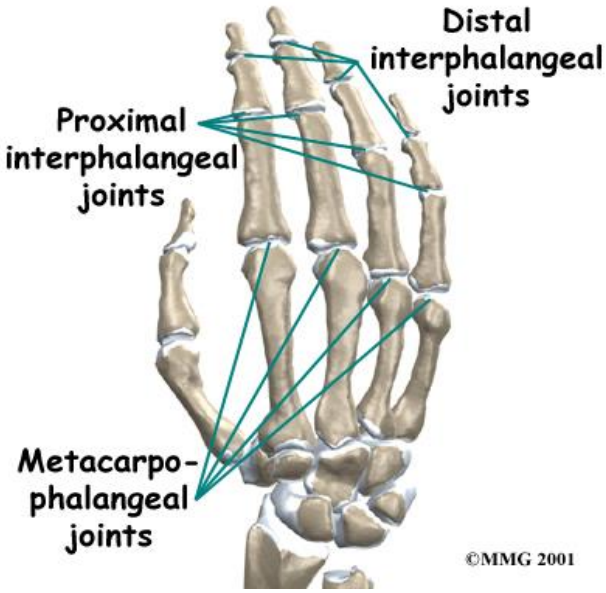

Figure 2.4: Human finger joints [36]

2.2.4 Blood

Blood flow velocity and vessel size in the human finger

Blood flow velocity in human vessels is an important factor to be known in order to simulate the blood or blood analogy fluids into artificial parts such as vessels, heart valves, etc. Blood flow velocities in the human index finger were measured of five healthy men subjects, with a mean age of 30.6 years. The measurements were performed by using a whole body 3 Tesla magnetic resonance (MR) scanner, which has the ability of high resolution imaging within a short echo time (TE = 6.5 msec). It was found that the range of arterial blood flow was from 4.9 to 19 cm/s whereas the venous blood flow was slower (1.5 to 7.1 cm/s). Vessel diameters are ranged between 800 µm to 1.8 mm. The blood flow rates in arteries ranged from 3.0 to 26 ml/s while in veins it ranged from 1.2 to 4.8 ml/s [37].

Blood analogue fluids

Blood is a shear-thinning and viscoelastic fluid (non-Newtonian) which is often taken as a Newtonian fluid at high shear rates (above 500 s^{-1})[38, 39]. Therefore, Newtonian fluids are widely used as blood analogue fluids for applications of artificial parts, such as heart, valves and vessels [39-41]. The justification for using a Newtonian analogue is often based on the blood haemolysis, due to the strong shear and turbulence. Glycerine in water solution (40:60) is widely used as blood analogy fluid in various applications [39, 42, 43]. This mixture provides a viscosity 3.5 centipoise at temperatures ranging between 32 to 39 C° [41], which approximates the apparent viscosity of blood at high shear rates for a normal ratio of red blood cells to the total volume of blood (haematocrit, 40%) [39, 42].

2.2.5 Human somatosensory system

The somatosensory system consists of various sensors which are responsible for perception in the human body and indicate touch, vibration, pain, temperature, pressure, movement and position [44].

Nerve fibres

The propagation rate of impulse is largely dependent on two factors: the diameter of the axon and the degree of myelination. A faster impulse conductivity is apparent with a larger axon diameter. This is due to low resistance to the flow of a local current. On non-myelinated axons, the impulse conductivity is relatively slow due to actions that are generated at sites immediately adjacent to each other, whereas the impulse propagation rate of the axon increases rapidly with the presence of a myelin sheath. This is due to the fact that myelin works as an insulator to avoid almost all charge leakage from the axon [45]

The nerve fibres are classified with respect to the conduction speed of signal and their size into three different categories, A, B and C, as shown in Figure 2.5 below:

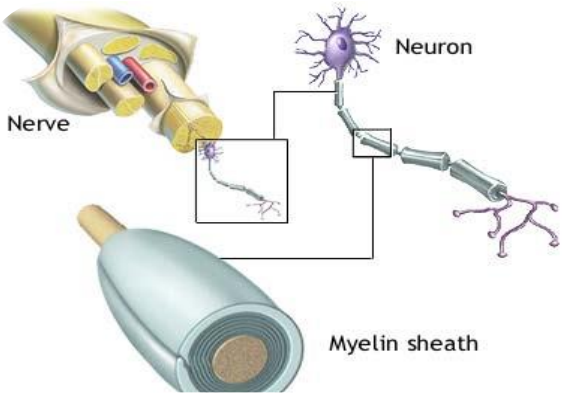

Figure 2.5: Myelin and nerve structure [46]

Type A fibres

This type is a myelinated nerve fibre and structurally is made from several parts: the axis cylinder, myelin sheath, neurolemmal sheath, and endoneurium. The structure of the myelinated fibre is shown in Figure 2.5 above. In addition, it is classified as having the thickest diameter range, from 1.5 to 20 µm. These nerves also have the fastest conductivity of the signal among the nerves to the brain at a speed range from 4 to150 m/ s. The group A nerve fibres are mainly used by mechanoreceptors to transmit the sense of skin touch and pain [45].

Type B fibres

These are lightly myelinated nerves and are of a medium size when compared to the type A fibres and type C fibres. They have a diameter ranging between 1.5 and 3.5 µm, and a conductivity speed ranging between 3 and 15 m/s. The group B nerve fibres are normally responsible for the sense of touch and for transmitting impulses from cutaneous and subcutaneous mechanoreceptors [45].

Type C fibres

This type is a non-myelinated nerve fibre. These are the smallest in size and the thinnest among all fibres with the diameter ranging between 0.1 and 2 µm. They have the slowest speed conductivity of signal among fibres, of 0.5 to 4 m/s. The group C nerve fibres are mainly responsible for transmitting impulses received by the thermal mechanoreceptors [45].

2.2.6 Human mechanoreceptors

An important characteristic of the sensors in human skin is that they are linked to the adaption rate. Most of the human mechanoreceptor cells respond to exterior changes such as temperature, pressure, or vibration (see Figure 2.6). Immediately after the external stimulus has changed, a voltage pulse is produced through neurons. The adaption rate is known as the rate of the mechanoreceptors pulse which returns to normal status after a stimulus changes. The adaption rate is related to the function of receptors themselves that need to be adapted to become faster or slower so as to ensure that the brain does not receive unnecessary information; for instance, when the skin is in long-term contact with objects such as clothes.

The mechanoreceptors in the human skin are classified, with respect to their adaption rate, into three categories: fast, moderate and slow.

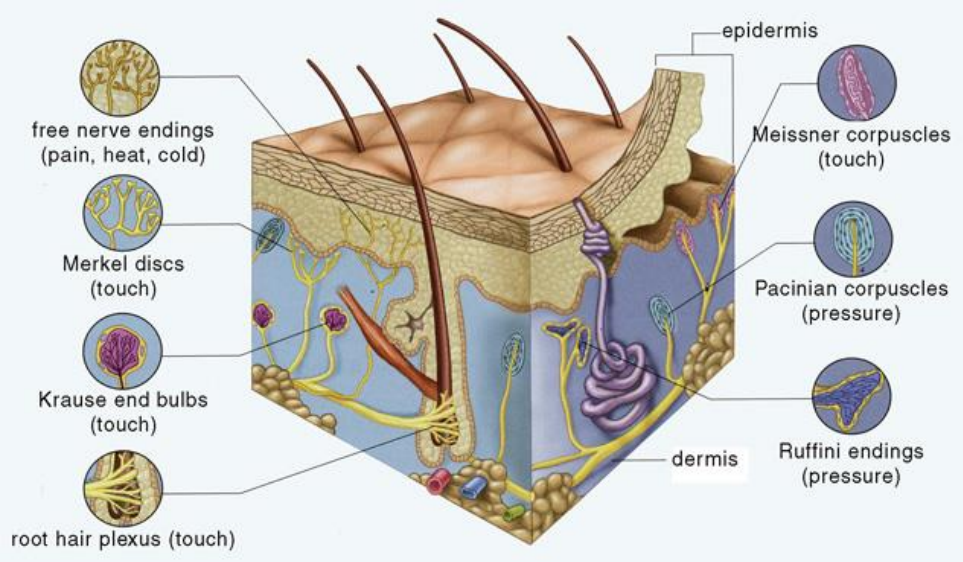

Figure 2.6: Sensory receptors in human skin [47]

Fast adaption

Pacinian Corpuscles are quick-adapting mechanoreceptors in the human skin and the cells are often sensitive to small variations of stimulus, such as the tactile force. These cells rapidly return to the normal range of pulses in less than 0.1 seconds. They are usually sensitive mechanoreceptors in the subcutaneous layer of the skin where they are protected from damage that can happen on the external surface of the skin. This type of

receptor is known as human perception system, and used in detecting the roughness of surfaces as well as sensing vibration frequencies in machines. This is due to the location of the receptors in the subcutaneous layer of the skin and the skin's role in transmuting the signal. The Pacinian corpuscles act as a filter that only allows the transmission of high level frequencies from 250 to 350 Hz to activate nerves endings [48].

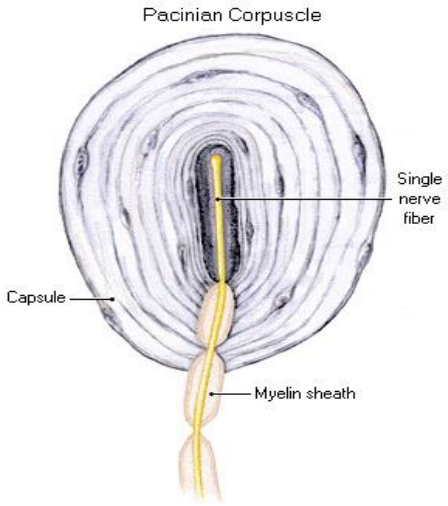

Figure 2.7: The structure of Pacinian Corpuscles [49]

Moderate adaption

Meissner's Corpuscles and hair follicles are mechanoreceptors which have a moderate rate of adaption, and adapt to external stimulus change within the time of one second. These receptors are located close to the skin surface, such as near hair follicles and they also detect insects (such as ticks, flies, or mosquitoes), on the human skin which may cause a threat. These corpuscles transmit vibration information with low frequencies from 30 to 50 Hz, which happens when objects are moved through the skin [48].

Slow adaption

Merkel's Cells, Tactile Disks, and Ruffini Endings have slow adapting rates, and are generally located close to the skin surface. These are responsible for static perception. They include, for instance, thermal sensitivity on the human skin, which is classified as slow adapting sort of receptors, as well as many tactile sensors which help in terms of maintaining the grip force on everyday objects, such as a cup. Moreover, these sensors have slow adaption rates

which may help human beings to avoid dropping objects. These receptors have an adaption time ranging between 10 and more than 100 seconds [48].

2.2.7 Human sensitivity to vibrations

A study by Verrillo [50] has carried out research on the effect of aging on the sensitivity of human hand. Vibrotactile threshold measurements were performed for five groups of six subjects. The groups were divided with respect to age and each group involved had the same number of male and female participants. The age range was between 8 and 74 years old. 11 frequencies were applied on the globous skin of the right hand by using a sinusoidal wave. The results show a gradual decrease in sensitivity at high frequencies, over the entire age range (8 to74 years) listed in the study, with the largest decline among the 50 to 65 age range. The reasons for low sensitivity can be a decrease in the number of Pacinian corpuscles receptors which are responsible for receiving high frequency vibration, as mentioned before, and this occurs with age, or as a result of structural changes in the corpuscles. At low frequencies (25 and 40 Hz) the threshold remained stable among all age groups, suggesting that the changes in non-Pacinian receptors do not affect the psychophysical threshold responses. When the youngest age group (10 years old) was then retested after 30 years, the changes in threshold paralleled those differences apparent in groups of different individuals separated by approximately the same period of years. There were no fixed differences in gender related to vibrotactile sensitivity [50].

In addition, the vibrotactile sensitivity of humans can help in detecting vibration induced white finger (VWF). According to Pyykko and Starck, it has been observed that if the vasoconstriction in the arteries is caused by a fault in the receptors, then the normal vasoconstrictor nervous tone can lead to increased peripheral resistance, which is associated with the occurrence of VWF though the strong vasoconstriction of the artery and arteriovenous shunts. If excessive, this vasoconstriction, in conjunction with decreased blood flow, can finally lead to the collapse of the blood vessel wall and an attack of VWF [23]

2.3 Loading conditions for vibrating hand tools

The nature of the vibrations transmitted into the hands and arms of workers is affected by many factors, as listed in Table 2.4 .

Table 2.4: The affected factors for vibrations transmitted into hands [19]

1. Physical	- Input vibration amplitudes to hand - Input frequencies - Years of exposure to vibration - Daily exposure - Vibration direction - Non occupational exposure
2. Biomechanical	- Hand grip force - Contact surface area - Hand parts location during the vibration exposure - Posture
3. Individual	- Operator skills of controlling - Tools maintenance - Type of tool in use - Hand size and weight

2.3.1 Force applied by hand during use of tools

The contact force between the hand and handles of vibrating tools is likely to be an important factor affecting the nature of vibrations that are transmitted into the human hand-arm system [51]. Previous case studies have indicated that the contact force tended to decrease with increasing tool handle diameter [52]. This result was based on measured grip forces from three different handle diameters [51]. In addition, another study found that the coefficient of the mean push force was almost the same for all vibrating tool handles. Moreover, the contribution of the grip force to the total contact force is three times higher compared to the contribution of the push force [53]. Regarding the effect of

vibration on the contact forces (grip and push forces), a directly proportional relationship was found, with an increase in the transmitted vibration occurring for increase in contact forces [14]. Another study indicated that the absorbed power of vibration at frequencies above 40 Hz increase in general with increases in the push and grip forces[54]. Whilst the increase observed is non-linear, the absorbed power at frequencies less than 40Hz also increases with an increase in handle diameter [54].

Many studies have been carried out with regard to the influence of grip and push forces applied to tool handles [55]. One study examined three different diameter tool handles (30, 40 and 48 mm). The main objective of the experiment was to measure the hand forces and the distribution of pressure. A capacitive pressure-sensing grid was located around the three handles. The test data was collected from ten adults male to monitor and analyse the distribution of contact forces on the surface of the right hand as a function of grip and push forces. A water displacement method was used to measure hand volume and the size of hand was measured according to the European Standard ES-420 (1994) and the design of the experiment was based on three factors:

- Handle diameter (30, 40, 48 mm)
- Grip force (Fg) (0, 15, 50, 75 N)
- Push force (Fp) (0, 25, 50, 75N)

As a result, the large handle (48 mm) yielded the highest peak of interface pressure and the small handle (30 mm) caused the higher contact force, and a more uniform distribution of pressure occurred over the small handle. Also, the localized pressure peaks in the workers' hands depended on the size of the handle and the applied grip and push forces [55].

It has been suggested that the harmful risk caused by exposure to hand-held tools vibrations is strongly linked to the contact force. Also, the estimated value of overall and localised contact forces may become essential for studying the biodynamic response of the hand-arm system rather than the gripping and pushing forces [55]. According to Dong et al., the biodynamics of the human hand-arm system is defined as a branch of biomechanics that applies engineering concepts and physics laws in order to identify the motions and forces on the hand-arm system during exposure to vibration, as well as their relationships regarding the occurrence of HAVS [56]. A recent study has shown that finger biomechanical

response could be used to determine the vibration exposure of fingers, and that the palm biomechanical force could be used to study disorders of the wrist-arm system [56]. This is due to the significant differences in the characteristics of finger and biomechanical forces which are related to deformation and stresses on the hand-arm system at different positions [56]. The human hand structure is very flexible; therefore, there were differences in the biomechanical responses distributed in between the fingers and palm of the hands. Therefore, the transmitted and absorbed energy at these parts (fingers and palm) of the hand were also found to be different [57].

Many methods have been used to measure the grip force applied to different handle diameters. A dynamometer is often used to measure the grip strength [52], the Jamar type being used widely [58], [59]. Also, it can be measured by using an instrumental split cylinder [60]. Finally, the grip force can be measured by including a strain transducer into the design of the handle [1]. According to Seo and Armstrong [52], the Jamar grip strength and handle diameter can describe around 61% of the variance of the grip strength that measured using the split cylinder.

Many lab measurements have illustrated that an increase in hand grip force leads to an increase in the vibration transmitted to the hand-arm system [61]. A high impedance can be produced generally by stronger gripping, and this applies to all frequencies in (x, y, z) directions. [62]. Previous studies have indicated that the transmissibility of vibration depends on the vibration direction [1]. However, Dong et al. [56] indicates that the vibration exposure duration has been confirmed in the recent studies as the most important parameter regarding the risk assessment of the transmitted vibration into the operator's hand-arm system. However, Gurram et al. [15] indicated that the magnitude and frequency of a tool handle vibration have been identified as the most significant factors which are related to vibration transmissibility into the workers' hand-arm system. The transmitted vibration into the human hand increases when the grip forces increase [63].

2.4 Existing technologies and protocols for HAVS research

Reducing vibration exposure can help in decreasing the risk of development of HAVS. There are several ways to reduce such exposure and risk, and some possible methods are as follows: [11]

- Work modification (e.g. using a robot when human skills are unnecessary)
- Use less vibration in tools (every tool has different specifications)
- Tool maintenance (ensure that tools are tested and used regularly)
- Operator training (operators should be trained in order to reach the best performance while limiting exposure to vibration)
- Damping vibration in tool handles (filling tool handles with absorbent material will help reduce the vibration being transmitted into hands)
- Keep hands warm and dry
- Padded gloves: vibrating-tool users should wear gloves, which need to be padded, especially in the palm and finger zones

Due to High levels of hand transmitted vibration and the high rates of prevalence of VWF symptoms among workers who intensively used hand-held vibration tools, the International Organization for Standardization (ISO) have established many standards for assessing and evaluating the exposure levels of hand-transmitted vibration.

2.4.1 ISO Standards

There are many current ISO standards that cover hand-arm vibrations with the most relevant of these are outlined in the following sections. ISO 5349-1 and ISO 5349-2 describe the factors that affect hand-arm vibrations, and how human exposure to hand-arm vibrations should be measured and evaluated. ISO 10819 covers how gloves should be evaluated and assessed, and the requirements that must be fulfilled before they can be labelled as “anti-vibration”.

ISO 5349-1-2001

Part one of ISO 5349 specifies the general requirements for the measurement and evaluation of human exposure to hand-transmitted vibration. It highlights several factors that are known to affect the hand-arm vibrations experienced in the workplace [64]. They

are the frequency spectrum of vibration, the magnitude of vibration, the duration of exposure per working day; and the cumulative exposure to date.

The daily exposure to hand-transmitted vibration is based on the eight-hour energy-equivalent acceleration value as a reference duration and identified as "$A(8)$", which is shown in Equation 4. This value is depending on the vibration magnitude, frequency and exposure duration, while the effect of hand grip force is ignored.[12, 64]

$$A(8) = a_T \sqrt{\frac{t}{t_0}} \qquad \textbf{Equation 2.5}$$

Where a_T is the total root-mean-squared, or RMS, acceleration, t is the duration of exposure to the acceleration, and t_0 is the reference duration of eight-hours (28800 s).

A frequency weighting curve (W_h) in the one-third octave bands from 6.3 to 1250 Hz is also provided in this standard that signify the assumed importance of various frequencies in resulting in health risks to the hand-arm system. Furthermore, this standard states that vibration should be measured in three directions *x*, *y*, and *z* as shown in Figure 2.8.

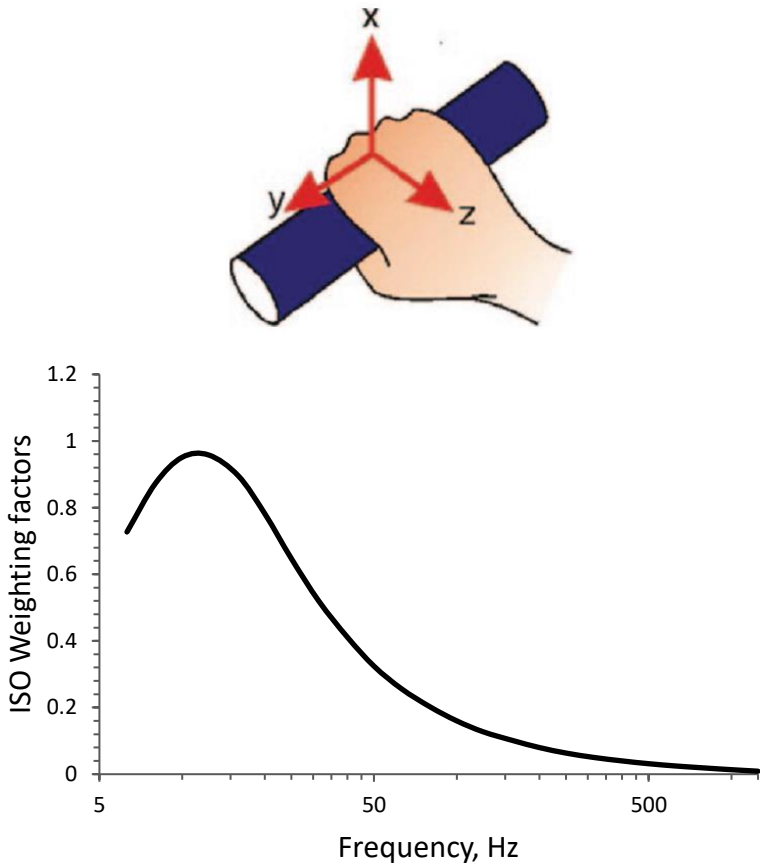

Figure 2.8: Diagram of the three orthogonal directions, *x, y* and *z* and the frequency weighting curve (Wh) as outlined in ISO 5349-1 2001 [64, 65].

The Health and Safety Executive (HSE) have used ISO 5349-1 in order to develop guidelines for employers. They state a daily exposure action value of (2.5 ms^{-2} *A(8))*, above which employers must be able to prove they are minimising the risk to their workers, and a daily exposure limit value of (5 ms^{-2} *A(8))*, where exposure values above this are illegal [66].

ISO 5349-2-2002

This standard provides the most practical guidelines based on part one ISO 5349-1 , and describes aspects of gathering the vibration data, such as mounting locations, how they should be mounted, and how the data should be gathered and processed.

Gathering methods of digital data are included in this standard and it recommends that both Fast Fourier Transform, or FFT and digital filtering, analyses should have a wide enough range to cover the full frequency range covered by the one-third-octave bands, whilst maintaining a good resolution at low-frequencies, and a high enough sample rate to ensure that accurate data can be collected at high-frequencies.

ISO 10819

The original version of this standard was established in the year 1996, and stated that there was no evidence of anti-vibration gloves providing a sufficient attenuation of vibration to prevent the injuries they caused, which agrees with research at the time [67], as well as more recent studies [68, 69] that find attenuation at low frequencies is negligible.

This standard mentions that gloves are evaluated on their performance at the palm of the hand but in actuality vibrations are transmitted into the fingers as well and states that a different measurement technique would need to be used to evaluate the effect glove on vibrations transmitted to the fingers.

When testing the gloves the standard specifies a particular palm adaptor, which is shown in Figure 2.9. It contains three orthogonal accelerometers to capture the vibration signal, and the shape is designed so that it fits comfortably inside a glove while still conforming to the shape of the handle used in testing, as shown in Figure 2.10. The issue with this method is that such a large adaptor affects the measured transmissibility [70], and as it is inside the glove, it can be difficult to assess the alignment of the adaptor with the handle [71].

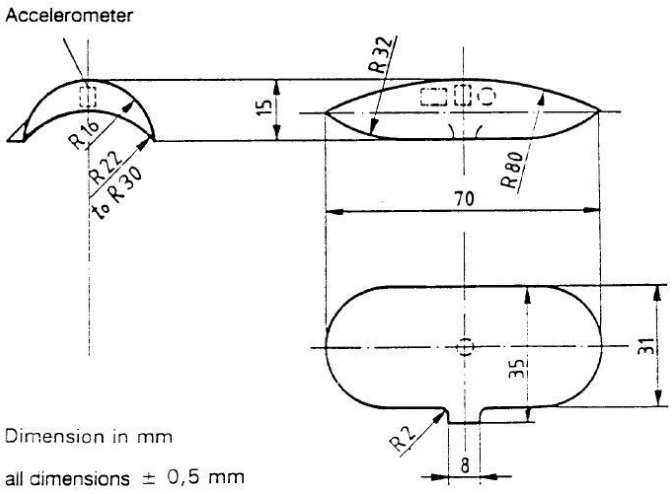

Figure 2.9: Diagram of the palm adaptor used in ISO testing method [72].

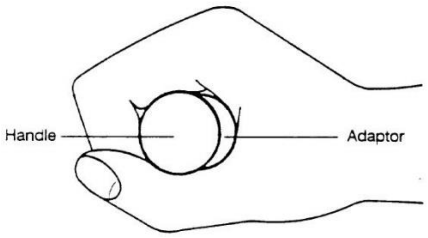

Figure 2.10: Diagram of how the palm adaptor is used when holding the handle during testing [72].

The handle is excited by a shaker that can generate vibrations in three directions and is capable of measuring both the gripping force from the hand, as well as the feed force applied by the operator, which is the force the operator pushes with. The diagram in Figure 11 shows this setup, along with the posture that operators are required to adopt when taking part in the experiment.

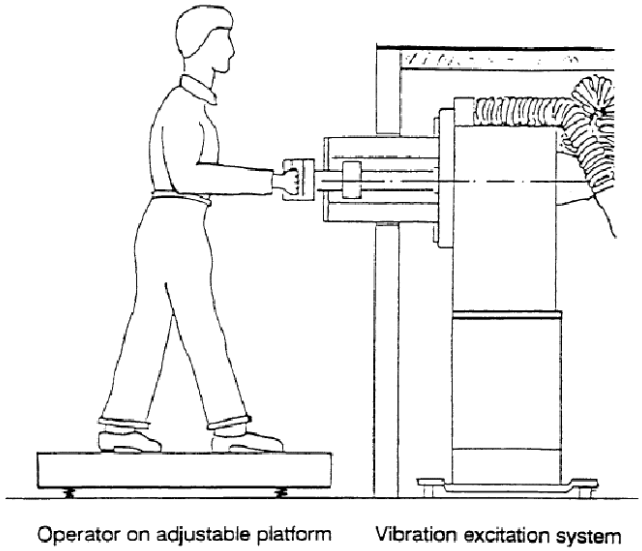

Figure 11: Standardised vibration system for measuring glove transmissibility as outlined in ISO 10819 [72].

In order to establish whether a glove can be labelled as “anti-vibration” (AV) this standard measures glove transmissibility twice, once at the medium frequency (TRM) ranged between 31.5Hz and 200 Hz (25 Hz-200 Hz in the revised version); and one at the high frequency (TRH) ranged between 200 Hz and 1250 Hz. According to an original version of this standard 1996, the glove should fulfil the requirement of both of following criteria of the average transmissibility: TRM < 1.0 and TRH < 0.6

Further, this standard states that a glove can only be identified as an AV glove if both the fingers and palm of the hand are covered with the same material [72]. This criterion outlined in the original glove standard were inconsistent. This due to if a glove has reduction capability of vibration in z direction at the high-frequency spectra about 40% or greater, whereas this same glove can be reduced the vibration by greater than 10% at the medium-frequency spectra[73, 74]. Due to most of the vibrating handheld tools are operated within medium-frequency spectra, the above criteria was unreasonable. Anti-vibration gloves were required to provide a significant attenuation at a high-frequency range, not only for the low-frequency range produced by the majority of hand-held powered tools, which shows disagreement with the purpose of the use of AV glove. Therefore, this criterion has been revised in the latest version (from TRM < 1.0 to RTM ≤ 0.90), while (RTH ≤ 0.60) which is actually as it was in the original version of the glove standard [75].

Due to the challenges of measuring a glove transmissibility at the fingers, the standard does not provide any methodology of identifying glove performance in this area. It is considered that the effectiveness of the AV glove in reducing vibration in the fingers would be as good as in the palm of the hand. Many recent studies have indicated that some of the AV gloves show similar finger transmissibility spectra to that of some non-AV glove at frequencies under 400 Hz; non-AV gloves show more effective compared with the AV gloves. These findings demonstrate unnecessarily of covering both fingers and palm of the hand with same material properties (e.g. thickness and softness). Also, it is extremely difficult to use the materials with the same thickness to cover palm and fingers of AV gloves. The AV gloves that met the standardised criteria of both (transmissibility and thickness) of the palm and the fingers is unlikely to be achieved a safe using of the tools. That is because it is too bulky, and requires more hand grip force [69, 76]. Now, none of the AV gloves that meet thickness requirement at fingers can be found on market.

Because of this, the requirement of material thickness that covered fingers was relaxed in the revised revision of the standard ISO 10819, 2013. That requires “The thickness of anti-vibration material placed in the fingers and thumb parts of the glove should be (≥ 0.55) times the thickness of the anti-vibration material placed in the palm part of the glove.” The revision of the standard also recommends that “the thickness of anti-vibration material

placed in the palm part of the glove should not be > 8 mm." It could be considered excessive to require such certain thickness limitations on the AV glove design, and the bulkiness of the glove should be tested with the different functional test such as a grip strength test [77].

The revision version of ISO 10819, 2013 comes with some other significant technical changes and simplifications. A single vibration range is replaced in the latest version with the two ranges (M and H) that are outlined in the original standard. This improvement reduces the testing time to half, whilst maintaining of the quality. For improving the reliability of vibration measurement of the AV glove, the number of test subjects is raised from 3 to 5 and the number of tests per subject from 2 to 3. Moreover, the bare-hand adapter test in the original standard is replaced instead by a bare adapter test (transmissibility was measured using the only adapter strapped on the bare handle without the use of the human subjects) to carry out the in-situ response of the adapter and handle accelerometer, which avoids any unwanted interference of the hand biomechanical response on the internal calibration. It has been noticed that the direct contact of palm with the accelerometer inserted into the adapter may affect the measurement at low frequencies in some cases. this was one reason for the bare-hand test in the original version of glove standard ISO 108019, 1996 [72].

Even though it is not required by the revised version of the standard, Xu et al. suggest performing one more bare-hand test with both grip and push forces (30 N and 50 N), in order to check the in-situ dynamic response of the accelerometer. To ensure that the adapter is aligned with the handle during the test, the adapter can be attached to the handle using double sided tape and secured with two thin elastic bands to ensure good surface contact [78].

Evaluation of the standardised frequency-weighting curve on finger

Based on the theory of biomechanical response by Dong et al. [79], it could also be acceptable to utilise the palm-transmitted vibration exposure to evaluate the risk of possible injury and disorders in the palm wrist-arm system. These findings suggested that it may be acceptable to use the transmissibility of the AV glove measured on the palm of the hand to assess its vibration reduction advantages for this system. Also, vibration-induced finger injury and disorders such as vibration-induced white finger are more likely

closely relating to finger-transmitted vibration exposures than palm-transmitted vibration exposures. Due to this fact, the benefit of an AV glove in protecting fingers can be assessed dependent on its reduction of transmitted vibration into fingers.

A review study by Hewit et al. states that AV gloves could have a slight reduction of transmitted weighted vibration on fingers comparing to its reduction to the palm, except in some cases [65]. This finding disagrees with the findings of some studies, which reported that an AV glove can help reduce some HAVS on the fingers by about 30%. It is challenging to explain such benefits of the AV gloves when using the reduction vibration measured on the palm to estimate reduction at fingers. According to Hewit et al., this disagreement may link to the following hypothesis. First, the benefits of AV gloves in reducing the health risk could be overestimated in some studies that focused the health effects, or some of the findings are typically not applicable to many other cases. Second, the current frequency weighting does not sufficiently provide the frequency-dependency of the vibration-induced finger or hand health problems, or the high-frequency effects were underestimated [65]. One study also claimed how the using of unweighted vibration produced better estimates of the vibration-induced white finger than using weighted vibration [80].

The finger biomechanical frequency weighting also suggests that the weighting peak of the fingers is likely to be in the medium-frequency spectra ranged (25-300 Hz) where the primary occurrence of finger resonances happen [79]. Another study suggested that the peak weighting resonance occurs at the frequency of 63 Hz and gradually reduced at frequencies beyond [81]. If these finger weighing suggestions are confirmed, the actual benefit of AV gloves could be between the predictions using both the weighted and unweighted vibration in lots of incidents. The real mechanisms of the occurrence of finger disorders have not been specified, and strong relationships between hand-transmitted vibration exposures and the health effects factors have not been found [64, 82]. With no such understanding, it is extremely hard to identify an appropriate finger frequency weighting for disorders. Additionally, the suggested finger frequency weightings were not sufficiently investigated or supported [83]. As a result, the determination of a reliable finger frequency weighting is a big research task. It is not likely that the standardised

method and the current frequency weighting for assessing the risk of exposure of HTV, can be improved very soon in the future [84].

Hand-transmitted vibration measurement

The measurement of the vibration transmissibility of gloves can be affected by many factors, such as: variability between and within subjects [85, 86], controlling feedback and grip forces, test rig behaviour, and temperature. One previous study has investigated the effects of several variables on measuring the vibration transmissibility of gloves; it has found that misalignment of the palm-adaptor can reduce the measured transmissibility by approximately 20%. Other variables include inter-subject variability (±10%), temperature variation (±4%) and controlling feed forces(±4%) [85]. Further, the vibration transmissibility measured at the finger can vary depending on the location of the measurement on each of the fingers [87], and using the finger-adaptor method may change the geometry of the finger, which may in turn affect the dynamic properties of the finger and produce unreliability in measurement [88].

Many studies have indicated that the effect of hand force has to be taken into account as a contributing factor in evaluating the potential risk related to hand-transmitted vibration [51]. This requires the real identity of the relationship between the hand force, the vibration transmission and health issues. Furthermore, an exact description, together with a measurement approach for the hand force, is required [15]. Some health effects and workplace studies have claimed that AV gloves would be helpful in protecting operators' hands from injuries caused by hand-transmitted vibration, such as the effects on blood circulation in the fingers [65, 89, 90]. However, there is still doubt regarding the effectiveness of gloves for attenuating vibrations transmitted to the hand and fingers [67, 86, 91-93]. Also, gloves can impair dexterity whilst raising the effort of hand grip force, and these factors may pose a safety risk. The balance between vibration reduction and dexterity impairment will depend on tool specifications and work conditions. To help determine this balance, it is important to know how much vibration an AV glove can reduce.

Vibration-induced damage to the fingers is the main component of HAVS [91], so the fingers are likely to be the most important substructures of the hand-arm system that need to be taken into consideration. Mostly due to technical challenges such as the mounting

and alignment of instrumentation, the study of the vibration transmissibility to the fingers has been limited [86, 94]. The standardised AV glove evaluation is usually dependent on the vibration transmitted through the palm of the hand along the *z* direction [72, 75]. A recent study measured vibration transmissibility on the hand-arm system and indicated that the major resonance occurring on the forearm is in the range of 16-30 Hz, and it happens in the *y* direction in the wrist. On the dorsal surface of the hand the main resonance occurs at a frequency ranging from 30 to 40 Hz. At frequencies above 50 Hz, the transmission of vibration to the hand and fingers was limited. In fingers, the major resonance occurred at about 100 Hz in the *x* and *y* directions and about 200 Hz in the *z*. Also, the resonance peak was lowest in the *z* direction [95].

No in-vivo method has been established which can directly measure the effect of transmitted vibration inside the soft tissues of the hand-arm system [64, 96]. Alternatively, the determination of transmitted vibration is usually dependent on the modelling of the system. The reliability of these models is dependent on their capability to represent the actual hand-tool system and the accuracy of the measurements that are used for validation and calibration [97].

There are several types of handheld tools where each type is classified specifically with regard to many factors such as weight, acceleration and frequency. The Health and Safety Laboratory (HSL) has measured vibration magnitudes for many different vibrating tools, as shown in Table 2.5.

Table 2.5: The measured magnitudes by HSL on different vibrating tools in use at work [66].

Tool type	Model classification	Acceleration
Road breakers	-Typical	12 m/s2
	-Modern tool design, good operating conditions and trained operators	5 m/s2
	-Worst tools and operating conditions	20 m/s2
Demolition hammers	-Typical	8 m/s2
	- Modern tools	15 m/s2
	-Worst tools	25 m/s2
Hammer drill / combined hammer	-Typical	9 m/s2
	-Best tools and operating conditions	6 m/s2
	-Worst tools and operating conditions	25 m/s2
Needle scalers	-Modern tool designs	5-7 m/s2
	-Older tool designs	10-25 m/s2
Scrabblers (hammer type)	-Typical	20-40 m/s2
Angle grinders (large)	-Modern vibration-reduced designs	4 m/s2
	-Other types	8 m/s2
Angle grinders (small)	-Typical	2-6 m/s2
Clay spades / jigger picks	-Typical	16 m/s2
Chipping hammers (metal-working, foundries)	-Typical fettling	18 m/s2
	-Modern tool designs	10 m/s2
Pneumatic stone-working hammers	-Modern vibration-reduced hammers and sleeved chisels	8-12 m/s2
	-Older tools, conventional	30 m/s2
Chainsaws	-Typical	6 m/s2
Brush cutters	-Typical	4 m/s2
	-Best	2 m/s2
Sanders (random orbital)	-Typical	7-10 m/s2

2.5 Previous research on VWF

2.5.1 In-vivo studies

Many studies have indicated that vasoconstriction is dependent on vibration frequency, acceleration magnitude and exposure duration [3, 8, 10, 98]. A large number of in-vivo studies have been carried out on the effect of vibration on blood flow circulation of the human hands. In 2001, Bovenzi el al set up an experiment to examine the response of finger circulation during and after vibration exposures. The measurements of finger blood flow (FBF), finger systolic blood pressure (FSBP) and finger skin temperature (FST) were taken from the middle finger of both hands before, during and after the exposure to vibration [7, 9]. The experiment set up is shown in Figure 2.11

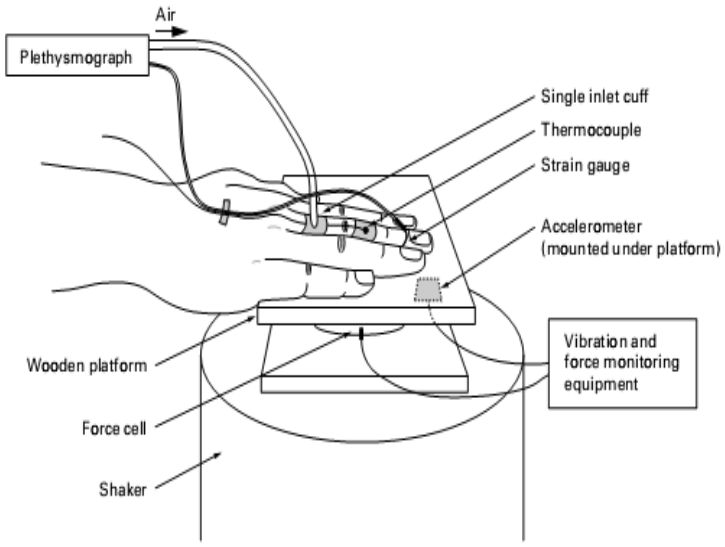

Figure 2.11: The experimental set up of vibrating, controlling contact forces and measuring finger blood flow [7].

The strain gauge and pressure cuff were linked to the plethysmograph (Digitmatic DM2000, Medimatic A/S, and Copenhagen) which is an instrument for measuring and recording those changes linked to blood flow. The FBF was measured by a technique, is called a venous occlusion, by Greenfield et al.: the pressure cuffs were inflated to a pressure of between 40 and 60 mm Hg and the rise of volume was detected by means of the strain gauge [99]. This technique provides a non-invasive method to measure a direct blood flow and its quantity [100]. Moreover, the finger skin temperature (FST) is measured by a K-type thermocouple linked to an HVLab. The HVLab vibrotactile perception meter is a developed device (by Institute of Sound and Vibration Research at the University of Southampton)

with software to measure human response to vibration. Many studies have measured the effect of transmitted vibration into human fingers as listed in Table 2.6.

Table 2.6: Blood flow measurement of the effect of vibration in human finger.

Author	Measurement technique	Measurement region
Juhani et al., 1973 [101]	Strain gauges and plethysmograph	Vibrated and un-vibrated finger
Bovenzi et al., 2001 [7]	Pressure cuff and strain gauge connected to plethysmograph (Digitmatic DM2000)	Both middle fingers
Bovenzi et al., 2000 [98]	Pressure cuff and strain gauge linked to plethysmograph (Digitmatic DM2000	Both middle fingers
Ye et al., 2012 [102]	Pressure cuff and strain gauge linked to a multi-channel plethysmograph HVLab	Right middle and little finger
Bovenzi et al., 2004 [10]	Pressure cuff and strain gauge linked to a five-channel plethysmograph HVLab	Right middle and little finger of both hands
Bovenzi et al., 1999 [8]	Pressure cuffs and strain gauges connected to a plethysmograph (Digitmatic DM2000)	Middle finger of both hands
Bovenzi et al., 1998 [9]	Strain gauge and the pneumatic cuffs connected to plethysmograph (Digitmatic 2000)	Middle finger of both hands
Hokanson et al., 1975 [103]	Strain gauge and pressure cuff connected to plethysmograph	Index finger
Bovenzi et al., 1995 [5]	Pneumatic cuff and strain gauge connected to plethysmograph (Digitmatic DM2000)	Index finger of both hands
Furuta et al., 1991 [104]	Blood flow meter connected to three channel recorders (Graphtech, SR-6335).	Right hand
	Laser Doppler flow meter based on thermal diffusion method in both hands.	Left middle finger

A study was carried out by Bovenzi et al. on the influence of the duration of acute exposure to vibration on finger blood flow. FBF were measured in the middle finger of both the right and left hand of ten healthy males. The right finger was exposed to vibration at 125 Hz and acceleration of 87 ms^{-2} rms for three durations: 7.5, 15 and 30 minutes while a static load 10N was applied. The static load was used as a control. FBF was measured before exposure to the static load and vibration as well as specific periods during exposure to vibration and also after 45 minutes of recovery. The results did not show significant changes with the applied static load. However, a significant reduction was produced in finger blood flow during the exposure to vibration and vascular resistance increased each vibration duration when compared with results from pre-exposure and un-vibrated finger values. Moreover, immediately after each exposure to vibration, temporary vasodilation occurred in the vibrated finger. After 7.5 minutes, the recovery of FBF and vascular resistance was complete, whereas a progressive FBF reduction occurred in both the vibrated and un-vibrated finger, after 15 and 30 minute of exposure. The longer vibration exposure duration yielded a stronger vasoconstriction in the vibrated finger during recovery [9].

A recent experimental study by Ye et al. [3] showed that blood flow in fingers depends on the shock repetition rate, the peak and rms magnitude of acceleration. 14 healthy men subjects were used in this study, and all these volunteers were either university students or office workers, who did not have a history of occupational and/or leisure exposure to vibration. A force of 2 N was applied on a vibrator in contact with the palm of the right hand. Mechanical shock was applied at 125 Hz with one of the following repetition rates (1.3, 2.5, 21 or 83.3 s^{-1}) and one of the following rms un-weighted acceleration (2.5, 5 or 10 ms^{-2}). FBF measurements were taken from the middle and little fingers of both vibrated and un-vibrated hands. The results showed that there was no change in FBF in both hands when the force of 2 N was applied. A similar vasoconstriction occurred in the fingers of the left and right hands, when repetitive mechanical shocks with a frequency of 125 Hz were applied to the right palm and constant rms acceleration whereas the rate of shock repetition was varied from 1.3 to 83.3^{-1}. When shocks had the same peak acceleration, a greater reduction in FBF was produced with increases of the rms acceleration and the rate of repetition [3].

There are several different handheld vibrating tools; these tools can affect different zones on the hand-arm system. According to Heaver et al., different areas of the hand-arm system could be affected by vibration, depending on its level and type. For instance, high-frequency impact tools are related with a high occurrence of wrist syndromes, whereas impact tools with a low frequency are related to proximal joint syndromes [105] .

Despite the differences in the affected areas on the hand-arm system and where the vibration is applied (fingers, palm or whole hand-arm system), all previous and recent studies have stated that the high vasoconstriction occurred with a high magnitude of vibration. A daily measurement of vibration exposure can be calculated from un-weighted (rms) acceleration above the frequency range of 6.3-1,250Hz based on one-third octave bands which achieve a better prediction of VWF and vascular disorders in workers who use vibrating handheld tools compared with the rms acceleration frequency weighted as presented in ISO 5349-1 [17]. Moreover, the vibration at a frequency of 31.5 Hz could result in a more powerful vasoconstrictor effect than the vibration at frequency 250 Hz. On the other hand, different experimental studies have indicated that the vibration at frequency 250 Hz, rather than high and low frequencies, produces a greater change in the blood circulation of fingers [106].

Relatively low frequency vibration causes discomfort in using vibratory handheld tools, vibration at a range of frequencies 40-200 Hz substantially reduces the blood flow in the skin, and it was found that vibration at frequency 120 Hz was the most effective [5]. Earlier studies have reported that power transferred through the hand is dissipated within the cutaneous and subcutaneous tissue of the hand and only occurs at a low level of vibration: less than 10% was only transmitted into the wrist and beyond at excitation frequencies over 250 Hz. Additionally, the resonance occurred at closed frequencies to 125 and 500 Hz and it was found that at frequencies over 300 Hz, the transmitted vibration tended to become localised to the hand. [63]. There were changes demonstrated in finger blood flow (FBF) at vibration frequencies 31.5-63 Hz and 250-500 Hz, and ISO 10819: 1996 states that "medium" and "high" frequencies of 31.5 Hz and 250 Hz [90]. On the other hand, the vibration at very high-frequencies (around 1 MHz) from the handles of ultrasound devices might also have an effect. This appeared in patients who had been exposed to vibration

using ultrasound device handles and who were found to be suffering from weaknesses of vibration perception [13].

Many studies have been carried out in order to measure the response of finger circulation to vibration exposure under different conditions. These studies are shown in Table 2.7

Table 2.7: Summary of published studies with regards to the influence of vibration exposure on finger circulation

Citations	**Exposure Characteristics**	**Effects of vibration exposure**
Bovenzi et al., 2001 [7]	Frequencies: 125 Hz Accelerations: 44, 62, 88, 125 and 176 m/s^2 rms Durations: 30, 15,7.5, 3.75 and 1.88 min	• FBF reduction was stronger in a vibrated right middle finger than an un-vibrated left middle finger where FBF was measured. • Progressive decrease in FBF was found in both vibrated and un-vibrated hands after the exposure to vibration at 44 m/s^2 for 30 min and 62 m/s^2 for 15 min • Similar degree of vasoconstriction was found in the vibrated right middle finger during exposures to vibration at all five applied accelerations and durations • No significant vasoconstriction was found for short duration exposures
Bovenzi et al., 1999 [8]	Frequencies: 125 Hz Accelerations: 5.5, 22, 44 and 62 m/s^2 rms Durations: 15 min	• Significant reduction in FBF was found in the vibrated finger compared with FBF measured before the exposure and FBF in the un-vibrated finger • Vasoconstriction was present during the recovery period after exposure to vibration magnitudes greater than 22 m/s^2 rms • Highest vibration magnitude produced the strong reduction of FBF in both vibrated and un-vibrated fingers during and after the end of exposure to vibration • The strong effect was found with the vibrated hand than with the un-vibrated

Citations	Exposure Characteristics	Effects of vibration exposure
Bovenzi et al., 1998 [9]	Frequencies: 125 Hz Accelerations: 87 m/s^2 rms Durations: 7.5, 15 and 30 min	• Vibration yielded a significant reductions in either FBF and increased the peripheral resistance of vascular wall at each exposure duration when compared with pre-exposure and measured values of the un-vibrated finger • Immediately after each exposure to vibration, temporary vasodilation occurred in the vibrated finger, but this was only significant after exposure to 30 minutes vibration when compared with the FBF in the un-vibrated finger. • Progressive FBF reduction occurred after 15 and 30 minutes in both the exposed and unexposed fingers • The longer exposure duration produced strong vasoconstriction in the exposed finger during recovery
Bovenzi et al., 2000 [98]	Frequencies: 16, 31.5, 63, 125 and 250 Hz Accelerations: 5.5, 11, 22, 44 and 88 m/s^2 rms Durations: 15 min	• FBF did not change significantly when only a static load was applied • The greater reduction in FBF with the vibrated right finger was found at frequencies of 31.5-250 Hz rather than at 16 Hz and with the static load • FBF in un-vibrated finger at frequencies of 63-250 Hz was significantly less when compared with that measured with static load only • FBF reduction during the exposure to any of the applied frequencies was stronger in the vibrated hand than in the un-vibrated one • Progressive reduction in FBF was found in both vibrated and un-vibrated fingers after the exposure to vibration with applied frequencies of 31.5-250 Hz • Highest frequency yielded strong reduction in FBF in both vibrated and un-vibrated finger after the end of the exposure (recovery period)
	Frequencies: 125 Hz	

Citations	Exposure Characteristics	Effects of vibration exposure
Bovenzi et al., 2004 [10]	Accelerations:44 m/s^2 rms Durations: 30 min for each of five conditions: 30 min 30/2 min 30/4 min 30/8 min 30/16 min	• Significant reduction in FBF was found in all five conditions when compared with premeasured FBF • A similar degree of vasoconstriction was found in the vibrated finger during the exposure to vibration in all five conditions • After the end of the exposure to vibration for 30 minutes continuously, there was found to be a progressive reduction in FBF • There was not a statically significant reduction following the intermittent exposure to vibration
Ye et al., 2012 [102]	Frequencies: 125 H Accelerations: 0, 22 or 88 m/s^2 rms Durations: 7.5 or 15 min	• The reduction in FBF was found in both vibrated and un-vibrated during and after (recovery) vibration exposure • An increase in duration of vibration did not show changes in vascular response during the exposure whereas an increase in vasoconstriction was found after vibration exposure and longer recovery period • With the greater vibration magnitude, the reduction in FBF through the exposure was linked to the recovery period after the exposure • An increase in vasoconstriction was found after vibration exposure and longer recovery period

2.5.2 In-silico modelling

Finite element modelling is a very useful technique that enables engineers to develop, simulate and study very complicated problems which are normally extremely difficult or impossible to test and study by conducting experimental work alone. In order to avoid complications with the developed model, some assumptions and simplifications are acceptable, whereas the predicted results from FE modelling are usually comparable in

accordance with the results of a real case. Many studies have indicated that prolonged exposure to segmental vibration can lead to vibration-induced white finger (VWF), but the mechanism of occurrence of VWF is still unclear. Wu et al. analysed the dynamic responses of the fingertip, by using a multi-2D finite element model including the major anatomical substructures such as skin, subcutaneous tissue, bone and nail as shown in Figure 2.12 [107]. The simulations were conducted using a finite element software package (ABAQUS). As a result, it was found that the fingertip has a major resonance at a vibration excitation of about 100 to 125 Hz and a second resonance at about 250 Hz. In addition, the resonance in the fingertip did not depend on the direction of the vibration exposure (normal or shear). Furthermore, it was indicated that the dynamic strain which occurs due to low-frequency vibration will penetrate deeper through the tissue (> 3 mm) whereas the high-frequency vibration will be concentrated in the superficial skin layers (< 0.8 mm), as shown in Figure 2.13 [107].

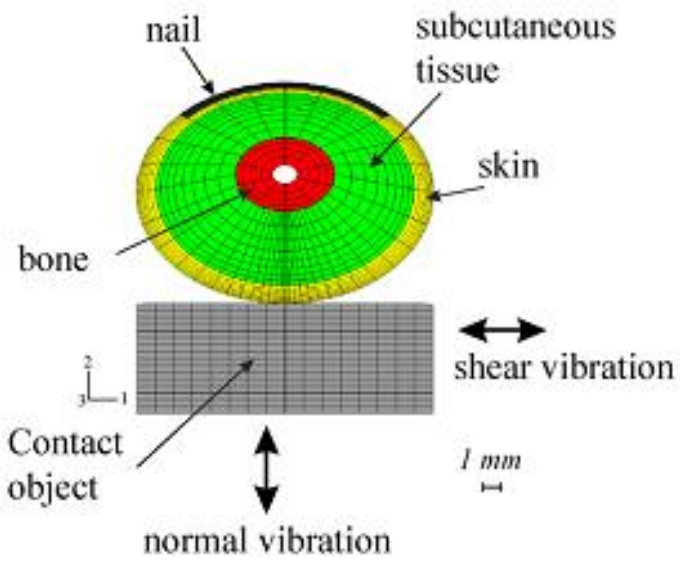

Figure 2.12: A two-dimensional (2D) finite element model of a fingertip in contact with a flat surface reproduced from [107].

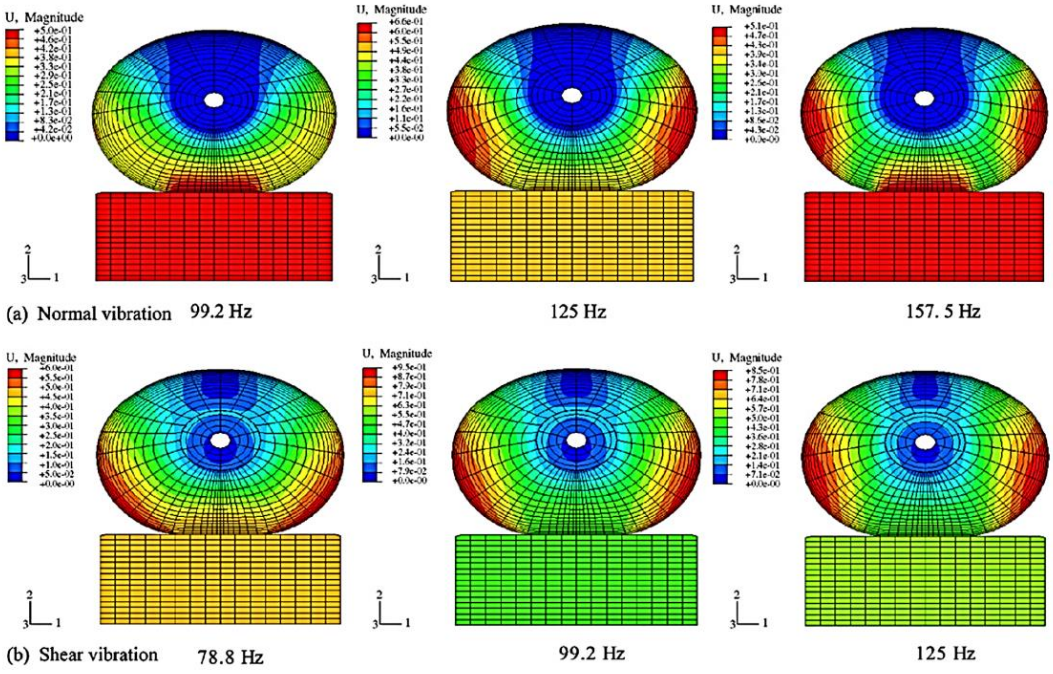

Figure 2.13: The distributions of vibration magnitude (U, mm) across the tissues of the fingertip around the major resonance. (a) Normal vibration. (b) Shear vibration reproduced from [107].

2.5.3 Synthetic test-bed

The mechanical properties of human skin vary and could be affected by many factors such as hydration, age and anatomical structure [108, 109]. This variation produces a complication in measuring reliable and consistent data of individuals. To gain a reliable measurement that replicates the mechanical behaviour of human skin, a few studies have been conducted that investigated the stiffness and friction properties of human skin, an artificial model of a fingertip was developed for experimental use. Many alternative materials have been investigated in studying the mechanical properties (including softness and friction) of the human skin at the fingertip. Ramkumar et al. [110, 111] developed and evaluated an artificial model using polyvinylsiloxane. Derler et al. [109] used different silicone and polyurethane materials as mechanical friction equivalents to the skin and polyurethane coated polyamide fleece with a surface structure was found similar to that of skin showed the best friction correspondence to human skin under dry conditions. A recent study by Shao et al. [108] used 101RF silicone rubber (cured hardness: 30 Shore A) to replicate the mechanical properties (including softness and friction) of the anatomical

structure of a real fingertip. The results show that an artificial fingertip that used only pure silicone showed a difference in friction behaviour compared to the real fingertip. However, the soft multi-layer artificial fingertip (see Figure 2.14) was found to be closer to the real one [108]. These previous studies have only investigated the mechanical properties of materials (friction and stiffness), and not the dynamic response of materials. More investigation is therefore required to examine the materials dynamically.

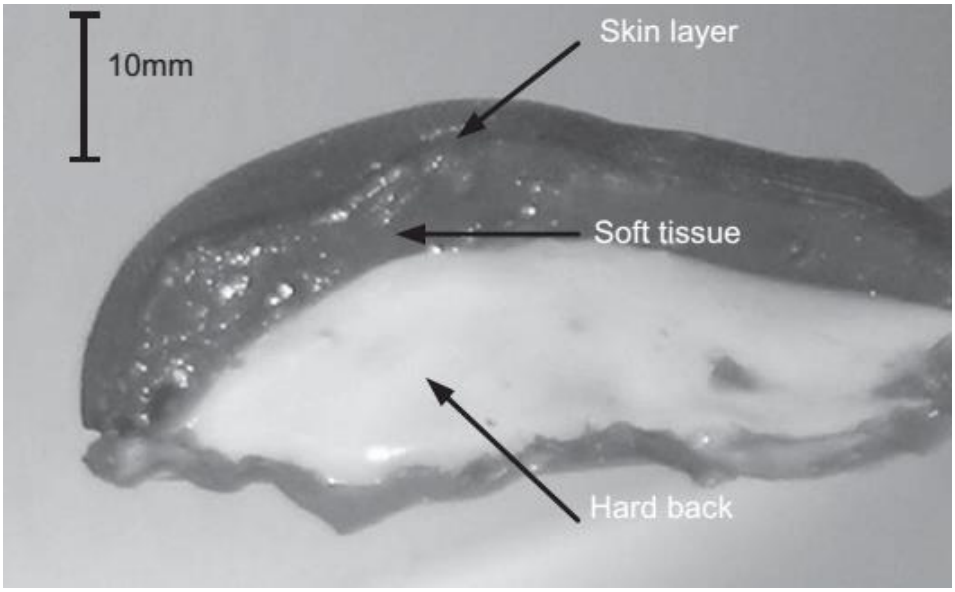

Figure 2.14: Sectional structure of the multi-layer artificial fingertip [108].

2.6 Conclusion

The findings of this literature review are that the prolonged use of vibrating hand-held tools widely affects the human hand-arm system, and that vibration-induced white finger (VWF) is the most common hand-arm vibration syndrome. VWF occurs in workers who are continually using vibrating handheld tools, and many researchers suggest that the aetiology of VWF is related to vasoconstriction and vasodilation due to the vibration that is transmitted. Therefore, the human anatomy has been reviewed in order to understand the mechanical properties of each organ individually. This is for the purpose of developing the artificial finger that can be used instead as an alternative experimental test-bed in assessing the vibration transmitted into fingers. Several tools can affect different zones of the hand-arm system, depending on many factors such as vibration directions, frequency, and magnitude, and these differ according to the vibrating tools. The grip and push forces

applied on different sizes of the handle have an effect on the vibration transmitted into the hand, and the influence of the grip force on this vibration process has also been reviewed. The biomechanical response is widely suggested to be involved in hand-arm vibration system assessments. The relevant ISO standards for assessing hand-arm vibration are also reviewed, including the two parts of ISO 5349-1-2: 2001 that addressed both general and practical requirements of the measurement of human exposure to hand-arm vibration, and both versions of ISO 10819:1996:2013 that outlined the evaluation and assessment method for measuring the transmissibility of AV gloves. Since the current frequency weighting curve and standardised methods are specified for the palm of the hand and are not applicable for the finger, a number of studies have suggested that studying finger transmitted vibration has become a major research topic. Further research will be needed that investigates finger transmitted vibration, and this could be achieved by developing a new methodology that may provide a better understanding of this topic. This includes developing both a vibration test rig and a synthetic test-bed for finger transmitted vibration purposes

Chapter 3: Development of vibration test rig

This chapter outlines the development of a new methodology that measures vibration transmission for HAVS. The research is based on existing techniques reviewed in the literature section (Chapter 2). Firstly, it presents the development of the entire design of the vibration excitation test rig including the instrumentation, software and equipment which is used in producing and gathering data as well as the signal processing method that is being applied. Secondly, it describes how the grip force system was designed and calibrated to meet the purpose. Finally, this chapter presents hammer testing of the dynamic response of the entire rig, followed by a number of pilot studies to assess the validity of the approach including two-dimensional finite element modelling of the index finger.

3.1 Introduction

Based on the reviewed literature in Chapter 2, the primary aim of this research is to develop a new method to measure and evaluate vibration transmission for HAVS research, which can be used for the human finger testing and development of synthetic test-bed. The new vibration test rig is designed to gain an understanding of finger transmitted vibration (FTV) that is associated with the occurrence of vibration-induced damage into the human index finger in contact with different vibrating hand-held tools whilst measuring and controlling the grip force.

3.2 Methodology

The vibration test rig was designed and built to investigate FTV that can be produced by several types of handheld vibrating tools, such as angle grinders or drills. The instrumentation set-up includes the vibration controlling and response measurement system, as well as a grip force and display system, as shown in Figure 3.1.

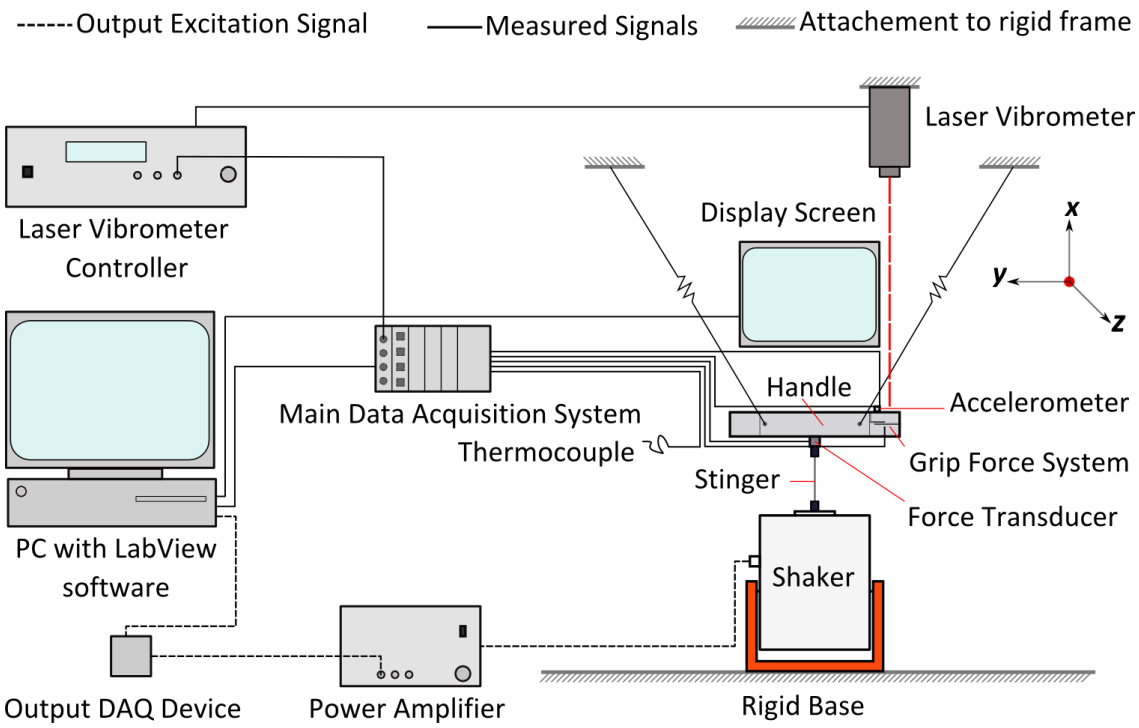

Figure 3.1: Instrumentation set up showing the vibration generation and response measurement systems, as well as a grip force and temperature measurement and display system

3.2.1 Vibration excitation system

A generic handle made from aluminium (based on ISO 10819 1996) was developed and instrumented for measuring finger transmitted vibration and grip force. The handle was freely suspended at the ends and attached via a thin stinger to an electrodynamic shaker to provide a vertical excitation (*x* direction). To determine the excitation force, the handle was attached to the stinger via a piezoelectric force transducer.

The main features outlined here are described in more detail below.

Handle

The set-up of the entire handle is shown in Figure 3.2. The handle was made from aluminium, it measured 40 mm in diameter and 250 mm in length, and its surface was drilled with threads tapped at various points for measurement mounting purposes. Four of the mounting points were selected to be used to attach four suspension lines connected via springs (with a tensile stiffness of 0.14 N/mm) to a rigid aluminium frame that would act to stabilise the entire handle in a "free" state, and several mounting points on a top surface of the handle were used to attach a reference accelerometer. A

piezoelectric force transducer with a sensitivity of 10.29 mV/lb (PCB Model 208C03) was mounted to the excitation driving point at the lower mid-point of the handle and connected to the shaker via a stinger (the diameter of which is discussed later). Furthermore, two guitar tuner pegs were modified and attached at both ends of the handle to be used for mounting the physical models of the finger later in the study.

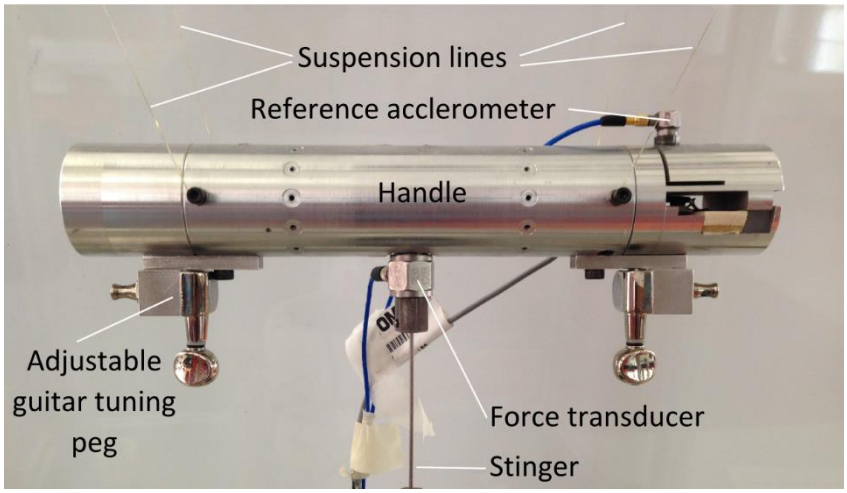

Figure 3.2: Setup of the entire handle including its suspension method

The entire handle was machined at the University of Sheffield. The right end of the handle (see figure 3.3) was designed and instrumented to measure a grip force ranging from 10 N to 50 N in order to control the gripping force of the right index finger and the thumb of the human subjects as well as the physical models. The design used a split cylinder with a full bridge strain gauged beam element (LCL -040), supplied from Omega, using a design as outlined by ISO 10819 1996.

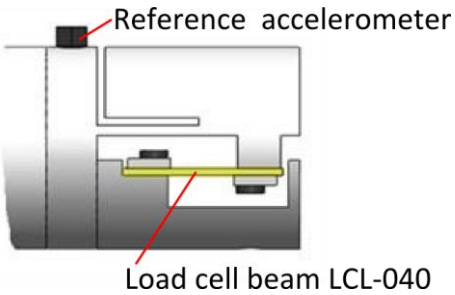

Figure 3.3: Cross-sectional diagram of the instrumented end of the handle

Photos of the handle installed in the vibration test rig can be seen in Figure 3.4.

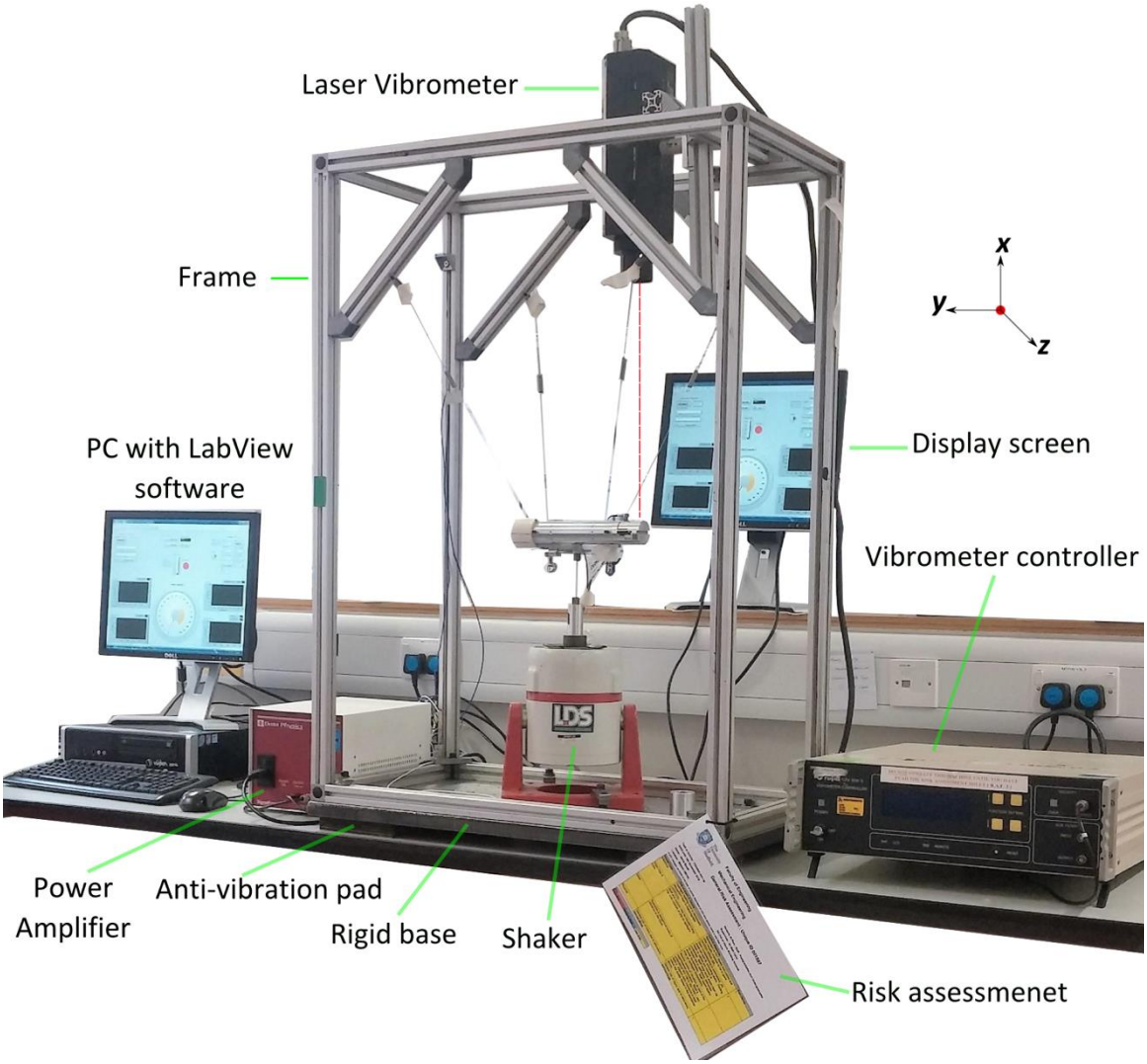

(a)

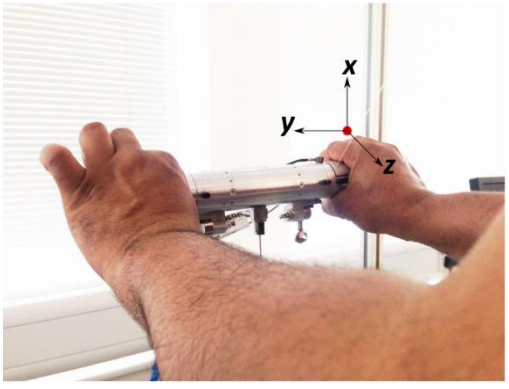

(b)

(c)

Figure 3.4: a) Setup of the entire vibration test rig including vibration excitation system and vibration measuring system; b) Close-up view of the handle being held during a test; c) The standing upright posture maintained during all the vibration testing.

Shaker

The vibration test rig used an electrodynamic exciter (LDS V406, Permanent Magnet Shaker) with a maximum force capability of 196 N to provide a vertical excitation in the *x* direction (see Figures 3.1 and 3.4). The shaker is commonly used to test dynamics of small lightweight components, as it can be used for a wide range of applications. The shaker was firmly attached to a rigid base throughout testing.

The shaker excitation signals were outputted from the desktop computer, via an output NI USB DAQ card, model NI-6002, which provided an analogue input to the shaker power amplifier, as described below.

Power amplifier

The amplifier used in this setup was a SignalForce amplifier, from Data Physics Corporation, with a maximum power of 100 Watts (see Figures 3.1 and 3.4). This amplifier is suitable for driving electrodynamic shakers from all manufacturers and also for different laboratory applications.

Frame and rigid base

In order to suspend the entire handle and for other purposes such as mounting a laser probe, an aluminium alloy strut profile, 30 × 30 mm, was used in order to make a frame (see Figure 3.4). The frame was designed with dimensions of 765 mm width, 420 mm depth and a height of 1060 mm. The frame was then placed on the rigid base, made from a steel plate manufactured with many thread holes that allowed the aligning and mounting of the shaker and the frame, as shown as in Figure 3.4. The design and dimensions of the rigid base are shown in Figure 3.5. The rigid base including the shaker and the frame was isolated from the main table using TICO anti-vibration pads with dimensions of 150 × 185 mm and 25 mm in thickness, one under each corner and one in the middle of the rigid base. This isolation was to ensure that external vibrations would not affect the experiment, and this also had the benefit of reducing the noise produced during experimentation.

The frame and the rigid base (steel plate) were designed and built in the University of Sheffield workshop.

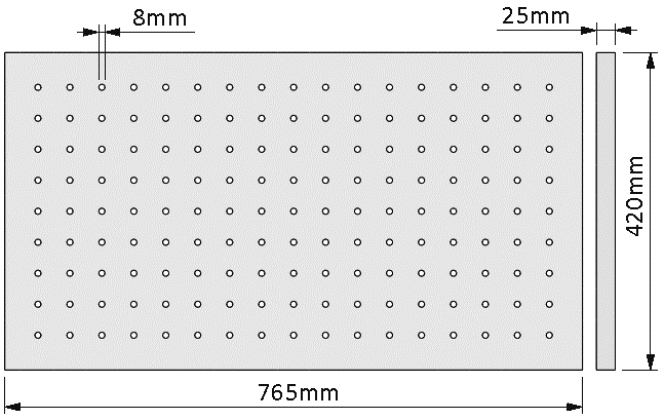

Figure 3.5: 2D drawing showing the dimensions of the rigid base

3.2.2 Dynamic measurement system

In order to measure the dynamics of the system, different models of accelerometers and a laser vibrometer were used as described in more detail below.

Accelerometers

Three different accelerometers were used for measuring vibration transmitted from the handle into the finger. A reference accelerometer was used to measure input excitation and mounted at the right end of the handle, close to the measuring point of the finger. Another similar accelerometer was used for measuring finger excitation with a finger adaptor (described later), whilst small accelerometer was used for measuring vibration across the finger and mounted on the back of the finger. The specifications of these accelerometers are listed in Table 3.1.

Table 3.1: Specifications of accelerometers used for measuring vibration

Model type	Serial number	Sensitivity (mV/g)	Mass (gram)
PCB (353B15)	16699	10.65	2.0
PCB (353B15)	52451	10.30	2.0
Dytran (3224B)	2790	10.19	0.3

Finger adaptor

Because it was difficult to mount an accelerometer between the finger and the handle/or material interfaces, a small finger adaptor was made to fit in between the handle and index finger as a mounting point for the accelerometer (see

Figure 3.6). The design used was similar to that outlined in ISO 5349 2 [12]. A single piezoelectric accelerometer was mounted to the adaptor using adhesive. A rubber strap was to ensure that the adaptor remained attached to the finger throughout testing.

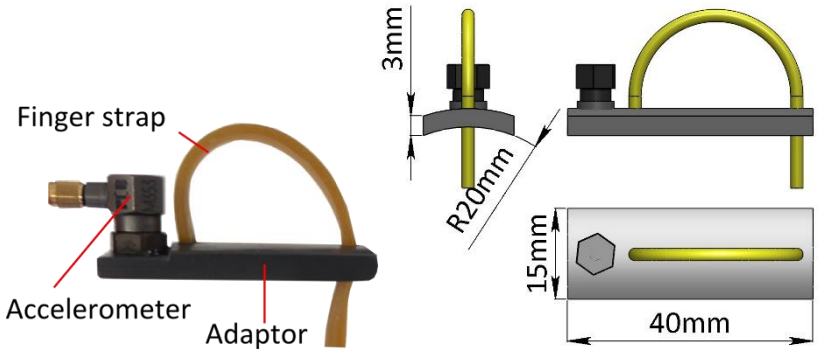

Figure 3.6: The entire finger adaptor including the measuring accelerometer and strap

Table 3.2 shows the properties of the finger adaptor. To reduce the effects of the adaptor, the mass of adaptor including the accelerometer should not exceed 15 g [72], and so the one used in this study had an entire mass of 5.8 g. The curve contour of the adaptor allowed it to fit flush with the bare handle, thus minimising the possible misalignment of the adaptor to the handle during testing.

Table 3.2: The properties of the finger adaptor

Material type	Width (mm)	Mass (gram)	Radius (mm)
Rigid plastic (PVC)	14.8	5.8	20

Laser vibrometer

A laser doppler vibrometer was used in the set-up with a OFV-3001 controller and OFV-303/-353 sensor head. The vibrometer was set up to measure the surface vibrations at the back of the finger, as shown in Figures 3.1 and 3.4. The vibrometer had different sensitivities and its selection depended on the distance between the laser head and the measuring point. It also had a tracking filter built in and was set up in a fast mode that would allow the noise of a measured signal to be reduced. For this set-up, the sensitivity

used was 0.025 m/s/V.

3.2.3 Data acquiring system (DAQ)

The main DAQ system used with the test rig (see Figure 3.1)was a National Instruments NI CompactDAQ USB chassis, model cDAQ-9174 that can integrate many different measurements types such as measuring voltage, and bridge-based sensors, temperature and acceleration into one signal device that outputs all measured data through the same interface. The chassis has a USB connection to the PC and four slots that can be used for four different IN DAQ assistant cards. Three different DAQ cards were used as discussed below:

- An NI 9234 DAQ assistant card (Integrated Electronics Piezo Electric, IEPE) was used to read and record the acceleration data. It had four channels for signal acquisition, with one being used for measuring excitation force, and two for acceleration signals, whilst the fourth one was used for the laser vibrometer signal. The DAQ card had a maximum sample rate of 51.2 kHz. This card was also used for another test, a hammer testing, during system calibration.
- An NI 9237 DAQ was used to measure the grip force data. It had four channels for data acquisition, although only one was used in this setup, and it had a maximum sampling rate of 50 kHz.
- An NI 9211 DAQ card was used to measure temperature via thermocouples. It had four channels with a maximum sampling rate of 14 kHz. This DAQ card was used for measuring room temperature using only one channel and was also used for a glove temperature test using all four channels.

The cDAQ USB chassis was connected to a desktop computer that had LabView software (Version 2014), from National Instruments installed. This allowed the computer to record data supplied by data measuring the DAQ cards used. Another DAQ system was used to provide excitation signals for the shaker (see Figure 3.1) as mentioned earlier in the shaker section.

To obtain a measurement with a high resolution, the LabView program was coded to record only the raw data (including vibration, grip force and temperature) continuously with a maximum sampling rate of 10 kHz and saved as a .tdms file, which is a file that can be used with other software, DIAdem View (NI, Version 2014). This software was

designed to rapidly process large data files. It also contains many useful functions built in for processing, analysis and graphing vibration data such as the Fast Fourier Transform (FFT).

The main LabView programme used in this test rig was coded as a project for producing outputs sinusoidal signals for controlling the shaker, and it had two signal generation functions. One was for producing sequence signals and another for swept signals that could be either in linear or logarithmic scale.

The sequence function used an external .tdms file that was created separately and saved, using another LabView function for generating sequential waveforms before was called to the main LabView program. However, the sweep function could be directly used as it was built into the main LabView program. This allowed direct control of the vibration parameters from the front panel.

The main program was also coded to display and monitor signals measured including excitation force, accelerations and the FFT measured from the output accelerometer as well as the room temperature via the thermocouple and grip force via the force gauge. The front panel was displayed on both the main desktop screen and a secondary screen located in front of the subjects, for monitoring the grip force, as shown in Figure 3.4. The front panel of the main LabView program used in this setup is shown in Figure 3.7.

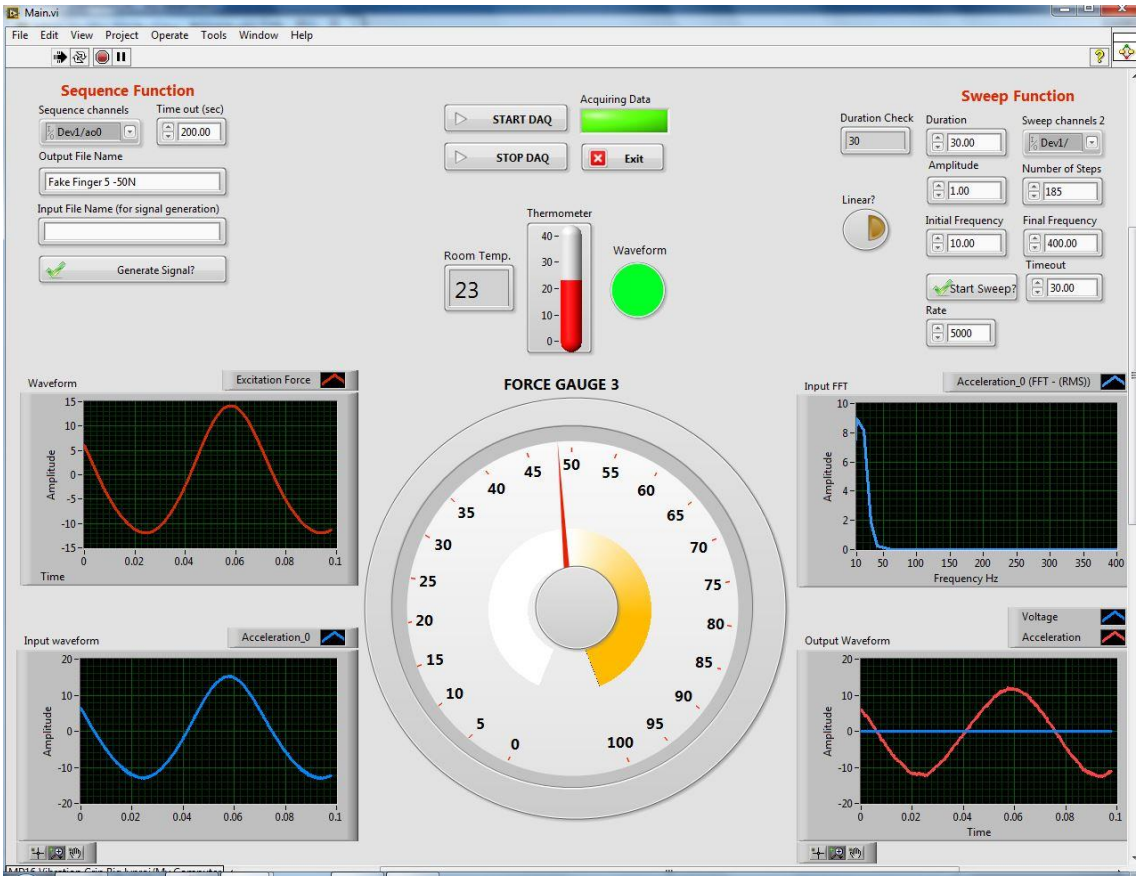

Figure 3.7: Front panel of the main LabView program showing vibration generation functions and display features used in this setup.

3.2.4 Signal processing of the vibrations measurement

Part two of the standard ISO 5349-2[12] states that FFT analysis should use appropriate time windowing, and the Hanning window function is commonly used for continuously operating tools. However, the ISO also suggests that a suitable window function should be considered depending on the vibration characteristics of the tools used [12]. In this study, the vibration measurements were conducted using both the sequence and the swept sinusoidal excitations, and were processed by DIAdem view software. The flow chart diagram of both methods is shown in Figure 3.8.

Sequence sinusoidal vibration

The first step in processing the data obtained using the sinusoidal sequence vibration was to cut the raw data into separate channels that were relevant to the times when an excitation input had been applied to the shaker. In order to minimise the effect of a transient response signal, only the middle section response of measured signal was selected [112].

Next, the FFT with the Hanning window function (as outlined in ISO 5349-2) was applied to each separated signal obtained from both the vibration input and output data. This ensures that the effects of any external noise are reduced.

The maximum peak values obtained from the FFTs were then used to produce one single channel of the maximum responses at each of the frequency inputs. Then, the transmissibility was identified as a ratio of the output response to that of input vibration, with this being the criteria for assessing the finger-transmitted vibration and AV glove materials.

Swept sinusoidal vibration

The LabView program started acquiring data before the vibration inputs had been applied, which allowed the human subjects to maintain the target grip force. Therefore the measured data was then cleaned from any data recorded before and after the vibration spectra had been applied. This process ensures that the effects of random noise outside the spectra are removed. The digital bandpass filter, type Butterworth, was then applied to each of the input and output measured time signals. Due to the limitation of the use of sinusoidal vibration in assessing human vibration, the FFT function was applied with a rectangular window that was considered a suitable window for swept signals, with this being used for processing all the swept vibration signals in this project.

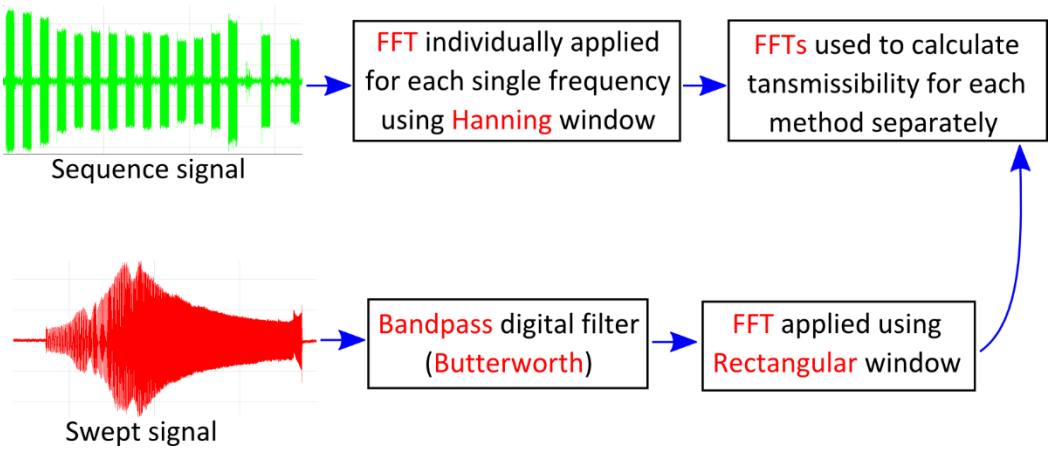

Figure 3.8: Diagram of signal processing of sequence and swept methods used

3.2.5 Transmissibility measurement

Three methods were used for measuring finger-transmitted vibration: one was the use of a novel finger-adaptor, which was used for evaluating the transmissibility of AV glove materials; the second was the miniature accelerometer, which was directly attached to the back of the right index finger (proximal), for measuring the transmissibility across the finger. The third method used was the laser vibrometer, to investigate the effects of the accelerometer mass on finger transmissibility. The three methods are detailed below.

Finger-adaptor method

The purpose of the testing was to measure the transmissibility between the interface of the glove material and the human index finger, as well as the physical model of the finger whilst gripping the handle. Thus the method used for measuring the glove transmissibility was that outlined in the original version of the glove standard ISO 10819 1996 [72]. Because it was difficult to obtain the transmissibility at the same measuring position, with and without the handle being covered, the transmissibility can then be identified indirectly. As an alternative, the result was obtained using two steps. Firstly, the transmissibility of the bare handle (T_{bare}) was identified as follows:

$$T_{bare} = \frac{A_{Fb}}{A_{Hb}} \qquad \textbf{Equation 3.1}$$

where: A_{Fb} is the acceleration of the bare index finger, measured using the "finger-adapter" accelerometer; and A_{Hb} is the acceleration of the handle, measured from the "reference" accelerometer (see Figure 3.9 a).

The transmissibility was then determined for glove materials (T_{glove}) by the following formula:

$$T_{glove} = \frac{A_{Fg}}{A_{Hg}} \qquad \textbf{Equation 3.2}$$

where: A_{Fg} is the acceleration of the gloved index finger, measured from the "finger" accelerometer; and A_{Hg} is the acceleration of the handle, measured from the "reference" accelerometer (see Figure 3.9 b).

Lastly, these two obtained transmissibilities were expressed to gain one corrected transmissibility ($T_{corrected}$) that allowed the removal of any effects that had been caused due to the frequency response of the handle-adapter system. The transmissibility was identified using the formula below:

$$T_{corrected} = \frac{T_{glove}}{T_{bare}} \qquad \textbf{Equation 3.3}$$

This criterion was used for evaluating the transmissibility for the bare handle and the glove materials when the finger-adaptor method was being used.

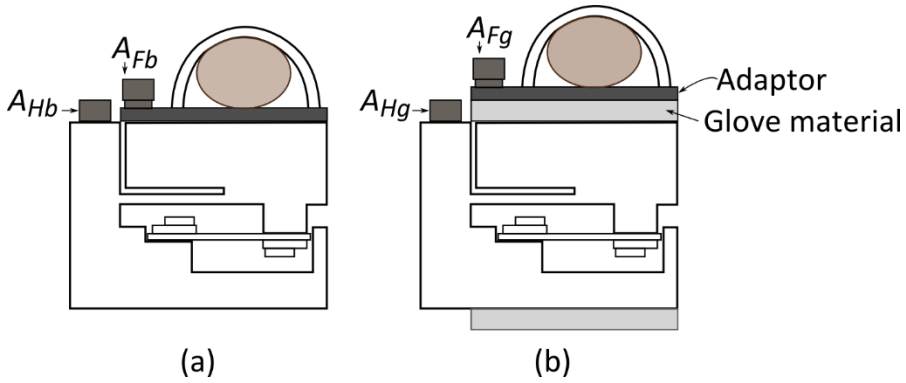

Figure 3.9: cross-sectional drawing showing transmissibility measurement when the finger adaptor method adaptor was used: a) transmissibility measured on the bare handle; b) transmissibility when the handle was being covered by glove material

Back finger method

As the purpose of the measurements was to investigate the transmissibility through the finger (front to back), both with and without wearing the glove, as well as the glove transmissibility, when gripping a handle, this was indirectly measured [65]. First, the transmissibility of the bare handle ($T_{bare\ handle}$) was identified as:

$$T_{bare\ handle} = \frac{A_{output}}{A_{Input}} \qquad \textbf{Equation 3.4}$$

where: A_{output} is the acceleration measured at the surface of the bare handle at the finger measuring position (from the "finger" accelerometer); and A_{input} is the acceleration of the reference accelerometer attached to the handle close to the finger position, as shown in Figure 3.10 a.

The transmissibility across the bare finger ($T_{bare\ finger}$) was then measured by the

following formula:

$$T_{bare\ finger} = \frac{A_{bare\ finger}}{A_{input}} \qquad \textbf{Equation 3.5}$$

where: $A_{bare\ finger}$ is the acceleration measured at the back of the bare finger (from the "finger" accelerometer), as shown in Figure 3.10 b.

The transmissibility through the gloved finger ($T_{gloved\ finger}$) was also measured using Equation 3.6 below:

$$T_{gloved\ finger} = \frac{A_{gloved\ finger}}{A_{input}} \qquad \textbf{Equation 3.6}$$

where: $A_{gloved\ finger}$ is the acceleration measured at the back of the gloved finger (from the "finger" accelerometer), as in Figure 3.10 c.

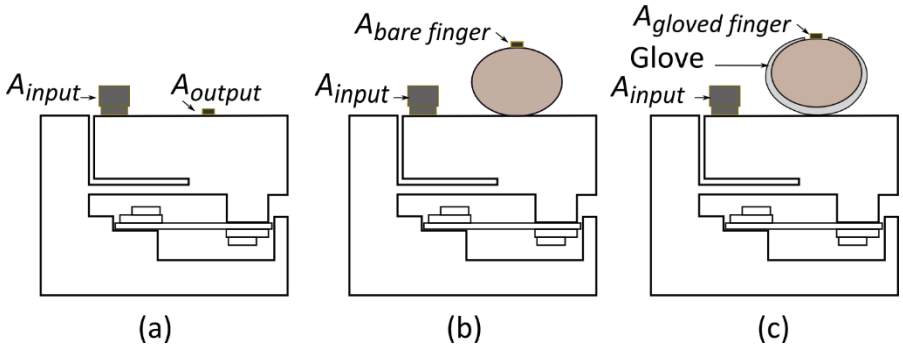

Figure 3.10: Cross-sectional drawing showing transmissibility measurement of finger ; a) transmissibility measured on bare handle; b) transmissibility through the bare finger; c) transmissibility through the finger when wearing a glove

The transmissibilities obtained were expressed in one corrected transmissibility of the finger without and with the glove ($T_{corrected-bare-finger}$ and $T_{corrected-gloved-finger}$), and were calculated using Equations 3.7 and 3.8 below:

$$T_{corrected-bare-\ finger} = \frac{T_{bare\ finger}}{T_{bare\ handle}} \qquad \textbf{Equation 3.7}$$

$$T_{corrected-gloved-finger} = \frac{T_{gloved\ finger}}{T_{bare\ handle}} \qquad \textbf{Equation 3.8}$$

After the corrected transmissibilities of the finger with and without wearing the glove were obtained, the glove transmissibility at the finger (T_{glove}) was measured using the

following formula:

$$T_{glove} = \frac{T_{corrected-gloved-finger}}{T_{corrected-bare-finger}} \qquad \textbf{Equation 3.9}$$

The same criteria were used when the laser vibrometer method was used for measuring the vibration transmissibility at the back of the finger.

3.2.6 Calibration of the grip force system

As the right end of the handle was instrumented to be used in controlling and measuring the grip force applied, it was calibrated using a Mecmesin MDD test stand with a digital force gauge with a maximum force of 500 N (from Mecmesin), and a displacement device (Absolute Digimatic Scale) attached. The instrumented end was detached from the entire handle. However, its signal cable remained connected to the NI 9237 DAQ card as described in Section 3.2.3 above. It was then placed and supported using the V-block, as shown as in Figure 3.11.

Static forces ranging from 0 to 80 N, increments of 10 N were individually applied to the area where the finger would make contact using hemispherical indenter, 20 mm in diameter, attached to the force gauge. All outputs voltage signals were directly read and recorded from the front panel of the main LabView program.

It should be noticed that the displacement measurement device was only used for monitoring the deflection of the strain gauged beam element (LCL -040), which had a deflection limit of 1.27 mm.

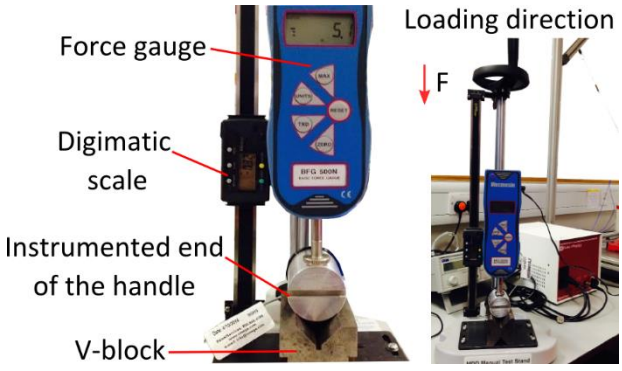

Figure 3.11: Calibration of the grip force system showing the Mecmesin MDD stand and equipment used

All the values measured were used to compare the voltage outputs units applied grip

force in N. The relationship between the force and volt values was found to be linear, as shown as in Figure 3.12.

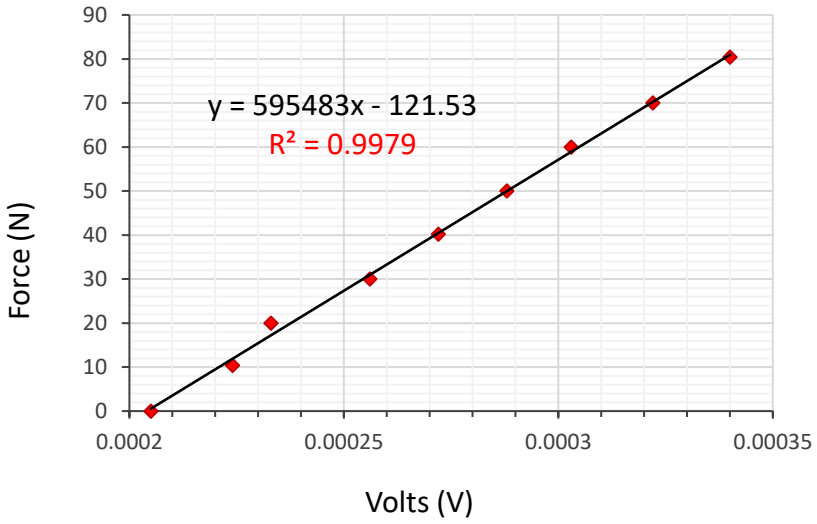

Figure 3.12: Force-volt relationship of the grip force system

The slope and intercept values obtained from this relationship were used to provide a calibration of the force measurement. The R-squared value was found to be close to one, meaning that the strain gauged split cylinder design functioned well to provide a linear response. The calibration equation was used with LabView software to display and record the forces in N.

3.2.7 Dynamic response of the entire system

Methodology

According to the international standard 10918 2013, an ideal handle should not have any resonances within the frequency range of 25-1250 Hz [75]. In order to identify the natural frequencies of the entire handle, the frequency response functions (FRFs) of the system were measured at six positions across the handle length, using an instrumented hammer, from PCB, with a plastic tip and a sensitivity of 2.194 mV/N, and a miniature accelerometer to record the response located at the left end of the handle, from Dytran (model 30302A), with a sensitivity of 10 mV/g and 1.5 grams in mass. The experimental setup of the FRF test was as shown in Figure 3.13.

The FRF values were measured and analysed using a separate LabView code written for this purpose with a sampling rate of 1.024 KHz and 4.096 k samples to read. An exponential window was applied to the signals measured from the response accelerometer, and a force window for the hammer signal, in order to cut any force produced after the maximum force obtained from hitting the surface. Fast Fourier Transforms (FFTs) were calculated using LabView, version 2014 and saved to an Excel file.

To minimize random errors, responses from ten hammer hits were taken for each position. The test was conducted with and without the handle being gripped. It should be noted that the system was designed to operate in only the vertical direction (parallel to the stinger) so only resonances with a significant motion in this direction were considered.

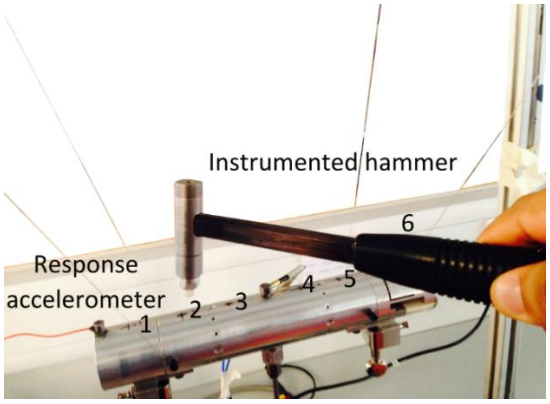

Figure 3.13: Set up for the hammer test

Result and discussion

The FRFs of the handle were calculated using:

$$FRF = \frac{FFT_{output}}{FFT_{input}} \qquad \textbf{Equation 3.10}$$

where: FFT_{output} is the Fast Fourier Function of acceleration measured from the response accelerometer, and FFT_{input} is the Fast Fourier Function of input force measured from the impact hammer.

The FRF test for the entire vibration test rig system was carried out with the FRF data measured at each of six positions, as shown in Figure 3.13. Analysis of the data showed that the dynamic behaviour of the handle including the stinger and the suspension wires had three resonances at low frequencies of 8.2, 17.5 and 38.5 Hz, and no other resonances were shown at high frequencies above up to 600 Hz, as shown in Figure 3.14.

When only the right end of the handle was gripped by the index finger and thumb, the peak heights at all the resonances were reduced presumably due to increased damping from the hands (Figure 3.15). However, the resonance frequency of 38.5 Hz was within the frequency range of interest. It was felt that the stiffness of the stinger could affect the shaker, so in order to examine this potential resonance, the 4 mm stinger was replaced with another stinger, with a diameter of 1.6 mm which was used throughout the remainder of the study. The close view of the two stingers used is shown in Figure 3.16.

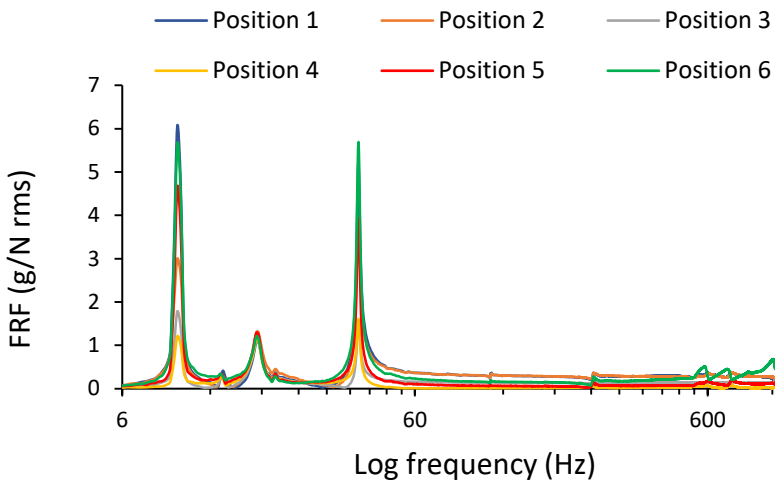

Figure 3.14: Frequency response function FRF for the six positions along the handle when the stinger of 4 mm in diameter was used

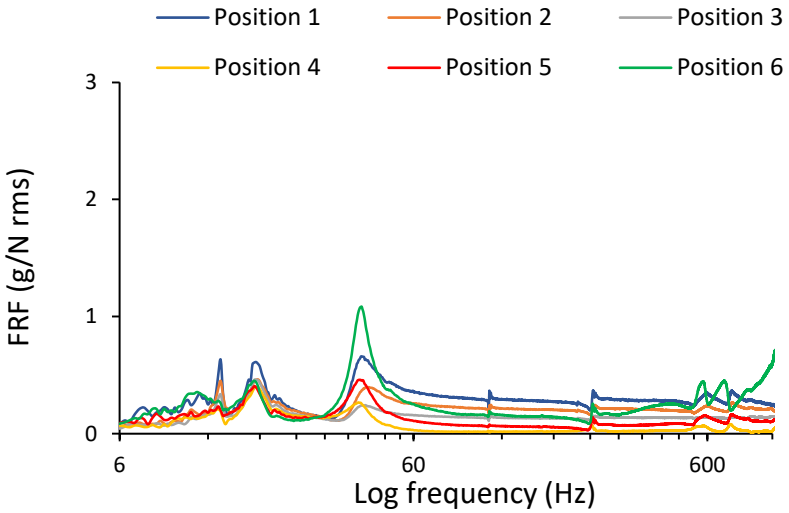

Figure 3.15: Frequency response function FRF for the six positions along the handle when the stinger of 4 mm in diameter was used and the right end was gripped by index finger and thumb

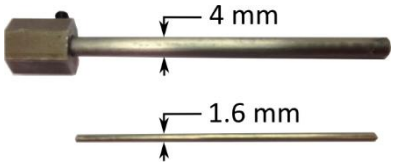

Figure 3.16: Initial stinger (4 mm) and the one being used (1.6 mm) with the vibration test rig

The FRF data measured at each of the six positions showed that the dynamic system of the handle with the new stinger (1.6 mm in diameter) had three resonances at low frequencies (2, 11 and 17 Hz), and no other resonances showed up to a frequency of 550 Hz. (Figure 3.17).

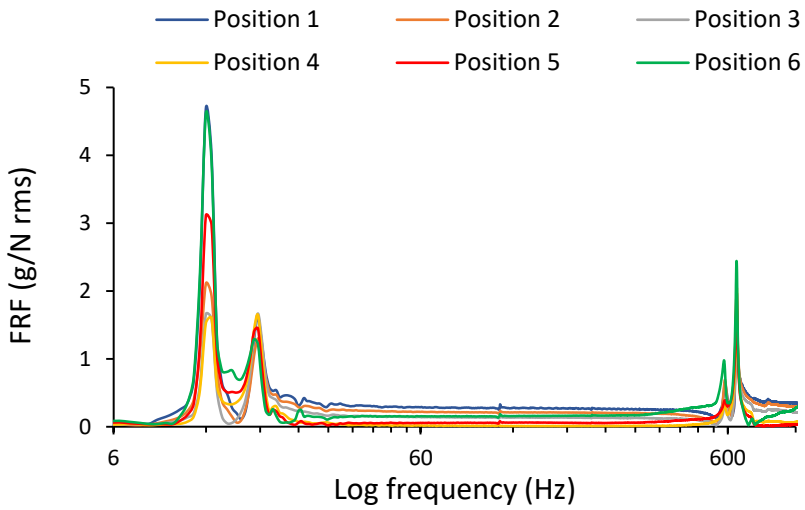

Figure 3.17: Frequency response function FRF for the six positions along the handle when the stinger of 1.6 mm in diameter was used

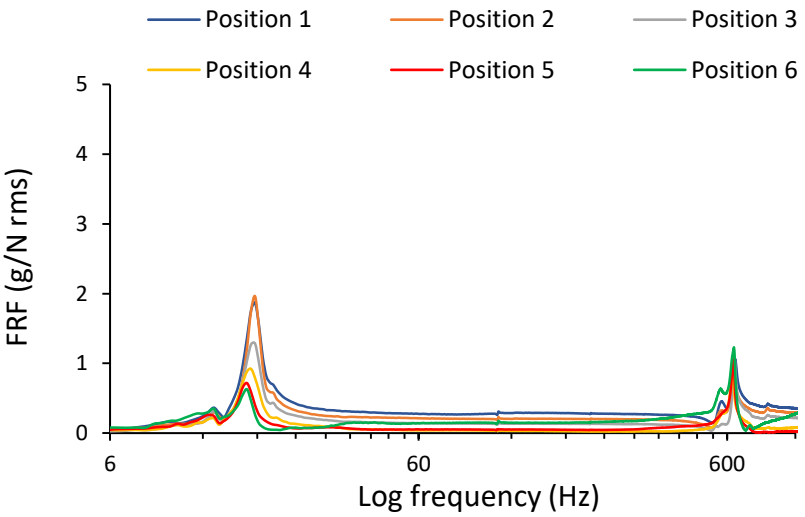

Figure 3.18: Frequency response function FRF for the six positions along the handle when the stinger of 1.6 mm in diameter was used and the right end was gripped by index finger and thumb

At low frequency, the most significant resonance was the one at 11 Hz. For this peak, the FRF magnitudes at the ends (positions 1 and 6) were much higher than that in the middle (positions 3 and 4), which indicated rocking behaviour relative to the shaker connection point. The resonance at the frequency of 17 Hz on the other hand, showed similar amplitudes at all points, indicating a vertical bouncing mode resulting in extension and compression of the stinger. The high-frequency modes above 550 Hz are thought to be flexural modes of the handle dominated by the split-bar section.

When only the right end of the handle was gripped, the peak heights at all the resonances were reduced. This was probably due to increased damping from the hands (see Figure 3.18). The frequencies of the low-frequency modes dropped, reflecting the increase in effective mass from the addition of the hand. The shape of the bouncing mode (near 17 Hz) also changed somewhat with the maximum motion occurring at the free end (position 1) and minimum motion at the gripped end (position 6).

Overall, the findings of this study have led to the conclusion that the new test rig is suitable for measuring vibration transmissibility for HAV research. This is reasonable for testing vibration transmissibility of glove materials at frequencies ranging from 20 Hz to 400 Hz, and this information is of importance to this research, as outlined in the original and revised versions of AV glove standard ISO 10819, 1996, 2013 [72, 75]. Also, most of the hand-held vibrating tools operate within this vibration range and the existing AV gloves are effective at a frequency range beyond 250 Hz only on the palm of the hand, not on the fingers [65].

3.3 Pilot studies

3.3.1 Vibration test rig evaluation under “no hands” condition

Methodology

In order to ensure that the entire vibration test rig was working well, before any large scale studies were conducted, the entire system was tested including the vibration excitations system and the measurement system including vibration, the grip force and room temperature. Two accelerometers were mounted on the right end of the handle: one was used to measure “reference” accelerations, and another was used to measure the accelerations on the split portion of the handle, mounted on the bare handle at the

measuring location of the index finger, using wax as shown as in Figure 3.19 below.

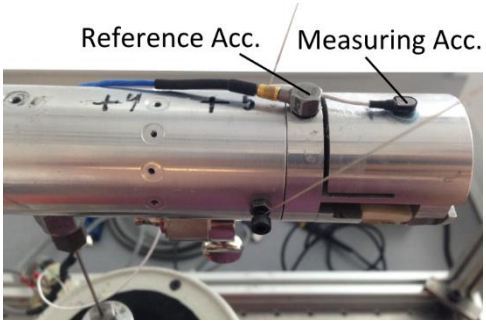

Figure 3.19: Setup of the reference accelerometer (input) and measuring accelerometer (output)

Even though the FRFs showed that the handle has no resonance at frequencies ranging between 20-600 Hz, moving both accelerometers to one end allowed measuring transmissibility even at frequencies below 20 Hz (e.g. 10 Hz). This was also stated in ISO 10819 1996, which recommended testing the transmissibility at low frequencies if necessary [72]. The bare handle was subjected to a swept sinusoidal excitation ranging from 10-400 Hz over 30 sec. The sinusoidal excitations and all the measured signals were produced and gathered using the LabView program as outlined in Section 3.2.3 above. The raw data was then examined using DIAdem view.

Results and discussion

The raw time data obtained showed that the entire system was producing vibration outputs and continuously reading and recording all vibrations signals and the grip forces signal as well as room temperature via a thermocouple.

The LabView program was written to acquire data before the excitation was applied that allowed maintaining the grip target force and to stop acquiring data by selecting “stop” after the vibrations ended (see Figure 3.20). It should be noted that the signal measured from the grip force system responded slightly to vibration behaviour, probably as a result of the inertia of the section of the handle beyond the transducer and the strain gauge beam element. In order to explain this, a power spectral density (PSD) analysis was conducted of the time history of the grip force (see Figure 3.21) measured from the bare handle when exposure to vibration excitation ranged between 10-400 Hz.

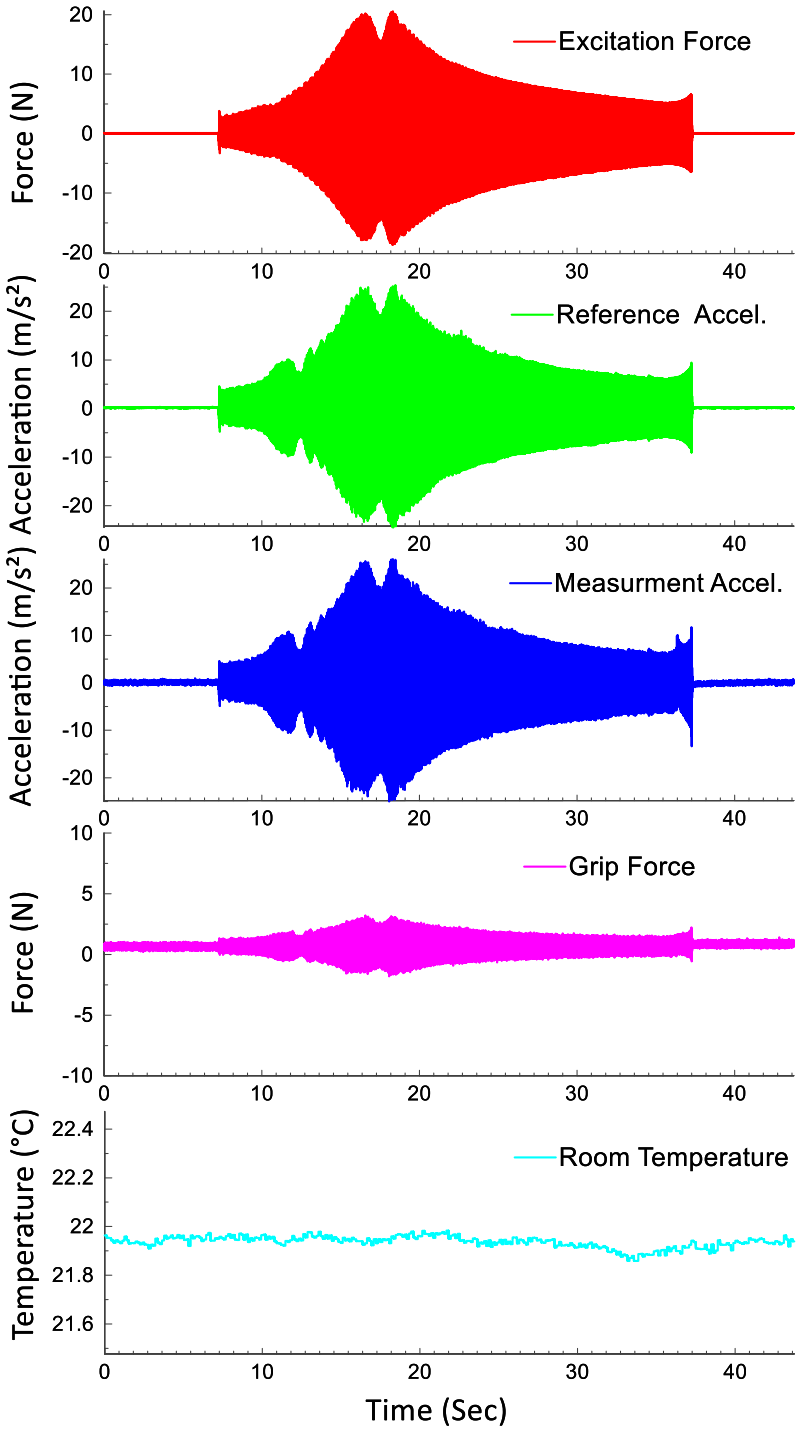

Figure 3.20: Example set of raw data (sampling rate 10 kHz) measured by testing the vibration test rig including the excitation force, accelerations (input and output) and the grip force as well as room temperature.

The PSD showed the power distribution of the grip force over the frequency range which was found to have three peaks at low frequencies (12, 17 and 18.38 Hz) and was higher at 17 Hz (see Figure 3.21). Moreover, the PSD also showed a spike at a frequency of 50

Hz, and at frequencies beyond this and up to 400 Hz the PSD was found to be stable at about zero, thus indicating that the grip force measurement may lead to variations in the transmissibility measurements at low frequencies below 50 Hz.

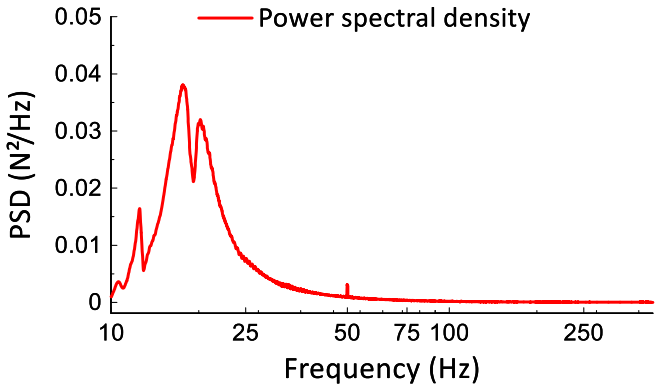

Figure 3.21: PSD of grip force time history measured for the bare handle

3.3.2 Grip force study

Methodology

Since the grip force system was designed to measure the finger grip forces while gripping the vibrating handle, the system was tested under three different grip forces (15, 30 and 50 N) with vibration applied. This pilot study was conducted by the researcher. First, the bare handle was gripped by the index finger and thumb at both ends as shown in Figure 3.22. Next, the grip force of 15 N was maintained and monitored by participant using the display screen as outlined earlier. Then, the handle was subjected to swept vibration as outlined in Section 3.3.1.

To ensure the reliability of the system, the measurement was repeated five times for each of the three grip forces (15, 30 and 50 N).

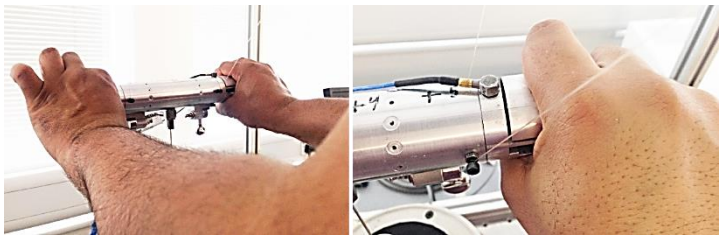

Figure 3.22: Test setup showing the posture of gripping the bare handle and the close-up view of the right end

The grip force system used in this study was different from that outlined in the glove standard ISO 10819 1996, 2013 as this was a new study, which was developed to measure transmissibility across the index finger (proximal), not at the palm along from the arm, as outlined in the standard. The comparison is shown in Figure 3.23.

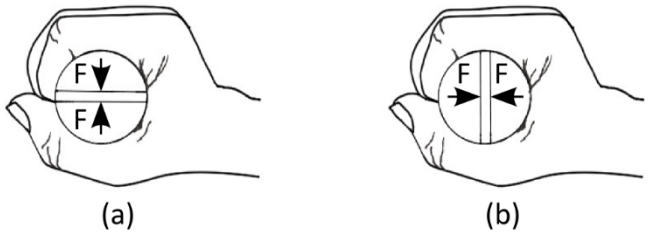

Figure 3.23: (a) Finger-thumb grip force used in this study (b) Palm-fingers grip force outlined in ISO 10819 1996, 2013

Results and discussion

The descriptive statistics of both grip force and temperature measurement were obtained using DIAdem view.

The mean grip force measurement over a frequency range between 10-400 Hz was found to vary among the five repetitions of each grip force (see Table 3.3).

Table 3.3: Descriptive statistics of the mean grip force measurement

Target grip force	15N			30 N			50 N		
Repeat	Mean	SD	CoV (%)	Mean	SD	CoV (%)	Mean	SD	CoV (%)
1	15.60	2.03	13.00	30.49	2.23	7.33	47.58	3.31	6.96
2	14.52	2.16	14.88	30.51	2.54	8.32	49.83	3.40	6.83
3	15.19	2.04	13.44	30.33	2.54	8.38	49.00	3.02	6.16
4	15.78	2.91	18.46	29.91	2.50	8.35	49.25	3.20	6.50
5	15.45	2.31	14.94	30.37	2.28	7.51	48.24	2.99	6.20
Mean	**15.31**	**2.29**	**14.96**	**30.32**	**2.42**	**7.98**	**48.78**	**3.19**	**6.53**

The mean, standard deviations and coefficient of variation (CoV %) calculated from all five measurements showed that the variance in grip forces measured at 15 and 30 N was found to be within the range whilst the grip force of 50 N was unreachable for all five tests. This indicates that maintaining the grip force of 50 N might be difficult to reach by different subjects. However, the coefficient of variation obtained showed that the grip force measurement at 50 N was found to have less variation (6.53 %) when compared with that measured at 30 N (7.98 %) and 15 N (14.96 %), thus indicating that the variation in grip force measurement of the finger-thumb system decreases as grip force is increased.

The mean and SD for ambient temperature of the lab was measured by a thermocouple for all tests and found to be 21.61 ˚C (0.04)

3.3.3 Investigation of the effects of an accelerometer mass on finger vibrations

In order to study the vibration transmitted throughout the finger (front to back), a small accelerometer was used and the effects of its mass on finger transmitted vibration was investigated using two different techniques: finite element modelling and laser vibrometer as follows:

Two-Dimensional Finite Element model (2D-FE) of proximal index finger

Methodology

FE model:

The finger segment was considered to be composed layers representing the skin (including epidermis and dermis), subcutaneous tissue and bone, as shown in Figure 3.24. The cross-sections of both the finger itself and the bone were considered circular, with external diameters of 20 and 8 mm respectively, while their centroids were offset by 4.27 mm [24, 113-115]. This offset resulted in the subcutaneous tissue having an asymmetric thickness around the bone. The skin however, was considered to have a constant thickness of 0.8 mm [58, 116].

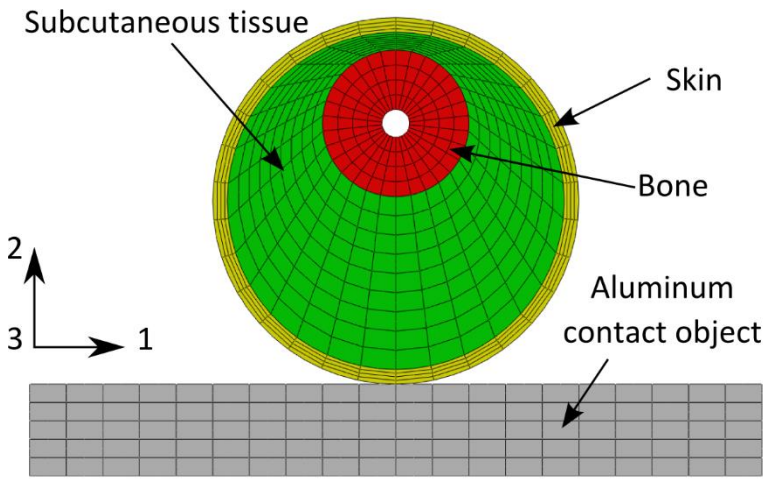

Figure 3.24: 2D finite element model of an index finger proximal in contact with an aluminium plate

In this study, the finger was pressed against a rigid surface and the response to sinusoidal excitation over a range of frequencies obtained at the accelerometer location. The rigid surface was assumed to be aluminium and the contact between it and the skin layer was considered frictionless.

As motion across the diameter of the finger was of primary interest, the model consisted of a 2D slice of the finger. Quadratic plane-strain elements (element type: CPE8R) were utilised in the mesh and analysis was conducted using the commercial software Abaqus (version 6.13).

Material properties used in the model are summarised in Table 3.4. Both the bone and the aluminium surface were assumed to display isotropic, elastic behaviour. The soft tissues were considered to have linear hyperelastic and linear viscoelastic behaviour. The linear hyperelastic material is a type of constitutive model for elastic material for which the stress and strain relationship derives from a strain energy potential function (Neo-Hooke) whilst the linear viscoelastic material is that for which there is a linear relationship between stress and strain at any given time.

Table 3.4: Material properties used in modelling [58, 115-118]

Material	Density	Long term Young's modulus	Poisson's ratio	Structural damping
	kg/m^3	Pa		
Aluminium	2700	70×10^9	0.33	0.0
Bone	1800	1.5×10^9	0.33	0.0
Skin	1000	1.0×10^5	0.48	0.6
Subcutaneous tissue	1000	3.4×10^4	0.48	0.6

For the soft tissues, the hyperelastic (NeoHooke potential) and viscoelastic (Prony series[119]) material parameters are shown in Tables 3.5 and 3.6 [116] and were based on data obtained from published experimental work by fitting constitutive models to stress/strain and stress relaxation curves [119, 120].

Table 3.5: Hyperelastic and viscoelastic parameters for the skin

i	C_{10i} (MPa)$^{-1}$	D_{1i} (MPa)$^{-1}$	g_i	τ_i (s)
1	0.01689	2.4	0.0864	0.2136
2	0.0	0.0	0.2136	8.854

Table 3.6: Hyperelastic and viscoelastic parameters for the subcutaneous tissue

i	C_{10i} (MPa)$^{-1}$	D_{1i} (MPa)$^{-1}$	g_i	τ_i (s)
1	0.005743	7.059	0.2566	0.3834
2	0.0	0.0	0.2225	4.6731

The viscoelastic damping arising from these models is relatively low, with loss factors below 0.01 in the frequency range of interest, as they were originally developed for studying creep rather than vibration behaviour. To account for over the frequency range (10-400 Hz), structural damping was considered in this FE model for the skin and the subcutaneous tissue and ignored for bone and aluminium in this FE model (see Tables 3.5 and 3.6).

Simulation procedure:

In order to generate the frequency response of the finger pressed against a vibrating surface, the procedure was conducted in two steps.

The first step involved a finite-strain, quasi-static analysis in which the nodes at the centre of the bone were pressed by applying a concentrated force of 0.1 N that allowed the nodes moving 2 mm towards the rigid surface. This was in order to obtain the static deformation behaviour of the finger model. In this static analysis, the geometry and material nonlinearities were considered, as the model consisted of three different layers.

The second step was a steady-state, frequency domain analysis using infinitesimal strain assumptions starting from the state reached at the end of the first step. In this step, the rigid surface was assumed to oscillate over a frequency range from 10 to 400 Hz. The output from this step was the transmissibility at the location of the finger-mounted accelerometer with reference to the handle.

In the physical experiment, the mass of the accelerometer is 0.3 grams. In the 2D simulation where the cross-section depth used was 1 mm, the accelerometer mass therefore represented as a point mass of 0.06 grams that added to the outer top point of the skin layer.

Result and discussion

Frequency analysis of the model

The transmissibility measurement shows the dynamic response of the finger without and with the mass added (see Figure 3.25). The results showed that the FE model has a major resonance around 112 Hz. It can be seen that adding a small mass does not affect the transmissibility at frequency ranging from 10-400 Hz.

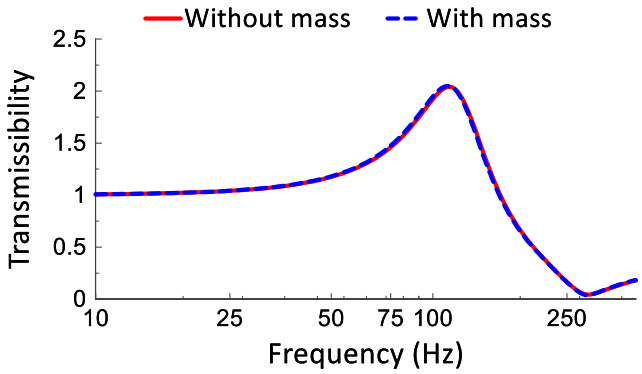

Figure 3.25: Transmissibility of measurement obtained from finite element model of the finger showing the effect of adding a small point mass (accelerometer mass) on the finger vibration response.

Measuring finger transmissibility using laser vibrometer and small accelerometer

Since the aim of this study was to investigate experimentally the transmissibility through the finger (front to back), using a small accelerometer (Dytran, 0.3 grams), the effect of the use of an accelerometer on the finger vibrations was further studied using a single axis laser vibrometer, and (its specifications were outlined earlier in Section 3.2.2

Methodology

The measurement was conducted using a small accelerometer, followed by measurement carried out with the usage of the laser vibrometer (see Figure 3.26). For each measuring method, the measurement was conducted under three different grip forces: 15, 30 and 50 N. Before testing the finger measurement, the transmissibility was first measured on the surface of the bare handle, as mentioned earlier, for evaluation purposes (see Figure 3.19). The small accelerometer was attached to the back of the index finger (proximal), using double-sided tape and the accelerometer's wire was secured using tape, as shown in Figure 3.26 (a). Then, the human subject was asked to grip the handle at both ends and apply the grip target force before the handle was finally subjected to swept vibration excitation ranging from 10 to 400 Hz, as outlined in Section 3.3.1.

There is established evidence by (Laszlo et al., 2011) on the transmission of vibration through gloves: effects of push force, vibration magnitude and inter-subject variability, which suggested that the inter-subject variability (coefficient of variance) increases as the vibration magnitude is increased [121]. Also, due to the limitations in finger-transmitted vibrations, this project used a new method to gain a better understating how finger-transmitted vibration can be affected by different factors, including anthropometry, skin characterisation and behaviour under loading. Therefore, only vibration magnitude of 5 ms-2 rms was for assessing aspects might affect the finger-transmitted vibration.

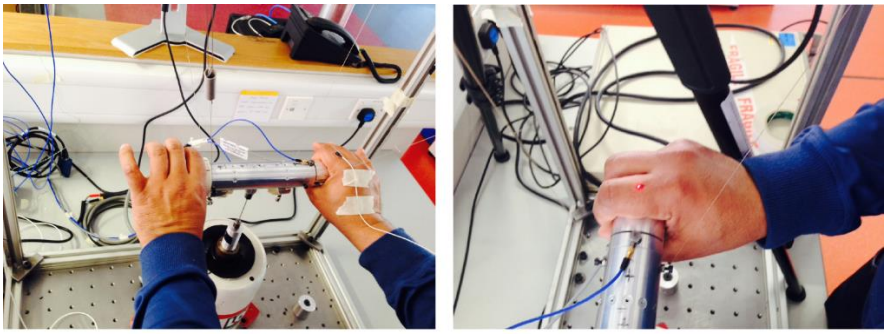

(a) (b)

Figure 3.26: The set-up of transmissibility measurement: a) when measured using an accelerometer method; b) when a single axis laser vibrometer was being used

For the laser measurement, it was difficult to obtain an accurate measurement, due to the sensitivity of the laser sensor and the nature of the handle which had free suspended ends. It should be noted that all pre-testing in this study used the project researcher as the testing subject. Once the subject was comfortable, to obtain better results under the vibration range at all grip force levels, the laser vibrations were measured to be evaluated and compared with those measured by the accelerometer. The velocity signal (V) measured using the laser was then converted, in the frequency domain (f), to an acceleration signal (A) using the formula (A=$2\pi fV \approx 6.28fV$) before it was used for transmissibility evaluation. Since the frame suspended the laser sensor, the transmissibility between the handle and the laser sensor was also measured to investigate the effect of external vibration on the laser measurement. This was conducted by attaching the small accelerometer onto the top surface of the laser sensor as a response accelerometer (output) while the reference accelerometer (input) remained connected to the handle surface, as shown in. The transmissibility was then evaluated using Equations 3.4, 3.5 and 3.6, as outlined earlier in Section 3.2.3 .

Results and discussion

Transmissibility obtained from both methods showed the finger had resonance around the same frequency and increased as the grip force increased (see Figure 3.27). At a grip force of 15 N, the vibration behaviour was similar at frequencies below 150 Hz, and differences in behaviour emerged as the grip force increased.

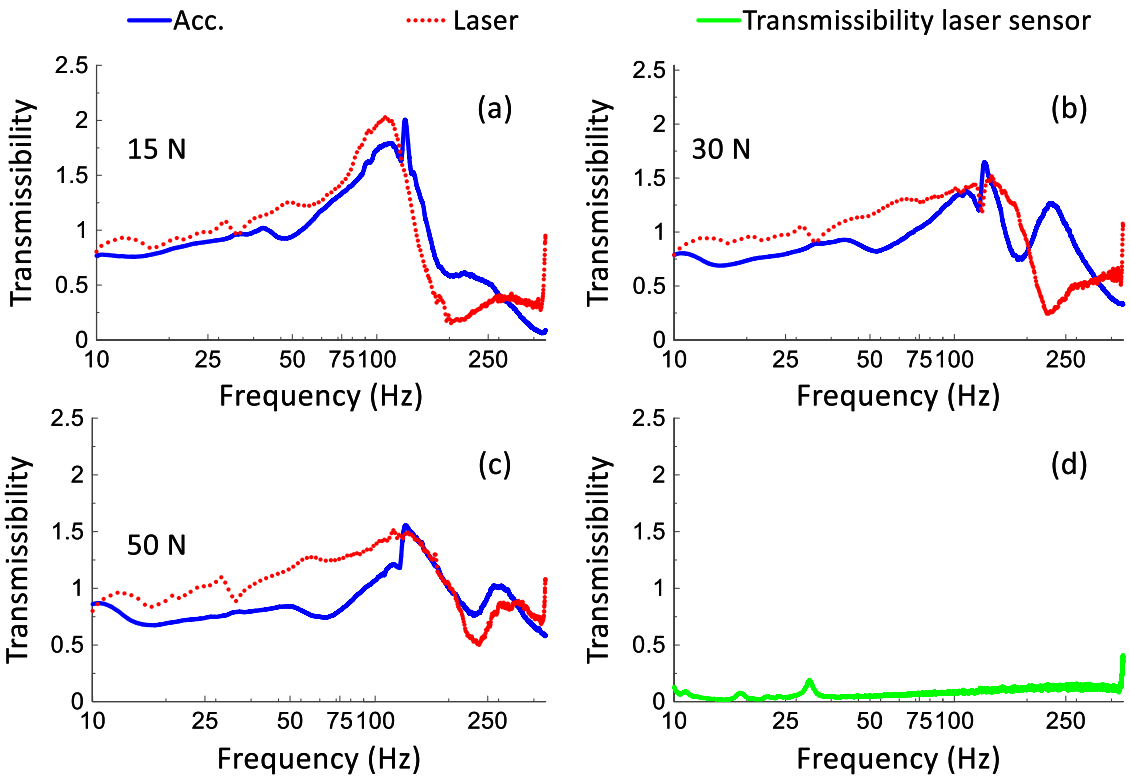

Figure 3.27: Transmissibility measurement through the human right index finger (proximal) when measured using a small accelerometer (0.3 grams) and laser vibrometer and transmissibility measured from the laser sensor investigating how the laser measurement can be affected by dynamic response of the entire vibration system.

Due to the use of the tape in mounting the accelerometer, some restrictions and damping were added to the split handle, which may also have decreased the unevenness to the vibration distribution on the handle [65].

The results showed that using such a small accelerometer attached to the right index finger (back) did not have a significant effect on the resonance frequency of the finger.

Comparing the transmissibility obtained from the FE model with human testing obtained when the laser-accelerometer method was used, both showed a resonance at a frequency ranging between 100-120 Hz. The effect of adding a small mass of accelerometer did not significantly affect the dynamic response of the finger, especially when the grip force of 15 N was applied. However, the resonance frequency increased with grip force, and also the vibration response measured from the laser and the accelerometer was not the same. This is probably due to the limitations of using the laser vibrometer [69] as it was found to be a challenge to obtain the laser measurement at the same point along with maintaining the target grip force.

A pilot study on finger transmitted vibration measurement

Before the large scale of the human vibration measurement was conducted, the test rig and the methodology were tested in this pilot study to check the reliability of measurement using this newly developed test rig.

Methodology

The transmissibility was measured throughout the right index finger (front to back), using the small accelerometer. In order to select the right position for mounting the accelerometer, the human subject was asked to grip the handle using the index finger and the thumb, with the proximal finger being horizontally positioned with the handle. Then, the alignment point with respect to the reference accelerometer was marked, using a pen, and the mounting position was selected as the centre point of the back surface of the finger, as shown in Figure 3.28.

Figure 3.28: Close-up view of the Dytran accelerometer attached to the back of the right index finger (proximal) after being aligned with the reference accelerometer connected to the handle.

The AV glove used for this testing had a section of material removed to allow accelerometer positioning (see Figure 3.29 a)

(a) (b)

Figure 3.29: Close-up view of the gloved hand: a) position of the accelerometer when wearing an AV glove; b) the gloved right hand gripping the handle.

The transmissibility was measured for the bare handle (see Figure 3.19), the ungloved and gloved finger. These measured transmissibilities were finally used for assessing the AV glove. The measurements were conducted using swept vibrations ranging from 10 to 400 Hz, as outlined earlier in Section 3.3.1 above, and different grip forces (15, 30 and 50 N). Each of the test parameters of six (15, 30 and 50 N, with and without wearing a glove) was measured five times, and the mean of measured transmissibilities was also calculated each time. The evaluation of transmissibility measurement was detailed earlier (see Section 3.2.5 , back finger method).

Results and discussion

Figure 3.30 shows the vibration transmissibility and phase angles measured on the surface of the bare handle. The magnitudes generally ranged from 0.99 to 1.1, and phase angles generally ranged from -2.11 ° to 1.04 °. The vibrations at all the points were very similar at frequencies below 300 Hz and very slightly increased as frequency increased. However, they were generally within the very acceptable range, as the magnitudes average was found to be 1.02. This increase was suggested as a reason for the major resonance of the handle which was found to be around 550 Hz (see Section 3.2.7).

Figure 3.31 shows the vibration transmissibility of the bare (ungloved) and the gloved index finger at grip levels of 15, 30 and 50 N, together with their mean values. The results showed how the transmissibility could vary within one subject.

The results also showed the consistency in the transmissibility behaviour at frequencies below 100 Hz at all grip forces. The peak transmissibility magnitude was higher when the finger was gloved than for the ungloved finger.

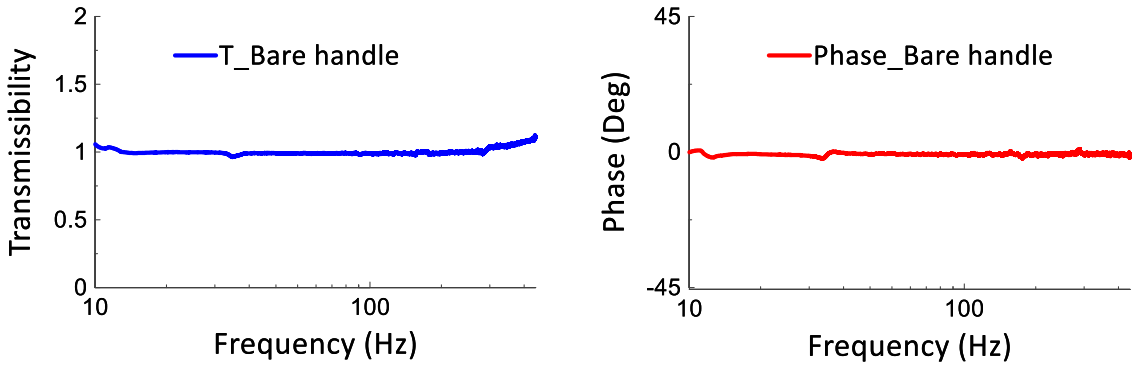

Figure 3.30: Vibration transmissibility measured on the surface of the bare handle

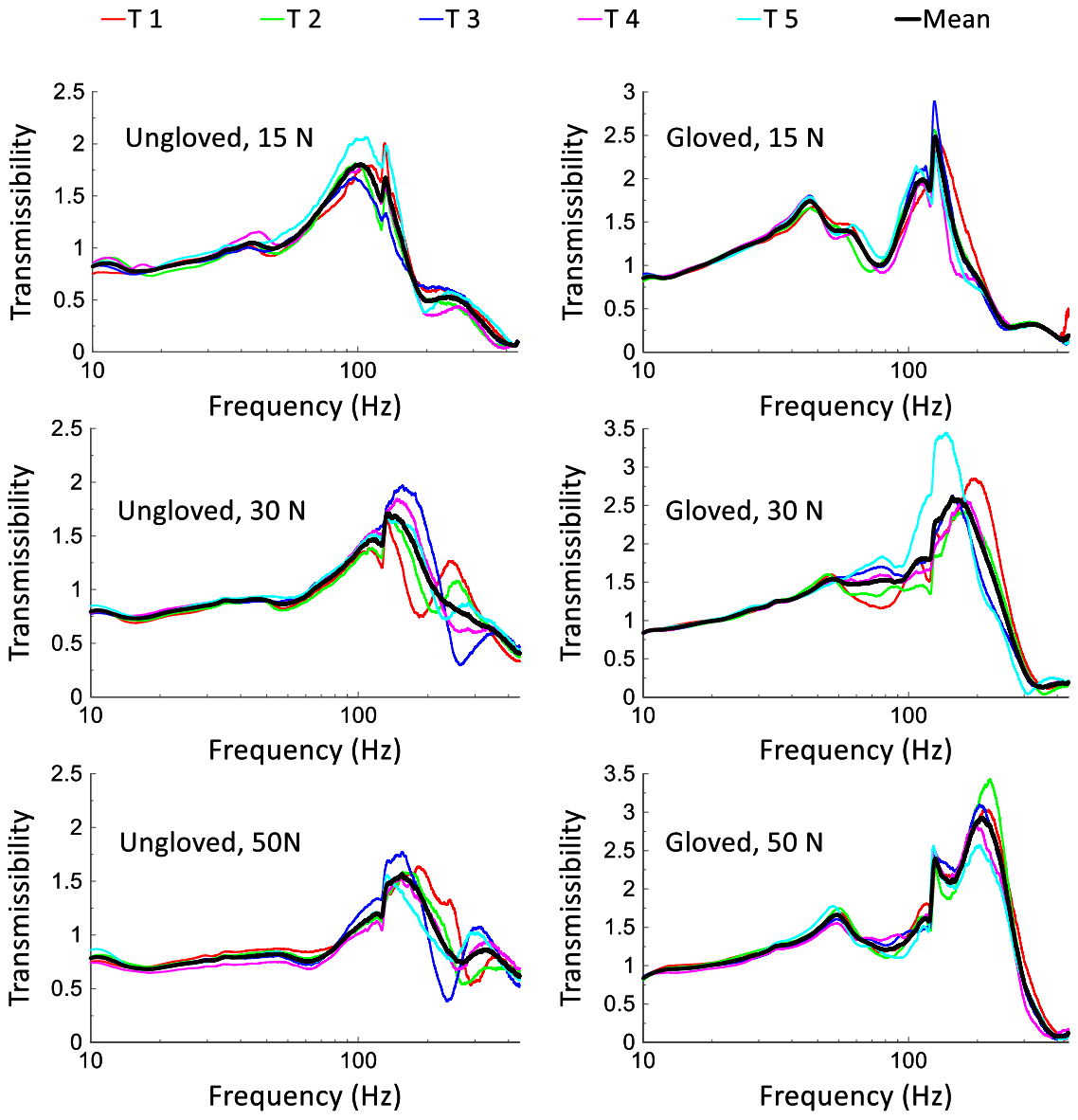

Figure 3.31: Transmissibility measurement of both ungloved and gloved index finger under grip forces of 15, 30 and 50 N, for one subject with 5 repeats.

In order to investigate the effect of the dynamic response of the grip force system on grip force measurements, which is suggested as one factor that affects transmissibility measurement, the power spectral density (PSD) of the grip force time history was calculated (see Figure 3.32) for each of five repeats that were measured along with the transmissibility. The PSD results obtained from all five repeats showed a similar grip force distribution to that measured from the bare handle (see Figure 3.21), over a frequency spectral range between 10-400 Hz.

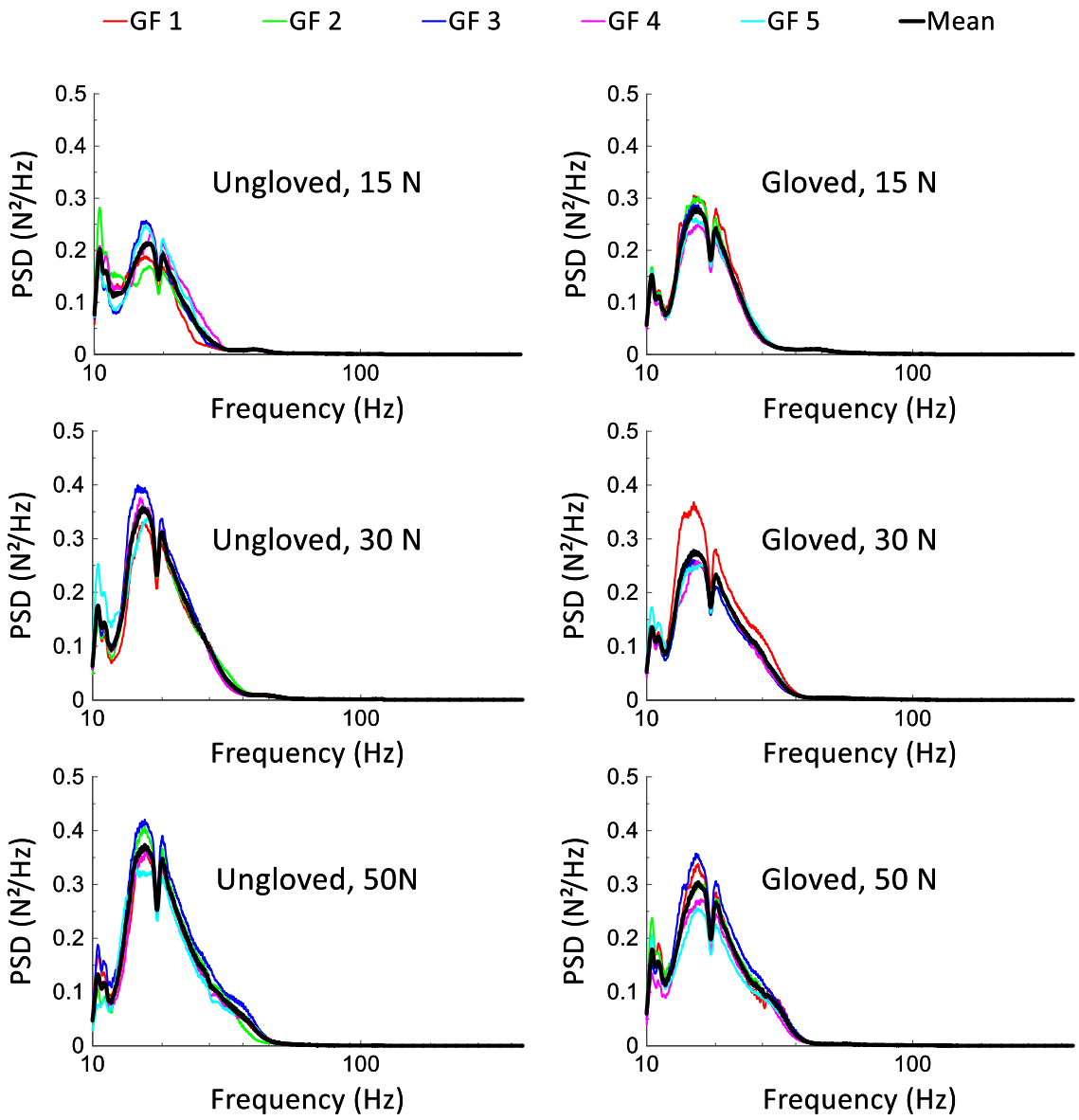

Figure 3.32: Power spectral density of grip force time history of both ungloved and gloved index finger under grip forces of 15, 30 and 50 N, for one subject with 5 repeats.

The results showed that the PSDs were found to have three peaks at frequencies below 50 Hz (12, 17 and 18.38 Hz). However, at frequencies beyond this, the PSDs were found to be consistent at about a magnitude of zero, thus indicating that the transmissibility might only be affected by the grip force at low frequencies. Moreover, in both cases (gloved and ungloved fingers), the PSDs increased with the grip force. However, the increase was significant between 15 and 30 N, whilst the PSDs were found to have slightly increased at 50 N. In addition, the PSDs were higher when the glove was not worn than for the gloved finger.

For the glove transmissibility, it was found that the AV gloved test shows another resonance frequency, of around 60 Hz, and increased as the grip force increased. This result showed agreement with the results from the previous study that examined the transmissibility of AV gloves at the same position using the laser vibrometer [65].

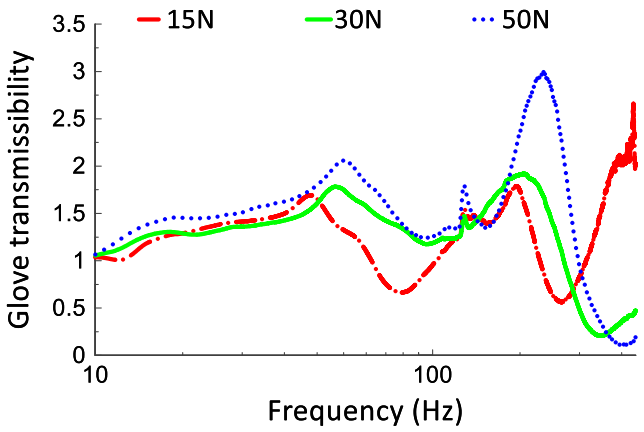

Figure 3.33: Transmissibility of the AV gloved test used in the study.

3.4 Conclusion

This chapter introduced the development of a new test rig for measuring finger vibration when gripping a handle, which allows vibration to be measured over a range of different frequencies under different grip levels. The frequency response function (FRF) testing showed that the system is suitable for testing in the frequency ranging from 20 to 400 Hz. There are no system resonances close to this range. The grip force testing showed the capability of the system in measuring the grip forces with vibration applied, as well

as monitoring the ambient temperature while each test was being conducted.

The 2D finite element model and experimental pilot studies using the laser vibrometer and the small accelerometer allowed the prediction of resonance frequencies of the proximal finger and how the finger vibration may affect when the accelerometer used. Finally the system was found to be able to measure the effect of wearing an AV glove on vibration transmissibility

Chapter 4: Human participant measurements

Since the main aim of this study was to develop a new artificial finger model for assessing transmitted vibrations, the next stage of the study was to carry out a set of different measurements of the right hand and index finger for evaluation and validation purposes. Firstly, anthropometric measurements were carried out using either existing, modified or developed techniques. Secondly, skin characterisation measurements were conducted using Cutometer and Corneometer devices. This was followed by load-deflection measurements of the finger using a modified indentation test rig. Finally, a set of finger transmitted vibration measurements were carried out under different excitation conditions, with and without a glove

4.1 Introduction

Many of the studies regarding HAVS research have conducted hand measurements in order to examine the effects of anatomical differences. Hand size is the key measurable factor associated with hand-transmitted vibrations, especially when assessing anti-vibration gloves, as it allows the researchers to determine the right size of gloves. However, most of the studies considered basic hand dimensions based on the method outlined in British Standard BS EN 420:2003 [122]. The international standard ISO 5349-1: 2001 states that in addition to vibration magnitude, frequency and duration, the hand-transmitted vibration could be influenced by many factors including age, hand or body temperature, and diseases that affect blood circulation [64].

Based on the existing literature, the main aim of the work presented in this chapter is to measure many different parameters of the human hand-finger system including anthropometrics, skin characteristics and stiffness response to loading. Also, vibration measurement of the right index finger was carried out to investigate the related factors that could affect the nature of finger-transmitted vibration. The obtained data would help to provide a better understanding of the factors involved in HAVS and could also be used for evaluation and validation of the physical models developed later.

4.2 Methodology

4.2.1 Participants and consent

Before the human participants were recruited, the experimental design and testing procedures were reviewed and approved by the Research Ethics Committee at the University of Sheffield (refer to Appendix A1 and A2). Participants from the University of Sheffield with no health disorders were invited via the university mailing list and direct conversation with department colleagues and academic staff. As a result, eleven students and academic staff from the University of Sheffield and six technicians working within the Faculty's workshop took part in the test. Therefore, the technician's group involved five people aged 41 to 61 and the non-technicians group involved 12 people aged 21 to 46. There were only two inclusion criteria for taking part in the study: participants should be male individuals and with no known hand disorder.

4.2.2 Collection of measurement

The participants who agreed to take part in the study were invited to the Human Interactions laboratory in the University of Sheffield one at a time. On arrival at the lab, each participant was given an information sheet and a consent form (refer to Appendix A3). The participant was given time to read the information sheet and then briefed about the measurement procedure and also about the objectives of the study. All participants were informed that they were allowed to stop the study at any time if they felt uncomfortable in any way. They were also given the freedom to decide whether they intended to participate in the study and those who agreed were asked to sign the consent form. Before starting, each participant was asked a set of questions in order to collect the following information: age, weight, height and whether they had regular exposure to hand vibrations (refer to Appendix A4).

Once this information was gathered, the measurement procedure began. Figure 4.1 illustrates the design of the experiment, the category and the order of taking all measurements performed in the study.

Despite three of the participants being left handed, all measurements and testing were carried out on the right hand. This is because the majority of hand-held vibrating tools need

two handles to control them, which means that both hands may be affected by vibration exposure.

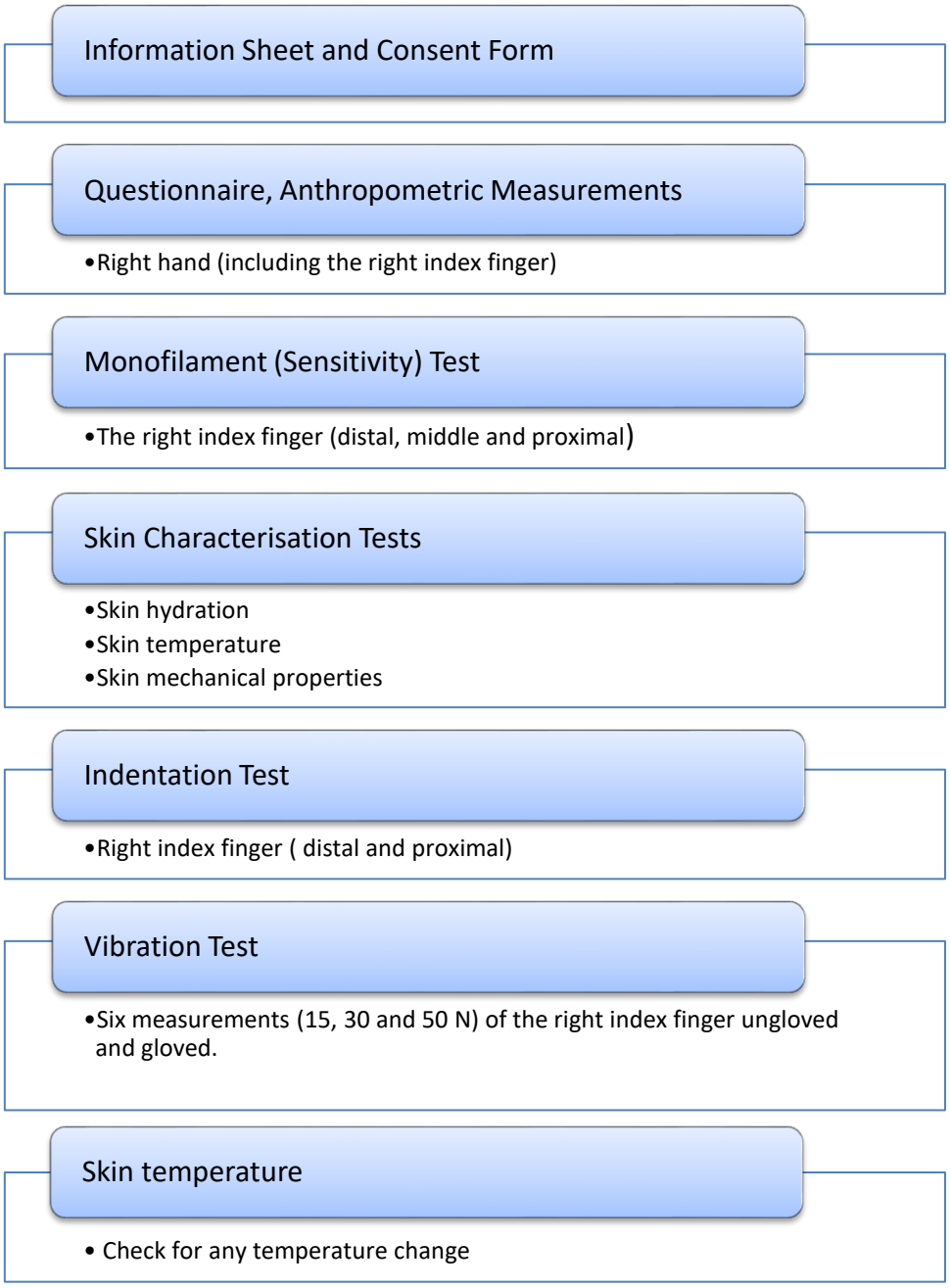

Figure 4.1: Order and category of measurements conducted in this study

The procedures of measurements are described in more detail below in relation to their category and order.

4.2.3 Anthropometric measurements

The procedures for measuring each dimension are based on the descriptions of British Standard BS EN 420:2003 [122], Hall et al. [123] and Jee et al. [124], with some adjustments made. The procedure for each measurement is explained in detail to allow repetition. The dimensions that were considered necessary to be measured are shown in Figure 4.2.

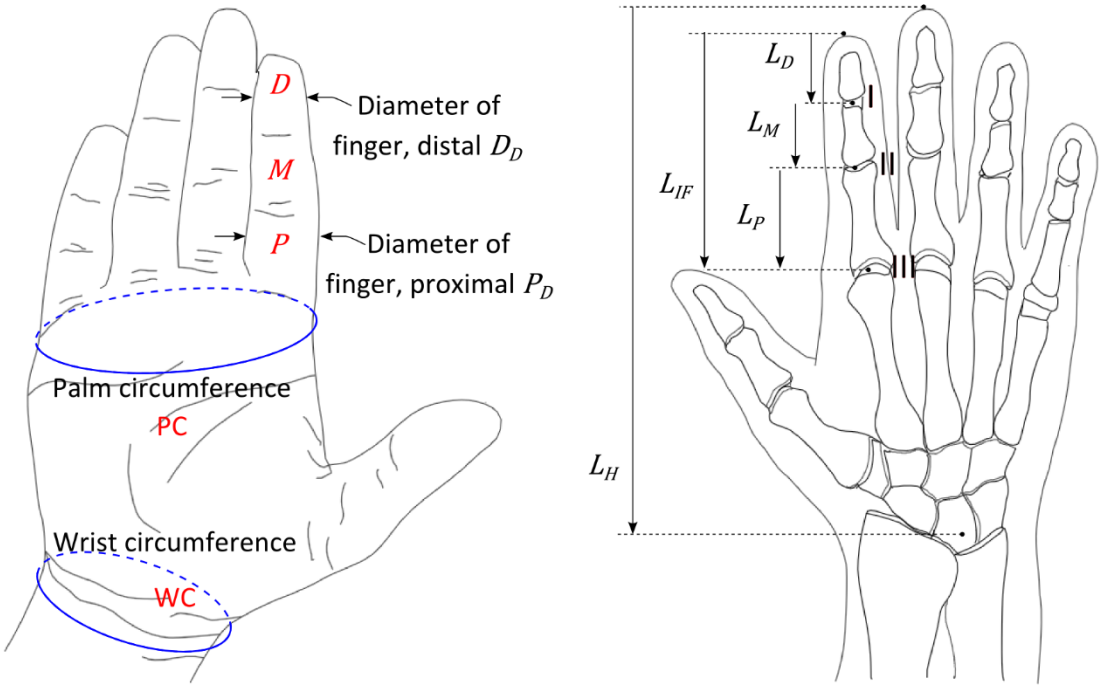

L_D, L_M, L_P= Length of distal, middle and proximal phalanxes of index finger, L_{IF} = Length of index finger. I, II = Distal and proximal interphalangeal joints, III= Metacarpophalangeal joint of index finger and L_H= Hand length.

Figure 4.2: Anthropometric dimensions for hand and index finger to be measured

Index finger length

The length of the index finger (L_{IF}) was measured as the distance from the fingertip to the metacarpophalangeal joint of the index finger (see Figure 4.2), using a ruler with a length of 15 cm, which was found to be more practical than a measuring tape. Participants were asked to place their fingers at the edge of the table (see Figure 4.3), so that the joint was more visible. They were also asked to stretch their finger in order for it to be parallel to the table. A ruler was placed above their finger and the distance from their fingertip to the major line of the metacarpophalangeal joint was measured.

Although many previous studies have measured the L_{IF} as the length from the fingertip to the proximal metacarpophalangeal crease [124, 125], in this study the length until the actual joint and not the crease was believed to be more useful. The reason for this was that under vibrations measurements, the whole proximal finger was considered as being investigated, including its joints. Even though it is easier to measure the distance to the crease, with the right attention and making a simple adjustment, the distance to the joint can be measured accurately.

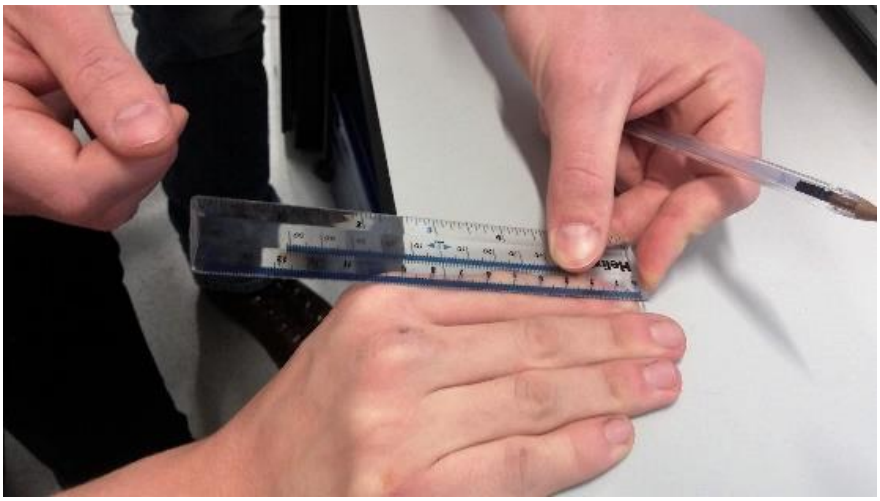

Figure 4.3: Measuring the index finger length of a participant

Length of segments of index finger

For these measurements, the participants were asked to place their hand on the table with their palm facing the ceiling. A ruler was placed above their index finger, and two lengths were measured. The first distance (L_D) was measured from the fingertip up to the distal interphalangeal joint crease and the second distance (D_2) from the fingertip up to the proximal interphalangeal joint crease. The lengths of the three finger parts were determined as follows:

$$L_M = D_2 - L_D \qquad \textbf{Equation 4.1}$$

$$L_P = L_{IF} - D_2 \qquad \textbf{Equation 4.2}$$

where DL, ML and PL are the length of distal, middle and proximal segments of the right index finger as defined in Figure 4.2 above. Similar to that of the index finger length, other studies measured the length of proximal segment up to the proximal metacarpophalangeal crease, not to the joint.

The diameter of the index finger segments "distal and proximal"

The diameters of the index finger segments distal D_D and proximal P_D (see Figure 4.2) were measured using a ring sizer. The ring sizer was first placed at the middle of proximal segment and was tightened until a regular fit was achieved. The reading of the ring sizer was recorded before the ring sizer was removed. A similar procedure was then repeated for distal segment. The readings obtained from the ring sizer were then converted into the corresponding diameters.

Figure 4.4: Diameter measurement of the proximal segment of the index finger

Indicative volumes of index finger

The volumes of the distal and proximal finger segments D and P were estimated using their corresponding lengths and diameters. The estimation of the volume was expected to be a useful measure of the size of the finger as it combines both the length and the area of the finger and was defined as:

$$Indicative\ volume\ of\ D = L_D \times \pi \times (\frac{D_D}{2})^2 \qquad \textbf{Equation 4.3}$$

$$Indicative\ volume\ of\ P = L_P \times \pi \times (\frac{P_D}{2})^2 \qquad \textbf{Equation 4.4}$$

Where D_D and P_D are the measured diameters of segments D and P. Although this method assumes that the finger segments are cylinders with a constant diameter, which is not realistic, this study is more interested in comparing the volume rather than finding its exact value.

The indicative volume of the index finger (IV_{IF}) was found by assessing an average of the diameters of distal and proximal segments (IF_D). The volume was calculated using the following equation:

$$IV_{IF} = L_{IF} \times \pi \times (\frac{IF_D}{2})^2 \qquad \textbf{Equation 4.5}$$

Hand length

Hand length was measured as the distance from the tip of the middle finger to the wrist crease base line, based on the method outlined in BS EN 420:2003 [122]. While participants had their hand resting on the table with their palm facing the ceiling, a measuring tape was used to measure the required distance. This measurement required more attention than the previous measurements, as the wrist crease baseline was not always very clear. In those cases, the researcher asked the participant to fold their hand so that the crease line was more visible (see Figure 4.6 a)

(a) **(b)** **(c)**

Figure 4.5: Measurement of the right hand: a) Length of hand; b) Palm circumference; c) Wrist circumference

Palm Circumference

The measuring tape was then passed around the palm of participants at a regular fit, and the circumference was measured as described in BS EN 420:2003 [122]. To be as consistent as possible, the tape was always placed at the same position, right next to the lines of the joints of the index and little finger, as shown in Figure 4.6, b.

Wrist Circumference

For this measurement, a measuring tape was passed around the wrist of participants to measure their wrist circumference. To increase consistency, the tape was always placed at the point above the wrist joint, or where the circumference was lowest at a regular fit (see Figure 4.6, c).

Hand Grip Circumference

In this study, the hand grip circumference (HGC) was measured as the longest circumference of a surface that gripped when the thumb and index finger just touching. Most of the previous studies have measured this parameter as the outer circumference of the hand [114] or the circumference with the thumb and middle finger touching [126]. The traditional method for measuring hand grip diameter is the “cone method”. However, a new method was developed which allows the shape of the hand grip circumference to adapt to fit around a deforming shape.

Participants were asked to grip as many identical thin plastic sticks as they could, with their index finger and thumb just touching, as shown in Figure 4.8. The plastic sticks were enclosed in a transparent plastic bag to prevent them from falling during the test and to make it simpler. Sticks were added or taken out from the bag until the participant’s index

finger and thumb were just touching. Based on how many sticks each participant was able to hold, his hand grip circumference could then be evaluated. The accuracy of the measurements depended on the diameter of the plastic sticks. The sticks with a diameter of 3.8 mm was used and provide very close approximations to the actual hand grip circumference.

Therefore, it would be interesting to investigate the effect of hand grip area on transmitted vibrations.

(a) **(b)**

4.6: a) Method used for measuring hand grip circumference; b) A close-up view of thumb just touching the index finger

4.2.4 Physical characteristics

Hand grip strength

Hand grip strength (HGS) is considered to be a measure of the performance of hand and forearm muscles, and it is widely used as it is easy and quick to measure. In this study, a Jamar hand Dynamometer was used [127] (see Figure 4.7), with a range of 0-90 kg and graduation of 1 kg. Participants were advised to sit comfortably and grip the dynamometer in any way that felt most natural. The chosen grip size setting of the dynamometer was the one closest to the handle diameter (40 mm) that was being used for the vibration test. A measure of the particular hand grip strength at the specific setting rather than the maximum grip strength was more desirable as in industry handles come in specific sizes.

Moreover, even though the dominant hand is stronger [128], the three left-handed participants still performed the grip test with their right hand since the vibrations test will be performed on their right hand too. Each participant performed the grip test three times; the recorded results were converted into Newton values, and the averages were calculated.

Index finger grip strength

The same procedures of the hand grip strength were repeated for just the participant's index finger gripping the dynamometer as shown in Figure 4.7 b.

(a) (b)

Figure 4.7: a) Hand grip strength measurement; b) Grip strength of the right index finger

4.2.5 Tactile sensitivity test

Monofilament testing is the most comprehensive way of assessing the sensitivity of a particular body part. For this study, sensitivity was tested at the three segments of the right index finger (D, M and P), using a Sammons Preston monofilament kit (20PC, A835-1) as shown in Figure 4.8. However, only 12 monofilaments were used. The thinnest one was monofilament C (max. force, 0.0275 g) and the thickest was monofilament N (max. force, 11.70 g).

During the experiment, participants were asked to indicate every time they could sense the filament applied and at which finger segment they felt it. Throughout the test, participants were asked to either close their eyes or to look away so they could not see if and where the examiner applied the monofilament. The common way of using the filament, applying enough force to bend the monofilament, and keeping it for about two

seconds, was followed in this study (see Figure 4.9). Each monofilament should not be bent too much as any contact of the side of the monofilament with the skin would have a negative impact on the consistency of the test.

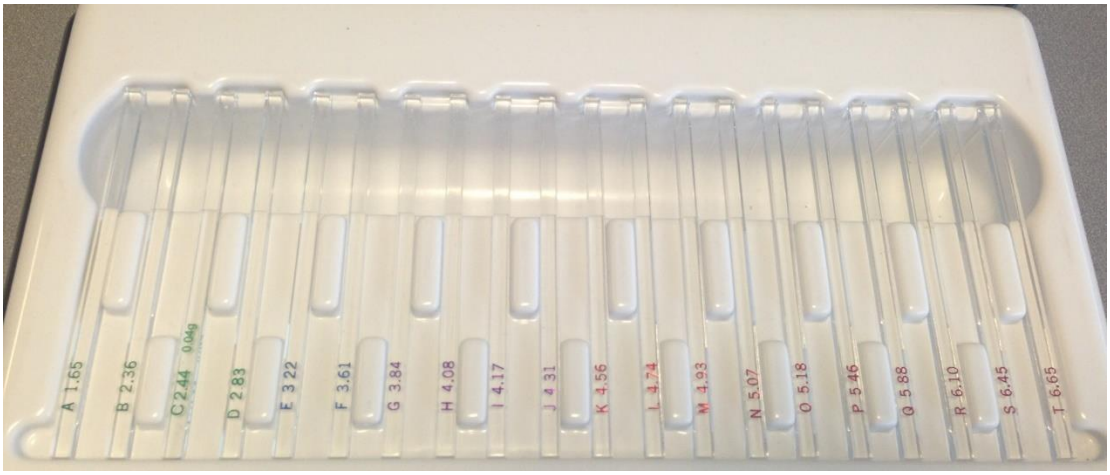

Figure 4.8: Monofilament test kit used in the study. A-T represent the filaments from thinnest to thickest

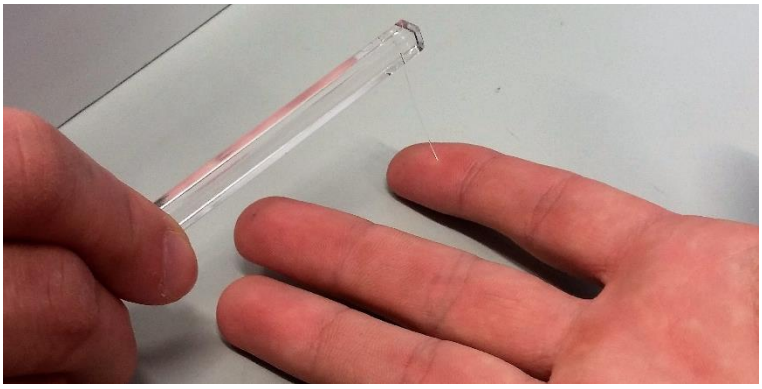

Figure 4.9: Filament applied to the index distal finger (*D*)

The testing procedure is described by the block diagram shown in Figure 4.10. A large monofilament was applied several times on each finger segment in a random order. During the pilot studies, it was highlighted that many times subjects gave inconsistent responses. Therefore, it was decided to record the results when the participant's response was the same three consecutive times. If successfully sensed, a thinner monofilament was chosen and the process repeated. If not sensed a thicker monofilament was used.

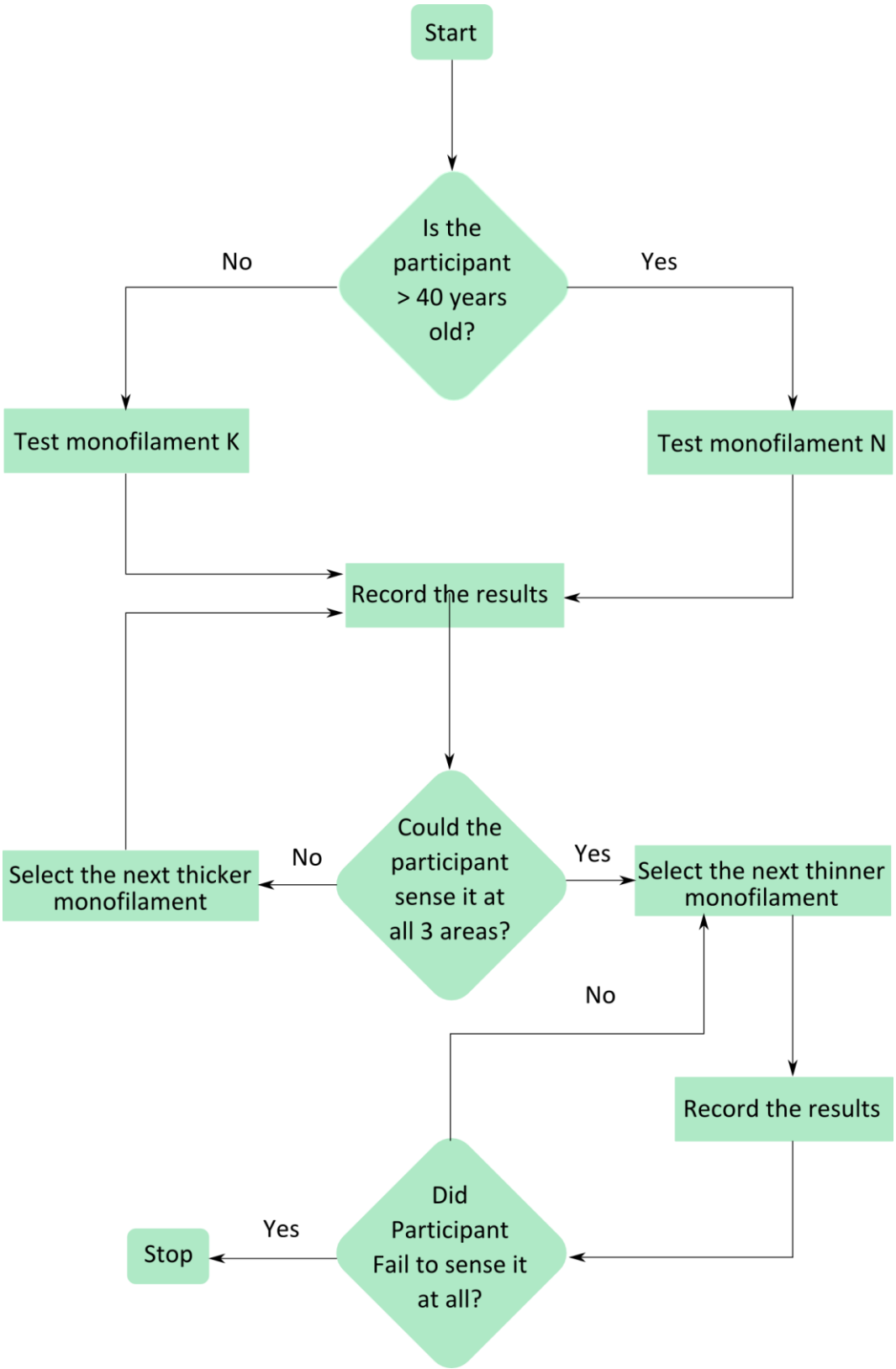

Figure 4.10: Flowchart diagram for assessing finger sensitivity

All participant were able to sense monofilament N. The results obtained from the monofilament tests were converted into a sensitivity measurement which was given by

dividing the number of the sensed filaments of each individual over the number of 12 monofilaments ranged between C and N, and was calculated as follows:

$$sensitivity\ \% = \frac{monofilaments\ sensed}{12} \times 100 \qquad \textbf{Equation 4.6}$$

4.2.6 Skin characteristic measurement

Many previous studies have reported that hand transmitted vibrations may be affected by many factors including hand temperatures and environmental conditions, as well as the mechanical properties of the hand during operating the vibrating tools either indoors or outdoors [64, 85]. Moreover, the mechanical properties of human skin differ and can be influenced by a number of factors including hydration, age and anatomical structure [108, 109]. This variability creates a complication when attempting to obtain consistent and reliable results from individuals. Therefore, this study measured skin characteristics of the finger including skin hydration, temperature and mechanical loading behaviour, as well as the ambient temperature and humidity. The set-up of the equipment used for testing is shown in Figure 4.11.

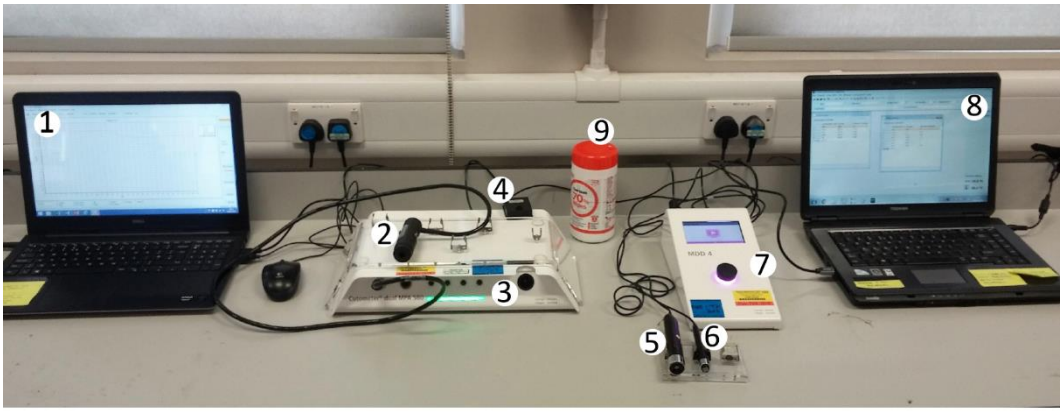

1. Cutometer PC and softwware
2. 8 mm diameter prode
3. Multi Prove adapter MPA
4. Ambient condition sensor RTH 100
5. Skin thermometer ST 500 probe
6. Corneometer CM 825 probe
7. Multi display device MDD 4
8. MPA PC and software
9. Alcohol wipes

Figure 4.11: Experimental set-up and equipment used for the skin characteristics testing

4.2.7 Skin hydration

Skin hydration refers to the water content of the skin, and it was measured with the Corneometer CM 825 (see Figure 4.11). The skin hydration was measured at index finger segments D and P on the palm side, and six readings were taken via the MPA software, with a time difference of at least five seconds between them. The first reading was ignored and the other five readings were averaged according to standard protocol. It should be noted that this test was performed before the skin temperature and viscoelasticity measurements were done, to avoid excessive contact of the finger. However, skin hydration was measured after the sensation testing, to allow the skin hydration level to acclimatise to the room conditions value. The Corneometer probe was cleaned with alcohol wipes after measuring each participant.

4.2.8 Skin temperature

The Skin-Thermometer ST 500 (see Figure 4.11) was used to measure the skin temperature of the index finger at segments D and P. The probe head was placed straight onto the skin and the measurement is recorded by pressing a button. Five measurements were taken and recorded by the MPA software. The probe head was cleaned with alcohol wipes after the measurements of each participant. This procedure was repeated immediately after the vibration test was conducted.

4.2.9 Skin viscoelasticity

Skin viscoelasticity was assessed using the MPA 580 Cutometer device, based on the suction method which was used to characterise the mechanical properties of human skin, via measuring the vertical deformation of the skin surface with response to the negative pressure applied. As shown in Figure 4.11, the device consists of a handheld probe with a central suction head (either 2 or 8 mm in diameter). The probe used in this study was the one with a diameter of 8 mm that connected to the main MPA unit via an air and electric cable. The MPA unit contains a vacuum pump that generates a maximum pressure of 500 mbar.

This device provides two measuring modes: a stress-strain mode and a strain-time mode. The strain-time mode was chosen for this study and a constant negative pressure was applied for 30 seconds followed by a pressure relax 30 seconds to allow relaxation. The

displacement of the skin is determined by optical measuring (see Figure 4.12). The device records the displacement values to the nearest micrometre every 10ms.

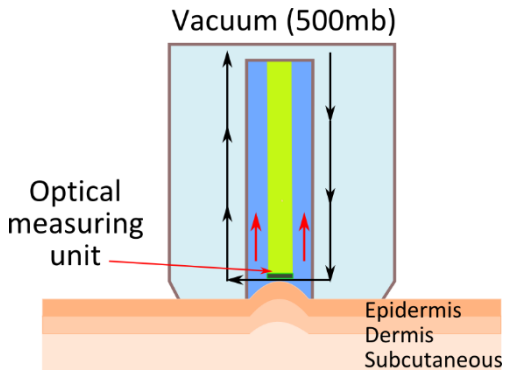

Figure 4.12: Measuring principal of the cutometer

Before applying the probe to the skin, participants were asked to sit comfortably and remain stable during the test as any kind of movement would affect the accuracy of results. The data were recorded by the MPA 580 software and analysed using Microsoft Excel.

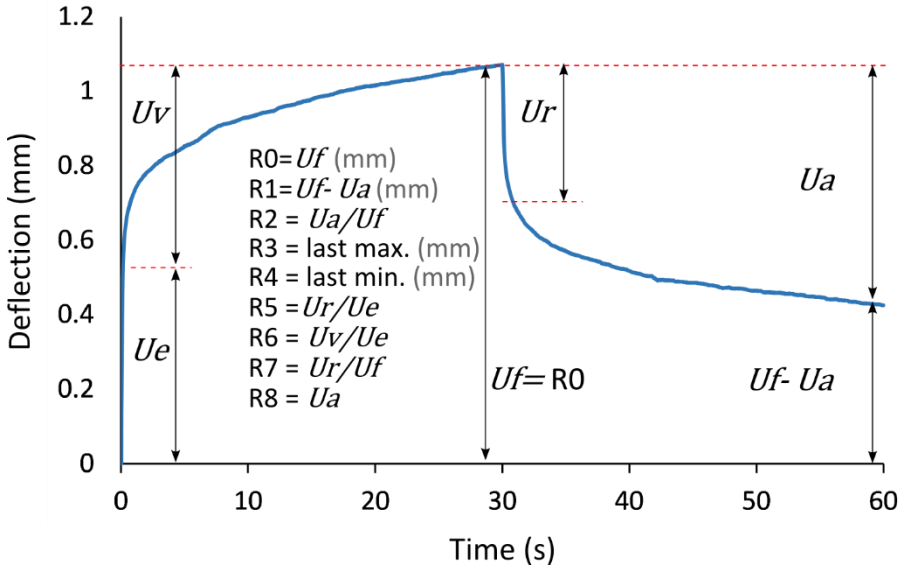

Figure 4.13: Example of the cutometer deflection-time curve of human skin for mode one and measuring parameters as described by Cua et al. [129]

Figure 4.13 shows an example of the real deflection-time curve of finger skin obtained from the cutometer. R values R0 to R8 are those referred by device software.

According to Agache et al. [130], the deformation parameters of the skin are described as follows: immediate distension-skin extensibility (Ue); delayed distension reflecting the viscoelastic contribution of the skin (Uv); immediate skin-retraction (Ur); final deformation of skin distensibility (Uf); ability of the skin to return to its first state after the vacuum was removed (Ua); gross elasticity of the skin, including viscous deformation ($Ua/\ Uf$) which was highlighted as an important parameter; net elasticity of the skin with no viscous deformation ($Ur/\ Ue$); the portion of the viscoelasticity on elastic segment of the curve ($Uv/\ Ue$); elasticity compared with the complete curve($Ur/\ Uf$)[129].

4.3 Indentation measurement

In order to study the load-deflection behaviour of the right index finger, a Mecmesin MDD test stand with a digital force gauge (described in Chapter 3, section 3.2.6) was modified to be used horizontally instead as shown as in Figure 4.14. A support base was designed to be attached to the main test stand. A cylindrical indenter made from polypropylene, 12.25 mm in diameter and 30 mm in length, attached to a digital force gauge (500 N limit) was used with a displacement transducer (spring return linear sensor, 9615, BEI Sensors) attached. This allowed measurements to be recorded continuously using Lab View software version 2014, and via an NI USB-6002 DAQ card. Before any testing was carried out, the displacement transducer was calibrated using the displacement measurement system (Absolute Digimatic Scale) that was originally attached to the test stand (see section 3.2.6). Figure 4.15 shows displacement readings, from the digimatic scale, plotted against the corresponding voltage values of the displacement transducer. The negative gradient is due to the approach used for attaching the transducer to the test stand and also the gradient was more accurate than the one measured in the positive gradient, probably because of the effect of the spring. The R^2 value of 0.997 demonstrates the high corrleation between the two measurements. The linear fit calibration was used in the LabVIEW programme to gain the displacement measured in mm.

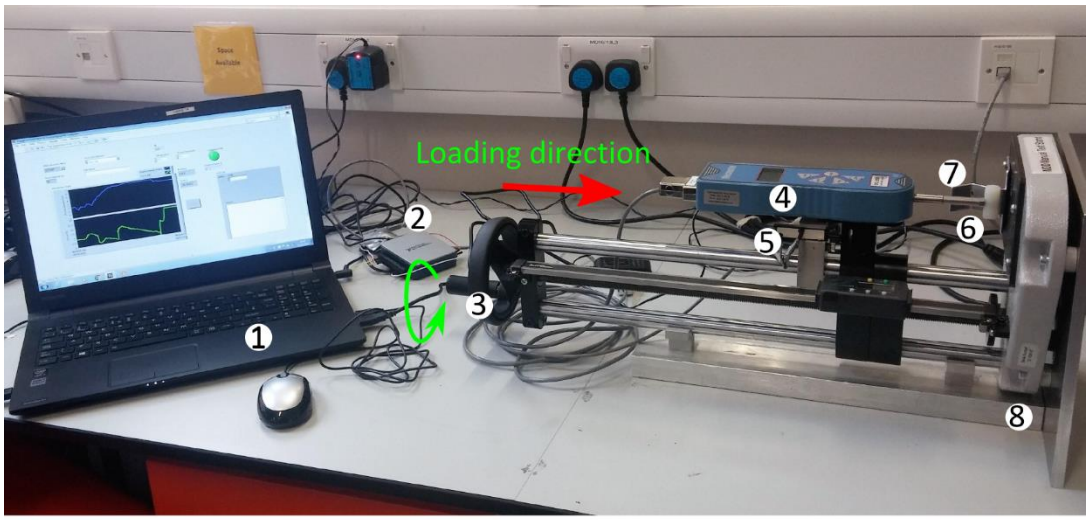

1. PC and LabView softwware
2. NI USB-6002 DAQ card
3. Mecmesin manual test stand - MDD
4. Mecmesin digital force gauge- 500 N
5. Spring return linear position sensor- 9615
6. 12.25 mm diameter indenter
7. Finger supporter
8. Modified base

Figure 4.14: Experimental set-up of an indentation test rig used in the study

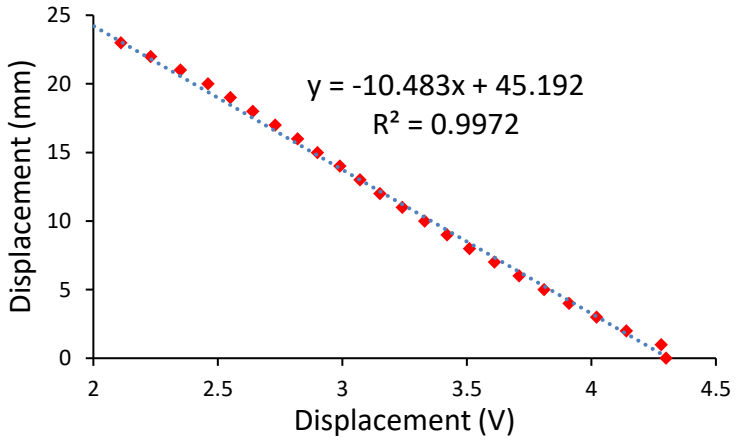

Figure 4.15: Calibration of displacement device used with the indentation test rig

For each participant, two indentation measurements were carried out as shown as in Figure 4.16. In order to replicate posture when gripping, the proximal segment was measured with a bend finger. To ensure that all participants maintained the same posture, an aluminium finger supporter (2 mm in thick) was made and attached to the test system. The distal segment was measured with the finger straight as it was felt its properties were less affected by posture.

To remove any friction between the indenter and the skin that might affect the load-

deflection behaviour of the finger, a water-based lubricant (Boots Lubricating Jelly) was applied to the indenter before each individual test began. Once the finger was in position with the indenter lightly touching, loading was applied manually by turning a handle at a consistent rate. Participants were asked to indicate whenever they felt pain in their fingers so testing could be stopped.

(a) **(b)**

Figure 4.16: Close-up view of indentation test rig: a) When the curved proximal finger was tested and a finger supporter was attached; b) Measurement of the distal finger

The results obtained from indentation measurements used to determine the stiffness at a given loading force by fitting a 4th order polynomial to the data and finding its derivative. In this study, the stiffness was measured under two different loading forces (5 and 10 N). The 4th polynomial fitting and stiffness at a certain load were calculated as follows:

Firstly, the normal forces were converted into logarithm values, base 10 and the coefficients of the 4th order polynomial were calculated for each individual, using the Linest function (Microsoft Excel). These coefficients were then used to calculate the fitting forces (log,10) with their corresponding displacement (x) and returned to their normal force values, as listed in Table 4.1. A sample of measured and fitted of force-displacement data are shown in Figure 4.17.

Table 4.1: An example of the 4th order polynomial fitting used in this study

Measured data			Fitted data		Coefficients	
Displacement (x, mm)	Force (N)	log10(Force)	log10(F) =	Force, N =	c_0	-0.63159
			$c_0 + c_1x + c_2x^2 + c_3x^3 + c_4x^4$	$10^{\log10(F)}$	c_1	0.24912
0.244565372	0.3	-0.52288	-0.568484	0.270095	c_2	0.03773
0.244565372	0.3	-0.52288	-0.568484	0.270095	c_3	-0.00544
0.352746196	0.3	-0.52288	-0.539246	0.288904	c_4	0.00074

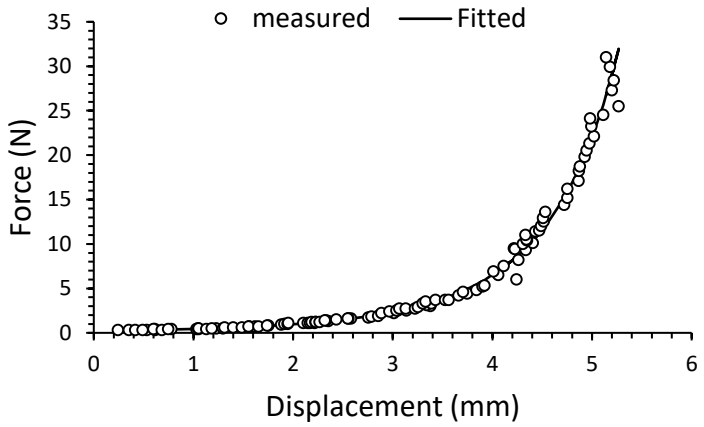

Figure 4.17: A sample of the measured and 4th order polynomial fitted indentation data

For the stiffness at a single point estimate, a grade fraction of 0.001 was considered to be either added or removed from a certain x value. This produced lower and higher x values that were used to calculate two log 10 forces with those x values (lower and higher).

Finally, the stiffness (k) was calculated as the force difference (dF) over displacement difference (dx).

Table 4.2: An example of a method used for measuring a stiffness at a certain force.

Variable	Value	Variable	Value
Grade fraction	0.001	Force with lower x	0.689632
x, mm	7	Higher x = x*(1+ 0.001)	7.007
Log(f)	-0.16016	log force with higher x	-0.15895
F, N	0.691568	Force with higher x	0.693513
Lower x = x*(1- 0.001)	6.993	k = dF/dx , N/mm	0.277155
log force with lower x	-0.16138		

4.4 Finger transmitted vibration measurement

The measurement methodology used in this large-scale study including the transmissibility evaluation was the same to that outlined in detail in Chapter 3, section 3.3.4. For finger vibration measurement, each participant was subjected to six unweighted swept vibrations ranging from 10 to 400 Hz with an amplitude of 5 ms^{-2} rms, for 30 seconds on the right proximal finger. The measurements were carried out when the finger was ungloved and when gloved and under three different levels of grip forces (15, 30 and 50 N respectively).

Once the vibration test was finished and the glove and the accelerometer were taken off, each participant was immediately asked to take another skin temperature reading at the distal and proximal of the same finger to check if testing affected finger temperature.

4.5 Results and discussions

4.5.1 Anthropometric measurements

Once the anthropometric data of all the participants had been collected (all the data in Appendix B), the descriptive statistics including average, standard deviation, minimum and maximum values of each dimension were calculated. These statistics were performed using SPSS statistical software (IBM SPSS Statistics, version 22), which was also used for calculating the one-way ANOVAs to compare between groups and correlation analysis across variables measured. The results obtained from the anthropometric measurements are listed in Table 4.3 below.

Table 4.3: Descriptive statistics of measured anthropometric dimensions

Variable	Mean	SD	Min.	Max.
Age	40.47	14.01	21	61
Height / m	1.77	0.07	1.63	1.95
Weight / kg	76.09	9.85	60	91
WC / mm	175.88	9.92	163	196
PW / mm	212.82	11.70	194	248
Hand size / inch	8.41	0.62	8	10
L_{IF} / mm	99.47	3.18	93	105
L_D / mm	27.29	1.83	25	32
L_M / mm	22.65	1.77	19	26
L_P / mm	49.53	3.52	43	58
D_D / mm	16.51	1.68	14.3	19.91
P_D / mm	20.74	1.04	19.5	22.69
IF_D/ mm	18.63	1.25	17.105	21.3
IV_D / mm³	5946	1514	4019	8713
IV_P / mm³	16786	2374	13938	23440
IV_{IF} / mm³	27257	4246	22812	35971
HGC / mm	152.24	7.71	136	164

4.5.2 Hand grip circumference

The hand grip circumference was an indirect measurement as the weight of the sticks had to be converted into the corresponding grip circumferences, using rubber bands. The results obtained from the test are shown in Table 4.4. R was calculated as the ratio between the hand grip circumference and the circumference of the handle used in the vibration test. Furthermore, a previous study [131] reported that the ideal diameter of the handle was found to be 33 mm, which is a bit lower than the handle used for vibration test rig, which has a diameter of 40 mm, as outlined in the glove standards ISO 10819 [72, 75]

Table 4.4: Hand grip circumference as measured for all subjects

	Corresponding grip circumference (mm)	Ratio R
Mean	152.24	1.21
SD	7.71	0.06
Max.	164	1.31
Min.	136	1.08
* The circumference of the handle used in the vibration test = 125.66 mm		

4.5.3 Hand and index finger grip strengths

All data in Appendix C and the average results of the hand and index finger grip strengths are shown in Table 4.5. The results indicated that the mean hand grip strength was found to be about three times greater than that measured with using only the thumb and index finger.

Table 4.5: Mean values of grip strength measured with hand and index finger

Variable	Mean	SD	Min.	Max.
Hand grip strength average (N)	417	84.73	215.82	555.9
Index finger grip strength average (N)	130	24.66	94.83	179.85

4.5.4 Sensitivity test results

Figure 4.18 shows the sensation levels among individuals when measured at the distal, middle and proximal of the right index finger. The results obtained from the analysis of variance (ANOVA) was found to be statistically different ($p<0.05$, $p=035$) among the three

measured regions. The sensitivity measured at the distal segment was found to be significantly higher than that at the proximal segment, which was found to be the lowest ($p< 0.05$, $p= 0.033$). However, no significant difference ($p> 0.05$) was found between the sensitivity measured at the middle segment and at both the distal and proximal segments. Eight participants were able to sense all tested monofilaments in at least one segment (sensitivity of 100%).

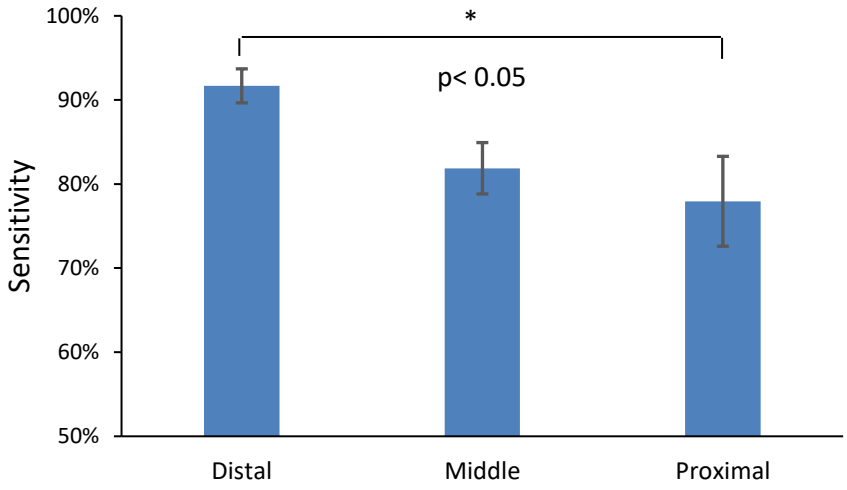

Figure 4.18: Sensitivity values measured for all participants

4.5.5 The effect of vibration testing on the finger temperature

Skin temperature values obtained before and after exposure to vibration for all individuals were averaged and the drop in skin temperature for each participant was calculated, as shown in Table 4.6 and Figure 4.19 respectively. The results obtained showed that skin temperature generally decreased by approximately 2.1˚C and 1.6˚C after exposure to vibration testing, at both measured regions, distal and proximal, respectively. The temperature drop at both measured regions was found to be significantly different ($p<0.05$, $p= 0.025$) and was the highest at distal. Since the last three measurement of the vibration test were conducted when a glove was worn, the decrease in temperature was therefore also considered to have been due to gripping the test handle rather than due to the effect of contact with the metal handle.

Table 4.6: Mean values of finger temperature at distal and proximal measured before and after exposure to vibration

	Temp. before vibration exposure, ˚C		Temp. after vibration exposure, ˚C		Temperature drop, ˚C	
Region	D	P	D	P	D	P
Mean	31.75	31.73	29.64	30.07	2.1	1.6
SD	3.69	2.98	3.16	3.01	__	__
Min.	21.60	23.60	22.48	23.92	__	__
Max.	34.92	35.22	33.96	34.40	__	__

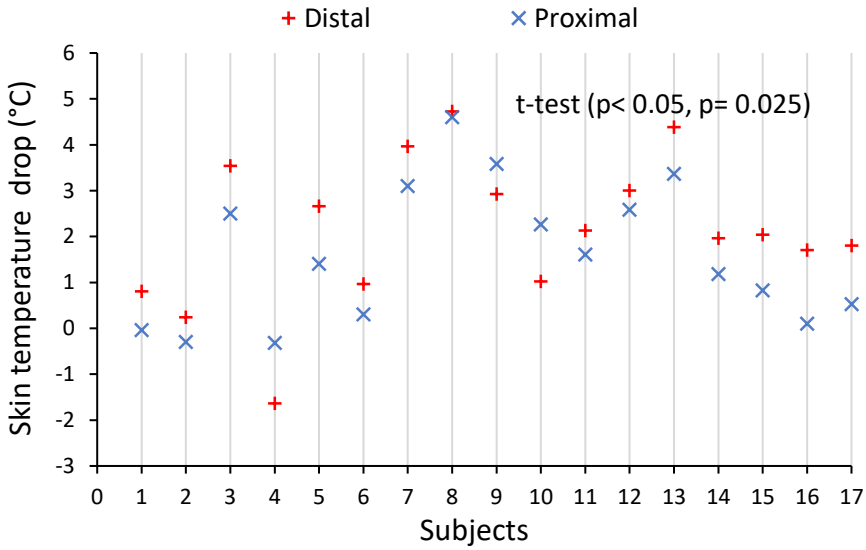

Figure 4.19: Temperature drop after vibration exposure for all participants

In order to check the hypothesis of what the temperature drop was related to, a pilot study was carried out using only one subject who had taken part in the entire study as this had been reported in a previous study that measured the finger blood flow under a static load with no vibration applied [98].

The measurement was carried out using the same method that was used for the entire testing (see Section 4.2.8). In this test, the participant was given enough time for acclimation before testing began. The skin temperature was first measured at room temperature; second, the participant was asked to wear a glove and grip the test handle with no vibration applied, for 30 seconds; then immediately after the glove was removed, the skin temperature was measured again in the same order (distal and proximal). The

procedure was repeated ten times with 90 seconds acclimation time between tests. The results obtained from this test are shown in Table 4.7 below.

Table 4.7: Mean values of finger temperature at distal and proximal measured before and after griping the test handle when the hand was gloved.

	Temp. before gripping, ˚C		Temp. after gripping, ˚C		Temperature drop, ˚C	
Region	D	P	D	P	D	P
Mean	32.1	33.0	32.2	32.9	-0.2	0.2
SD	1.5	1.1	1.0	0.8	1.1	0.7
Min.	29.6	31.1	30.1	31.4	-1.6	-0.8
Max.	34.1	34.6	33.3	33.9	2.2	1.6

The results obtained from this test found that gripping the non-vibrating test handle when a glove was worn did not affect the skin temperature measured at both regions (D and P) of the finger, thus indicating that the decrease in skin temperature was an effect of vibration, not of gripping the test handle.

The temperature and humidity of the room were also measured and found to be stable during the tests (temperature = 22.45±0.1 ˚C and humidity = 36.64±0.6 au)

4.5.6 Skin hydration results

Average hydration values of the distal finger (D) and proximal (P), are shown in Table 4.8. The results indicated that skin hydration measured at D was about twice as high as skin hydration measured at P. It should also be noted that any value less than 30 is considered as dry skin and anything above 40 is considered well-hydrated skin. Skin hydration levels of all participants are shown in Table 4.7 below.

Table 4.8: Mean of finger hydration values measured at distal and proximal

Region of finger	Mean	SD	Min.	Max.
Distal	52.26	15.26	25.38	77.08
Proximal	29.08	12.62	14.10	66.14

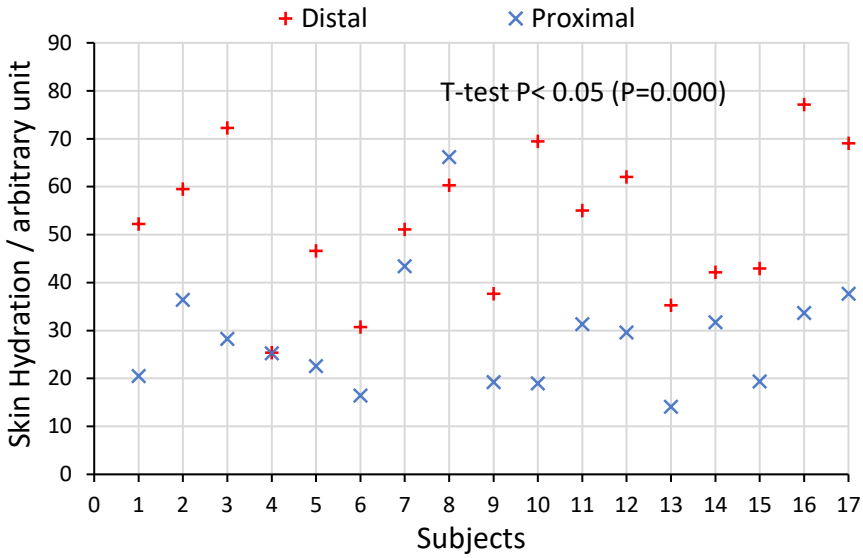

Figure 4.20: Skin hydration measured at D and P of finger for all participants

4.5.7 Skin viscoelasticity results

The useful cutometer parameters (R values) in relation to skin viscoelasticity as defined earlier (see section 4.2.9) were selected and averaged, as listed in Table 4.9. The distensibility of the skin (R0) was found to be slightly higher at the distal segment than the proximal, indicating that the skin at the distal is softer than at the proximal. Also, the ability of the skin to return to its first state (R1) at the distal was found to be double compared to that measured at the proximal. However, other R values (R2, R5 and R7) were found to be greater at the proximal region of the finger than at the distal, indicating that the proximal skin is generally more elastic compared to skin at the distal region of the finger.

Table 4.9: Mean of cutometer parameters (R values) measured at distal and proximal

Region of the finger	Distal				Proximal			
R- values	Mean	SD	Min.	Max.	Mean	SD	Min.	Max.
R0	1.70	0.83	0.71	2.78	1.18	0.39	0.88	2.62
R1	1.19	0.79	0.33	2.15	0.55	0.41	0.31	2.12
R2	0.37	0.18	0.17	0.61	0.56	0.11	0.19	0.65
R5	0.23	0.17	0.07	0.47	0.31	0.09	0.09	0.43
R7	0.10	0.05	0.05	0.21	0.14	0.03	0.07	0.2

R0: distensibility (Uf); R1: ability to return to its original state ($Uf - Ua$); R2: gross elasticity (Ua/ Uf), R5: skin pure elasticity (Ur/ Ue) and R7 elasticity compared with the complete curve (Ur/ Uf).

4.5.8 Room temperature and humidity

Both room temperature and air humidity were recorded using the Ambient Condition Sensor RHT 100, and the average values are shown in Table 4.10. The standard deviation of the values indicated that both variables, especially temperature, were generally stable throughout the whole study.

Table 4.10: Mean values of temperature and humidity measured during all tests

Temperature, ˚C					
Min.	Max	Mean	SD	5th %tile	95th %tile
20	22.2	21.3	0.43	20.4	21.8
Humidity, au					
Min.	Max.	Mean	SD	5th %tile	95th %tile
29.2	37.6	33.0	2.18	30.0	37

4.5.9 Indentation and stiffness measurements

The results obtained from the indentation test of the distal and proximal regions of the right index finger for all participants are shown in Figures 4.21 and 4.22. The results showed that the loading-deflection behaviour of the human finger was found to be generally consistent for a loading force ranging from 0-2 N, for both distal and proximal regions of the finger. However, this behaviour was found to vary as the loading force increased. It should be noted that that the load-deflection behaviour (and the peak load tolerated) for a human finger was found to vary among individuals, mostly depending on the geometry of the finger. For example, participants T9 and TS5 indicated to stop loading at below 10 N at the proximal finger (see Figure 4.22), therefore their stiffness at the proximal and 10 N were not calculated. The stiffness measured for both distal and proximal, for all participants, are shown in Figure 4.23 and Appendix D.

The mean and standard deviations of stiffness at each measured position were calculated. The results obtained showed that the stiffness at the distal, and at both targeted loading forces (5 and 10 N) was found to be about twice as high (5.96±1.12 and 14.6±2.55, respectively) as that measured at the proximal (3.84±0.80 and 8.67±3.54, respectively). The differences in the mean and standard deviations of stiffness at both distal and proximal at each loading force were also calculated (2.11±1.28 and 5.63±2.86 at 5 and 10 N,

respectively). Statistically significant differences ($p<0.05$) were found in both conditions. However, individual data (see Figure 4.23) showed that in some cases, some participants appeared to have similar stiffness at both distal (5 N) and proximal (10 N). However, one participant (TS3 = 14) showed the same stiffness at 5 N at both distal and proximal (3.87 and 3.99 N/mm), as well as at 10 N for both regions (9.50 and 9.53 N/mm).

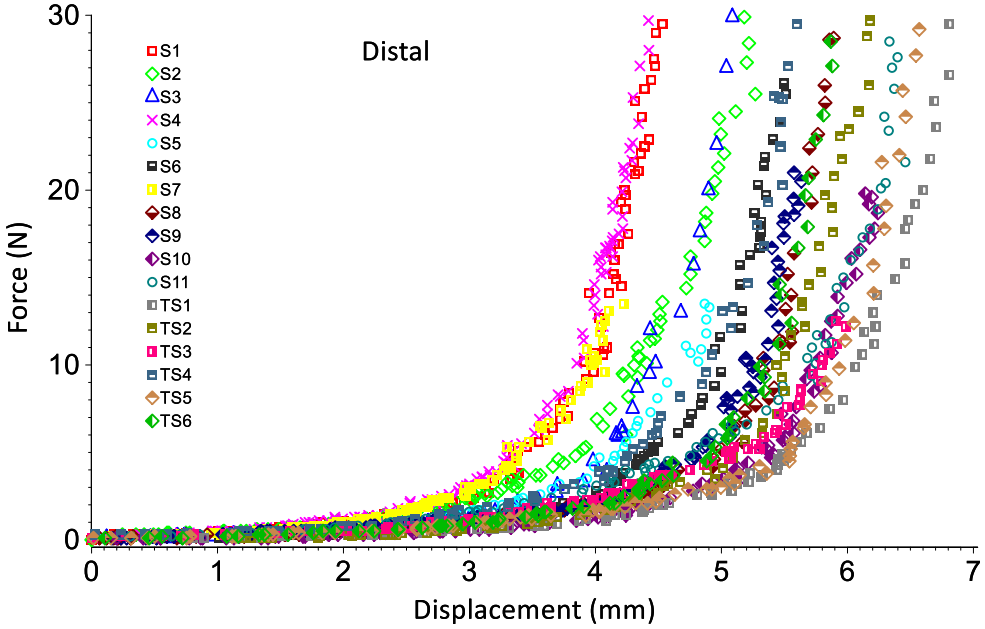

Figure 4.21: Indentation load-deflection measured at distal finger for all participants

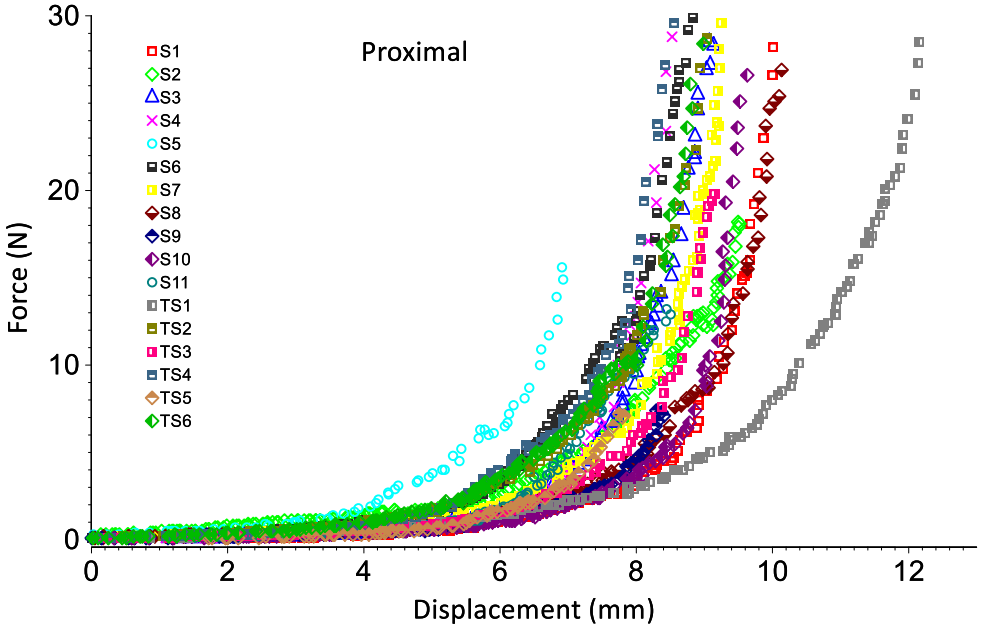

Figure 4.22: Indentation load-deflection measured at proximal finger for all participants

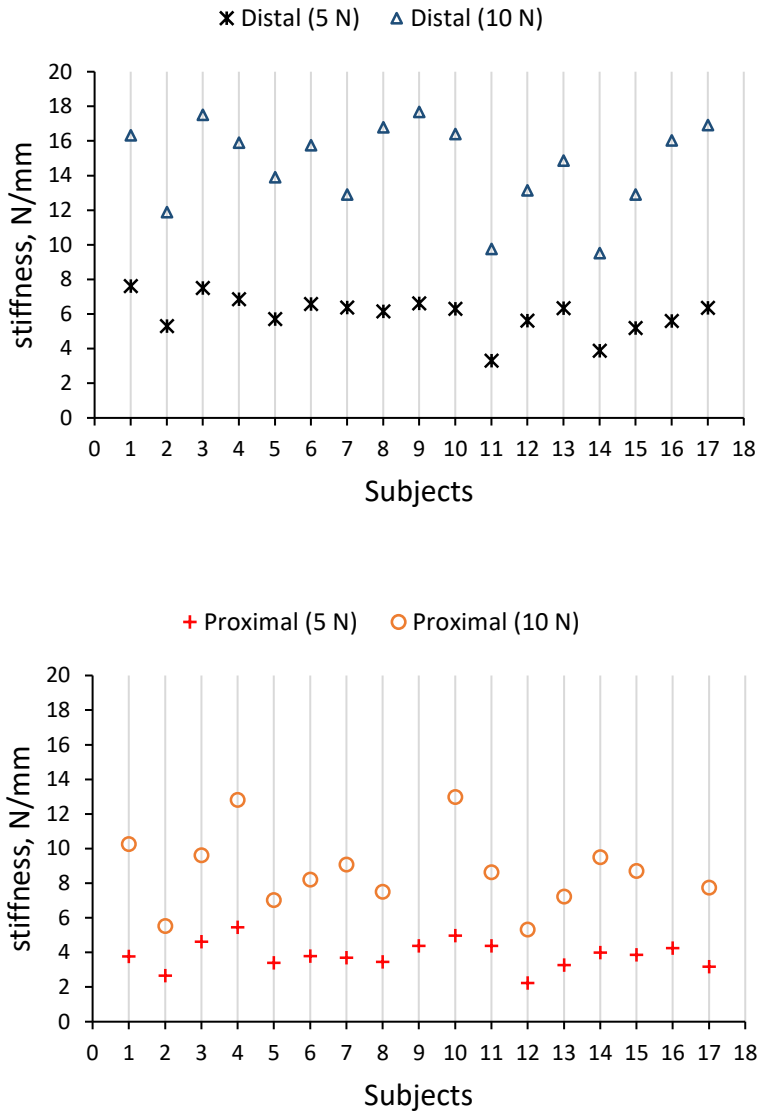

Figure 4.23: Stiffness measured at distal and proximal finger for all participants, at indentation loads of 5 and 10 N

4.5.10 Transmissibility measurements

The transmissibility measurements of the bare (ungloved) right index proximal finger and the ones while wearing the glove, as well as the transmissibility of the glove, are shown in Figures 4.24, 4.25 and 4.26, respectively.

The transmissibility measured from the bare finger at three grip forces (15, 30 and 50 N) was found to vary among individuals (see Figure 4.24). This variation was found to decrease as the grip force increased. In general, the transmissibility measured for all participants showed resonance at frequencies slightly above 100 Hz and increased with the grip force.

However, for some reason, the participant TS2 showed resonance at 10 Hz, and S7 showed some noise at frequencies above 250 Hz when the grip force of 15 N was applied and these were reduced as the grip force increased. This strongly suggested an association with issues of a signal acquiring and an accelerometer attachment to the finger, as well as its wire.

The effect on finger transmissibility of wearing a glove is shown in Figure 4.25. Similar to the results from the ungloved finger, the results of the gloved finger were also found to vary among individuals. However, the peak that appeared at about 50 Hz for all participants became a little higher when the glove was being worn than it was when measured for the bare finger, which is possibly due to the variance in grip force.

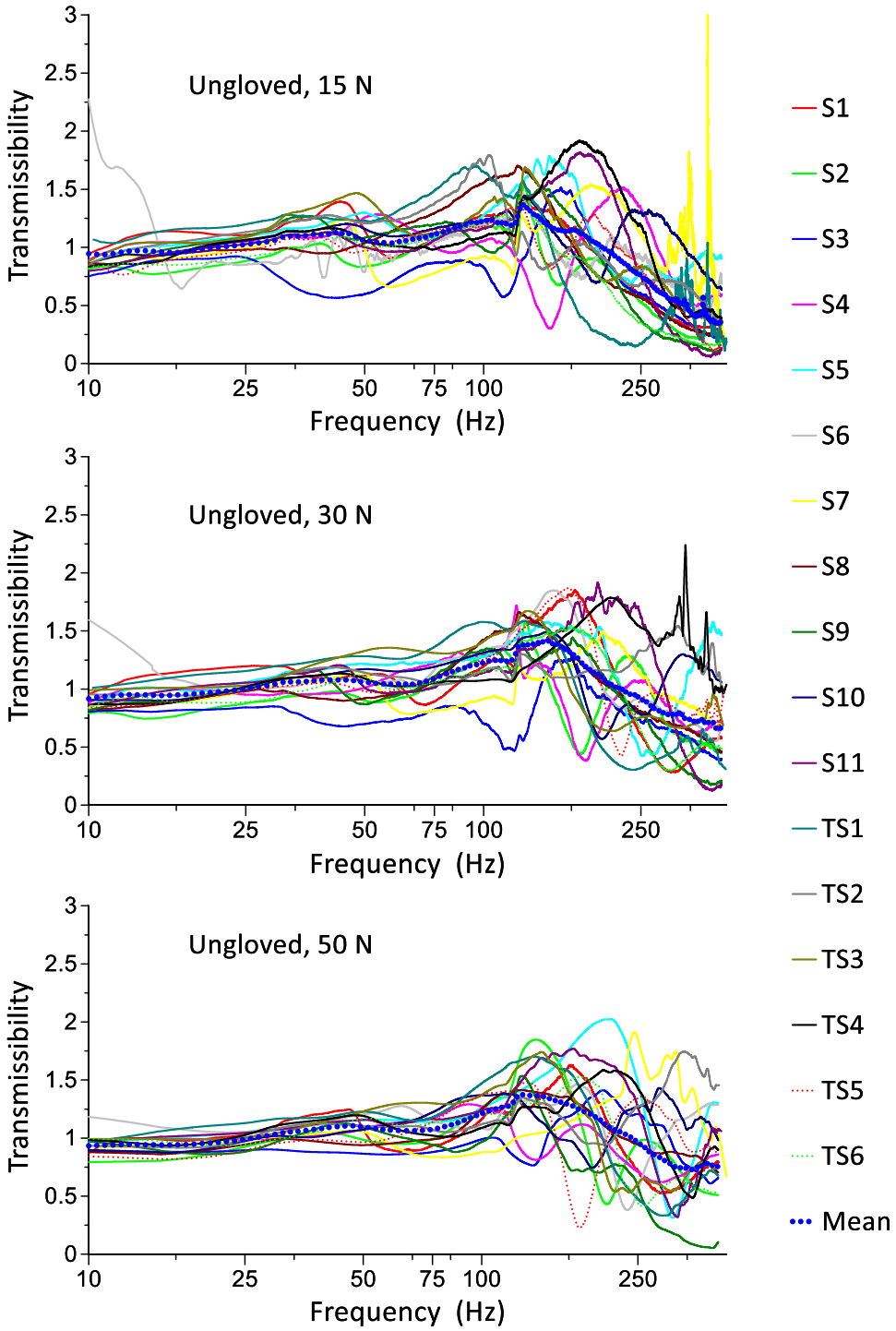

Figure 4.24: Transmissibility measured throughout the bare proximal (ungloved) right index finger under grip forces 15, 30 and 50 N, for all participants

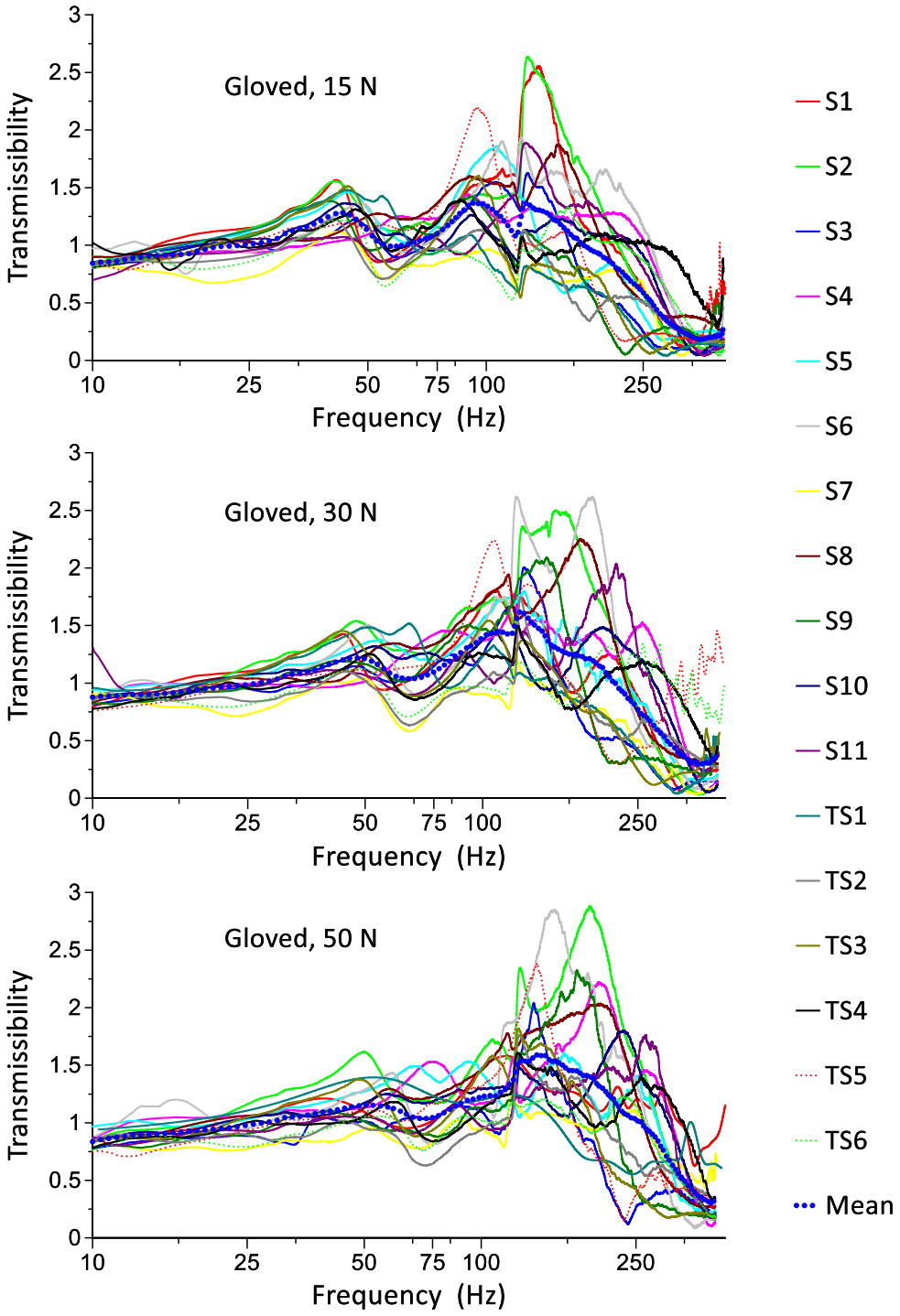

Figure 4.25: Transmissibility measured throughout the gloved proximal of the right index finger under grip forces (15, 30 and 50 N), for all participants

The glove transmissibility measured for all participants as shown in Figure 4.26, and showed that the glove has two resonance frequencies at about 50 Hz and slightly beyond 100 Hz, which is increased as the grip force increased.

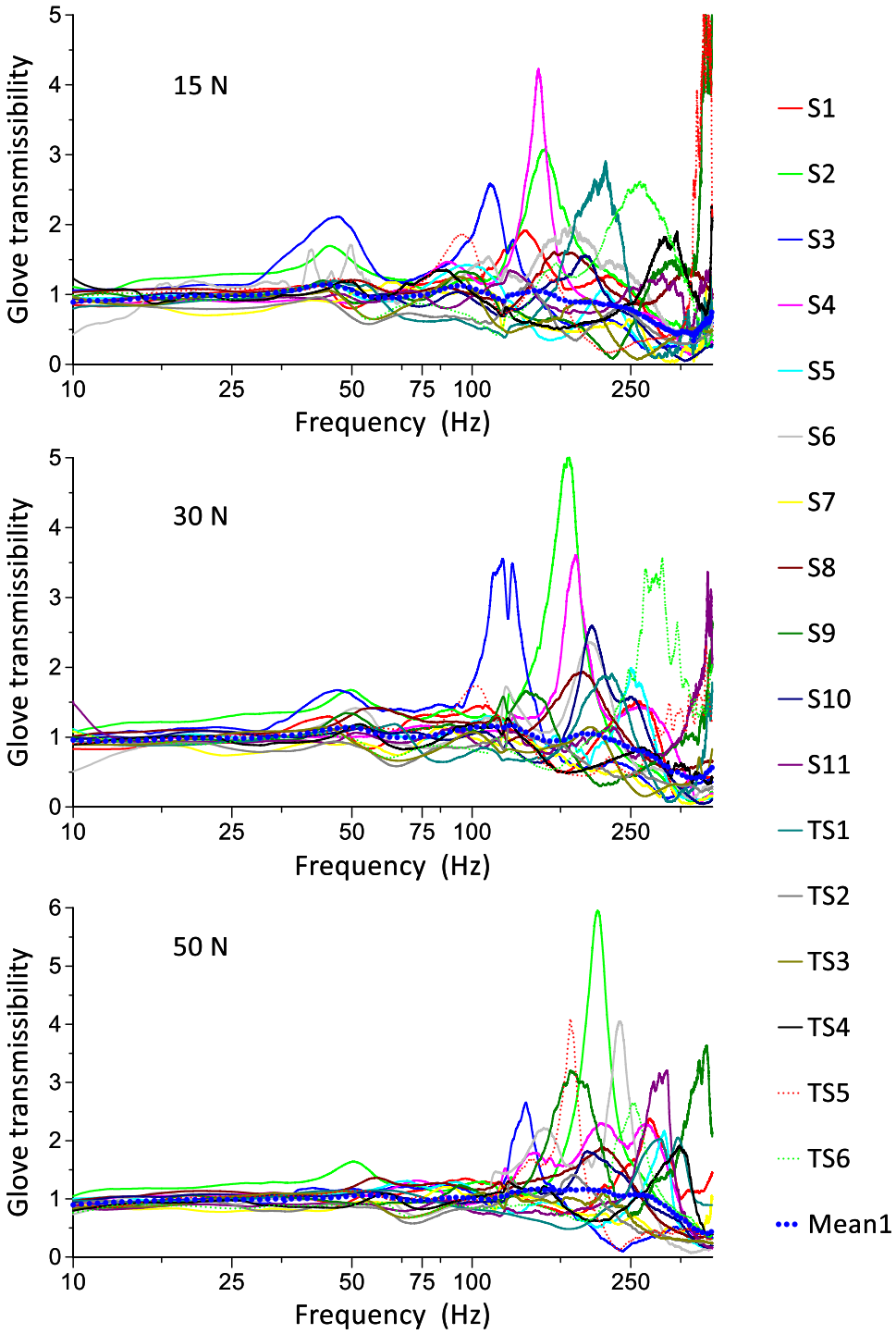

Figure 4.26: Transmissibility of the glove used in this study and under grip forces 15, 30 and 50 N for all participants

The variance in transmissibility among individuals was found to be related to the variance in finger grip force applied during exposure to vibration and how different subjects respond to each frequency. During each vibration test, the finger grip force was continuously

recorded along with vibration signals. Therefore, the mean grip force was calculated for each participant and each targeted grip force, which was then used to calculate the descriptive statistics for all force measurements among individuals, as shown in Table 4.11.

Table 4.11: Descriptive statistics mean grip forces for all participants

Measured grip force	Mean	SD	Minimum	Maximum
Ungloved, 15 N	15.77	1.23	13.50	17.50
Gloved, 15 N	16.10	1.20	14.07	18.87
Ungloved, 30 N	29.69	1.71	26.49	33.25
Gloved, 30 N	29.87	1.71	27.37	33.20
Ungloved, 50 N	48.40	1.87	45.32	52.05
Gloved, 50 N	48.52	1.85	44.85	52.15

The results in Table 4.11 showed that wearing the glove had increased the mean grip force when participants were asked to grip with the targeted force of 15 N. However, the glove did not have much effect on the participants' grip force for targeted forces of 30 and 50 N. The targeted grip force of 30 N was the most controllable among individuals, as the standard deviation remained the same in both cases.

The resonance frequency and its amplitude were also calculated from the measured transmissibility for each participant and all six measurements. It should be noted that these peak values were only calculated for frequency ranging from 25-250 Hz to remove the effect of any an invalid data. The measurements of peak transmissibility against resonance frequency, the mean measured grip force against resonance frequency and peak transmissibility against the mean measured grip force for each participant are shown in Appendix E1, E2 and E3.

Figure 4.27 shows the average of transmissibility measured for all subjects, bare and gloved finger, where three grip levels (15, 30 and 50 N) were applied. The results showed that the glove had affected the vibration transmissibility of the proximal finger. It increased the peak amplitude that appeared at about 50 Hz, which was very little when measured without the glove being worn. Also, the amplitude of major resonance was slightly increased.

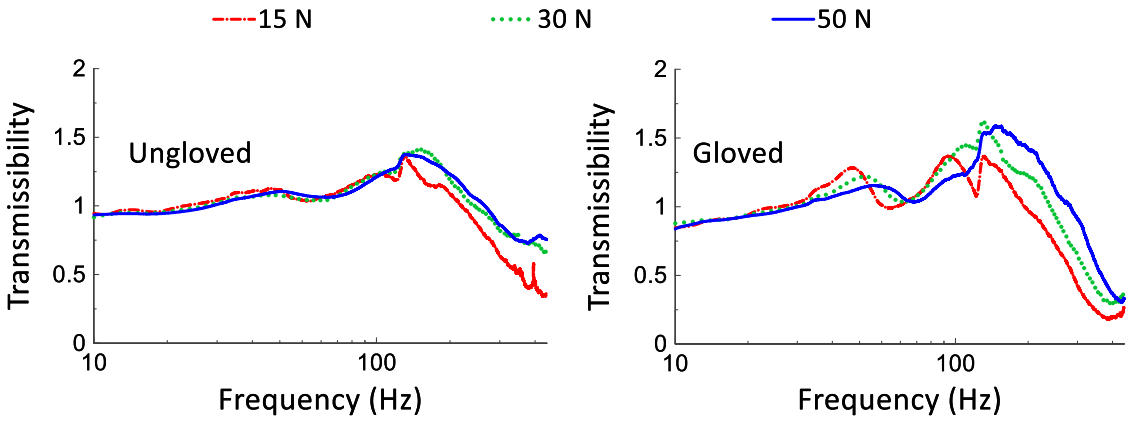

Figure 4.27: Mean transmissibility measurements of the bare (ungloved) and gloved finger and three grip forces (15, 30 and 50 N), for all participants

The effect of the glove at low frequency was decreased as the grip force increased. Also, the results showed that the higher grip force had a lower amplitude at low frequencies and increased as frequency increased (see Figure 4.27). These findings showed agreement with a recent study that measured vibration transmissibility through different points of fingers including the proximal index finger, using the laser vibrometer method [65]. The mean frequencies and peaks amplitudes for all three measurements are shown in Table 4.12.

Table 4.12: Mean resonance frequencies and amplitudes of mean transmissibility for all participants

	Resonance frequency Hz			Peak amplitude		
Target force N	15 N	30 N	50 N	15 N	30 N	50 N
Ungloved finger	93.1	126.0	126.0	1.37	1.37	1.62
Gloved finger	145.9	139.3	127.0	1.41	1.59	1.38
Glove transmissibility	44.1	125.1	145.9	1.14	1.18	1.17

The mean transmissibility of the glove is shown in Figure 4.28, and the results showed that the glove used in this study has three resonance peaks at frequencies about 50, 92 and 144 Hz, which generally shifted to higher frequencies as the grip force increased. The results of the study suggested that the AV glove used did not significantly reduce the vibration at frequencies below 400 Hz in the proximal segment of the right index finger.

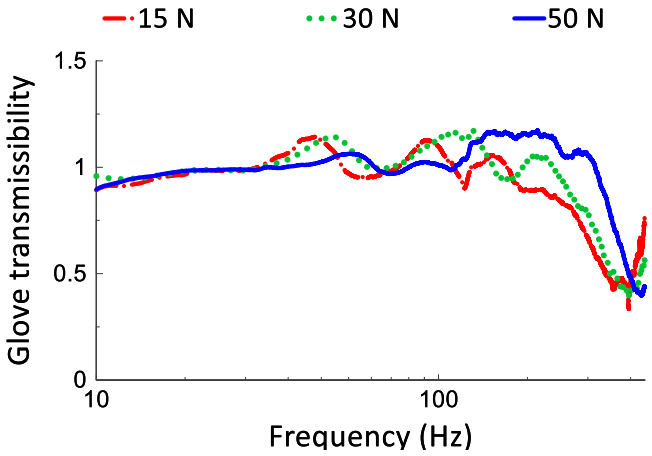

Figure 4.28: Mean transmissibility of the glove used in the study.

As transmissibility measurements of fingers are very limited, and no standardised method has been developed yet that measures finger transmitted vibration[86], more research is required.

Since one of project objectives is to investigate the dynamic response of human finger and to be used to validate the physical model of the finger. Averaging transmissibility measurements lead to losing some of individual behaviours. Therefore, only resonance/peak frequency was calculated for each individual and used for correlations and comparisons to find out factors might affect the exposure to finger-transmitted vibrations.

4.5.11 Statistical analysis – one-way ANOVA

This study is interested in finding the effects that prolonged exposure to vibration might have on the index finger. In order to investigate this, a group of technicans who were exposed to vibration in their daily activities was included in ths study. The purpose of this was to gain better a understanding of the factors that might affact finger transmitted vibration. In order to examine any differences between the two tested groups (technicians and non-technicians) over all the variables measured in this large-scale study, one-way ANOVA was calculated, using SPSS statistical software (IBM SPSS Statistics, version 22), when differences were considered significant at the p- value less than 0.05 level.

The details for the entire comparison between the groups are shown in Appendix F.

The results obtained from the one-way ANOVA showed that there are some staticical differences between technicians and non-technicians. In particular, these parameters are:

- Age: the technicians were older.
- Hand size: the length of proximal segment of index finger (L_P), diameter of the distal segment, the averaged diameter of the finger segments, the Indicative volume of the distal index finger (IV_D) and indicative volume of the index finger (IV_{IF}): the technicians hand were bigger except $L_{\_P}$ was smaller.
- Vibration behavour: the resonance frequency (RF_15 N) of the ungloved finger, resonance frequency of the glove (RF_GT30N) and resonance peak of the glove (RP_GT15N) were higher for technicians.
- Sensitivity at the proximal finger was higher for non-techniciants.

These were all found to be significantly different at the level of $p < 0.05$. However, no significant difference was found between other parameters among the two groups.

4.5.12 Statistical analysis – correlation

The relationships between all measurements were analysed using the Pearson correlation coefficient based on the two-tailed. The single asterisk (*) correlation refers to significance at the $p < 0.05$ level whilst the double asterisk (**) refers to the significance at the 0.01 level.

The entire analysis showed that there were strong correlations between all anthropometric variables and grip strength measured (see Appendix G). These correlations were positive, thus indicating that there is a link between the general size of someone's hand and hand characteristics, and this is a sensible outcome. For example, it can be expected that someone with relatively thick phalanx bones will generally have thick fingers and a larger wrist circumference as well. There was another correlation between the cutometer parameters (R-values) that measured at the distal finger with a temperature drop for both distal and proximal of the finger as shown in Table 4.1. However, no correlation was found between skin characteristic measures and temperature drops at the proximal finger.

Table 4.13: Pearson coefficients between R values and temperature drop at distal and proximal of the finger

	Temp. drop_D	Temp. drop_P
R0_D	.527*	.674**
R1_D	.504*	.644**
R2_D	-0.409	-.534*
R3_D	.527*	.674**
R4_D	.504*	.644**
R5_D	-0.419	-.572*
R6_D	-.621**	-.667**

As mentioned earlier, one of the two sets of data obtained from the cutometer measurements were the R values which represent some characteristics of the skin. Each of the R values is described in Section 4.2.9 . The results showed that the R values measured at the distal had a significant correlation at 0.001 level with a temperature drop at the proximal, and also a significant one at 0.05 level with a temperature drop when measured at the same region (distal). R2, R5 and R6 showed negative correlations.

Based on the definition of R values (see section 4.2.9) and correlation found between R values and temperature drop of the finger, the R values with negative correleation were reported to be critical parameters which were defined as R2 gross elasticity of the skin, including viscous deformation which was highlighted as the most important parameter; R5 net elasticity of the skin with no viscous deformation; R6 the portion of the viscoelasticity of elastic segment of the curve [129].

The correlation analysis also indicated that the sensitivity of three measured regions of the finger was found to be inversely correlated to age (see Table 4.14) and this was reasonable with the findings obtained from the monofilament test conducted in this study. The ANOVA showed the technicians group had lower sensitivity than that of non-technicians. In particular, sensitivity at finger segments D, M and P was found to be 7%, 10% and 28% lower compared to that measured for non-technicians. Therefore, since the technicians were older, there was not clear evidence as to whether the technicians have less sensitivity due to the activities that they are involved in or because they are older and it is natural to experience loss of sensation as age increases. To investigate this, the sensitivity test should be conducted on a group of younger people that are using vibrating tools.

Table 4.14: Correlation between the sensitivity at distal, middle and proximal with age

Region	Age
Sensitivity _D	-.673**
Sensitivity_M	-.489*
Sensitivity_P	-.507*

4.5.13 Comparison of measured characteristics with other studies

The data obtained from this study were compared with measurements of previous studies to see the similarities and differences of the participants tested in this present study with the general population. In general, the results showed the characteristics of the participants does not differ much from that measured in previous studies of other people [114, 128]. The only major difference was that participants tested in this study were found to have bigger hand grip areas than Indian agricultural workers. However, a recent study concluded that Asians have smaller hand dimensions compared with non-Asians [127] and therefore it cannot be concluded that the participants of this study have particularly large hands.

4.5.14 Vibrations affect finger temperature

As shown earlier (Table 4.6), the skin temperature dropped by 2.1°C and 1.6 °C at both finger distal and proximal respectively after the vibration test. A paired t-test conducted on both measured regions of the finger illustrated that this difference was significant ($p< 0.05$, 2-tailed). Since the second part of the vibration test was conducted for the gloved finger, the results strongly suggested that exposure to vibrations decreases finger skin temperature, and also indicated that finger circulation may be affected by vibration exposure, as this was also the conclusion reached in many previous studies [7, 8, 82]. The fact that skin temperature drop might happen due to static gripping the test handle was investigated (see section 4.5.5, Table 4.7). A paired t-test conducted on both measured regions of the finger found that this difference was not significant ($p> 0.05$, 2-tailed).

4.5.15 Parameters affect vibration behaviour

No correlations were found between skin characteristics measured (R values) at both regions of the finger (D and P) and any of the vibration measurements. However, a positive correlation was found (see Appendix H) between resonance frequency (RF_15N) and

age, L_D, D_D (p< 0.05), and IV_D (p< 0.01). The resonance peak (RP_30N) was found to be positively related (p< 0.05) to the length (L_P) and the volume (IV_P) of the proximal segment, whilst the resonance peak (RP_50N) showed a negative correlation with the length of the middle segment (L_M).

4.6 Conclusions

Based on the findings of this large-scale study, a suitable protocol has been developed for measuring characteristics in relation to HAVS. This protocol with the identified improvements can be followed in similar research in the future to help researchers' understanding of the factors causing HAVS.

Both anthropometrics and physical measurements of the human hands obtained in the study showed similarities when compared with findings from previous studies. The inclusion of cutometer and corneometer measurements provided the characteristics of the human skin including viscoelastic properties, temperature and hydration of the skin, which allows a better understanding of how all these measurements might affect the finger transmitted vibration. The vibration transmissibility of the proximal index finger was measured and found to vary among individuals.

No strong correlations were found between any of the skin characteristics measured and the vibration behaviour of the right index finger. However, the vibration behaviour was found statistically to be related either positively or negatively to some of the anthropometric measurements of the finger. The data obtained from this study were found to be useful and will be used to evaluate and validate an artificial finger model that will be developed and describe later.

Chapter 5: Investigation of anti-vibration "AV" glove materials

This chapter addresses how the gloved materials might be affected by different factors such as temperature and geometry. The dynamic mechanical analysis was carried out on three glove materials using a Viscoanalyser VA2000 machine and followed by human participant testing for the same glove material in order to compare between data gathered from both methods. This work was published as a conference paper [93] presented at the 50th UK conference on human responses to vibration.

5.1 Introduction

According to the literature review, vibration transmissibility of gloves can be affected by many factors, such as the type of glove material and its properties, tool vibration conditions, temperature and grip force. Although the AV gloves fulfil the requirements of vibration transmissibility, their assessment had been performed under controlled conditions such as room temperature and grip force, as stated in ISO 10819[72]. Therefore, there is a motivation to investigate the glove materials under different temperature levels.

This study, however, was designed to carry out a dynamic mechanical analysis (DMA) of material specimens in order to predict the dynamic responses of glove materials against a frequency spectrum and the effects of temperature, followed by an investigation into how the properties of different glove materials affect the tool vibration transmission into the index finger, and how the transmissibility of a glove material can be affected when varying grip forces are applied.

5.2 Material analysis

5.2.1 Methodology

Three different materials were selected for analysis. Materials 2 and 3 were taken from gloves that had passed the ISO 10819:1996 test, while material 1 was used for comparison, being a material designed for mounting vibration sensitive equipment. The summary of the characteristics of the specimens are shown in Table 5.1.

Table 5.1: Characteristics of the specimens used in the study

Material order	Material description	Thickness (mm)
1	Latex foam, new	6.10
2	Rubber, old	6.56
3	Foam, new	6.60

A Dynamic Mechanical Analysis (DMA) was conducted for all three materials in order to gain material properties for comparison, and specimens were prepared depending on their structures as seen in Figure 5.1. Also, the specimens were imaged using optical microscope (Zeiss Axio Imager A1m, AxioCam ERc 5s), as shown in Figure 5.2). DMA involves measuring the mechanical response of a material specimen when sinusoidal loading is applied

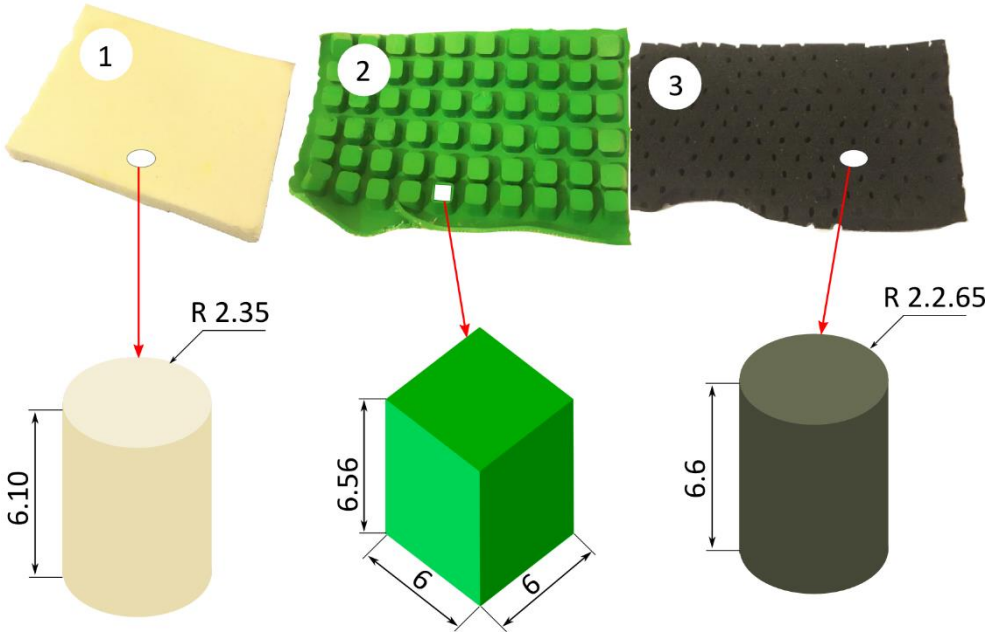

Figure 5.1: Material structures and dimensions of specimens used for DMA testing (in mm)

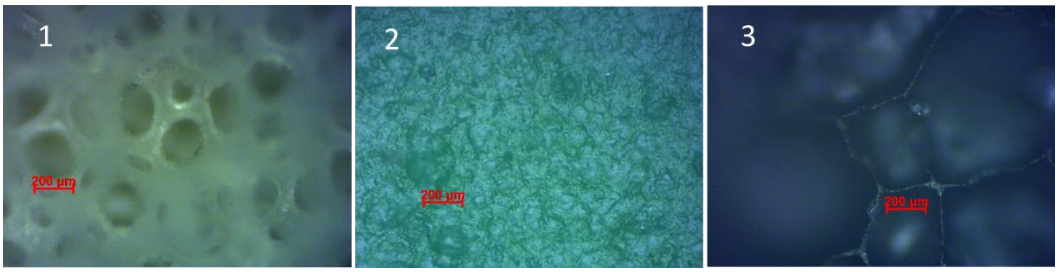

Figure 5.2: Optical microscope images (200 µm) of three glove materials used in the study

The DMA was conducted using Metravib Viscoanalyser equipment as shown in Figure 5.3 (a). Each specimen was installed between compression plates located in an analysis chamber, as shown in Figure 5.3 (b). The specimen temperature was measured using a thermocouple probe located in the chamber. At the start of the test, the chamber was cooled using liquid nitrogen to -60 °C to obtain the glass transaction temperature (T_g) as expected for most rubber and foam materials. Once the temperature had stabilised, the specimen was subjected to sinusoidal vibrations with a dynamic strain amplitude of 10^{-3}. Measurement of the resulting force signal was made at seven different frequencies (values spaced evenly on a logarithmic scale between 1 and 31.5 Hz). The chamber was heated slowly by 5 °C until the temperature is stabilised and, after stabilisation, the vibration testing repeated. This process was repeated at 5 °C increments up to 80 °C to examine specimens of materials in long term use. However, frequency-temperature measurements were carried out on a set of relevant temperatures that ranged between 0 °C to 30 °C.

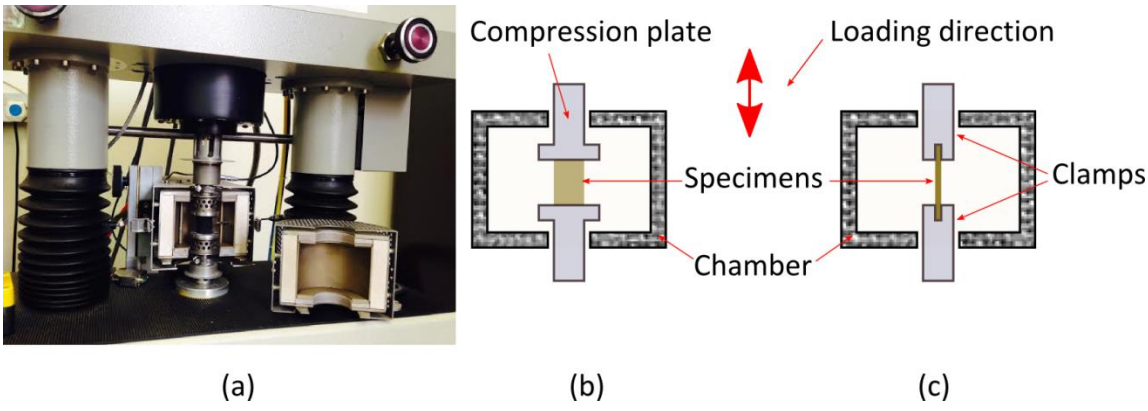

Figure 5.3: a) Viscoanalyser VA2000 machine; b) Sectional diagram of the chamber and specimens when using compression plates; c) Tension modes using clamps.

The results obtained from the DMA machine were used to produce viscoelastic master curves based on the Temperature-Frequency Superposition principle [132]. In this work, the software was employed to obtain the master curves that were then generated in-house and utilised the Differential Evolution Algorithm to find smooth spline curves that provide the best fit to the test data in a least squares sense.

5.2.2 Results from DMA of material specimens

The master curves generated from the DMA data were used to determine the glass transection temperature (T_g), which is defined as a loss factor peak against the temperature sweep (-60 to 80 °C) obtained from the master curve and to predict the Young's modulus and loss factor for each material at temperatures and loading frequencies of interest in hand-arm vibration studies. This data is shown in Figures 5.4, 5.5 and 5.6.

It can be seen that the Young's modulus of all three materials (1, 2 and 3) increased as the frequency of vibration increased and temperature decreased. A significant increase in the Young's modulus for all materials occurred when cooled to 0 °C, as at this condition the materials were closer to their glass transition temperatures. It should be noted that the modulus of Materials 1 and 2 was approximately ten times higher than that of Material 3.

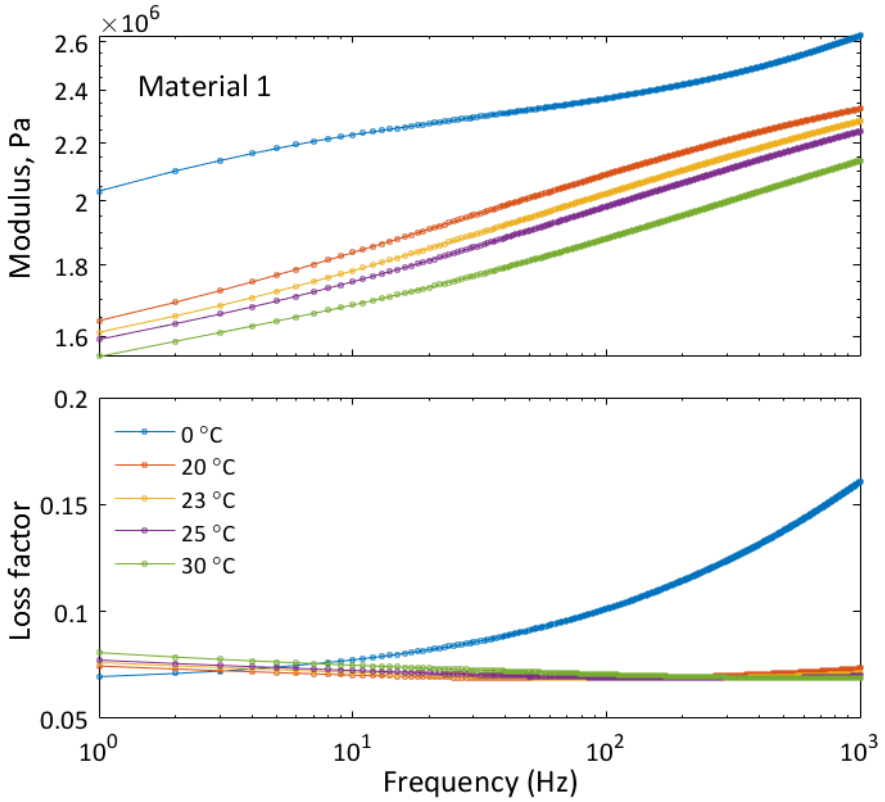

Figure 5.4: Young's modulus and loss factor against frequency for Material 1, Tg≈–23 °C

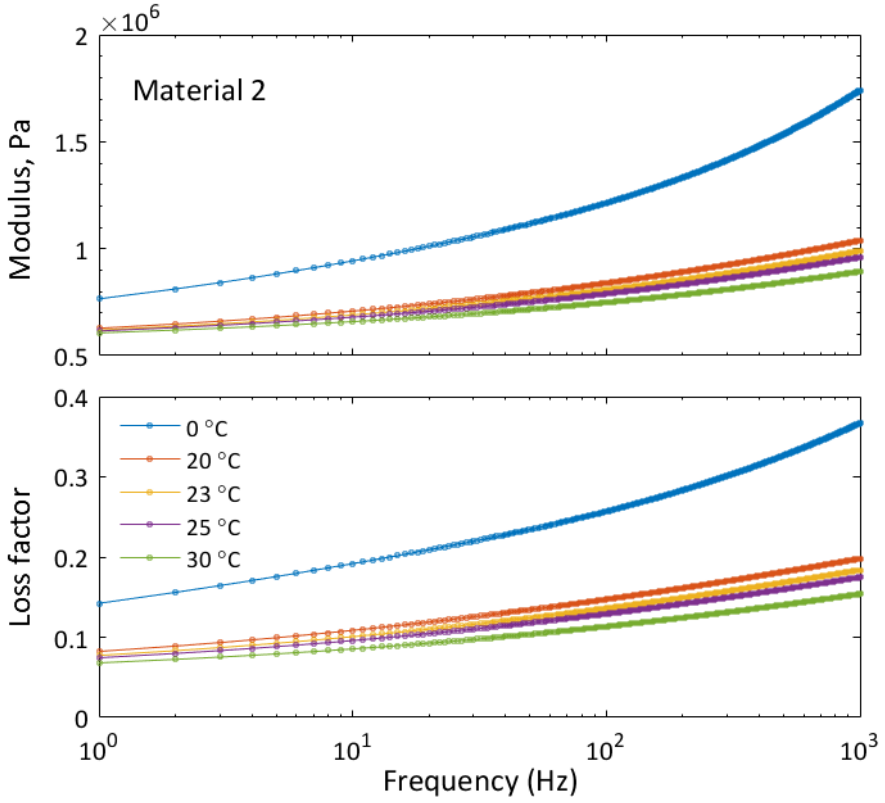

Figure 5.5: Young's modulus and loss factor against frequency for Material 2, Tg≈–30 °C

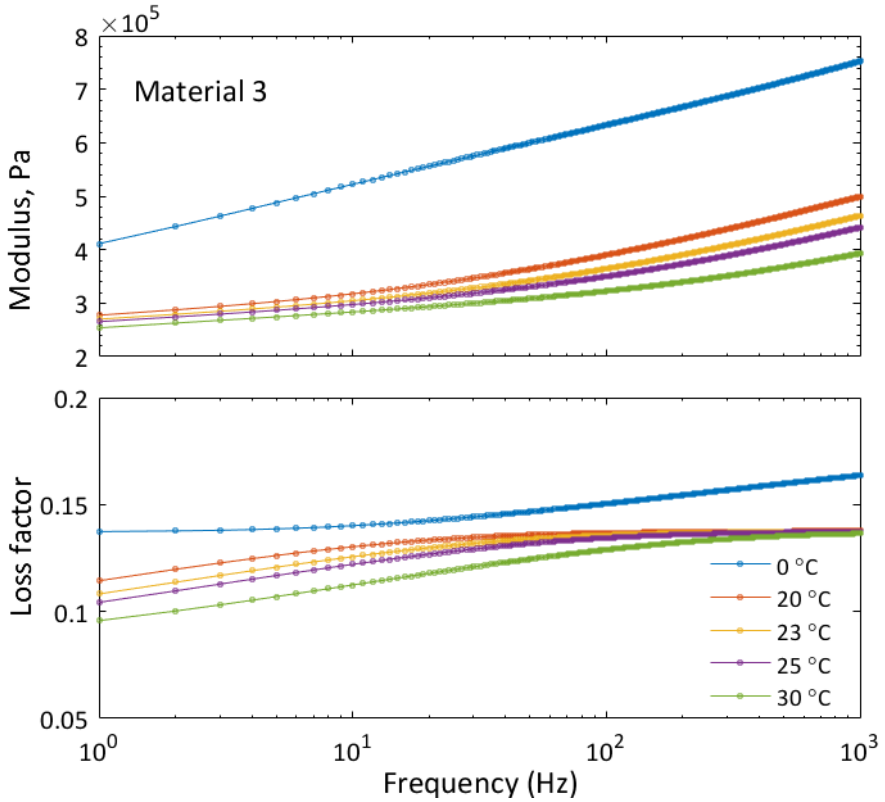

Figure 5.6: Young's modulus and loss factor against frequency for Material 3, Tg≈–41 °C

The loss factor of Material 1 was not significantly affected by frequency when subjected to a temperature range from 20 to 30 °C, but there was a dramatic increase with frequency when at 0 °C, as shown in Figure 5.4. The loss factor of Material 2 gradually increased over the frequency range, but this was most significant at 0 °C as shown in Figure 5.5. Material 3 showed different loss factor behaviour, with a slight change at low frequencies and a tendency to have the same behaviour temperature ranging from 20 to 30 °C at frequencies beyond 100 Hz. However, it had a significantly higher loss factor at 0 °C, as shown as in Figure 5.6.

5.3 Human subject testing

5.3.1 Methodology

Participants

Twelve human subjects aged 22 to 48 were used for the testing, and their characteristics are provided in Table 5.2. The design of the experiment was reviewed and approved by the Research Ethics Committee of the Faculty of Engineering at the University of Sheffield.

Table 5.2: Characteristics of the human subjects used in the study

	Mean	SD	Minimum	Maximum
Age (years)	28.75	9.05	22	48
Height (cm)	177.08	7.39	160	185
Weight (kg)	71.75	6.98	63	88
Hand length (cm)	18.25	1.03	17	20
Hand circumference (Cm)	19.83	1.54	17	22
Hand size EN 420:2003	7.75	0.75	7	9

Experimental setup

The setup of the vibration test rig including the finger adapter used in this study was described in detail earlier, in Chapter 3.

Two piezoelectric accelerometers with nominal sensitivity 10 mV/g (PCB Models 353B15 and 353A15) were used for measuring the acceleration data (see Chapter 3, Section 3.2.2): one was attached to the handle and used as a reference accelerometer, whilst the other was mounted on an adapter strapped to the finger (see Figure 5.7, a). The material specimen was placed around the right hand end of the handle, and the adapter was fitted onto the index proximal (of the right hand of the participants being tested (see Figures 5.7 and 5.8).

The participants were asked to maintain a grip of 30 N, and once they were comfortable, the handle was excited using discrete sinusoidal vibration excitation signals that covered the range from 20 to 400, in one third octave band [64]. Once the vibration input sequence had been completed, the participants were then asked to maintain a grip of 15 N before being subjected to a vibration frequency of 125 Hz for 5 sec, and this was then repeated for a grip force of 45 N.

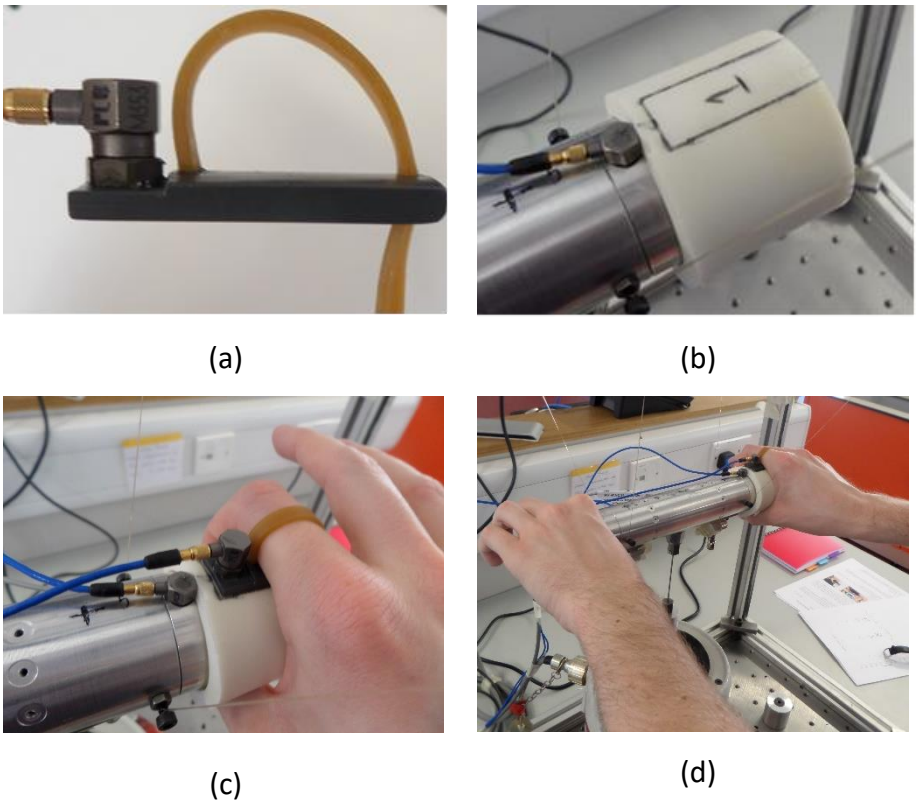

Figure 5.7: Testing setup showing: a) Finger mounting adapter; b) Material specimen and adapter alignment marked; c) Right end close-up (d) Posture of the handle being gripped.

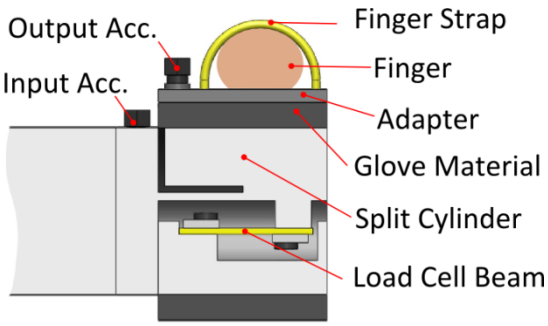

Figure 5.8: Cross-sectional diagram of the right end of the handle during the test.

All experiments were carried out with no glove material in place and with each of the three materials. The vibration amplitude produced by the rig was 1.47 ms^{-2} rms (unweighted). All vibration measurements were conducted at room temperature, which ranged from 22.9 °C to 23.4 °C.

5.3.2 Analysis of the transmissibility of gloves materials

All the measured data was processed and analysed using DIAdem view software (Version 2014). As mentioned earlier in Chapter 3, the Finger-adapter method was used in order to evaluate the transmissibility of glove materials, and was calculated using Equations 3.1, 3.2 and 3.3.

Transmissibility results

The transmissibility measurements obtained of all three glove materials for all 12 participants are shown in Figures 5.9, 5.10 and 5.11. No significant vibration attenuation was found for any of the materials at frequencies below 150 Hz. They all showed significant attenuation at frequencies above 315 Hz. Material 1 showed a good agreement between subjects for frequencies below 80 Hz. The true resonance frequency was found in the range 200-250 Hz (see Figure 5.9) and generally attenuated at frequencies above 315 Hz.

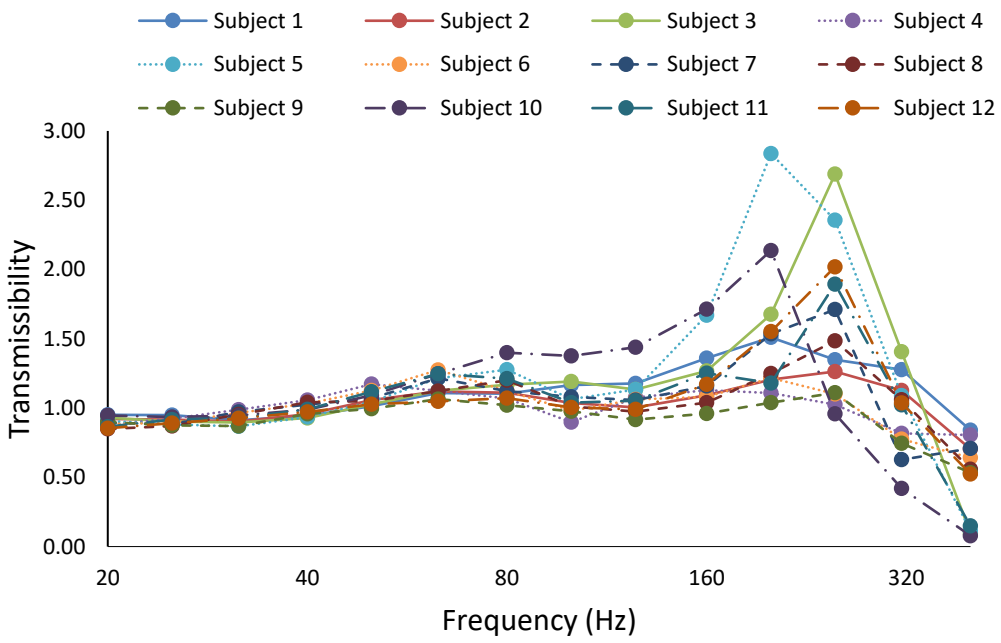

Figure 5.9: Transmissibility measurements against frequency for all participants when using Material 1

Material 2 showed variable transmissibility among individuals. A slight variation in the range of resonance frequencies was found at frequencies from 80 Hz to 200 Hz. However, generally attenuation started to occur at a frequency of around 250 Hz (see Figure 5.10).

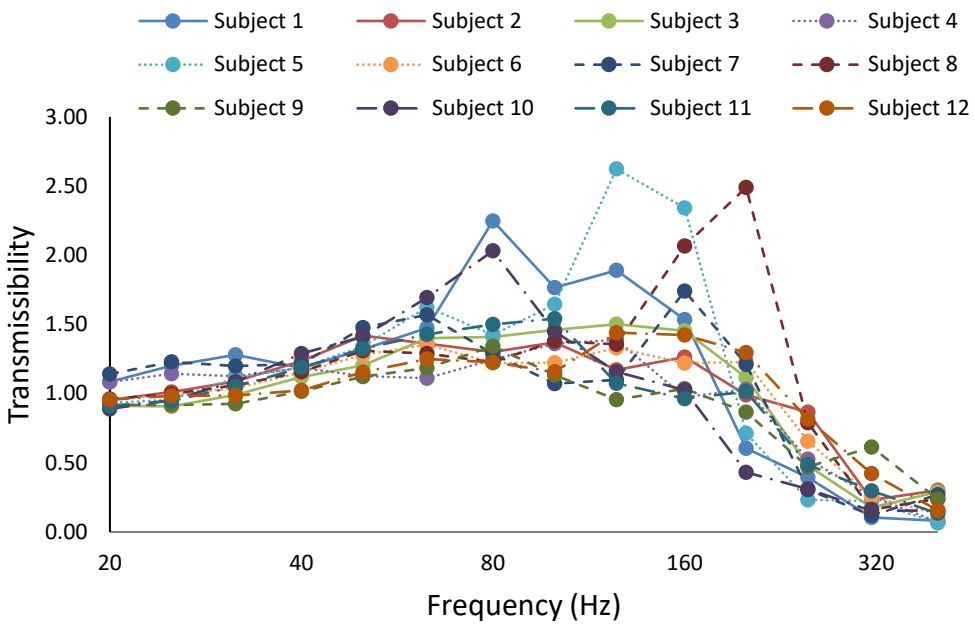

Figure 5.10: Transmissibility measurement against frequency for all participants when using Material 2

Material 3 showed less variation in transmissibility when compared with Material 2, but more than Material 1. The resonance response was mostly shown at a frequency of 160 Hz and generally started attenuating at a frequency of 250 Hz (see Figure 5.11).

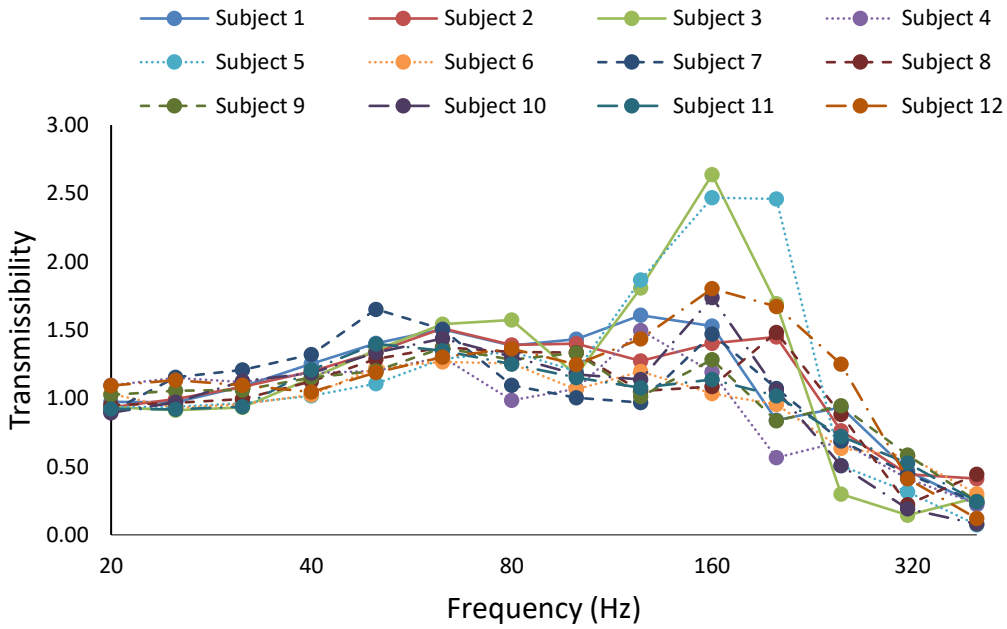

Figure 5.11: Transmissibility measurements against frequency for all participants when using Material 3

5.3.3 The effect of grip force on the transmissibility of materials

All the materials showed variation in transmissibility among indivduals, making any trends in behaviour due to grip force hard to establish. Material 1 showed least variation among indivduals and Material 2 the most (see Figure 5.12, below)

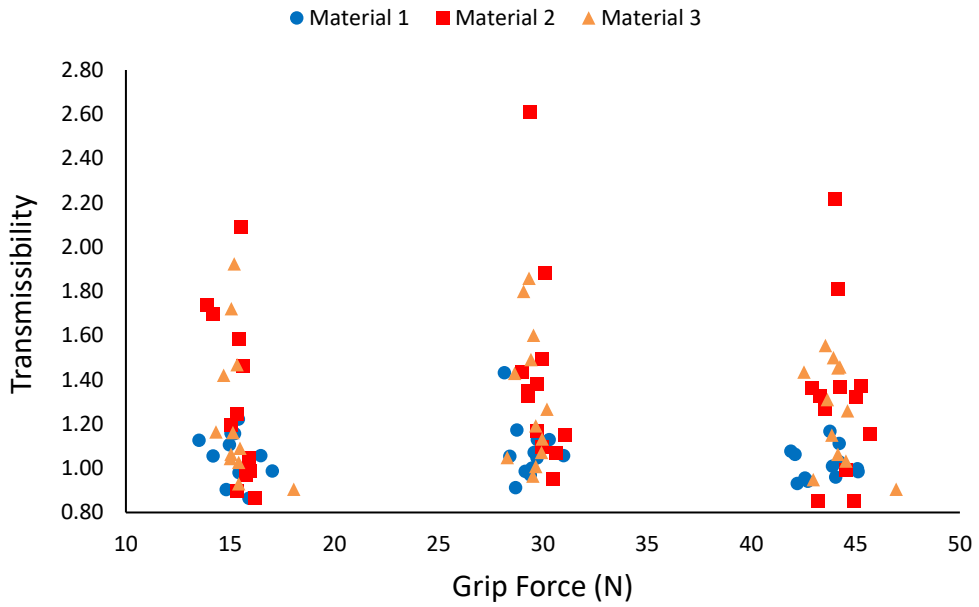

Figure 5.12: Transmissibility measurements against grip force for all participants, at frequency 125 Hz

5.4 Discussion

Many studies have been conducted using the palm adapter method, and most of the results show that there was very little attenuation below a frequency of 200 Hz [76, 82, 133]. Although the same method was used in this study, differences between this study and previous studies could be due to the difference in glove materials and participants used, as well as the hand location tested. Another study tested different gloves and found that the transmissibility of gloves was largely affected by the design of the gloves [65]. (e.g. number of layers and type of AV material used as well as its structure)

The AV glove materials examined in this study show little effect on vibrations below 100 Hz with possible amplification in the frequency range of 100-200 Hz and attenuation at frequencies beyond this. Comparing this study with others, the glove materials seem to be within the expected range of results for gloves.

One study measured the transmissibility of AV gloves using a 3-D laser vibrometer to measure vibration transmitted throughout the finger [65]. It found that the AV gloves showed very little attenuation across the entire spectrum of frequencies and resonance at a frequency of 125 Hz when a grip force of 30 N is applied with inter-subject variability of the height and position of the peak. It should be noted that the design of materials used in this present study did not match any of the glove designs that were used in the previous studies.

Findings from this study also show a strong agreement with the results obtained from a 3-D vibrometer [65], which is very promising as that is the only study that measures the transmissibility at the finger and not on the palm.

The non-glove material (Material 1) seemed to be the one with the worst performance, with less attenuation than AV materials, but this was expected as it is the stiffest and not used in AV gloves and was not optimised for this application.

Materials 2 and 3 did not show enough attenuation over the range 150 to 250 Hz to be labelled as AV in accordance with ISO 10819. Since they had passed the ISO standard test, it can be assumed that they have less effect on fingers than on the palm [65], and also the method for testing them is different from the standard method, which tests the entire glove. However, the present study used only AV materials – but not other layers which might be affected by bunching when placed around the test handle. The results of the present study suggested that the AV gloved fingers may only be effective at attenuating vibrations frequencies above 250 Hz.

According to a previous study, increasing the finger grip force increases the resonance frequency due to increased stiffness of the finger surface as well as the stiffness of the joints of the fingers [65]. This present study investigated the effects of grip force on vibration transmission of three different materials that could be found at a frequency of 125 Hz, with different grip forces (15, 30 and 45 N). As the results indicate (see section 5.3.3), all three materials showed no significant effect of grip force on transmissibility. This is reasonable, as unlike human tissue, polymers show relatively little nonlinearity at moderate strains.

The DMA results obtained represented the mechanical characteristics of the materials. Young's modulus affects the dynamic stiffness of the material layer, and is directly proportional to the energy stored during the loading period. The loss factor is the ratio of the energy lost to that stored and affects the mechanical damping of the material layer [ISO 6321-1134]. As the resonance is affected not only by the modulus but also the geometry and structures of the layers (see Figures 5.1 and 5.2, above), only modulus values can directly be compared in this study because the thickness is the same. The DMA results showed that Material 1 was stiffer than Material 2, and Material 3 was less stiff than the other two. This is reasonable when combining DMA data with human subject testing. The resonance frequency increases with an increase in material stiffness. Material 1 showed resonance at frequencies from 200 Hz to 250 Hz and Material 3 resonated at 160 Hz.

Material 2 showed most variation in resonance frequency among individuals. However, there is a probable reason for the large variation in the resonance frequency (80 Hz to 250 Hz), which could be due to fact that the surface of Material 2 was in blocks (see Figure 5.13) so that its effective area was less, thereby reducing the stiffness. It is hypothesised that these are the causes of the large variability.

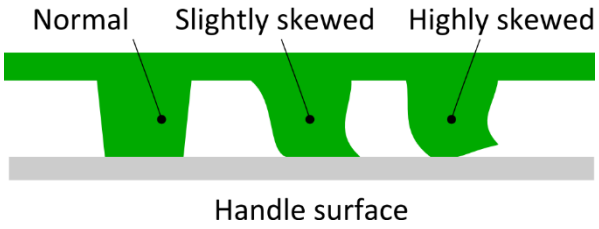

Figure 5.13: Diagram of possible loading behaviour of material 2.

The effects of the most effective frequencies and temperatures on Young's modulus of tested materials are shown in Table 5.3.

Table 5.3: The effects of frequency and temperature on Young's modulus of tested materials

Temperature °C		Material 1			Material 2			Material 3		
		Frequency Hz								
Young's Modulus, MPa		160	200	400	160	200	400	160	200	400
	0	2.40	2.42	2.49	1.29	1.33	1.48	0.66	0.67	0.70
	20	2.14	2.17	2.24	0.87	0.89	0.95	0.41	0.42	0.45
	23	2.08	2.10	2.18	0.84	0.85	0.91	0.38	0.39	0.42
	25	2.03	2.06	2.14	0.82	0.83	0.88	0.37	0.37	0.40
	30	1.93	1.95	2.03	0.77	0.79	0.83	0.33	0.34	0.36

DMA testing also allows the prediction of the behaviour of materials when affected by temperature change (e.g. cold conditions) and over the frequency range of interest. As the stiffness of the glove materials increases with an increase in vibration frequency, attenuation at higher frequencies could be lost due to an increase in resonance frequency. This can be noticed with human participant testing: the transmissibility of the stiffest material (material 1) showed resonance at a frequency range of 200-250 Hz, whilst materials 2 and 3 (less stiff) showed resonance generally at frequencies below 160 Hz.

5.5 Conclusion

Dynamic mechanical analysis testing for glove materials has shown that the mechanical properties of materials under sinusoidal loading and at different temperatures behave differently, largely depending on the structure of the materials (e.g. type of foam used). Thus, this study has suggested that the properties of different glove materials will change in real world work conditions (e.g. at low temperatures).

From the data obtained in this study, it can be concluded that AV gloves are less effective in protecting the fingers at the proximal segment from vibration than they are in protecting the palm of the hand. Combining DMA data with the testing of human subjects allows the AV performance of glove materials to be predicted for different temperatures.

Chapter 6: Development of an artificial finger

This chapter introduces the development of a novel physical model of a finger that can be used for assessing finger transmitted vibration (FTV) instead of the use of the human subjects. In order to replicate both the mechanical and the vibration behaviour of the human finger, many alternative materials were investigated using tensile testing and DMA testing. The finger models produced were tested statically and dynamically under the same protocol as that used for human testing. Also, the FE model of the finger that was originally shown in Chapter 3 was used for validation purposes.

6.1 Introduction

Several recent studies have used a 3-D laser vibrometer for measuring the transmissibility at the back of the fingers, and using such a technique reduced the unreliability associated with the use of the finger adaptor method [69, 87, 95, 135]. FE modelling is considered to be the best method for providing detailed biomechanical responses inside the soft tissues of the entire system, and several studies have developed FE models to replicate the biomechanical responses of the human finger to vibration [58, 96, 107, 136]. However, no experimental method has been established that directly measures the vibration responses inside the soft issues of the hand-arm system [64, 96]. The mechanical properties of human skin differ and can be influenced by a number of factors including hydration, age and anatomical structure [108, 109]. Several materials (see Chapter 2, Section 2.5.3) have been investigated in studying the mechanical properties (including stiffness and friction) of the human skin at the fingertip to replicate the mechanical properties of the anatomical construction of the real fingertip [108].

Base on existing knowledge of the index finger, this present study was designed to develop a new physical finger model for assessing finger-transmitted vibration that can replicate the mechanical and dynamic behaviour of the real human finger at room temperature. Load-deflection measurement and vibration measurement were carried out for validation and by making comparisons with a set of measurements from tests on human participants, obtained under the same conditions (see Chapter 4). Moreover, FE modelling was used to investigate both load-deflection and vibration behaviour of artificial models using parameters obtained from human finger and materials tested in this study.

6.2 Anatomy of an index finger

Figure 6.1 shows the anatomy of the human index finger, which is described in more detail in the literature section (Chapter 2, section 2.2). The finger skin consists of different layers, and each layer of the skin has different mechanical properties. For instance, the dermis fibres support the skin's structure and provide its elasticity properties, whilst the viscous behaviour of the skin is relevant to the delay in recovery from deformation. The mechanical behaviour of human skin is related to the contribution of the dermis and is often described using a nonlinear stress-strain relationship [137].

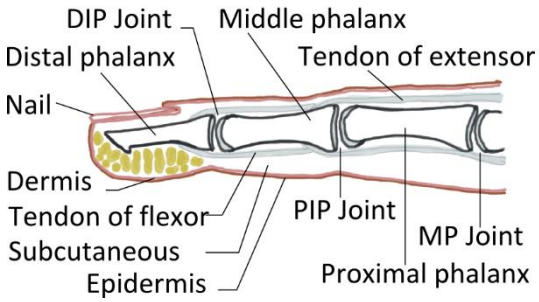

Figure 6.1: Anatomical diagram of the human index finger

Unlike typical solids, human skin behaves as an anisotropic, heterogeneous and nonlinear viscoelastic material which is similar to rubber [137, 138]. The mechanical properties of human skin consist of both viscous and elastic properties and are in depth associated with its complicated structure [139]. Possibly due to this complication some studies have considered the skin as one layer (representing both epidermis and dermis). Table 6.1 shows a summary of the mechanical properties for skin, subcutaneous tissue and bone that are used in different types of FE modelling of dynamic responses to vibration of the fingertip as well as that measured from different regions of the human skin.

Table 6.1: Mechanical properties of finger anatomy and relevant skin properties measured at different regions, gathered from literature

Citations	Property	Young's modulus	Poisson's ratio	Note
[118]	Bone	1.5 GPa	0.48	Each layer
	Skin	136 kPa		Epidermis 1 mm, dermis 0.75 mm
	Subcutaneous tissue	34 kPa		
[34]	Epidermis	136 kPa	0.48	Each layer
	Dermis	80 kPa		
	Subcutaneous tissue	34 kPa		
	Bone	1.5 GPa		
[116]	Skin	130-195 kPa	0.4	Hyperelastic and viscoelastic, 0.8 mm
	Subcutaneous tissue	59-112 kPa	0.4	Hyperelastic and viscoelastic
	Bone	17 GPa	0.3	
[140]	Skin, forearm front	101 kPa	0.5	$t_{epidermis}$ = 0.078 mm
	Skin, forearm back	69 kPa	0.5	$t_{epidermis}$ = 0.077 mm
	Skin, palm	25 kPa	0.5	$t_{epidermis}$ = 0.204 mm

The mechanical properties of skin have been investigated using both in-vivo and in-vitro techniques, and these properties are mainly identified by tensile tests, compression tests (e.g. indentation) and torsion tests. Many recent studies have used a compression test method in order to measure the elastic properties of the human skin [141].

In this part of the study, a new physical finger model was developed to have a three-layered system, which uses high modulus "bones", encased in a cylinder of low modulus (to replicate subcutaneous tissues), with an outer layer to replicate the skin, representing both dermis and epidermis

6.3 Materials

In order to replicate the mechanical and vibration behaviour of the human index finger, different materials were initially considered, as shown in Table 6.2.

Table 6.2: Candidate materials tested to replicate the finger layers

Layer	Material	Operating and storage temp.	Supplier
Skin	Tattoo skin	—	Skin UK
	Silicone sheet	—	
	Liquid latex rubber	5-25 °C	Polycraft
Subcutaneous tissues	Siliskin 10 silicone and deadener	23 °C	Polycraft
	Silicone gel based on polyorganosiloxanes	-60°C-200°C	Raytech
Bone	Polypropylene rod, 8 mm in diameter	—	Direct plastics

Materials were chosen that would have no adverse health effects on researchers during and after manufacturing processes and would be easy to manufacture at room temperature range. However, little information was available regarding the mechanical properties for all the candidate materials, except the polypropylene rod which is found to have the Young's modulus of 1.5 GPa, which is within the range of bone modulus (1.5-1.7 GPa), from the existing literature.

6.4 Tensile testing

6.4.1 Methodology

Preparation of tensile specimens

A tensile test was conducted to investigate materials that were chosen to replicate the skin layer, as listed in Table 6.2 above. Two sheets of rubber latex were produced, the thickness of which was varied using liquid latex. The latex layer was gently applied to the smooth surface using a sponge brush and curing was accelerated by using a heat gun before another layer was applied. This process was repeated until the estimated target thickness was achieved.

The dimensions of specimens used for the tensile test (see Figure 6.1) was based on the method outlined in ISO 37:2011 [142]. Each specimen was individually prepared and labelled as shown in Figure 6.3.

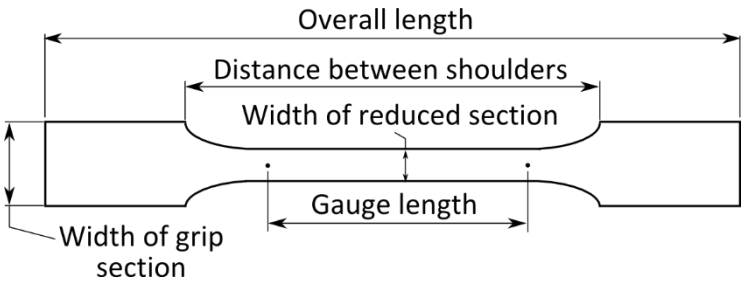

Figure 6.2: Dimensions of specimens used in tensile test

Figure 6.3: Specimens of materials tested

The characteristics of each tested material were measured before the tensile loading was applied, using Mitutoyo 500-181-30 Digital Callipers (150mm, 0.01mm resolution), as listed in Table 6.3 below.

Table 6.3: characteristics of material specimens used in the test

Materials of specimens:	Latex A	Latex B	Silicone sheet	Tattoo skin
Gauge distance (mm)	39.58	45.43	51.98	54.61
Thickness (mm)	0.73	0.78	1.44	0.91
Width of reduced section (mm)	9.25	9.32	9.86	10.52

Testing procedure

Figure 6.4 shows the set-up of the tensile test rig. The test approach used the same force-displacement stand as originally outlined earlier (see Chapter 3, section 3.2.6). The indenter was removed and two sets of serrated wedges were installed to hold the specimen. Firstly, the specimen was inserted in the right position (see Figure 6.4) and both the force and displacement devices were set to zero. A sequence tension force was applied manually using the wheel handle with an increment of 0.2 N. The tension force and corresponding reading were manually recorded for each force until the maximum limit was reached.

Due to the limitation of the test stand, all tested material reached the maximum distance of the test stand before any specimen failed. This procedure was repeated for other specimens.

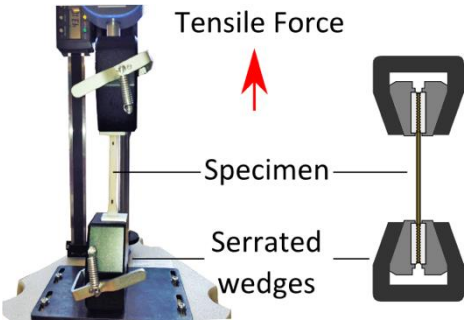

Figure 6.4: Experimental set-up of tensile test rig used in the study.

Once the testing had been conducted for all specimens, the data obtained from the tensile test was exported to Microsoft Excel to determine an engineering Young's modulus (E), which can be calculated as the ratio of the stress (σ) to the strain (Ɛ). The force measurement was used to determine the engineering stress, using the following equation:

$$\sigma = \frac{F}{A} \qquad \textbf{Equation 6.1}$$

where F is the tensile force and A is the cross-section of the specimen.

$$\varepsilon = \frac{\Delta L}{L_0} \qquad \textbf{Equation 6.2}$$

where ΔL is the change in gauge length, L_0 is the initial gauge length, and L is the length at each applied force.

6.4.2 Results and discussion

The stress-strain data obtained from the tensile test for all tested materials are shown in Figure 6.5. The results show that latex sheets A and B and the tattoo skin were found to behave similarly. However, the silicone sheet was found to be about three times as stiff compared to the other materials. The engineering Young's modulus calculated for latex A, latex B, silicone sheet and tattoo skin were 0.30, 0.44, 1.50 and 0.45 MPa, respectively.

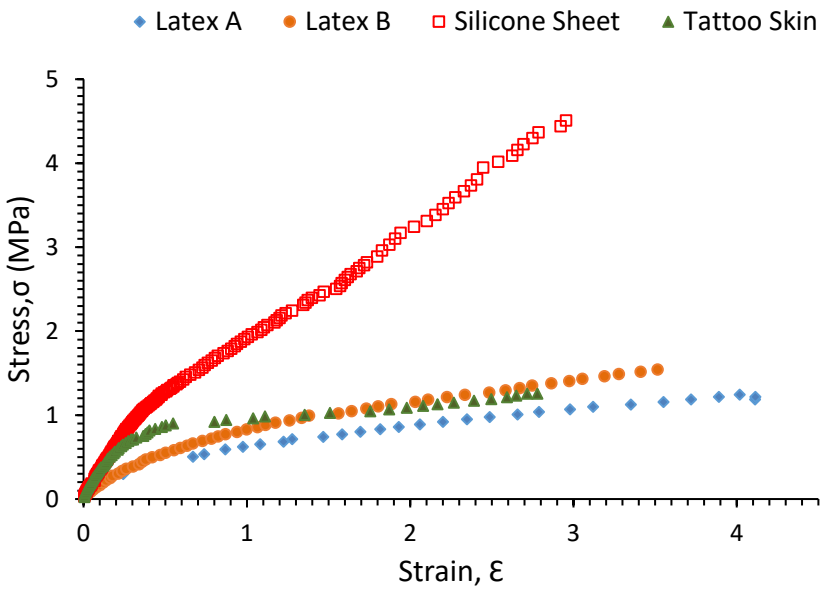

Figure 6.5: Stress-strain relationship obtained from tested materials

The variance found within the latex sheets was possibly due to the difference in the cross-section area, as it could be seen that the sheet B was thicker than the sheet A. It was reported that the skin's Young's modulus measured in a horizontal direction was found to be strongly associated with the thickness and stiffness of the skin within the tensile and compression tests [137, 138]. In addition, it might be related to the finish of the surface (i.e. the direction in which the brush was used). Even though the Young's modulus obtained from the tensile tests varied and were about 3-10 times higher than the target modulus for human skin which is 0.136 MPa, the latex material was selected in order to replicate the mechanical properties of human skin. This was because of its benefits in controlling the thickness and the possibility of applying it on other soft surfaces easily at room temperature.

6.5 Dynamic mechanical analysis (DMA)

6.5.1 Material initially investigated

A room temperature vulcanising (RTV) silicone, Silskin 10, from Polycraft (cured hardness 13±2 Share A) was first tested to replicate subcutaneous tissue. The RTV silicone is a polymer which consists of a base and catalyst mixed at a 1:1 ratio by volume before being left to cure at room temperature for 24 hours. In order to investigate the mechanical properties of silicone that approximate the behaviour of human finger, dynamic mechanical analysis was conducted using the Viscoanalyser VA2000 equipment described earlier (Chapter 5, section 5.2.1). Four silicone specimens were prepared with different percentages of deadener (S1=10%, S2=15%, S3=20% and S4=25%). Strain and temperature sweep tests were conducted on these specimens on the same day and these tests were repeated on specimens at later intervals (14, 28 and 43 days old). In the results which were obtained (see Appendixes I and J), the strain and temperature sweep tests indicated that the Young's modulus values increased in the period after each test, whereas the loss factor values decreased after each test. The results obtained from these tests indicated that the mechanical properties of the silicone change over time, which may be due to insufficient curing time and air bubbles occurring while the products were being mixed. Using this model to simulate vibration experiments would thus result in inaccuracies. Therefore, an improvement is needed in the product curing process.

After going through constructive consultation and discussion with the project supervisor and polymer experts in order to improve the mechanical properties of the utilised product it was suggested that five new silicone specimens (S1=0%, S2=10%, S3=20%, S4=30% and S5=40%) should be prepared, with the use of a degassing chamber before and after the pouring into the mould, in order to remove the air bubbles. This was done, and then the samples were cured for three days at room temperature, followed by baking in an oven for 24 hours at 70 °C. Each sample of five was then divided into three parts, and each part of one sample was tested once at intervals of one month between each test. The results obtained from the DMA (see Appendices I and K) showed that the Young's modulus values only changed slightly over time and did not change significantly with temperature changes when compared with the results obtained from the initial method for the curing process. This was especially the case with the specimen S=20% deadener, in which the loss factor

did not change significantly for the same sample in both the first test and the retested specimens.

6.5.2 Selected materials

Two materials were selected for analysis. A room-temperature curing silicone gel (Magic Power Gel, from Raytech) was used to replicate subcutaneous tissues while latex was used to replicate the outer layer skin (the dermis and epidermis). Two specimens of silicone gel were prepared with two different mixing ratios by volume (A:B) and one sample of latex sheet. The summary of the properties of the specimens are as shown in Table 6.5.

Table 6.4: Properties and dimensions of the specimens used in the study

Material	No. of specimens	Mixing ratios	Dimensions (mm)
Silicone gel	2	1:1 and 1:2	H = 35.5, Ø = 20
Latex	1	-	H = 29.3, L = 20, W = 1.6

In order to replicate the mechanical properties of the human index finger, a Dynamic Mechanical Analysis (DMA) was conducted to study the mechanical properties (Young's modulus and loss factor) of the selected materials and to investigate their sensitivity to temperature and amplitude changes. This information was used to determine the optimum mixing ratio of the silicone gel parts (base A and catalyst B) to provide a similar stiffness to that of the real human tissues.

The DMA was performed using the Metravib Viscoanalyser equipment described earlier (Chapter 5, Section 5.2.1, and Figure 5.3a). The installation of each sample varied, depending on its design. Each of the silicone gel specimens (1:1 and 1:2) was inserted between compression plates that were located in an analyser chamber, as shown in Figure 5.3b, whilst for the latex sheet sample, two clamps were used instead (see Figure 5.3c). Specimens were subjected to sinusoidal loading and the resulting force and displacement traces were used to find the Young's modulus and loss factor.

Each specimen was subjected to a strain sweep test at room temperature followed by a temperature sweep test. For the strain sweep test, each sample was tested under different dynamic strain amplitudes at room temperature, whilst the temperature test was conducted under a fixed dynamic strain amplitude over a range of temperatures. The

temperature of the specimen was measured using a thermocouple located inside the chamber. First, the chamber temperature was cooled down using liquid nitrogen until the target temperature was obtained, and then the specimen was subjected to sinusoidal loading with a selected dynamic strain. A frequency of 10 Hz was selected for all the tests and the specimens. The selection of the frequency was dependent on the calibration of the machine that showed the best dynamic response at 10 Hz and specimen size. The testing parameters are shown in Table 6.5.

Table 6.5: Parameters used for testing the specimens of materials

Test type	Strain sweep		Temperature sweep	
Material	Room temp.,˚ C	Strain range	Temp. range,˚ C	Dynamic strain
Silicone gel	23.3	0.0001-0.01	0-40	0.003
Latex sheet	25.4	0.0001-0.01	5-40	0.002

In order to check the consistency of the silicone gel (Power Magic Gel), only the specimen of mix ratio 1:2 was retested under the same condition after about 30 days whilst the geometry and dimension of specimen 1:1 were affected by the uninstallation process of the specimen. For example, it was difficult to remove the sample from the DMA machine due to the super glue used when installing, as it was very soft and sticky.

6.6 Results from DMA testing of materials

The latex specimen showed Young's modulus values of around 1.8 MPa (see Figure 6.6), typical of a rubbery polymer, which decreased somewhat with the dynamic strains as well as with the temperature. The loss factor was almost independent of the dynamic strain and decreased slightly as the temperature increased. The two silicone gel specimens showed insensitivity in both Young's modulus and loss factors to the dynamic strain levels and temperature changes (see Figure 6.7). The silicone sample with the 1:2 ratio (A:B) was about 5 times stiffer than the one with the 1:1 ratio. The results obtained for the silicone specimens allowed to determine an appropriate mixing ratio that would provide a Young's modulus value close that for subcutaneous tissues of the human finger.

The silicone gel (Magic Power Gel) with a mixing ratio of 1:1.013 was used to replicate the subcutaneous issues at room temperature. This mixing ratio was interpolated between two

known values obtained from the DMA results (dynamic sweep test) of the two silicone specimens (1:1 and 1:2) by volume at a room temperature of 23.3 °C.

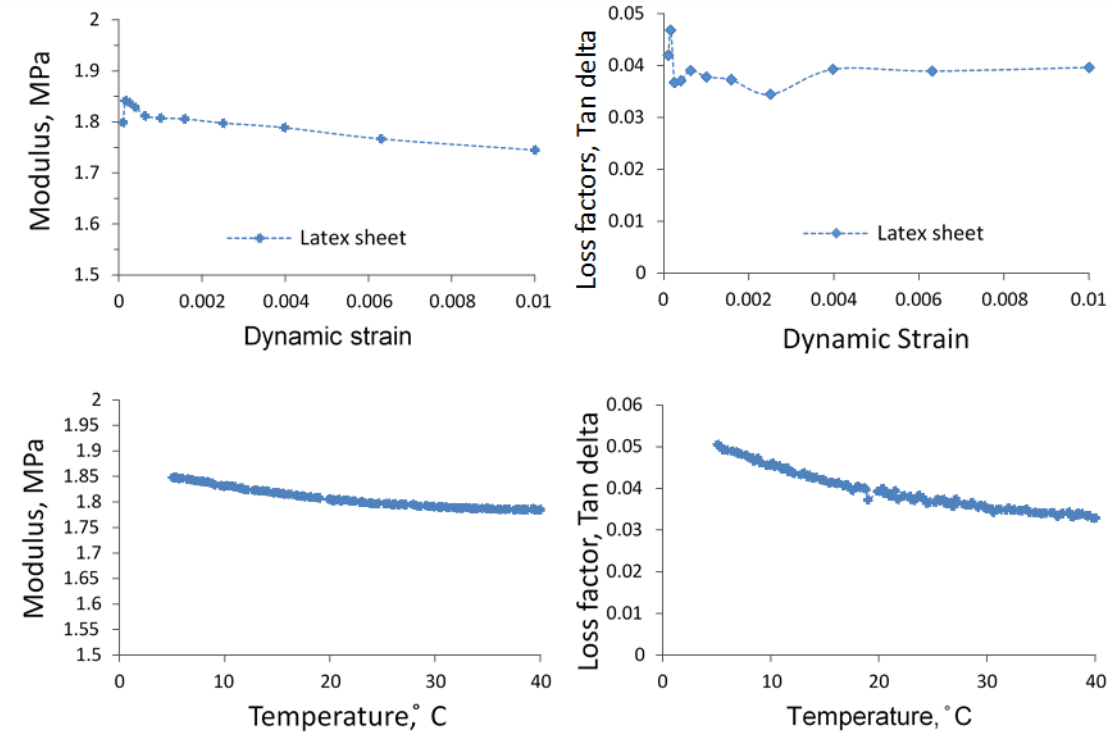

Figure 6.6: Young's modulus and loss factors against dynamic strain and temperature of latex specimen

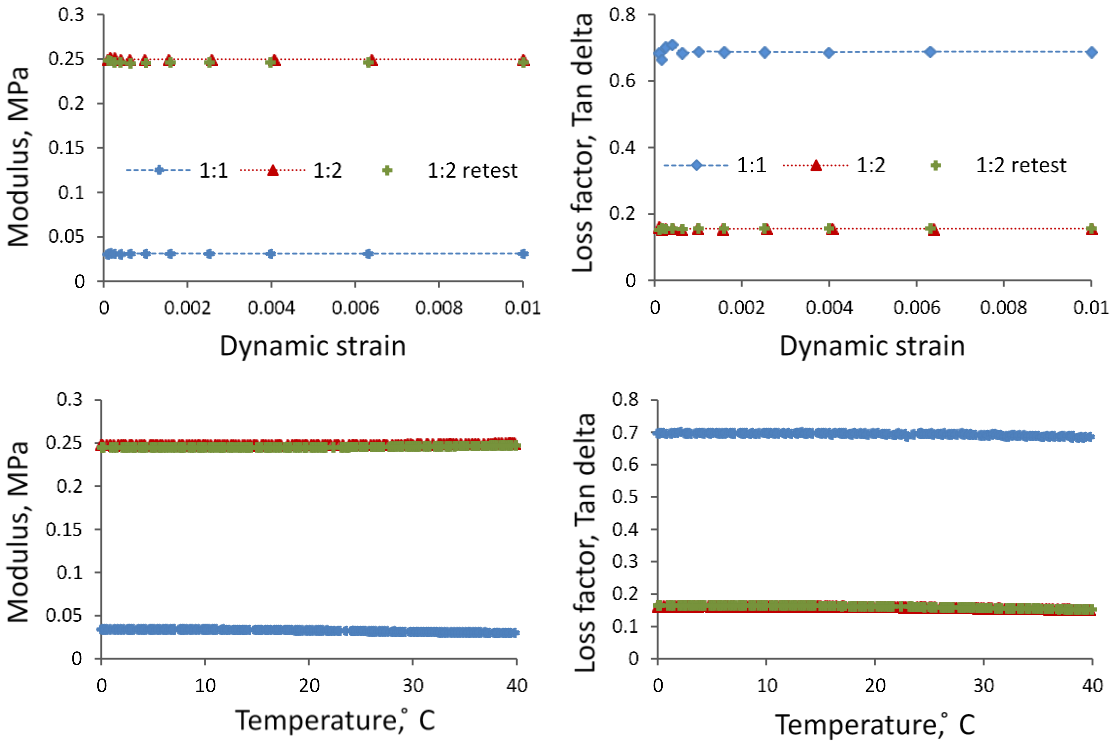

Figure 6.7: Young's modulus and loss factors against dynamic strain and temperature of silicone gel specimens

The retest results of silicone specimen 1:2 did not show any significant change in the mechanical properties over an interval of about a month, which indicates the material is a reasonable one to use for replicating both the loading and vibration behaviour of the subcutaneous tissue of the real finger. The values of Young's modulus obtained from the silicone gel materials were found to be within the range of interest. In addition, these materials (latex and silicone gel) can be stored within 5-23 °C and -60 to 200 °C, respectively.

6.7 Design idea of an artificial finger

In order to simulate the human finger, an artificial finger model was constructed, which includes the phalanx bones and its joints, and the vessels as well as the soft tissue. A proof-of-concept version of an artificial finger was made initially for the purpose of testing the pumping system. This used a pine wood rod as a single supportive structure representing the bones, as well as latex tubing for vessels. Room temperature vulcanising (RTV) silicone was moulded into a simple cylindrical shape for the main soft tissue structure. The mould itself was made using Chromatic alginate from Polycraft. This first attempt served its purpose and helped inform the next stage of design.

6.7.1 Initial prototype of an artificial finger

After the materials that approximate the behaviour of the human finger were investigated and adopted to replicate the real finger, the initial version of the finger model was designed and built, including the main arteries of the finger. A polypropylene rod (nylon), 8 mm in diameter, was used to make artificial phalanx bones that matched Young's modulus of human phalanx bones (1.5 GPa), and a nylon line was used to join them (see Figure 6.8, 1).

An artificial finger mould was then designed and manufactured from metal and considered as a uniform cylinder (see Figure 6.8, 2). The dimensions of the artificial finger were based on a man's index finger from measurement data taken from older adults, whereas the locations of the phalanx bones and the arteries are based on MRI and X-ray images of the human finger [113]. The Young's modulus of the human finger was previously defined and used for FE modelling of fingertip: for a bone (E =1.5GPa), skin(epidermis and dermis) (E = 0.136 MPa) and subcutaneous tissues (E =0.034 MPa) [34, 143]. Surgical latex tubing, ID=

1/16 (1.6 mm) and wall thickness =1/32 (0.8 mm), was used to replicate the digital arteries in the finger.

Manufacturing procedure

First, three polypropylene phalanx bones were prepared with three different lengths to replicate the length of the distal, middle and proximal phalanxes (15.82, 22.38 and 39.78 mm) [113]. These bones each had a hole along its axis, which made it possible to join them using a nylon line, 1.5 mm in diameter. Once positioned with the correct spacing between them, the bones were bonded to the line using cyanoacrylate adhesive (Krazy glue). Both the joined phalanx bones and surgical latex tubing were then installed inside a metal mould prepared for this purpose (Figure 6.8, 2). The silicone components (at a ratio of 1:1.013) were mixed using a wooden stick for about 1 minute and degassed using a self-assembled degassing chamber (a 3CFM Rotary Vane Vacuum Pump was used) as shown in Figure 6.8, 3 & 4) until it was clear and transparent (bubble-free), then the mixture was poured into the mould clamped and cured for 10 minutes, before being released (Figure 6.8, 5 & 6).

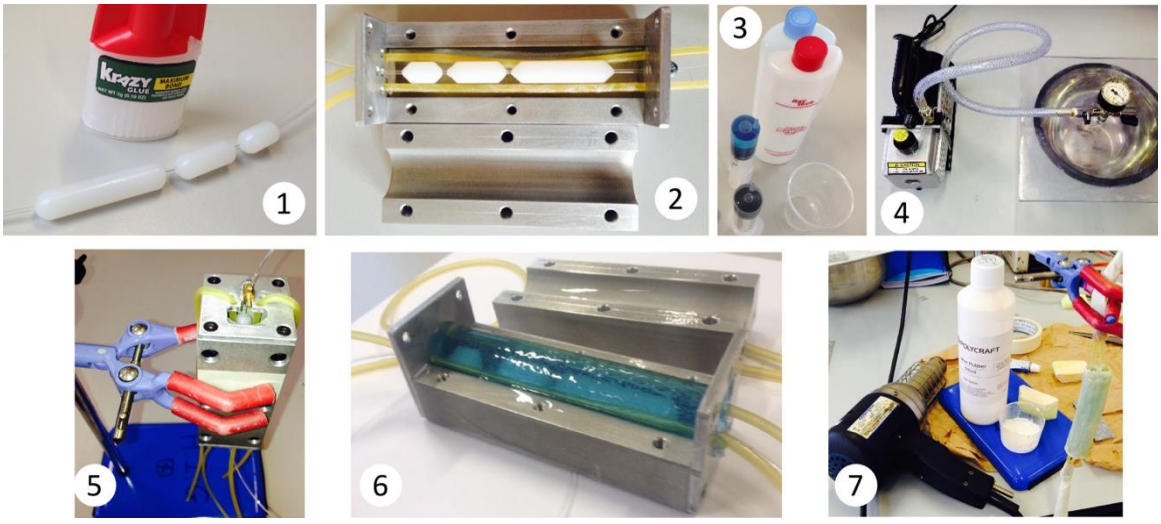

Figure 6.8: The stages of developing an artificial finger model

The artificial model was then painted with liquid latex to replicate the outer layer of the human skin. The latex was applied in layers and cured with a heat gun until the required thickness was gained (Figure 6.8, 7).

Thickness measurement of the skin layer finger model

Because the latex has a Young's modulus higher than that of human skin, the thickness of the outer layer was made to be thinner than that in a human index finger. It was found that it was a challenge to obtain an accurate and homogeneous thickness of the outer layer. Therefore, the outer skin layer of the model was then imaged using the Optical Coherence Tomography system (OCT), from VivoSight (see Figure 6.9), which is usually used for skin research. The OCT system used was based at the Royal Hallamshire Hospital, Academic Unit of Dermatology Research, Sheffield. The images were then analysed using a Matlab algorithm (Matlab version R2015a) based on an analysis of the light reflectivity/backscatter profiles (A-scans), to obtain an accurate measurement of the thickness of the outer layer [144], as shown in Figure 6.9 below.

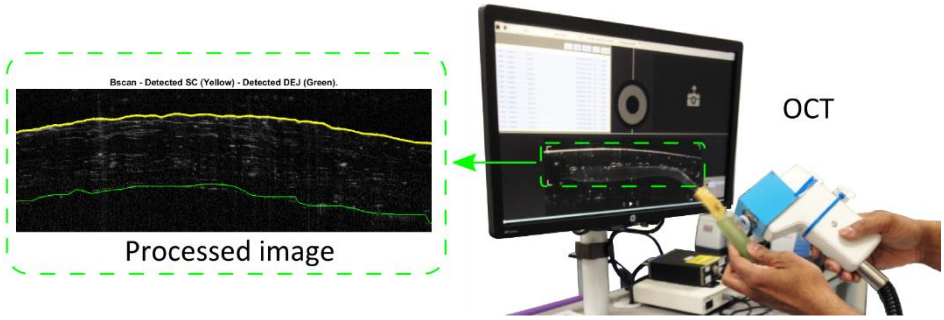

Figure 6.9: Optical Coherence Tomography system used and the processed image showing the detected outer and inner edges of latex layer

Using the OCT scanner allowed the measuring of the thickness of the skin layer and the structure quality of materials used. The parameters of the initial artificial finger are listed in Table 6.6 below.

Table 6.6: Characteristics of initial model of the finger.

Latex skin thickness		Total mass	Length	Outer radius	Volume
Mean, mm	SD, mm	grams	mm	mm	mm^3
1.071	0.060	37.1	102.1	11.1	39314

The main aim of this part of the study was to develop an artificial model of the finger which allowed the effect of vibration on finger circulation to be studied. However, attendance at a HAVS conference, early in the PhD study, greatly improved the researcher's under-

standing and facilitated discussions with leaders in this field. This led to a refinement of the project objectives, as a result of which the effects of other related factors were studied instead. Therefore, the final design of the finger model was kept as same as the initial model, but without the circulation system, as shown in Figure 6.10.

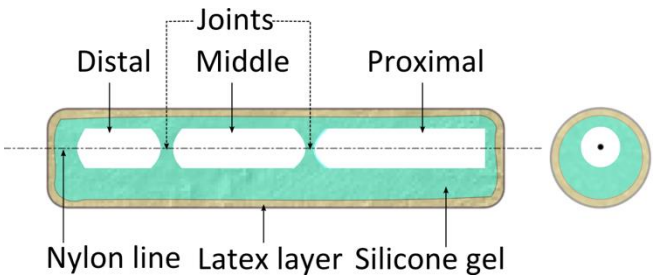

Figure 6.10: Final, adopted structure of the artificial model of the finger

However, the initial version of the finger model was used to develop a suitable concept for mounting the finger model on the test handle (see Figure 6.11). It was also used to assess the vibration system, along with human subjects (e.g. grip force and transmissibility).

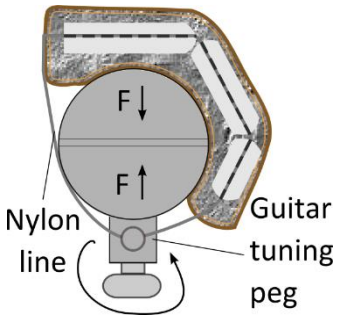

Figure 6.11: Cross-sectional diagram of the finger model mounted on the test handle

6.7.2 Development of an artificial model of finger

In order to study the effect of the thickness of the skin layer on both the static and dynamic behaviour of the finger model, five artificial models of the finger were produced: four of them used the same protocol utilised earlier in the initial version while one used a 1:2 mixing ratio for comparison. The outer layer was varied among all five models and their properties are listed in Table 6.7. The OCT images of the skin layer of all five produced models are as shown in Figure 6.12. To ensure that the finger model would not rotate when mounted on the test handle, a thick latex sheet was built into the top of the proximal end of the model and covered the nylon line. The sheet was crimped using double-barrelled crimps at the distal end. The final structure of the model is as shown in Figure 6.13.

Table 6.7: Characteristics of all five models of the finger used in the study

	Silicone gel	Latex skin thickness		Total mass	Length	Outer radius	Volume
Artificial Finger	Mixing ratio	Mean, mm	SD, mm	grams	mm	mm	mm^3
AF1	1:1.013	1.202	0.055	40.9	102.4	11.2	40353
AF2	1:1.013	1.195	0.051	40.3	102.4	11.2	40297
AF3	1:1.013	0.616	0.040	36.2	101.2	10.6	35820
AF4	1:1.013	1.285	0.056	39.9	102.6	11.3	41019
AF5	1:2	0.299	0.024	35.6	100.6	10.3	33503

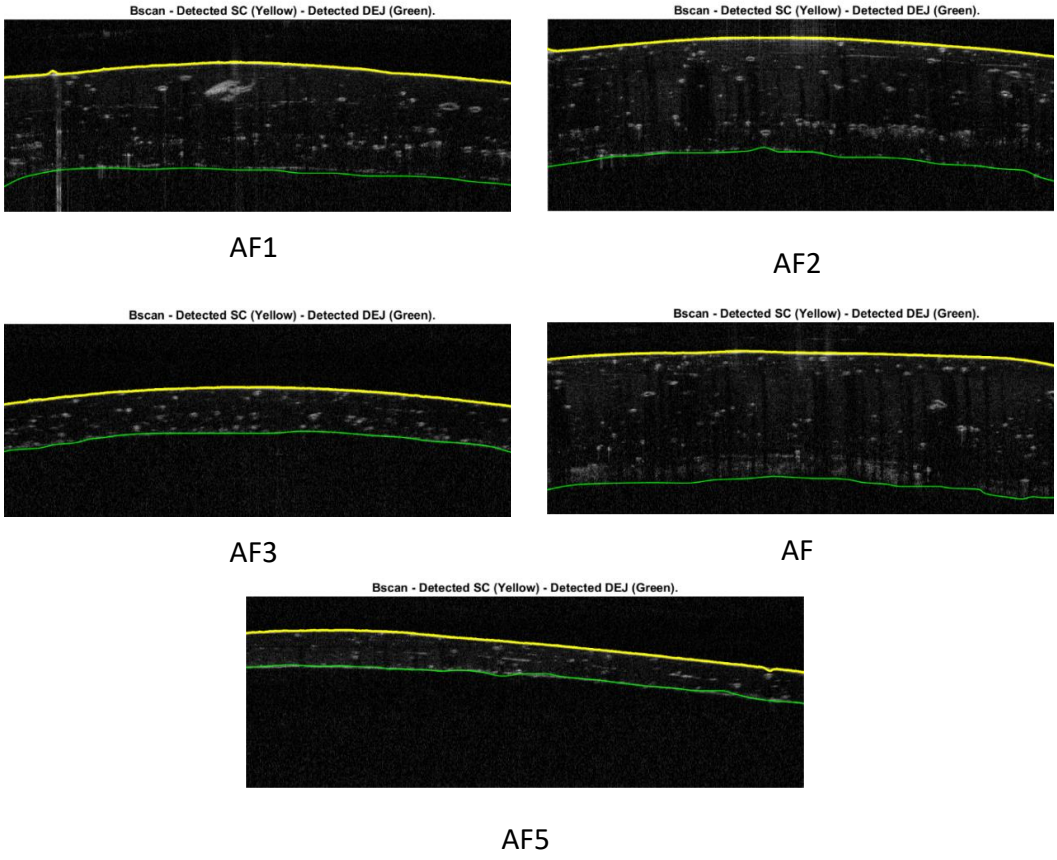

Figure 6.12: Processed OCT images of outer layer (latex) of five artificial fingers

Figure 6.13: Image showing the final version of an artificial model of the finger

6.8 Measurements of static behaviour

Cutometer measurement

Before both indentation and vibration measurements were conducted, the outer layer of each of the five models of the finger was characterised (see Figure 6.14) using an MPA cutometer device and protocol the same as used for human finger testing (see Chapter 4, Section 4.2.9).

Figure 6.14: Artificial model of the finger being tested using a cutometer probe.

Indentation test

The load-deflection behaviour of each of the five finger models was carried out using the same test rig described and used earlier for human measurement (see Chapter 4, Section 4.3). However, for the artificial models, the test rig was set up vertically instead. The testing set-up was as shown in Figure 6.15.

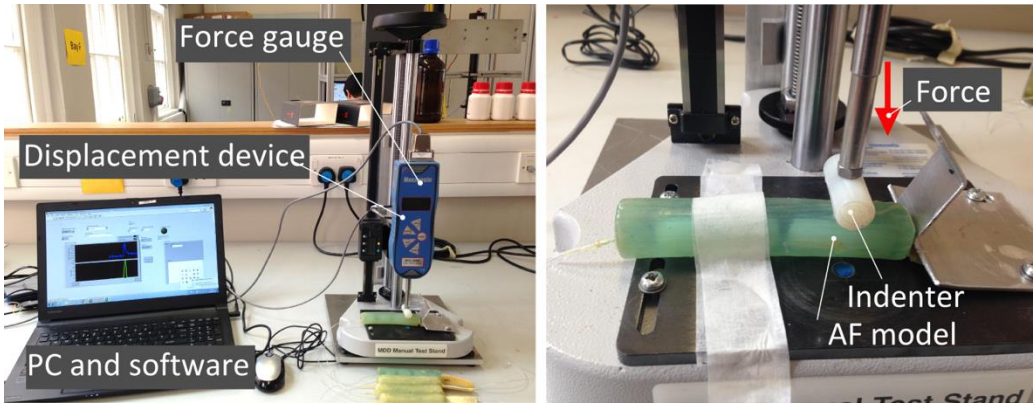

Figure 6.15: The experiment set-up for indentation measurement used for artificial fingers

However, because the geometry of the finger model was designed as a uniform cylinder, only the proximal segment of model was tested and left in its straight posture (see Figure 6.15) not curved like the proximal of the human finger. The reason for this was that the geometry of the finger model was less affected by posture than the human proximal. Testing and data analysis followed the same protocol as used for the human measurements.

Load-deflection of FE model

A 2D FE model of the proximal finger that was presented earlier (Chapter 3, Section 3.3.3) was used to produce indenter load-displacement data for comparison. The material parameters were set using the original FE model (human parameters). A second simulation was also carried out using material properties for the artificial finger AF3. Since the FE model was two-dimensional, the force-displacement behaviour was estimated to allow the comparisons with that obtained from testing. The method considered the force-displacement behaviour of a rigid cylinder (indenter with the same diameter as that used for testing, Section 4.3) being pressed against a soft cylinder (finger). It was assumed that the contact occurs between the curved faces and axes of the two cylinders are perpendicular to each other, as shown in Figure 6.16.

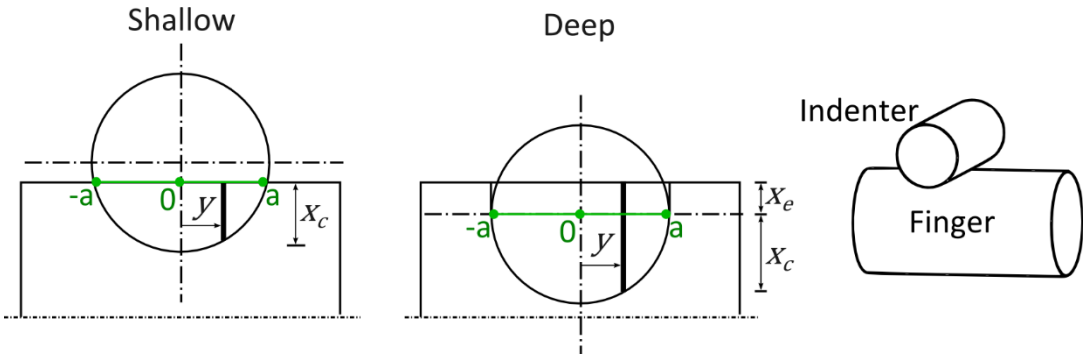

Figure 6.16: Cross-sectional diagram of method used to estimate force-displacement behaviour of 2D FE model of finger

The input to this calculation was the force-deflection data obtained from a slice of the soft cylinder (1 mm in thickness) as it is pressed against a flat surface. An estimate of the effect when pressing against a cylindrical indenter lying across the finger can be obtained by summing a series of slices, each at different depths. An analysis is slightly different if cylinder penetration x exceeds its radius r_{cyl} (see Figure 6.16). This calculation was

performed using a Matlab function (Matlab version R2016a) that estimates the total force (f_{total}) at each depth using Equation 6.3.

$$f_{total} = \int_{-a}^{a} f_y \, dy \qquad \textbf{Equation 6.3}$$

where a is the maximum contact distance at each depth and f_y is the force per unit width on the thin slice. This can be obtained from the 2D model for a given displacement x_y,

Shallow	Deep
$a = \sqrt{2r_{cyl}x - x^2}$	$a = r_{cyl}$
$x_y = x_c$	$x_y = x_c + x_e$
$x_c = \sqrt{r^2{}_{cyl} - y^2} - (r_{cyl} - x)$	$x_c = \sqrt{r^2{}_{cyl} - y^2} - (x - r_{cyl})$

The estimation ignores the effects of tensile loads generated along the length of the cylinder (indenter). It should be noticed that the displacement was higher in both human and artificial models testing than the FE models, this is due to the fact that force-displacement data obtained from the FE model only be calculated between the skin layer and the bone as mentioned above, but not across the finger as it does in testing.

Results

Properties of skin layer

Table 6.8 listed the R values obtained from the cutometer of all five artificial models of finger and its thickness obtained from OCT images, as well as the mean and standard deviation of R values measured previously from human testing, at proximal finger P (Chapter 4, Section 4.5.7) for comparison.

Table 6.8: Cutometer parameters and OCT thickness of skin layer obtained for artificial models and the mean and SD measured at proximal segments of human participants

	Skin thickness (mm)	R0	R1	R2	R5	R7
AF1	1.202	0.65	0	1	1.25	0.81
AF2	1.195	0.69	0.03	0.96	1.25	0.78
AF3	0.616	**1.17**	0.07	0.94	1.08	0.64
AF4	1.285	0.68	0.01	0.98	1.27	0.79
AF5	0.299	0.92	0.03	0.97	1.16	0.67
Human P	—	**1.18±0.39**	**0.55±0.41**	**0.56±0.11**	**0.31±0.09**	**0.14±0.03**

The distensibility of the skin layer of artificial models (R0) was found to increase as the thickness of the outer layer decreased. The R0 value of the AF3 model was found to be about the same as that of the human one. However, the AF5 has a thinner skin layer and behaved differently as its soft tissue was five times stiffer than others which were developed to have the same stiffness. Moreover, the ability of the skin to return to its original state (R1) was found to be about five times lower compared to that measured at the proximal of the human finger. However, other R values (R2, R5 and R7) were found to be lower at the artificial models of finger than at the human ones, indicating that the artificial skin is generally stiffer compared to the skin of the human proximal. This was expected from the material testing, where the outer layer was found to be about 10 time stiffer that human skin.

Load-displacement behaviour and stiffness measurement

The results obtained from the indentation testing for artificial fingers and the comparison data obtained from FE models (human data and tested material data) were displayed with the load-displacement data obtained from human participants, at the proximal finger (see Figure 6.17).

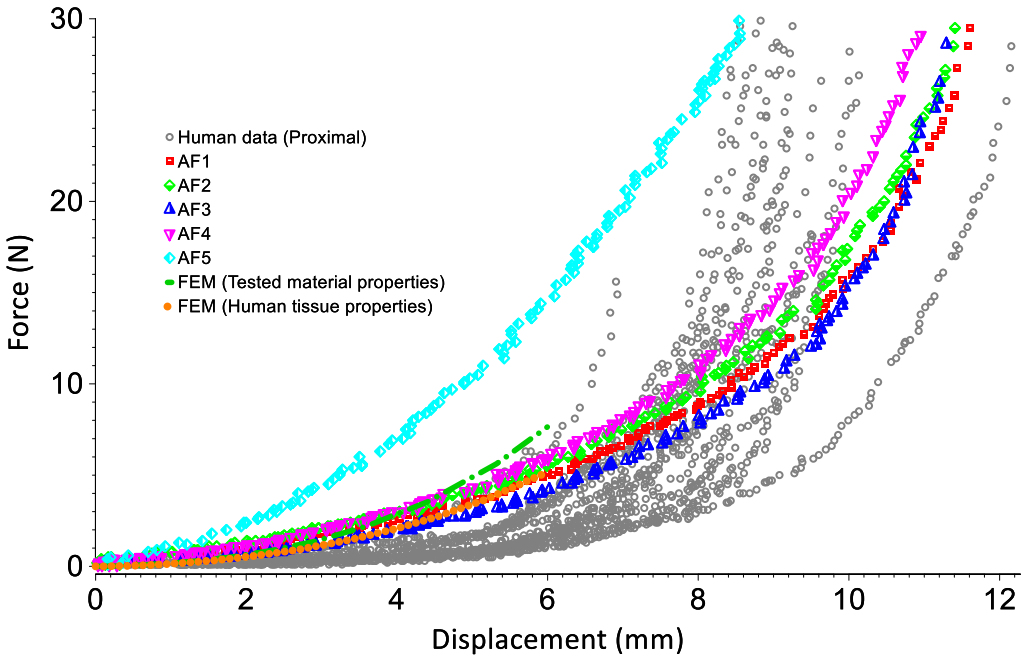

Figure 6.17: The load-displacement behaviour of five artificial finger models and the data obtained from the human right index proximal finger, as well as the FE models using human data and data from materials used in this study

The results showed that the artificial models appears to have similar loading behaviour to that in the human finger at low loading force ranging from 0-2 N, except AF5 which was developed with a different stiffness (5 time stiffer) for comparison. The AF3 model was found to be the closest to the human finger. The estimated load-displacement data obtained from FE models showed that the FE model of tested material properties was found to behave somewhat similarly to that of the artificial models (see Figure 6.18) and displayed slightly above the AF3 one. Also, that obtained from the FE model that used human data behaved like that of the human finger at low loadings. It should be noted that that the load-displacement behaviour (and the peak load tolerated) for the finger models

was found to vary among artificial fingers with similar stiffness of soft tissues, with the differences mostly depending on the skin thickness of the finger and the loading variance.

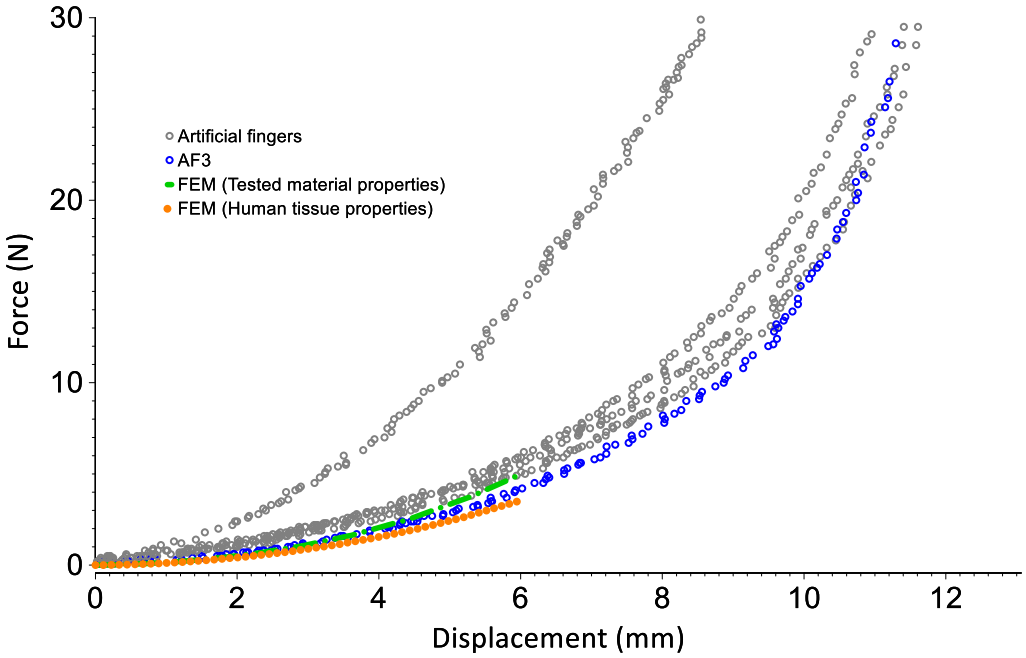

Figure 6.18: The load-displacement behaviour of FE models using human data and data from material tested in this study and the five artificial finger models

Table 6.9 shows the stiffness measured at loading forces of 5 and 10 N, for all five artificial models (see Appendix L), as well as that obtained from human measurement (see Chapter 4, Section 4.5.9).

At the loading of 5 N, the stiffness was approximately two to three times lower in the artificial fingers than in that of the human proximal and about three to five times that of the human distal. The AF5 model was the stiffest. The stiffness at the proximal was found to be doubled when the loading force of 10 N was applied. However, for the artificial models the stiffness increased by about double for all the fingers. This was mostly due to the geometry of the artificial finger layers which were designed as a uniform cylinder, which allowed an easier deflection than the human finger.

Table 6.9: Comparison of stiffness obtained from human testing and all five artificial models of finger

	Stiffness, N/mm						
	Human proximal	Human distal	AF1	AF2	AF3	AF4	AF5
At 5 N	3.84±0.8	5.96±1.12	1.32	1.18	1.38	1.51	2.82
At 10 N	8.67±3.45	14.60±2.55	2.72	2.77	3.27	2.61	3.50

6.9 Vibration measurement

The vibration measurement and transmissibility evaluation were carried out using the same protocol that was used for human testing (Chapter 3, Section 3.3.4). The finger model was first mounted on an instrumented cylinder (right end) to replicate a typical tool handle. The model was gripped using a nylon line inserted into guitar tuning pegs, one of which was attached to each end of the handle. Another model was mounted on the left end for balancing purposes. A miniature accelerometer (model 3224B) from Dytran, weighing 0.3g, was attached at the back of the proximal part of the model (see Figure 6.19). The finger model was then subjected to swept sinusoidal vibrations ranging from 10 to 400 Hz, all with an amplitude of 5 ms^{-2}. The transmissibility was measured with and without the glove and three different grip forces were used (15, 30 and 50 N respectively).

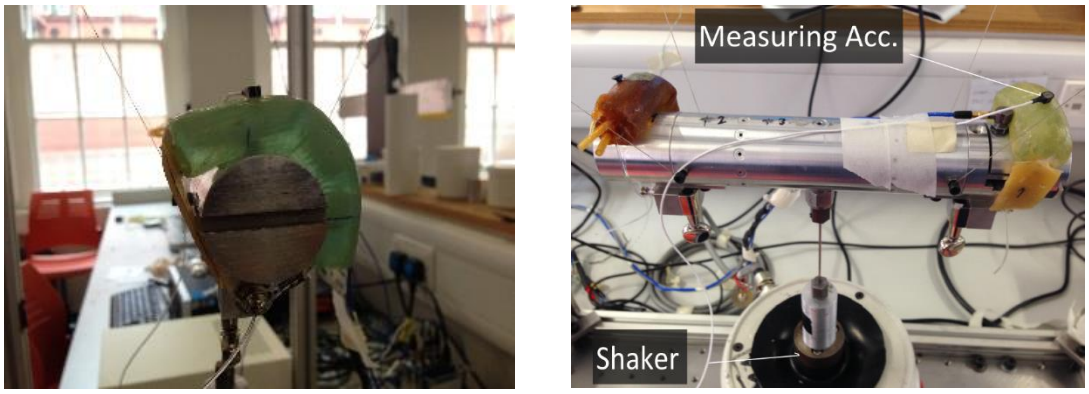

(a) (b)

Figure 6.19: The experiment set up for transmissibility measurement: a) side view of the finger model being mounted on the test handle; b) front view of tested model and balancing model (initial version) mounted on the left end of the handle

Before the final artificial fingers were tested, vibration measurement was carried out for the initial version of the finger model. The testing followed the same procedures but only

measured for the bare finger. The measurement was repeated twice, one with the accelerometer attached to the bone via a metal screw and one on the outer skin layer.

Results

Initial version of artificial model of finger

The results obtained from the initial model of the finger (see Figure 6.20) showed that the vibration responses of the skin layer and the bone were found to behave similarly at frequencies below 100 Hz. However, the transmissibility magnitude of the skin layer tended to be higher as the grip force increased. Thus, at frequencies above 100 Hz and a grip force of 15 N the resonance peak of the skin layer was higher than that of the bone. However, the resonance peak decreased as the grip force decreased, indicating that the response of the skin layer is more affected at high frequencies beyond 100 Hz than it is at low frequencies.

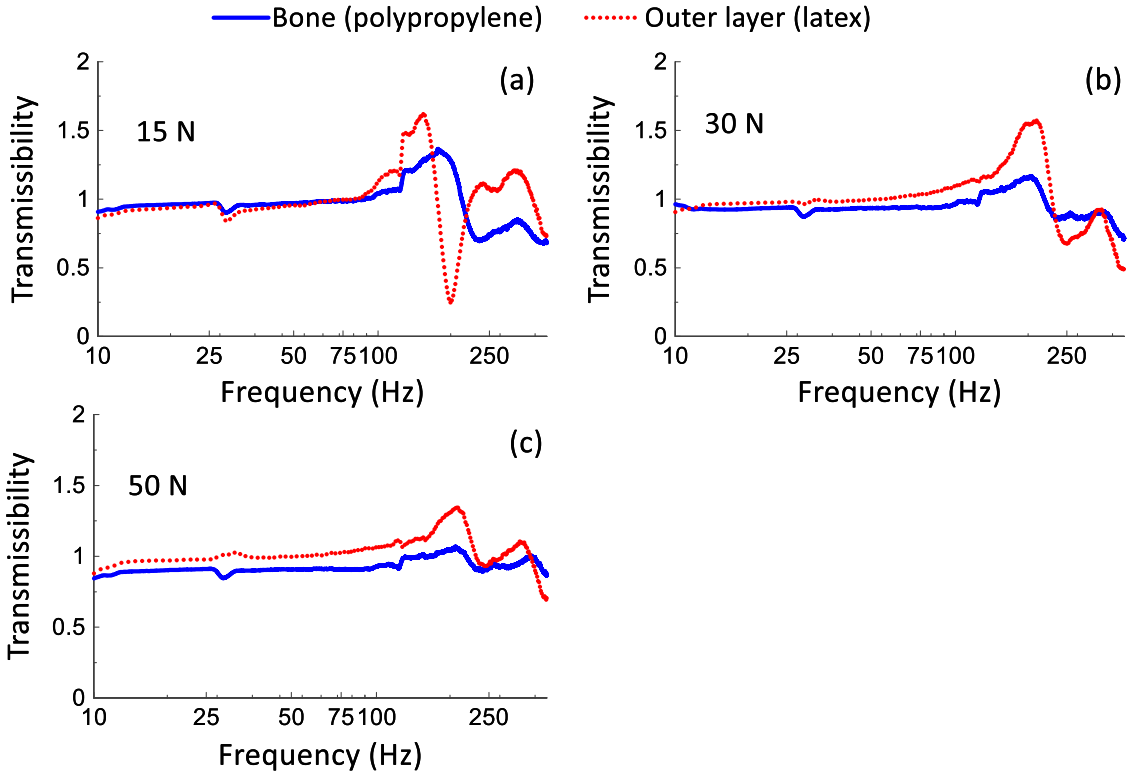

Figure 6.20: Transmissibility measured at the bone (polypropylene) and outer layer (latex) of initial finger model

Grip force measurement

In order to examine the consistency of grip force applied during on the transmissibility measurements, the grip force was first assessed. Table 6.1 shows the mean and standard deviation of grip forces measured for all five artificial fingers and that previously measured for the human ones in Chapter 4, Section 4.5.10, with and without the glove. The results showed that the finger models tended to obtain the target force more accurately than that measured for the human ones. The standard deviation showed that the fluctuation of the grip force during the test was within the accepted range force (both artificial and human) as ISO 10819 allowed the fluctuation of ±5 N of target force [72]. The results of the forces measured against frequency and transmissibility peaks, for artificial fingers, are shown in Appendix M. The grip forces measured were consistent and differentiated, and not affected by the vibration testing.

Table 6.10: Mean grip forces measured for the finger models and human fingers with and without the glove, target grip forces of 15, 30 and 50 N

Finger	Ungloved			Gloved		
	15 N(SD)	30 N(SD)	50 N(SD)	15 N(SD)	30 N(SD)	50 N(SD)
AF1	16±1.05	31±1.04	49±1.04	14±1.06	30±1.08	49±1.22
AF2	16±0.97	30±1.06	50±1.18	16±1.01	32±1.00	51±1.16
AF3	15±0.97	30±1.11	50±1.13	15±1.02	29±1.08	50±1.17
AF4	15±0.98	30±1.08	50±1.18	15±1.01	30±1.06	50±1.13
AF5	15±0.94	30±1.04	51±1.23	15±1.03	30±1.03	50±1.27
Human	16±1.23	30±1.71	48±1.87	16±1.20	30±1.71	50±1.85

Transmissibility measurement of artificial models

The transmissibility measurements of the finger models and the human measurement are shown in Figures 6.21, 6.22 and 6.23.

The transmissibility measured from the finger models showed similar behaviour to that measured from the human finger (see Chapter 4, Section 4.5.10) at all three grip forces (15, 30 and 50N) when measured without wearing the glove (Figure 6.21). Both the model finger and the human one showed resonances at frequencies slightly above 100 Hz, whilst the human finger had another peak at about 40 Hz that increased with the grip force, and it was a little higher when the glove was being worn (see Figure 6.22), which is possibly due to the variance in the grip force. However, with the gloved finger, the finger models showed consistency in transmissibility at frequencies below 100 Hz and the transmissibility magnitudes were found within the range of the data from the human fingers at all measured grip forces.

The glove transmissibility did not show any resonance at frequencies below 100 Hz, unlike the human finger, which showed resonance when wearing the glove (see Figure 6.23).

However, at frequencies above 100 Hz, the vibration responses were found to vary among both the finger models and the human fingers. Model AF3 was found to be the best model finger as it behaved most similarly to the human fingers. Model AF5 was the worst, at all testing conditions, as it was built differently (stiffer soft tissues, mix ratio of 1:2) from the other models.

For the other models (AF1, AF2, AF3 and AF4), the variance in the resonance peak was found to be strongly related to the thickness of the outer layer. The model with the thickest skin layer AF2 tended to resonate higher in most cases, and it was about double when the glove was worn (see Figures 6.21 and 6.22).

The glove transmissibility measured from finger models AF1, AF2, AF3 and AF4 was found to have similar behaviour of that obtained from the human fingers. However, at 50 N, the model AF5 tended to behave the same as the other models (see Figure 6.23). Also, the signals measured from the finger models were reliable compared to those measured from the human ones.

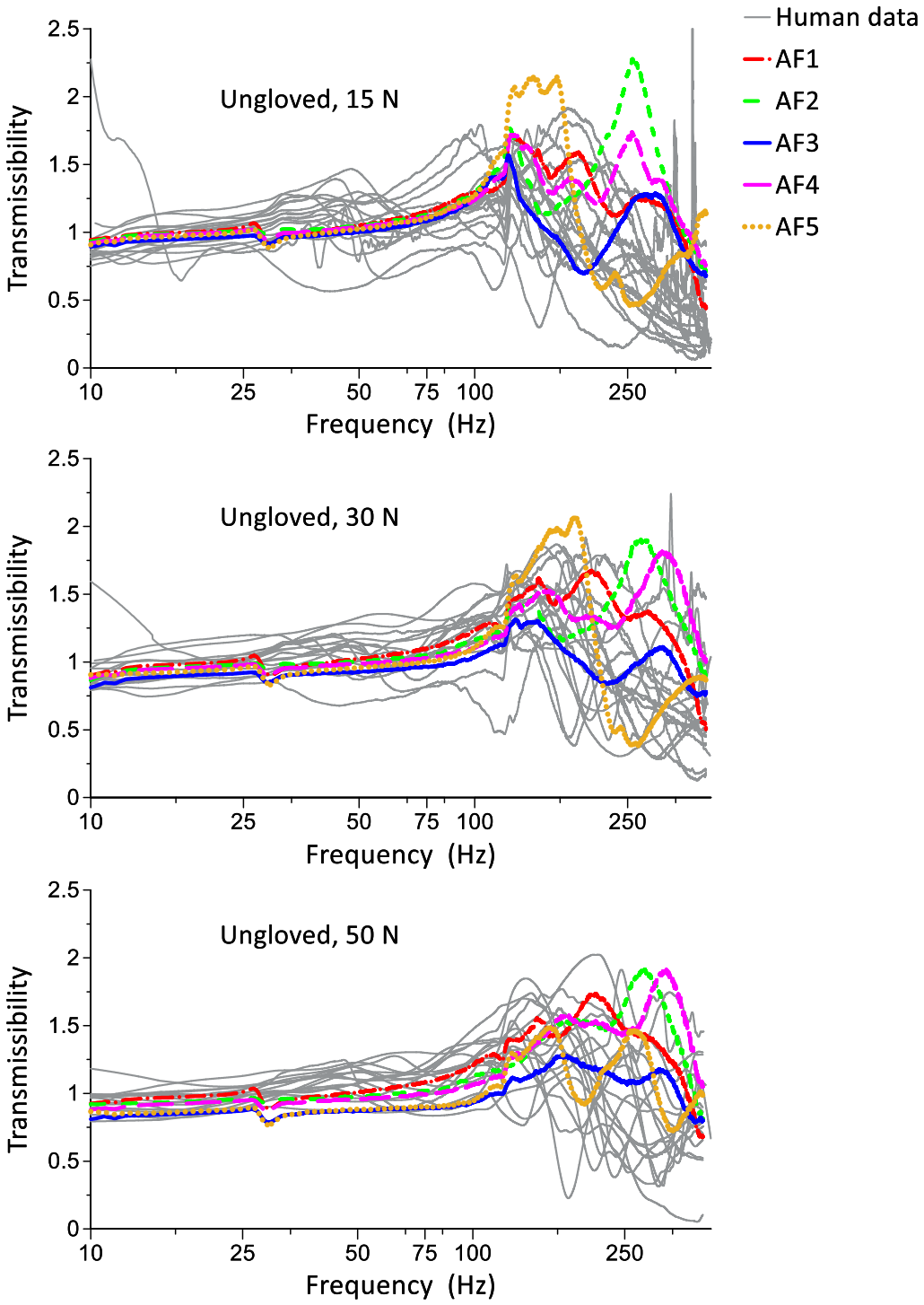

Figure 6.21: Transmissibility measured throughout artificial models of the finger (ungloved) and data obtained from ungloved human proximal right index finger under grip forces 15, 30 and 50 N

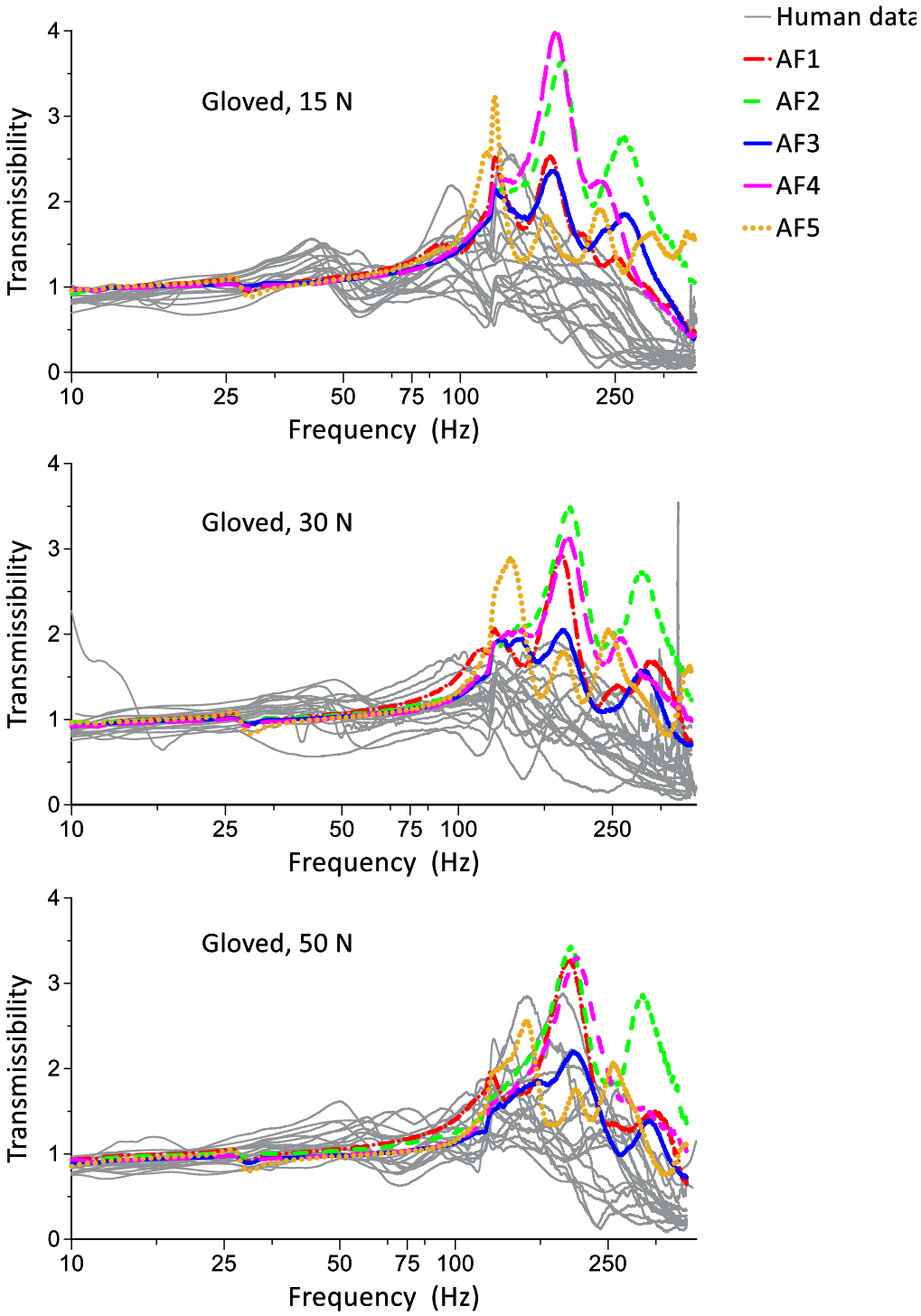

Figure 6.22: Transmissibility measured throughout the gloved artificial models of the finger and data obtained from gloved human proximal right index finger under grip forces 15, 30 and 50 N

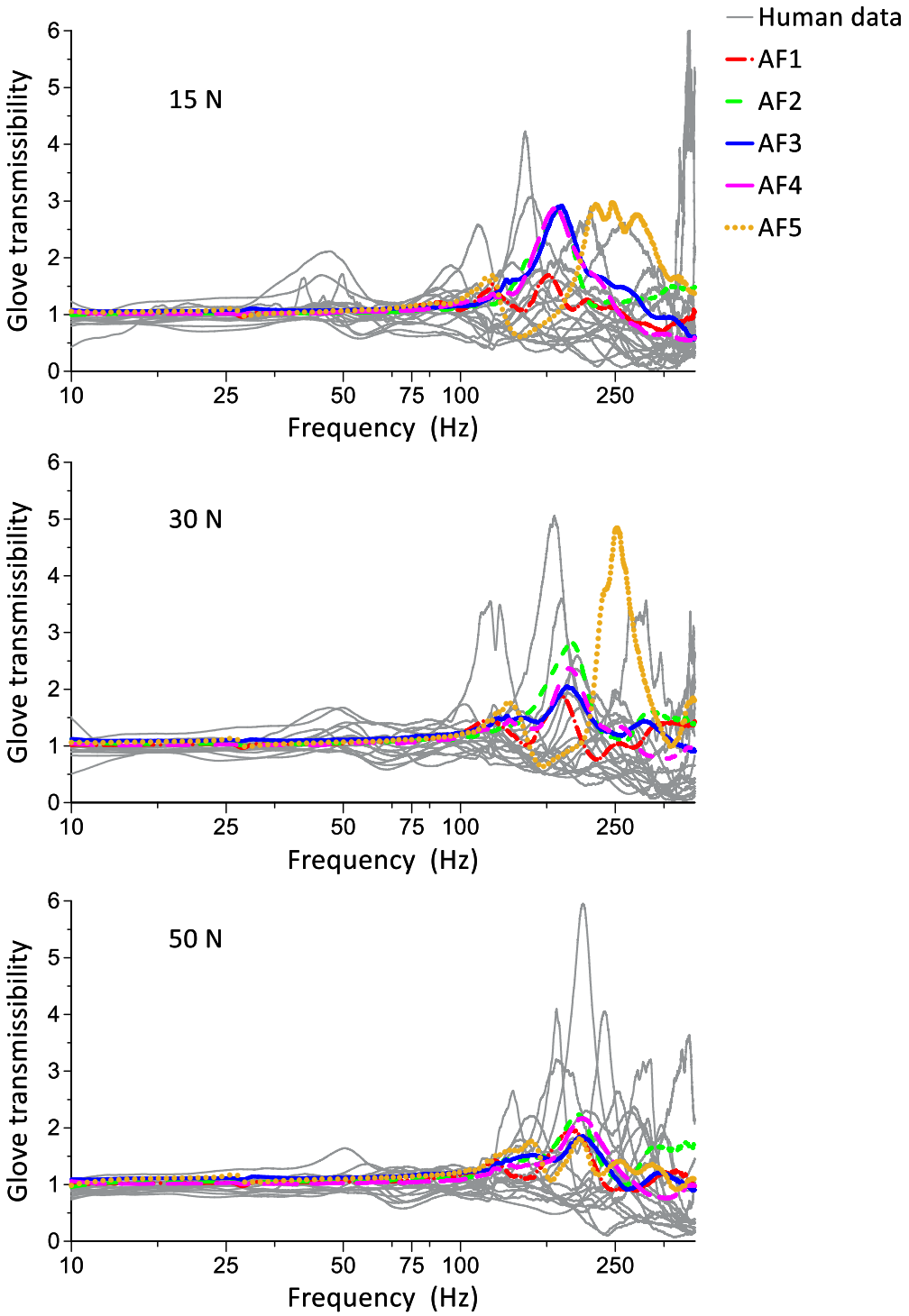

Figure 6.23: Transmissibility of the glove used in this study and under grip forces 15, 30 and 50 N for artificial models of the finger and all human data

6.10 Finite element model

The effect of grip force

The 2D FE model of the proximal finger (see Chapter 3, Section 3.3.3) was also used to examine the effects of the grip force on the transmitted vibration of the proximal finger. Figure 6.24 showed the transmissibility measured from the FE model when three different grip forces were applied (0.1, 0.2 and 0.3 N) such that produced a corresponding deflection of 2, 3 and 4 mm respectively towards the rigid surface. It should be noticed that the grip force applied was per slice (1 mm in thickness) and it was difficult to match the full finger-thumb grip force (15, 30 and 50 N) as it is distributed around the test handle. The results showed that the resonance frequency was found to increase with the grip force. However, the transmissibility magnitude at low grip force was found to be similar up to resonance frequency and decreased at frequencies beyond resonance frequency.

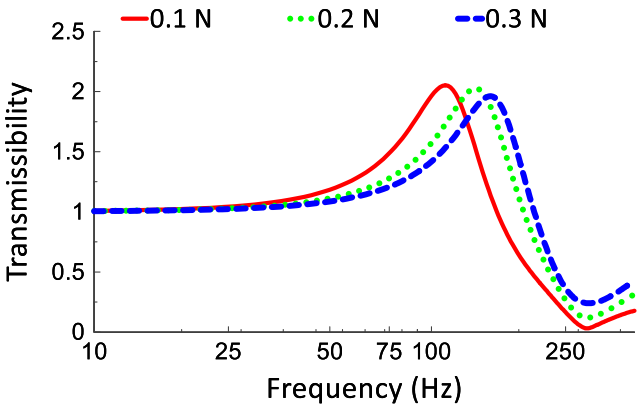

Figure 6.24: Transmissibility obtained from FE model of proximal finger under different grip levels

The distributions of strain at resonance frequency throughout the FE finger, for three different forces applied, are shown in Figure 6.25. The strain mainly occurred around the soft tissue including the position of the main arteries of the finger. At a low grip force, the high strain concentrated around the tissues between the bone and the skin. As the grip force increased, the high strain tended to be at the finger sides, as seen at 150 Hz (see Figure 6.25).

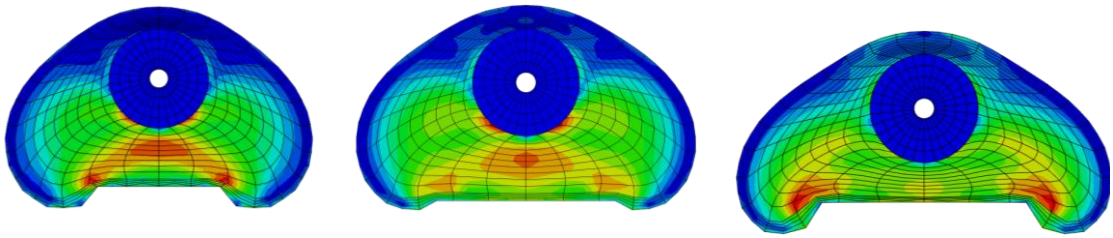

112 Hz 136 Hz 150 Hz

Figure 6.25: Mode shapes of the FE model showing the distribution of maximum strain at resonance frequency across the finger, for grip levels of 0.1, 0.2 and 0.3 N

2D FE model validation of parameters from tested materials

In this section, the FE model of the finger was used to validate the vibration behaviour of the artificial finger. The dynamic response was carried out for an FE model of the finger that used properties of the human finger (original FE model), followed by an FE model that used the properties of tested materials that were used to develop the artificial finger (latex and silicone gel). Both models were pressed from the bone towards the rigid surface by 6 mm in order to simulate the effect of the maximum gripping on FTV. The transmissibility measurement (see Figure 6.26) showed that both FE models were found to have similar behaviour at frequencies of 120 Hz. The FE model that simulated human data was found to resonate at a slightly lower frequency to the one that used the tested materials (190 and 198 Hz respectively). This is possibly due to Young's modulus of the skin layer (latex) being about ten times higher than that of human skin. However, the peak was higher for the tested material properties than for that of the human tissue properties of finger indicating that the loss factors of human tissue higher that found for latex (0.04).

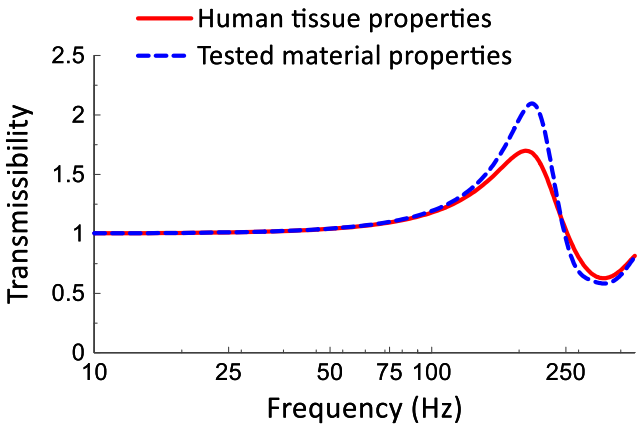

Figure 6.26: Transmissibility measured from FE model using both human and tested material parameters and deflection of 6 mm towards the handle.

Figure 6.27 shows the mode shapes of both FE models (human and tested materials), at the peak frequency and 400 Hz. In general, the strain distribution at resonance frequency appeared around the soft tissues of both models and was higher for the human one. At 400 Hz, the strain was found to be high at the finger sides. The skin layer was affected in the human model, unlike in the material model (see Figure 6.27 b) where the skin layer was not dynamically affected. As mentioned earlier, the material used in order to replicate the skin was ten times stiffer than the human skin. Also, both FE models at all conditions showed that the main arteries of the finger were found to be most affected by vibration, which was considered to be one of the factors that may lead to vibration-induced white finger.

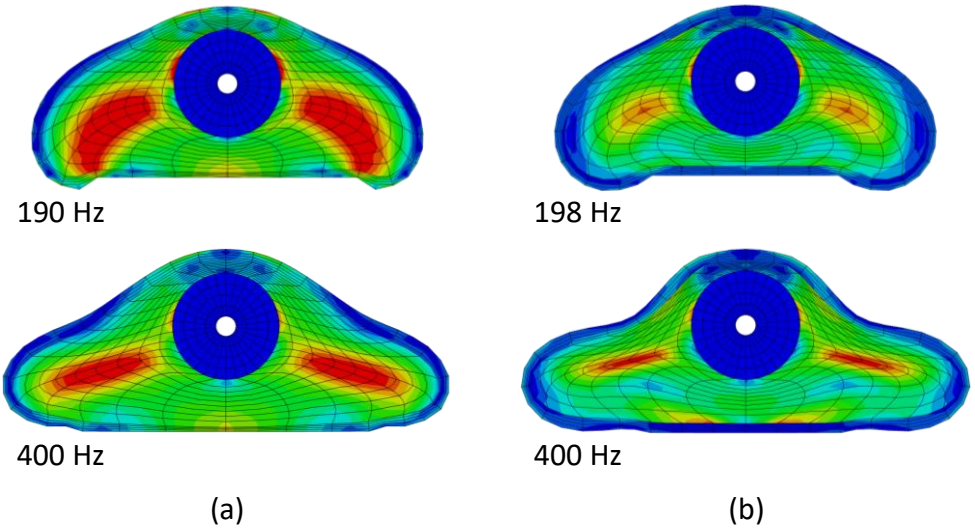

Figure 6.27: Mode shapes of FE models at resonance frequency and 400 Hz, during a deflection of 6 mm toward the handle: a) when human tissue parameters were applied; b) using parameters from tested materials

6.11 Discussion

A few studies that attempted to use artificial system to replicate the mechanical behaviour of the human fingertip, investigated many materials for the purpose of friction measurement and Young's modulus effects [108, 110, 111]. To date, no experimental protocol has been developed to measure the effect of transmitted vibration into the soft tissues of the finger, using an artificial test-bed.

This study investigated two types of material (latex and silicone gel) in order to obtain similar mechanical properties to those of the real finger, including the Young's modulus and loss factors, and to discover how these properties can be affected when subjected to different strain rates and temperature change.

The DMA data obtained from testing represented the mechanical behaviour of the tested materials. The Young's modulus represents how the energy can be stored by materials under loading conditions, and how it affects the dynamic stiffness of materials tested. The loss factors represent the ratio of the energy dissipated to that stored and affect the damping properties of the materials specimens [134].

DMA data obtained from two silicone specimens showed that the Young's modulus was within the range of interest and stability in the mechanical properties of these specimens over the time in which it was used and a range of dynamic strains and temperatures. Results allowed the appropriate mixing ratio to be selected in order to replicate the subcutaneous tissues of the human finger.

Even though the DMA data obtained from the latex sample showed that its Young's modulus was considerably higher than that of the outer layer of skin, it was found to be the best material for replicating skin as it has the strength required and can adhere to other surfaces such as silicone gel. It was also found useful in keeping all parts of the finger model enclosed, as the silicone is low modulus. The problems associated with the higher Young's modulus of latex material was reduced by decreasing the thickness of the skin layer.

This study showed the comparison in transmissibility measurements under different conditions between newly developed finger models and the data of human fingers tested under the same conditions. At frequencies below 100 Hz, all five finger models showed similar transmissibility to that of the real finger when the finger was ungloved. However,

at frequencies beyond 100Hz, the resonance frequency varied among the finger models, and increased as the grip force increased. [69]. The finger model AF3 was found to resonate at the same frequency range as that of the human fingers (122, 127 and 171 Hz), for grip forces of 15, 30 and 50 N respectively, and the finger model AF5 was the worst one as it was made from a different mixing ratio (1:2) for comparison, indicating the effect this subcutaneous tissue layer has on vibration transmission at the finger.

Additionally, the finger models showed consistency in transmissibility at low frequencies for all cases measured. This is possibly due to the fact that the finger model has a good capability of controlling the grip force at low frequencies, and this has been reported as one of the factors that may affect transmissibility measurements, especially when assessing the transmissibility of a glove [85].

It has hypothesised that the differences in transmissibility between the finger models and the human finger could be because the loss factors of the human tissues are higher than the gel, and the stiffness is probably nonlinear [145]. Also, it could be because the variance in the grip force of the human fingers that responds differently to each frequency [146].

The results obtained from FE modelling of the finger showed skin stiffness can affect the vibration behaviour of the finger. The strain distribution at resonance frequency was around blood arteries of the finger (for both human and artificial finger models), and was higher for the human finger model than the artificial finger model. This indication was reported to be one of the factors that are linked to the occurrence of VWF syndromes.

This study provided a new protocol for developing and assessing the artificial test-bed of the finger to replicate the mechanical behaviour of human finger, but with some limitations as follows:

- It was difficult to produce a homogenous thickness of the outer layer of the finger model (latex skin).
- The indentation test rig used in this study was found to be inconsistent in finding a zero deflection measurement, and it was hard to control the loading increment, which was found to vary among both human participants and physical models.
- Some participants found it slightly difficult to maintain a target grip force of 50 N during vibration tests when no AV glove was worn. This is reported as one benefit

of wearing AV gloves. However, the grip force measurement at 50 N was found to have less variation (6.53 %) compared to that of 15 N (7.98%) and 30 N (14.96%).

- Due to the creep of a nylon line that was used for mounting and gripping the finger, each target grip force required some time to ensure the accuracy of the grip force before vibration was applied.
- The comparison between vibration measurement between the human finger and on the artificial model was limited due to the fact that the human finger is connected to hand-arm system, whilst the artificial model was only represented the index finger.

These limitations require further investigation to be enhanced.

6.12 Conclusions

The findings from this chapter are as follows:

- A protocol of developing a reasonable artificial model to replicate the mechanical behaviour of the human finger has been established and can now be used in future experiments for assessing finger-transmitted vibrations.
- The model finger AF3 was selected as the best model for replicating both loading and vibration behaviour similar to that found from human measurements.
- The 2D FE modelling of the proximal finger segment used provided a good understanding of FTV and showed that the strain was found to be high around the arteries of the finger.
- The artificial test-bed provides consistent control of test parameters such as grip force.
- The AF model can help in assessing AV glove materials without the need for human subjects (which can sometimes be difficult due to ethical issues) and allows vibration to be measured inside the soft tissues.

Chapter 7: Conclusions and future work

This final chapter summarises and evaluates the main results and findings of the thesis. Some recommendations for further research into the topic of finger transmitted vibration are also outlined.

This thesis aims to gain a better understanding of the effects of hand-transmitted vibration on the human index finger in relation to the occurrence of HAVS, such as VWF.

7.1 Conclusions

The development of the new method for measuring finger transmitted vibration

This thesis has presented the development and assessment of a new method that measures finger transmitted vibration (Chapter 3). A vibration test rig has been designed and built to measure finger transmitted vibration, including a grip force system. The grip force system was calibrated at forces ranging from 0 to 80 N. In addition, the dynamic responses of the entire vibration system was assessed, using an impact hammer. The FRF data obtained showed that the system is capable of testing the vibration transmissibility of glove materials at frequencies ranging from 20 Hz to 400 Hz, and this information is of importance to HAVS research, as stated in the original and revised versions of AV Glove Standard ISO 10819, 1996, 2013[72, 75]. However, moving the reference accelerometer close to the measuring accelerometer has helped to remove handle resonance at frequencies ranging from 10 to 400 Hz.

The grip force system used in this work was different from that described in the Glove Standard ISO 10819 1996, 2013 [72, 75] as transmissibility was measured across the index proximal finger, not at the palm along from the arm, as stated in the standard. The grip force system was assessed with and without vibrations applied, with grip forces of 15, 30 and 50 N. The system was capable of measuring the finger-thumb grip force under a vibration excitation range of 10-400 Hz.

In this thesis, most of the finger-transmitted vibration measurement were made across the finger (front to back) with an accelerometer attached. The use of a small accelerometer allowed measuring FTV at the same measuring point, for all tests among individuals.

The effect of the accelerometer mass on the finger vibration was investigated using different techniques. 2D finite element modelling was used to simulate the proximal finger using material properties found from literature. The 2D FE model was designed to simulate both static loading and vibration behaviours of the proximal finger. In order to check the effect of the accelerometer mass, the vibration analysis of the finger was first conducted in the condition of no accelerometer attached, followed by the same analysis when the measuring accelerometer was attached. The accelerometer mass was simulated as a point mass at the accelerometer location. The transmissibility obtained showed that the FE model has a major resonance of around 112 Hz, suggesting that adding a small mass does not significantly affect the transmissibility at a frequency range from 10-400 Hz.

Furthermore, the effect of using a small accelerometer (0.3 grams) mounted to back of proximal finger was investigated using a single axis laser doppler vibrometer. The transmissibility obtained from both methods (accelerometer and laser) showed that the proximal finger resonated at about the same frequency of 125 Hz. However, due to the limitation of the use of the laser vibrometer, it was difficult to establish the transmissibility at the same measuring point of the finger and the laser sensor was found to be very sensitive to external noise. For example, the response of the frame that the sensor attached to. Comparing the transmissibility found from the FE model with that from human testing obtained when the laser-accelerometer method was utilised, both showed a resonance at around 100 Hz, especially at the grip force of 15 N. Also, the effect of adding a small mass of accelerometer does not significantly affect the vibration response of the proximal finger. However, the resonance increased with the grip force

Factors affecting finger-transmitted vibration.

As presented in Chapter 4, various experiments were carried out using human participants to study factors that might affect finger transmitted vibration. Characteristic measurements were conducted for hand and index finger, including anthropometric, physical and sensitivity measurements, skin characteristics and compared with finger transmissibility measurements.

Based on the findings of this study, a suitable protocol has been established for measuring human characteristics in relation to HAVS. This protocol with the identified improvements can be followed in similar studies in the future to help researchers to have a better

understanding of the factors causing HAVS. Anthropometric and physical measurements of the human hands used in this study were found to be similar to those used in previous studies (see Chapter 4).

Correlation analysis indicated that the sensitivity of three measured regions of the finger was found to decrease as age increased and to be high at the distal. The inclusion of the cutometer "MPA 580" and corneometer "CM 825" measurements revealed the characteristics of the human skin including viscoelastic properties, temperature and hydration of the skin, thus providing a better understanding of how all these measurements might affect the transmitted vibration of the finger. The vibration transmissibility of the proximal index finger was measured at vibration ranging from 10-400 Hz, under different conditions and was found to vary among subjects. This study has suggested that variance in transmissibility at frequencies below 100 Hz was found to be related to grip forces. Increase grip force led to an increase in resonance frequency.

No strong correlations were found between any of the skin characteristics measured and the transmitted vibration of the right index finger. However, the transmitted vibration was found statistically to be related either positively or negatively to some of the anthropometric measurements of the finger. A positive correlation was found between resonance frequency at 15 N and the age, length and diameter of the distal finger segment ($p< 0.05$), and the volume of the distal finger segment ($p< 0.01$). The resonance peak at 30 N was found to be positively related ($p< 0.05$) to the length and the volume of the proximal segment, whilst the resonance peak (RP_50N) showed a negative correlation with the length of the middle segment.

In addition, the finger temperature dropped by 2.1°C and 1.6 °C at both the distal and proximal respectively after the vibration test. The drop was found to be statically significant different ($p< 0.05$). Since the last part of the vibration test was performed for the gloved finger, the results strongly suggested that exposure to vibrations decreases finger skin temperature, indicating that finger circulation may be affected by vibration exposure even in a short testing time period. The fact that this finding might occur due to gripping the metal test handle was investigated and the results showed that gripping the unvibrated test handle did not significant change the finger skin temperature when no vibration was present ($p> 0.05$).

Temperature –frequency dependence of AV glove materials

From the reviewed literature, it has been reported that in order to evaluate the transmissibility of the AV gloves, and due to the limitations of glove transmissibility measurements at the finger, the AV glove material should be studied separately from the other layers of the glove. In this thesis Chapter 5, the temperature-frequency dependence of AV glove materials was investigated. DMA testing of the glove materials was first conducted, using a Metravib Viscoanalyser machine to provide mechanical properties (Young's modulus and loss factor) against the loading frequency and temperature. The findings from the DMA indicated that the vibration behaviour of materials would vary and this was largely related to the structure of the materials (e.g. the type of foam used). Therefore, this study has suggested that the properties of different glove materials will change in work conditions in the real world much as for example, at low temperatures. Findings obtained from the human subjects, suggested that AV gloves are less effective in protecting the proximal segment from vibration than they are in protecting the palm of the hand. Combining DMA data with the human testing results allows the AV performance of glove materials to be predicted for different temperatures, and this in turn allows manufacturers to design gloves to be more effective for the fingers as well as for the palm.

Development of an artificial model of finger

Chapter 6 presented the development of a new artificial finger that replicates the loading and vibration behaviour of the real index finger. Several materials have been statically and dynamically investigated in order to replicate the skin and soft tissues of a human finger at room temperature. The materials testing was carried out using tensile and DMA testing. The tensile testing showed that Young's modulus of latex samples was affected by the thickness. DMA testing of the silicone materials was used to select an appropriate mixing ratio to match properties of subcutaneous tissues.

Experiments using finger models

Comparing indentation data obtained from the human subjects in Chapter 4 and that measured from the artificial models of a finger showed similar load-displacement behaviour. The transmissibility measurements of the finger models showed similar vibration behaviour to that of the human index fingers at frequencies around the

resonance frequency. The peak magnitude of the finger models was strongly related to the Young's modulus and the thickness of the outer layer which was obtained by using an Optical Coherence Tomography (OCT) scanner.

The usage of a 2D FE model of the proximal finger provided a good understanding of finger transmitted vibration and indicated that maximum strain occurs in the vasculature region of the fingers. It also allowed the evaluation between the artificial finger and the human finger regarding the material properties used.

An examination of the different prototype artificial fingers suggested the most appropriate model was AF3 with alatex skin thickness of 0.62 mm and a silicone mixing ratio of 1:1.013. The artificial test-bed of finger and manufacturing protocol that was developed in this work can now be used in future experiments for assessing finger-transmitted vibrations; it can help in evaluating AV glove materials without the need for human subjects (which can sometimes be difficult due to ethical issues) and can also offer consistent control of test parameters such as grip force. It also allows instrumentation inside the soft tissues; for example, measuring vibration via the bone.

7.2 Contribution of the study

The main contribution of this thesis work are as follows:

- This work provided knowledge regarding the effects of different factors on finger transmitted vibration. The main finding was that exposure to vibration has a significant effect on finger temperature, even for a short time period of exposure, which is related to finger circulation. This finding will contribute to HAVS knowledge and allow researchers and organisations such as the Health and Safety Executive, who are working on controlling HAVS, to measure temperature affected by exposure to vibration as an indicator of changes in finger circulation.
- Investigation of AV glove materials using DMA showed that the mechanical properties of AV materials change under real world industrial conditions such as excitation frequencies and temperature. The outcome gained will allow AV glove manufacturers to investigate the frequency-temperature dependent on AV glove materials separately from other layers before being used for the entire glove. Also, evaluation of AV glove materials can be carried out using the newly developed

artificial test-bed of the finger which allows a better control of testing parameters such as a grip force.

- This work has been discussed with staff from the Health and Safety Laboratory (HSL) in the early stage of the project, and other leaders and researchers in the field of HAVS. The project has attempted to answer a large number of questions received from the HAVS committee. Most of the work presented in this thesis has been published, and the list of publications is as follows:

    1. Almagirby, A., J., Carré, M. J. and Rongong, J. A. A new methodology for measuring vibration transmissibility on a gripped handle for HAVS research. In *Thirteenth International Conference on Hand-Arm Vibration*. 2015. Beijing, China: Beijing University Health Science Center Capital Medical University.

    2. Almagirby, A., Walton, J., Rongong, J. A. and Carré, M. J. Vibration transmissibility measurement of glove materials under different grip forces. In *50th UK Conference on Human Responses to Vibration*. 2015: Human Factors Research Unit Institute of Sound and Vibration Research, University of Southampton, Southampton, England.

    3. Almagirby, A., J., Rongong, J. A. and Carré, M. J. The development of a new physical model of a finger for assessing transmitted vibrations. In *51st UK Conference on Human Responses to Vibration*. 2016: Institute of Naval Medicine, Gosport, England.

    4. Almagirby, A., J., Carré, M. J. and Rongong, J. A. A new methodology for measuring the vibration transmission from a handle to a finger whilst gripping. *International Journal of Industrial Ergonomics*,2016

7.3 Future work

The work represented in this thesis has provided a detailed study of different aspects of finger-transmitted vibration in order to fill the gaps in the current knowledge of the vibration transmitted across the index finger. A number of questions have arisen during this study, for which further research in different directions is recommended. Each of the aspects below contains a list of suggestions that could be undertaken in such future research.

Characteristics of human participants

- In this thesis, research into the skin characteristics of the index finger was carried out including cutometer and corneometer measurements to study the effect of the skin's mechanical properties on finger-transmitted vibration. For a better understanding of how the skin could affect the vibration behaviour of the finger, it is recommended that the effects related to variation in the skin thickness among individuals should be measured along with the skin characteristics measurements. This can be achieved by including OCT measurements of the human finger skin and a group of human participants selected to provide variation in this characteristic parameter.
- Finger sensitivity was studied in relation to HAVS, using two different groups of participants: technicians who were working in a workshop and non-technicians who had no vibration history. From the knowledge and results obtained from this study, the sensitivity of the human finger was found to be indirectly related to age, as the lower sensitivity measured from the technicians' group could be due to the effect of age (as they were older), rather than to vibration exposure. Therefore, further investigation is recommended, to study the effect of vibrations might have on finger sensitivity.
- This current study has carried out load-deflection using a modified indentation test rig. However, due to the limitations of the test rig, it was found difficult to identify the zero load point, and the loading increment was inconsistent across individuals. To investigate this technical issue, a new indentation test rig could be developed that would have more accurate force and displacement devices, and the loading increments could be achieved by using a small electric motor installed that would allow control by software (e.g. LabView).
- Human testing suggests looking in more depth at changes in finger temperature by measuring temperature changes during exposure to finger transmitted vibration. This can be done by inserting temperature sensors between a finger and a vibrating handle.

An artificial finger model

- The skin layer of the finger model used latex material which was found to be about ten times stiffer than human skin. Thus, further alternative materials could be investigated to find a material that has mechanical properties closer to that of human skin.
- FE modelling to study the parameters of materials of both the human and the artificial finger, it is recommended these should be analysed further using 3D FE modelling of the finger. This will provide a good comparison of the parameters, which may help in the design of the finger model. 3D FE model will allowed to study the vibration responses across the entire segment of proximal finger and can deliver grip forces as well as the load-deflection behaviour similar to that obtained from human finger and physical model.

References

1. Radwin, R. G., Armstrong, T. J. and Chaffin, D. B., Power hand tool vibration effects on grip exertions. *Ergonomics*, 1987. 30(5): pp. 833-855.

2. Bovenzi, M., Franzinelli, A. and Strambi, F., Prevalence of vibration-induced white finger and assessment of vibration exposure among travertine workers in Italy. *Int Arch Occup Environ Health*, 1988. 61: pp. 25-34.

3. Ye, Y., Mauro, M., Bovenzi, M. and Griffin, M. J., Acute effects of mechanical shocks on finger blood flow: influence of shock repetition rate and shock magnitude. *International Archives of Occupational and Environmental Health*, 2012. 85(6): pp. 605-614.

4. Pattnaik, S., Banerjee, R. and Kim, J., Spatial resonance in a small artery excited by vibration input as a possible mechanism to cause hand–arm vascular disorders. *Journal of sound and vibration*, 2012. 331(8): pp. 1951-1960.

5. Bovenzi, M., Griffin, J. and Ruffell, M., Acute effects of vibration on digital circulatory function in healthy men. *Occupational and Environmental Medicine*, 1995. 52: pp. 834-841.

6. Dong, R. G., Schopper, A. W., McDowell, T. W., Welcome, D. E., Wu, J. Z., Smutz, W. P., Warren, C. and Rakheja, S., Vibration energy absorption (VEA) in human fingers-hand-arm system. *Med Eng Phys*, 2004. 26(6): pp. 483-92.

7. Bovenzi, M., Lindsell, C. J. and Griffn, M. J., Response of finger circulation to energy equivalent combinations of magnitude and duration of vibration. *Occupational and Environmental Medicine*, 2001. 58: pp. 185-193.

8. Bovenzi, M., Lindsell, C. J. and Griffin, M. J., Magnitude of acute exposures to vibration and finger circulation. *Scandinavian Journal of Work, Environment & Health*, 1999. 25(3): pp. 278-284.

9. Bovenzi, M., Lindsell, C. J. and Griffin, M. J., Duration of acute exposures to vibration and finger circulation. *Scandinavian Journal of Work, Environment & Health*, 1998. 24(2): pp. 130-137.

10. Bovenzi, M., Welsh, A. J. L. and Griffin, M. J., Acute effects of continuous and intermittent vibration on finger circulation. *International Archives of Occupational and Environmental Health*, 2004. 77(4): pp. 255-263.

11. Tayyari, F. and Smith, J., eds. *Occupational Ergonomic* 2003, Kluwer academic: Boston,Dordrecht,London.

12. ISO 5349-2, *Mechanical vibration-Measurement and evaluation of human exposure to hand-transmitted vibration- Part 2: Practical guidance for measurement at the*

workplace. 2002, International Organization for Standardization: Geneva, Switzerland.

13. Palmer, R. A. and Collin, J., Vibration white finger. *British Journal of Surgery*, 1993. 80(6): pp. 705-709.

14. Muzammili, M., Khan, I. A. and Hasan, F., Effects of vibration, feed force and exposure duration performance drilling task. *Journal of human ergology*, 2003. 32: pp. 77-86.

15. Gurram, R., Rakheja, S. and Gouw, G. J., A study of hand grip pressure distribution and EMG of finger flexor muscles under dynamic loads. *Ergonomics*, 1995. 38(4): pp. 684-699

16. Andersson, E. R., Design and testing of a vibration attenuating handle. *International Journal of Industrial Ergonomics*, 1990. 6: pp. 119-125.

17. Bovenzi, M., A longitudinal study of vibration white finger, cold response of digital arteries, and measures of daily vibration exposure. *International Archives of Occupational and Environmental Health*, 2010. 83(3): pp. 259-272.

18. Youakim, S., The validity of Raynaud's phenomenon symptoms in HAVS cases. *Occupational Medicine*, 2008. 58(6): pp. 431-435.

19. Gurram, R., *A Study of Vibration Response Characteristics of the Human Hand-Arm System*, in *Mechanical Engineering*. 1993, Concordia University: Montreal Quebec, Canada.

20. Negro, C., Rui, F., D'Agostin, F. and Bovenzi, M., Use of color charts for the diagnosis of finger whiteness in vibration-exposed workers. *International Archives of Occupational and Environmental Health*, 2007. 81(5): pp. 633-638.

21. Bovenzi, M., Medical aspects of the hand-arm vibration syndrome. *International Journal of Industrial Ergonomics*, 1990. 6: pp. 61-73.

22. Lewis, T., *Vascular disorders of the limbs*. 2nd ed. 1949, London: MacMillan.

23. Pyykko, I. and Starck, J., Pathophysiological and hygienic aspects of hand-arm vibration. *Scandinavian Journal of Work, Environment and Health*, 1986. 12(4): pp. 237-241.

24. Eliot, G., *Human Anatomy for Artist*. 1991, Oxford University press: New York.

25. MedicineNet. *Finger anatomy*. 1996 March 2 2014; Available from: http://www.medicinenet.com/image-collection/finger_anatomy_picture/picture.htm.

26. dictionary, T. v. *Finger*. 2005 [cited 2013; Available from: http://www.infovisual.info/en/human-body/finger.

27. ENT Wellbeing. *Layers of skin*. [cited 2013; Available from: http://www.entwellbeing.com.au/skincare/skin-basics/layers-of-skin/.

28. Brannon, H. *Skin Anatomy*. 2007; Available from: http://dermatology.about.com/cs/skinanatomy/a/anatomy.htm.

29. Jones, L. A. and Lederman, S. J., *Human hand function*. 2006: Oxford University Press.

30. Wood, E. J. and Bladon, P. T., *The human skin, Studies in Biology*. 1985. p. 162.

31. Bowden, A. E., Rabbitt, R. D. and Weiss, J. A., Stress and strain in the human distal phalanx under indentation. *Advancing Technology*, 1999: pp. 512.

32. Daniela, D. N., Popa, D. and Roxana, Analysis of stress and displacements of phalanx bone with the finite element method. *Romanian Journal of Morphology and Embryology*, 2005. 46(3): pp. 189-191.

33. Fung, Y. C., *Biomechanics: Mechanical Properties of Living Tissues*, Springer-Verlag, Editor. 1981.

34. Wagner, M. B., Gerling, G. J. and Scanlon, J., Validation of a 3-D Finite Element Human Fingerpad Model Composed of Anatomically Accurate Tissue Layers. *Department of Systems and Information Engineering, University of Virginia, USA*, 2008: pp. 101-105.

35. Luxmoore, J. S., *Using finite element analysis for the assessment of human-product interaction*, in *Mechanical engineering*. 2008, University of sheffield: Sheffield.

36. Houston Methodist. *PIP Joint Injuries of the Finger*. [cited 2013; Available from: http://www.eorthopod.com/Booklet?ClinicID=6138752e01d21f68baaa5b7b82751802&TopicID=2a4d586af506d5af81ecfb33c9351281.

37. Klarho, M., Csapo, B., Balassy, C., Szeles, J. C. and Moser, E., High-resolution blood flow velocity measurements in the human finger. *Magnetic Resonance in Medicine*, 2001. 45: pp. 716-719.

38. Long, J. A., Undar, A., Manning, K. B. and Deutsch, S., Viscoelasticity of pediatric blood and its implications for the testing of a pulsatile pediatric blood pump. *ASAIO Journal*, 2005. 51(5): pp. 563-566.

39. Deutsch, S., Tarbell, J. M., Manning, K. B., Rosenberg, G. and Fontaine, A. A., Experimental fluid mechanics of aulsatile artificial blood pumps. *Annu. Rev. Fluid Mech*, 2006. 38: pp. 65-86.

40. Carey, R. F. and Herman, B. A., The effects of a glycerin-based blood analog on the testing of bioprosthetic heart valves. *Journal Biomechanics*, 1989. 22: pp. 1185-1192.

41. Legendre, D., Fonseca, J., Andrade, A., Biscegli, J. F., Manrique, R., Guerrino, D., Prakasan, A. K., Ortiz, J. P. and Lucchi, J. C., Mock Circulatory System for the Evaluation of Left Ventricular Assist Devices, Endoluminal Prostheses, and Vascular Diseases. *Artificial organs*, 2008. 32(6): pp. 461-467.

42. Mann, K., Deutsch, S., Tarbell, J., Geselowitz, D., Rosenberg, G. and Pierce, W., An Experimental Study of Newtonian and Non-Newtonian Flow Dynamics in a Ventricular Assist Device. *Biomechanical Engineering*, 1987. 109: pp. 139-147.

43. Hochareon, P., Manning, K. B., Fontaine, A. A., Deutsch, S. and Tarbell, J. M., Diaphragm Motion Affects Flow Patterns in an Artificial Heart. *Artificial Organs*, 2003. 27: pp. 1102–1109.

44. Nida Gleveckas-Martens, T. R. G. *Somatosensory System Anatomy*. 2013; Available from: http://emedicine.medscape.com/article/1948621-overview.

45. Marieb, E. N., *Human Anatomy and Physiology*. 5th ed. 2001: Daryl Fox.

46. Thixia. *Myelin Sheath and Nerve*. 2008 11/12/2016 [cited 2013; Available from: https://scamparoo.wordpress.com/2008/09/30/diagram-myelin-sheath-and-nerve/.

47. Gonzales, A. *Nerve Receptors*. 11/12/2016 [cited 2013; Available from: https://www.tes.com/lessons/dQ2HKFsZG5MAJQ/structures-of-the-integumentary-system.

48. Purves, D., Augustine, G. J., Fitzpatrick, D., Katz, L. C., LaMantia, A.-S., McNamara, J. O. and Williams, S. M., eds. *Neuroscience* 2nd ed. Mechanoreceptors Specialized to Receive Tactile Information. 2001, Sunderland, Mass. : Sinauer Associates, c2001.

49. Nerve Impulses. *The Pacinian Corpuscle*. [cited 2013; Available from: http://www.biologymad.com/nervoussystem/nerveimpulses.htm.

50. Verrillo, R. T., Age related changes in the sensitivity to vibration. *The Journals of Gerontology*, 1980. 35(2): pp. 185-193.

51. Welcome, D. E., Rakheja, S., Dong, R. G., Wu, J. Z. and Schopper, A. W., An investigation on the relationship between grip, push and contact forces applied to a tool handle. *International Journal of Industrial Ergonomics*, 2004. 34(6): pp. 507-518.

52. Seo, N. J. and Armstrong, T. J., Investigation of Grip Force, Normal Force, Contact Area, Hand Size, and Handle Size for Cylindrical Handles. *The Journal of the Human Factors and Ergonomics Society*, 2008. 50(5): pp. 734-744.

53. Marcotte, P., Aldien, Y., Boileau, P. É., Rakheja, S. and Boutin, J., Effect of handle size and hand–handle contact force on the biodynamic response of the hand–arm

system under zh-axis vibration. *Journal of sound and vibration*, 2005. 283(2-5): pp. 1071-1091.

54. Aldien, Y., Marcotte, P., Rakheja, S. and Boileau, P. E., Influence of hand–arm posture on biodynamic response of the human hand–arm exposed to zh-axis vibration. *International Journal of Industrial Ergonomics*, 2006. 36(1): pp. 45-59.

55. Aldien, Y., Welcome, D., Rakheja, S., Dong, R. G. and Boileau, P. E., Contact pressure distribution at hand–handle interface: role of hand forces and handle size. *International Journal of Industrial Ergonomics*, 2005. 35(3): pp. 267-286.

56. Dong, R. G., WU, J. Z. and Welcome, D. E., Rcent advances in biodynamics of human hand-arm system. *Industrial health*, 2005. 43: pp. 449-471.

57. Dong, R. G., Welcome, D. E., McDowell, T. W., Wu, J. Z. and Schopper, A. W., Frequency weighting derived from power absorption of fingers–hand–arm system under zh-axis vibration. *Journal of Biomechanics*, 2006. 39(12): pp. 2311-2324.

58. Dong, J. H., Dong, R. G., Rakheja, S., Welcome, D. E., McDowell, T. W. and Wu, J. Z., A method for analyzing absorbed power distribution in the hand and arm substructures when operating vibrating tools. *Journal of sound and vibration*, 2008. 311(3-5): pp. 1286-1304.

59. McDowell, T. W., Wimer, B. M., Welcome, D. E., Warren, C. and Dong, R. G., Effects of handle size and shape on measured grip strength. *International Journal of Industrial Ergonomics*, 2012. 42(2): pp. 199-205.

60. Wimer, B., Dong, R. G., Welcome, D. E., Warren, C. and McDowell, T. W., Development of a new dynamometer for measuring grip strength applied on a cylindrical handle. *Medical Engineering and Physics*, 2009. 31(6): pp. 695-704.

61. Farkkila, M., Pyykko, I., Korhonen, O. and Stark, J., Hnad grip forces during chain saw operation and vibration white finger lumberjacks. *British journal of industial medicien*, 1979. 36: pp. 336-341.

62. Lage, B., The influence of biodynamic factors on the mechanical impedance of the hand and arm. *International Archives of Occupational and Environmental Health*, 1997. 69(Sep 1996): pp. 437-446.

63. Gurram, R., Rakheja, S. and Gouw, G. J., Vibration transmission characteristices of the human hand-arm and gloves. *International Journal of Industrial Ergonomics*, 1994. 13: pp. 217-234.

64. ISO 5349-1, *Mechanical vibration — Measurement and evaluation of human exposure to hand-transmitted vibration — Part 1: General requirements*. 2001, International Organization for Standardization: Geneva, Switzerland.

65. Hewitt, S., Dong, R. G., Welcome, D. E. and McDowell, T. W., Anti-Vibration Gloves? *Annals of Occupational Hygiene*, 2014. 59(2): pp. 127-141.

66. HSE, ed. *Hand-arm vibration*. 2005, Health and Safety Executive. 1-144.

67. Griffin, M. J., Evaluating the effectiveness of gloves in reducing the hazards of hand-transmitted vibration. *Occupational and Environmental Medicine*, 1998. 55: pp. 340-348.

68. Hewit, S., *Triaxial measurements of the performance of anti-vibration gloves*. 2010, Health and Safety Executive: Buxton, Derbyshire.

69. Welcome, D. E., Dong, R. G., Xu, X. S., Warren, C. and McDowell, T. W., The effects of vibration-reducing gloves on finger vibration. *International Journal of Industrial Ergonomics*, 2014. 44(1): pp. 45-59.

70. Dong, R. G., McDowell, T. W., Welcome, D. E., Smutz, W. P., Schopper, A. W., Warren, C., Wu, J. Z. and Rakheja, S., On-the-hand measurement methods for assessing effectiveness of anti-vibration gloves. *International Journal of Industrial Ergonomics*, 2003. 32(4): pp. 283-298.

71. Boileau, P. E., Rakheja, S. and Boutin, J., An interlaboratory evaluation of the vibration transmissibility of gloves following the ISO 10819 test method. *Canadian Acoustics*, 2001. 29(3): pp. 18-19.

72. ISO 10819, *Mechanical vibration and shock — hand-arm vibration — Method for the measurement and evaluation transmissibility of gloves at the palm of the hand*. 1996, International Organization for Standardization: Geneva, Switzerland.

73. Dong, R. G., McDowell, T. W., Welcome, D., Barkley, J., Warren, C. and Washington, B., Effects of Hand-Tool Coupling Conditions on the Isolation Effectiveness of Air Bladder Anti-Vibration Gloves. *JOURNAL OF LOW FREQUENCY NOISE, VIBRATION AND ACTIVE CONTROL*, 2004. 23(4): pp. 231 – 248.

74. Welcome, D. E., Dong, R. G., Xu, X. S., Warren, C. and McDowell, T. W., An evaluation of the proposed revision of the anti-vibration glove test method defined in ISO 10819 (1996). *International Journal of Industrial Ergonomics*, 2012. 42(1): pp. 143-155.

75. ISO 10819, *Mechanical vibration and shock — Hand-arm vibration —Measurement and evaluation of the vibration transmissibility of gloves at the palm of the hand*. 2013, International Organization for Standradization: Geneva, Switzerland.

76. Welcome, D. E., Dong, R. G., Xu, X. S., Warren, C. and McDowell, T. W. TOOL-SPECIFIC PERFORMANCE OF VIBRATION-REDUCING GLOVES AT THE FINGERS. in *Proceedings of the 5th American Conference on Human Vibration*. 2014. Guelph, Ontario, Canada.

77. Wimer, B., McDowell, T. W., Xu, X. S., Welcome, D. E., Warren, C. and Dong, R. G., Effects of gloves on the total grip strength applied to cylindrical handles. *International Journal of Industrial Ergonomics*, 2010. 40(5): pp. 574-583.

78. Xu, X. S., Dong, R. G., Welcome, D. E., Warren, C. and McDowell, T. W., An examination of the handheld adapter approach for measuring hand-transmitted vibration exposure. *Measurement*, 2014. 47: pp. 64-77.

79. Dong, R. G., Welcome, D. E., Mcdowell, T. W., XU, X. S., Krajnak, K. and Wu, J. Z., A proposed theory on biodynamic frequency weighting for handtransmittd vibration exposure. *Industrual Health*, 2012. 50(5): pp. 412-424.

80. Griffin, M., J. , Bovenzi, M. and Nelson, C. M., Dose-response patterns for vibration-induced white finger. *Journal of Occupational and Environmental Medicine*, 2003. 60: pp. 16–26.

81. Tominaga, Y., New frequency weighting of hand-arm vibration. *Industrial Health*, 2005. 43: pp. 509-515.

82. Bovenzi, M., Exposure-response relationship in the hand-arm vibration syndrome:an overview of current epidemiology research. *International Archives of Occupational and Environmental Health*, 1998. 71: pp. 509-519.

83. Bovenzi, M., Epidemiological evidence for new frequency weightings of hand-transmittd vibration. *Industrial Health*, 2012. 50: pp. 377-387.

84. Pitts, P. M., Mason, H. J., Poole, K. A. and Young, C. E., Relative performance of Frequency Weighting Wh and candidates for alternative frequency weightings when used to predict the occurrence of hand-arm vibration induced injuries. 2012.

85. Hewitt , S., Assessing the performance of anti-vibration gloves—A possible alternative to ISO 10819, 1996. *The Annals of Occupational Hygiene*, 1998. 42(4): pp. 245-252.

86. Paddan, G. S. and Griffin, M. J., *Measurement of glove and hand dynamics using knuckle vibration*, in 9th International Conference on Hand-Arm Vibration. 2001: Nancy, France.

87. Welcome, D. E., Dong, R. G., Xu, X. S., Christopher, M., McDowell, T. W. and Wu, J. Z., Investigation of the 3-D vibration transmissibility on the human hand –arm system using a 3-D scanning laser vibrometer. *Canadian Acoustics*, 2011. 39: pp. 44-45.

88. Concettoni, E. and Griffin, M., The apparent mass and mechanical impedance of the hand and the transmission of vibration to the fingers, hand, and arm. *Journal of sound and vibration*, 2009. 325(3): pp. 664-678.

89. Jetzer, T., Haydon, P. and Reynolds, D. D., Effective intervention with ergonomics, antivibration gloves, and medical surveillance to minimize hand-arm vibration hazards in the workplace. *J. Occup. Environ. Med.*, 2003. 45(12): pp. 1312-1317.

90. Mahbub, M. H., Yokoyama, K., Laskar, M. S., Inoue, M., Takahashi, Y., Yamamoto, S. and Harada, N., Assessing the influence of antivibration glove on digital vasccular

responses to acute hand-arm vibration. *Journal of Occuptional Health*, 2007. 49: pp. 165-171.

91. Griffin, M. J., *Handbook of Human Vibration*. 1990, London: Academic Press.

92. Dong, R. G., McDowell, T. W., Welcome, D. E., Warren, C., Wu, J.Z., and Rakheja, S., Analysis of anti-vibration gloves mechanism and evaluation methods. *435-453*, 2009. 321.

93. Almagirby, A., Walton, J., Rongong, J. A. and Carré, M. J. Vibration transmissibility measurement of glove materials under different grip forces. in *50th UK Conference on Human Responses to Vibration*. 2015: Human Factors Research Unit Institute of Sound and Vibration Research, University of Southampton, Southampton, England.

94. Griffin, M. J., Macfarlane, C. R. and Norman, C. D., *The transmission of vibration to the hand and the influence of gloves in: Vibration Effects on the Hand and Arm in Industry*, Brammer, A.J., et al., Editors. 1982: New York.

95. Welcome, D. E., Dong, R. G., Xu, X. S., Warren, C., McDowell, T. W. and Wu, J. Z., An examination of the vibration transmissibility of the hand-arm system in three orthogonal directions. *International Journal of Industrial Ergonomics*, 2015. 45: pp. 21-34.

96. Wu, J. Z., Dong, R. G., Welcome, D. E. and Xu, X. S., A method for analyzing vibration power absorption density in human fingertip. *Journal of sound and vibration*, 2010. 329(26): pp. 5600-5614.

97. Dong, R. G., Jennie, H., Wu, J. Z. and Rakheja, S., Modeling of biodynamic responses distributed at the fingers and the palm of the human hand–arm system. *Journal of Biomechanics*, 2007. 40(10): pp. 2335-2340.

98. Bovenzi, M., Lindsell, C. J. and Griffin, M. J., Acute vascular responses to the frequency of vibration transmitted to the hand. *Occupational Environmental Medical*, 2000. 57: pp. 422-430.

99. Greenfield, A. D. M., Whitny, R. J. and Mowbray, J. F., Methods for the investigation of peripheral blood flow. *British Medical Bulletin*, 1963. 19(2).

100. Roddie, I. C. and Wallace, W., Methods for the assessment of the effects of drugs on the arterial system in man. *Br. J. clin. Phannac.*, 1979. 7: pp. 317-323.

101. Hyvarinen, J., Pyykko, I. and Sundberg, S., Vibration frequencies and amplitudes in the aeltiology of traumatic vasospastic disease. *The Lancet*, 1973: pp. 791-794.

102. Ye, Y., Mauro, M., Bovenzi, M. and Griffin, M. J., Association between vasoconstriction during and following exposure to hand-transmitted vibration. *International Archives of Occupational and Environmental Health*, 2012.

103. Hokanson, D. E., Baker, D. W., Sumner, D. S. and Strandness, D. E., An electrically calibrated plethysmograph for direct measurement of limb blood flow. *IEEE Transaction on biomedical engineering*, 1975. 22(1): pp. 25-29.

104. Furuta, M., Sakakibara, H., Miyao, M., Kondo, T. and Yamada, S., Effect of vibration frequency on finger blood flow. *Int Arch Occup Environ Health*, 1991. 63: pp. 221-224.

105. Heaver, C., Goonetilleke, K. S., Ferguson, H. and Shiralkar, S., Hand-arm vibration syndrome: a common occupational hazard in industrialized countries. *Journal of Hand Surgery (European Volume)*, 2011. 36(5): pp. 354-363.

106. Bovenzi, M., Welsh, A. J. L. and Griffin, M. J., Effect of prior exposure to hand-transmitted vibration on cold response of digital arteries. *International Archives of Occupational and Environmental Health*, 2006. 80(4): pp. 281-289.

107. Wu, J. Z., Welcome, D. E., Krajnak, K. and Dong, R. G., Finite element analysis of the penetrations of shear and normal vibrations into the soft tissues in a fingertip. *Medical Engineering and Physics*, 2007. 29: pp. 718–727.

108. Shao, F., Childs, T. H. C. and Henson, B., Developing an artificial fingertip with human friction properties. *Tribology International*, 2009. 42(11-12): pp. 1575-1581.

109. Derler, S., Schrade, U. and Gerhardt, L. C., Tribology of human skin and mechanical skin equivalents in contact with textiles. *Wear*, 2007. 263(7-12): pp. 1112-1116.

110. Ramkumar, S. S., Wood, D. J., Fox, K. and Harlock, S. C., Developing a Polymeric Human Finger Sensor to Study the Frictional Properties of Textiles Part I: Artificial Finger Development. *Textile Research Journal*, 2003. 73(6): pp. 469-473.

111. Ramkumar, S. S., Wood, D. J., Fox, K. and Harlock, S. C., Developing a Polymeric Human Finger Sensor to Study the Frictional Properties of Textiles Part II: Experimental Result. *Textile Research Journal*, 2003. 73(7): pp. 606-610.

112. Smith, J. O., *Introduction to digital filters : with audio applications*. 2008, United States]: United States : W3K, 2008.

113. Alexander, B. and Viktor, K., Proportions of Hand Segments. *International Journal of Morphology*, 2010. 28(3): pp. 755-758.

114. Dewangan, K. N., Owary, C. and Datta, R. K., Anthropometry of male agricultural workers of north-eastern India and its use in design of agricultural tools and equipment. *International Journal of Industrial Ergonomics*, 2010. 40(5): pp. 560-573.

115. Wang, Z., Wang, L., Ho, V. A., Morikawa, S. and Hirai, S., A 3-D Nonhomogeneous FE Model of Human Fingertip Based on MRI Measurements. *IEEE Transactions on Instrumentation and Measurement*, 2012. 61(12): pp. 3147-3157.

116. Wu, J. Z., Krajnak, K., Welcome, D. E. and Dong, R. G., Analysis of the dynamic strains in a fingertip exposed to vibrations: Correlation to the mechanical stimuli on mechanoreceptors. *J Biomech*, 2006. 39(13): pp. 2445-56.

117. Wu, J. Z., Dong, R. G. and Welcome, D. E., Analysis of the point mechanical impedance of fingerpad in vibration. *Med Eng Phys*, 2006. 28(8): pp. 816-26.

118. Zhongkui Wang, Y. A., Shinichi Hirai and Shigehiro Morikawa, A 3D FE Dynamic Model of Human Fingertip Basedon MRI Data. 2011. 1.

119. Zheng, Y. and Mak, A. F., An ultrasound indentation system for biomechanical properties assessment of soft tissues in-vivo. *IEEE Transactions on Biomedical Engineering*, 1996. 43(9): pp. 912-918.

120. Pan, L., Zan , L. and Foster, F., Ultrasonic and viscoelastic properties of skin under transverse mechanical stress in vitro. *Ultrasound in Medicine and Biology*, 1998. 24(7): pp. 995–1007.

121. Laszlo, H. E. and Griffin, M. J., The transmission of vibration through gloves: effects of push force, vibration magnitude and inter-subject variability. *Ergonomics*, 2011. 54(5): pp. 488-96.

122. BS EN 420, *Protective gloves — General requirements and test methods*. 2003, European Committee for Standardization (CEN).

123. Hall Judith G. , Allanson, J. E., Gripp, K. W. and Slavotinek, A. M., *Handbook of Physical Measurements Second Edition*. 2nd ed. 2007: Oxford Univesity Press.

124. Jee, S. C. and Yun, M. H., Estimation of stature from diversified hand anthropometric dimensions from Korean population. *J Forensic Leg Med*, 2015. 35: pp. 9-14.

125. Ishak, N. I., Hemy, N. and Franklin, D., Estimation of stature from hand and handprint dimensions in a Western Australian population. *Forensic Sci Int*, 2012. 216(1-3): pp. 199 e1-7.

126. Mohammad, Y. A. A., Anthropometric characteristics of the hand based on laterality and sex among Jordanian. *International Journal of Industrial Ergonomics*, 2005. 35(8): pp. 747-754.

127. Nurul Shahida, M. S., Siti Zawiah, M. D. and Case, K., The relationship between anthropometry and hand grip strength among elderly Malaysians. *International Journal of Industrial Ergonomics*, 2015. 50: pp. 17-25.

128. Nicolay, C. W. and Walker, A. L., Grip strength and endurance: Influences of anthropometric variation, hand dominance, and gender. *International Journal of Industrial Ergonomics*, 2005. 35(7): pp. 605-618.

129. Cua, A. B., Wilhelm, K.-P. and Maibach, H. I., Elastic properties of human skin: relation to age, sex, and anatomical region. *Archives of Dermatological Research*, 1990. 282(5): pp. 283–288.

130. Agache, P. G., Monneur, C., Leveque, J. L. and De Rigal, J., Mechanical properties and Young's modulus of human skin in vivo. *Archives of Dermatological Research*, 1980. 269(3): pp. 221–232.

131. Sancho-Bru, J. n. L., Giurintano, D. J., Pérez-González, A. and Vergara, M., Optimum tool handle diameter for a cylinder grip. *Journal of Hand Therapy*, 2003. 16(4).

132. Ferry, J. D., *Viscoelastic properties of polymers*. 3rd ed. 1980, New York: Wiley.

133. Boyle, M. and Griffin, M. J., *Inter-subject variability in the measurement of the vibration transmissibility of gloves according to current standards*, in 9th International Conference on Hand-Arm Vibration. 2001: Nancy, France. p. 8pp.

134. ISO 6321-1, *Plastics - Determination of dynamic mechnical properties - Part 1:General principles*. 1996, International Organization for Standradization: Geneva, Switzerland.

135. Dong, R. G. W., Daniel E. McDowell, Thomas W. Wu, John Z., Modeling of the biodynamic responses distributed at the fingers and palm of the hand in three orthogonal directions. *Journal of sound and vibration*, 2013. 332(4): pp. 1125-1140.

136. Wu, J. Z., Dong, R. G., Welcome, D. E. and McDowell, T. W. THREE-DIMENSIONAL FINITE ELEMENT MODELING OF THE EFFECTS OF GRIPPING FORCE ON FINGER VIBRATION TRANSMISSIBILITY. in *Thirteenth International Conference on Hand-Arm Vibration*. 2015. Beijing, China: Beijing University Health Science Center Capital Medical University.

137. Hendriks, F. M., *Mechanical behaviour of human epidermal and dermal layers in vivo*, Baaijens, F.P.T., Bader, D.L., and Oomens, C.W.J., Editors. 2005, Technische Universiteit Eindhoven.

138. Delalleau, A., Josse, G., Lagarde, J. m., Zahouani, H. and Bergheau, J. m., A nonlinear elastic behavior to identify the mechanical parameters of human skin in vivo. *Skin Research and Technology*, 2008. 14(2): pp. 152-164.

139. Payne, P. A., Measurement of properties and function of skin. *Clinical Physics and Physiological Measurement*, 1991. 12(2): pp. 105-129.

140. Liang, X. and Boppart, S. A., Biomechanical properties of in vivo human skin from dynamic optical coherence elastography. *IEEE Trans Biomed Eng*, 2010. 57(4): pp. 953-9.

141. Bader, D. L. and Bowker, P., Mechanical characteristics of skin and underlying tissues in vivo. *Biomaterials*, 1983. 4(4): pp. 305-308.

142. ISO 37, *Rubber, vulcanized or thermoplastic — Determination of tensile stress-strain properties*. 2011, International Organization for Standardization: Geneva, Switzerland.

143. Dandekar, K., Raju, B. I. and Srinivasan, M. A., 3-D Finite-Element Models of Human and Monkey Fingertips to Investigate the Mechanics of Tactile Sense. *Journal of Biomechanical Engineering*, 2003. 125(5): pp. 682.

144. Maiti, R., Gerhardt, L. C., Lee, Z. S., Byers, R. A., Woods, D., Sanz-Herrera, J. A., Franklin, S. E., Lewis, R., Matcher, S. J. and Carre, M. J., In vivo measurement of skin surface strain and sub-surface layer deformation induced by natural tissue stretching. *J Mech Behav Biomed Mater*, 2016. 62: pp. 556-69.

145. Kitazaki S. and Griffin, M. J., A data correction method for surface measurement of vibration on the human body. *Journal of Biomechanics*, 1995. 28(7): pp. 885-890.

146. Almagirby, A., Carré, M. J. and Rongong, J. A., A new methodology for measuring the vibration transmission from handle to finger whilst gripping. *International Journal of Industrial Ergonomics*, 2017. 58: pp. 55-61.

Appendixes

Appendix – A1: Ethics approval; vibration measurement

The University Of Sheffield.

20/11/2014

Almaky Almagirby
Mechanical Engineering

Dear Almaky

PROJECT TITLE: Measuring transmitted vibration through hand-held tools
APPLICATION: Reference Number 001465

On behalf of the University ethics reviewers who reviewed your project, I am pleased to inform you that on 20/11/2014 the above-named project was **approved** on ethics grounds, on the basis that you will adhere to the following documentation that you submitted for ethics review:

- University research ethics application form 001465 (dated 30/06/2014).
- Participant information sheet 001748 (30/06/2014)
- Participant consent form 001749 (30/06/2014)

If during the course of the project you need to deviate significantly from the above-approved documentation please inform me since written approval will be required.

Yours sincerely

Galina Balikhin
Ethics Administrator
Mechanical Engineering

Appendix – A2: Ethics approval; Investigation on the properties of the skin

The University Of Sheffield.

Downloaded: 23/02/2016
Approved: 15/02/2016

Raman Maiti
Infection and Immunity

Dear Raman

PROJECT TITLE: Investigation on the properties of the skin using mechanical and skin characteristic systems
APPLICATION: Reference Number 007424

On behalf of the University ethics reviewers who reviewed your project, I am pleased to inform you that on 15/02/2016 the above-named project was **approved** on ethics grounds, on the basis that you will adhere to the following documentation that you submitted for ethics review:

- University research ethics application form 007424 (dated 08/02/2016).
- Participant information sheet 1015207 version 1 (06/02/2016).
- Participant information sheet 1014814 version 3 (06/02/2016).
- Participant consent form 1015208 version 1 (06/02/2016).
- Participant consent form 1014810 version 2 (06/02/2016).

The following optional amendments were suggested:

The PIS needs the name of the study on it. The PIS and consent forms need dates and version numbers added as a footer / header.

If during the course of the project you need to deviate significantly from the above-approved documentation please inform me since written approval will be required.

Yours sincerely

Paula Blackwell
Ethics Administrator
Medical School

Appendix – A3: Participant consent

Title of Project: Skin characterisation and finger-transmitted vibration measurement.
Name of Researcher: Almaky Almagirby
Participant Identification Number for this project:

Please initial box

1. I confirm that I have read and understood the information sheet for the above project and have had the opportunity to ask questions. ☐

2. I understand that my participation is voluntary and that I am free to withdraw at any time without giving any reason. I may also request that my data/recordings be deleted at any time. ☐

3. I understand that my responses will be anonymised before analysis. I give permission for members of the research team to have access to my anonymised responses. ☐

4. I understand there is a very small risk of an allergic reaction to the medical tape adhesive used to attach a sensor. ☐

5. I understand that photos of task performance will be taken during the testing session and that I am free to stop any photos of me being taken. ☐

6. I agree to take part in the above project. ☐

_____	_____	_____
Name of Participant	Date	Signature
_____	_____	_____
Researcher	Date	Signature

Copies: One copy for the participant and one copy for the Principal Investigator / Supervisor

Appendix – A4: Measurement sheet used for the study

Participant's ref. number: ……..

Height: ……. m **Weight**: …….. Kg **Hand Dominance**: ……

Age group: 18-20 21-23 24-27 28-32 33-38 39-47 48-58 >58

On average, how often are you involved with any kind of manual work?

Never 1-2 / month 1-2 / week Daily …….hrs / Day

Index finger length: …… cm Wrist circumference: …….. mm

O*D*: …… cm Palm circumference: ……. mm

O*M*: …… cm Full hand length: …… mm

Circ. Of *D*: …… Circ. Of *P*: ……

Hand grip strength: ……. , ……. , ……

Index finger grip strength: ……. , ……. , ……

Hand grip area: …… g

Filament tested	Finger areas in which participant was able to feel the applied filament	Filament tested	Finger areas in which participant was able to feel the applied filament
H			I
G			K
F			J
E			N
D			M
C			L

Appendix – B: All anthropometric data measured for all participants

Subject	Age, years	Height, m	Weight, kg	WC, mm	PW, mm	Hand size, inch	Hand dominance	L_{IF}, mm	L_D, mm	L_M, mm	L_P, mm	D_D, mm	P_D, mm	IF_D, mm	IV_D, mm³	IV_P, mm³	IV_{IF}, mm³	HGC
S1	24	1.85	90	175	201	8	R	101	27	24	50	16	20	18	5338	16206	25960	152
S2	37	1.75	88	183	219	9	R	103	28	24	51	17	23	20	6693	20611	32569	153
S3	29	1.8	70	174	208	8	R	100	25	21	54	14	20	17	4019	16804	22981	156
S4	43	1.82	67	163	211	8	L	101	26	22	53	14	20	17	4174	16493	23197	164
S5	43	1.63	70	167	217	9	R	93	25	19	49	15	20	18	4703	15882	23392	139
S6	30	1.73	76	166	194	8	R	98	26	24	48	15	20	18	4648	14937	23560	136
S7	53	1.72	86	195	210	8	R	105	27	20	58	17	23	20	6454	23440	33201	153
S8	23	1.83	72	173	216	9	R	100	28	23	49	16	20	18	5536	15248	25124	156
S9	21	1.81	80	188	214	8	R	101	28	21	52	17	21	19	6093	17542	27696	163
S10	46	1.78	78	175	223	9	L	99	27	23	49	16	21	19	5338	17190	26612	145
S11	42	1.95	91	167	210	8	R	100	25	24	51	15	20	18	4703	15870	24579	159
TS1	58	1.8	89	196	248	10	R	101	28	26	47	20	23	21	8713	18995	35971	150
TS2	61	1.75	60	180	200	8	L	101	28	24	49	20	21	20	8713	16530	32737	148
TS3	60	1.7	67	174	216	9	R	100	30	24	46	18	21	20	7512	16138	29850	157
TS4	41	1.67	63.5	167	205	8	R	93	28	22	43	16	20	18	5536	13938	23904	159
TS5	21	1.75	70	168	211	8	R	95	26	22	47	15	20	17	4891	14029	22812	146
TS6	56	1.8	76	179	215	8	R	100	32	22	46	18	21	19	8013	15518	29225	152

Appendix – C: All data for hand and finger grip strength measured for all participants

Subject	Hand grip strength average (N)	Index finger grip strength average (N)
S1	317.19	130.8
S2	555.9	179.85
S3	389.13	124.26
S4	418.56	127.53
S5	215.82	94.83
S6	421.83	147.15
S7	385.86	130.8
S8	392.4	124.26
S9	415.29	124.26
S10	529.74	160.23
S11	317.19	94.83
TS1	444.72	111.18
TS2	438.18	143.88
TS3	480.69	101.37
TS4	454.53	107.91
TS5	379.32	130.8
TS6	526.47	170.04

Appendix – D: Stiffness measured at distal and proximal of the human finger at loading of 5 and 10 N for all participants

	c_0	c_1	c_2	c_3	c_4	k, N/mm at 5 N	k, N/mm at 10 N
Right index proximal finger							
S1	-0.38562	-0.81715	0.31643	-0.03796	0.00163	3.77	10.25
S2	-0.66937	0.41003	-0.09666	0.01331	-0.00057	2.65	5.52
S3	-1.44297	0.35648	-0.05506	0.00957	-0.00044	4.62	9.61
S4	-1.66506	0.62577	-0.11709	0.01254	-0.00028	5.45	12.81
S5	-0.53254	0.12638	0.02128	-0.00037	-0.00005	3.40	7.01
S6	-1.11190	0.46624	-0.09150	0.01336	-0.00059	3.78	8.20
S7	-0.85598	0.19030	-0.00052	-0.00084	0.00017	3.70	9.07
S8	-0.85662	0.17072	-0.01651	0.00350	-0.00014	3.46	7.50
S9	-1.11492	0.29560	-0.04602	0.00581	-0.00015	4.37	Invalid
S10	-1.00011	-0.02269	0.09282	-0.01576	0.00095	4.97	12.97
S11	-1.25501	0.41395	-0.09705	0.01688	-0.00084	4.38	8.63
TS1	-1.15910	0.26485	-0.00727	-0.00045	0.00006	2.24	5.31
TS2	-0.91269	0.24285	-0.00852	0.00127	-0.00001	3.27	7.22
TS3	-1.05713	0.17236	0.01099	-0.00207	0.00020	3.99	9.50
TS4	-0.94203	0.16742	0.02158	-0.00271	0.00021	3.85	8.70
TS5	-1.85295	0.67334	-0.15789	0.02419	-0.00120	4.25	Invalid
TS6	-0.99126	0.27803	-0.00009	-0.00229	0.00026	3.18	7.75
Mean	-1.04737	0.23615	-0.01359	0.00223	-0.00005	3.84	8.67
SD	0.37122	0.32423	0.10546	0.01402	0.00065	0.80	3.54
Right index distal finger							
S1	-0.76208	0.68700	-0.35402	0.11878	-0.01111	7.61	16.31
S2	-0.63159	0.24912	0.03773	-0.00544	0.00074	5.30	11.89
S3	-1.18594	0.65033	-0.15663	0.03180	-0.00113	7.49	17.50
S4	-0.85553	0.74528	-0.26390	0.07101	-0.00514	6.84	15.90
S5	-1.05178	0.34354	0.07502	-0.02701	0.00323	5.71	13.91
S6	-1.39681	0.62776	-0.07259	0.00364	0.00105	6.57	15.75
S7	-0.76301	0.35105	-0.02379	0.02266	-0.00269	6.36	12.90
S8	-0.97383	0.25109	0.10104	-0.03804	0.00432	6.16	16.78
S9	-1.14477	0.71043	-0.13735	0.00650	0.00166	6.62	17.67
S10	-1.06607	-0.01901	0.21319	-0.05060	0.00430	6.31	16.39
S11	-0.73243	0.07922	0.18345	-0.04724	0.00388	3.31	9.76
TS1	-1.48252	0.60315	-0.09761	0.01187	-0.00018	5.62	13.13
TS2	-1.84538	0.72746	-0.07730	0.00292	0.00075	6.34	14.86
TS3	-0.91550	0.32316	0.02199	-0.00961	0.00103	3.87	9.53
TS4	-0.54869	0.05319	0.12651	-0.02884	0.00286	5.18	12.90
TS5	-1.03293	0.24553	0.11262	-0.03968	0.00394	5.59	16.02
TS6	-1.06599	0.30900	0.07549	-0.03226	0.00390	6.36	16.91
Mean	-1.02676	0.40808	-0.01389	-0.00056	0.00067	5.96	14.60
SD	0.32723	0.25583	0.15566	0.04431	0.00402	1.12	2.55

Appendix – E1: Peak transmissibility against peak frequency measured for all subjects

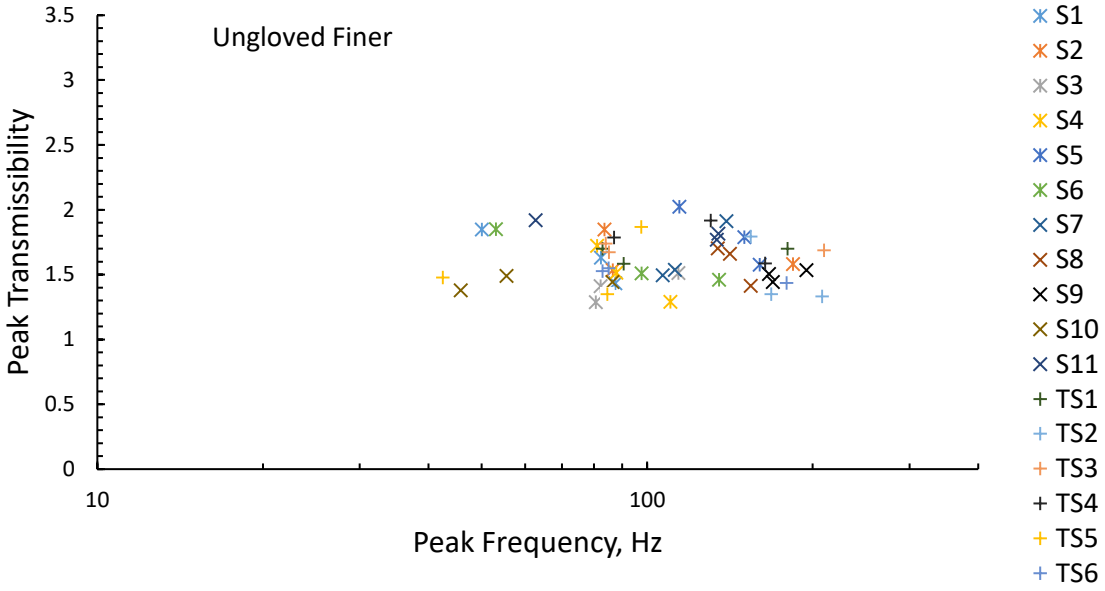

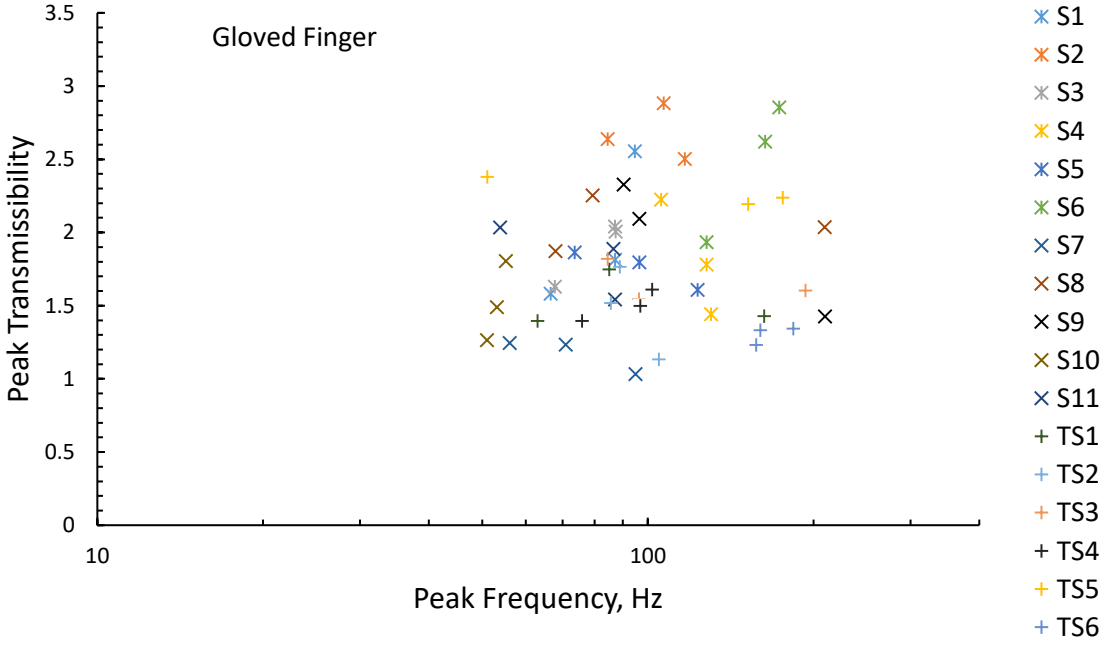

Appendix – E2: Mean grip forces against peak frequency measured for all subjects

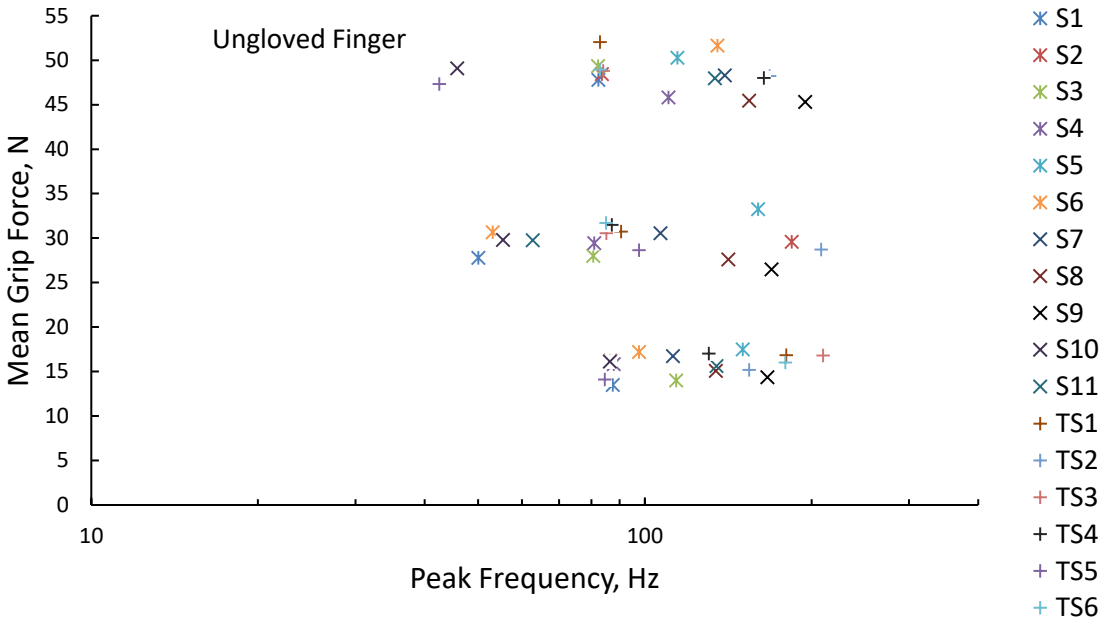

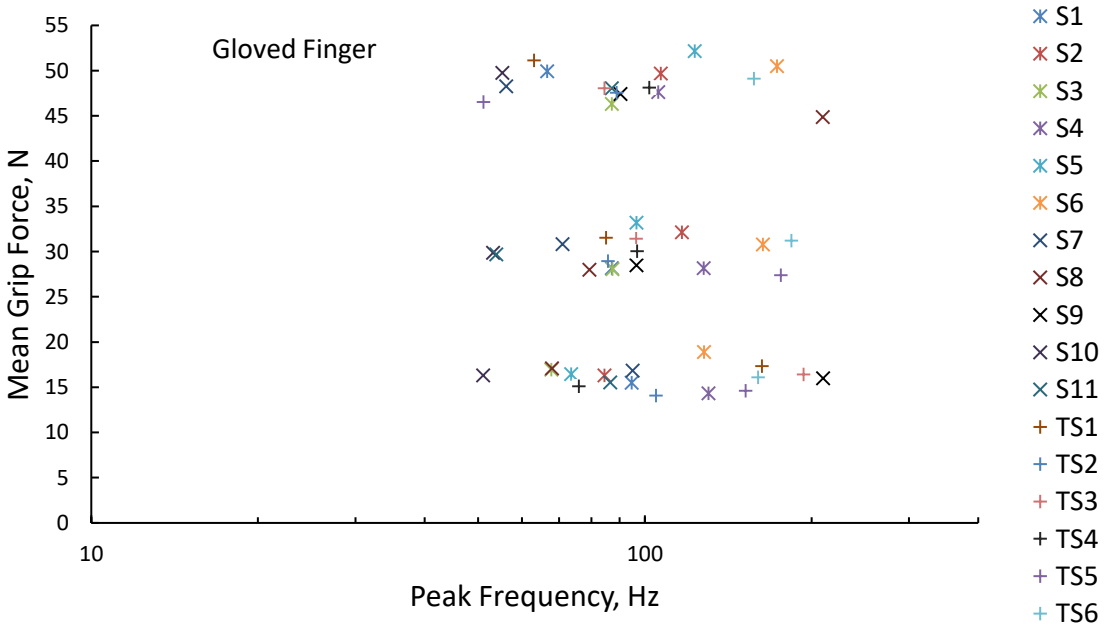

Appendix – E3: Peak transmissibility against mean grip forces measured for all subjects

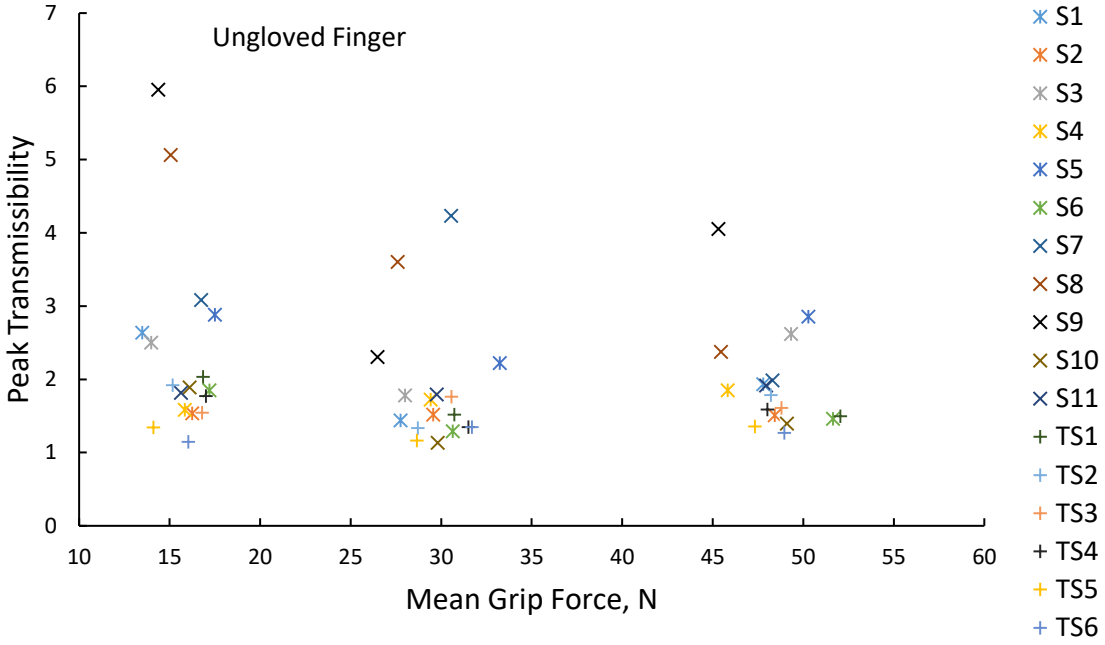

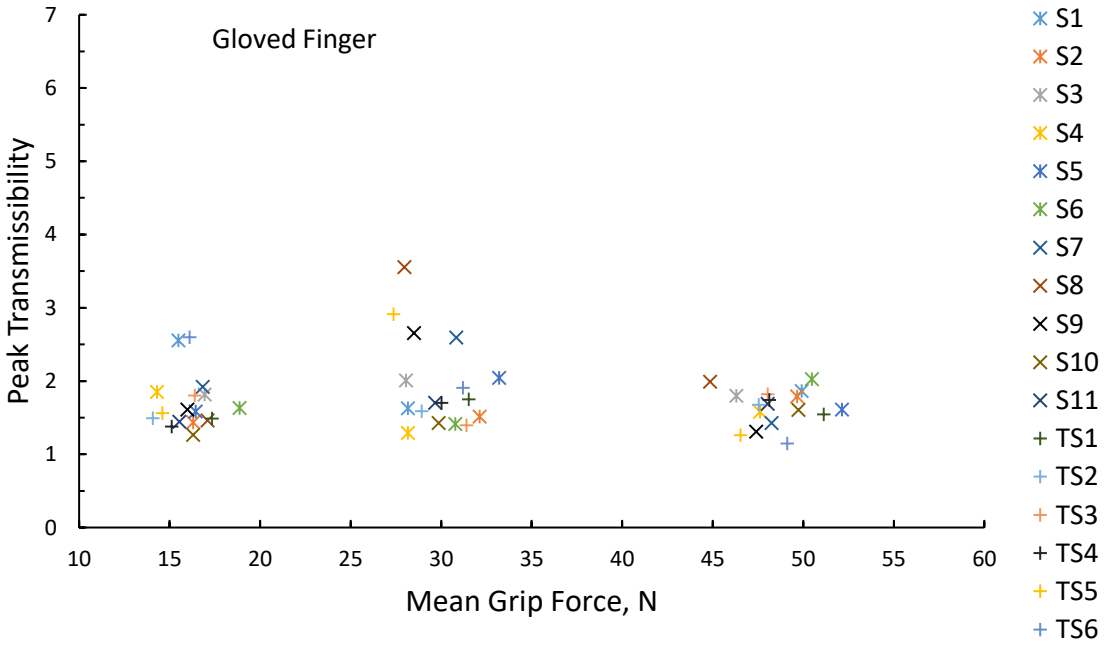

Appendix – F: One-way ANOVA between two groups (technicians and non-technicians)

Non- technicians (n=12)					Technicians (n =5)				
	Mean	SD	Min.	Max.	Mean	SD	Min.	Max.	Sig.
Age / years	34.33	11.03	21	53	55.20	8.17	41	61	**0.002**
Height / m	1.79	0.08	1.63	1.95	1.74	0.06	1.67	1.8	0.317
Weight / kg	78.17	8.71	67	91	71.10	11.64	60	89	0.186
WC / mm	174.50	9.71	163	195	179.20	10.71	167	196	0.391
PW / mm	211.17	7.85	194	223	216.80	18.70	200	248	0.383
Hand size / inch	8.33	0.49	8	9	8.60	0.89	8	10	0.436
L_{IF} / mm	99.67	3.23	93	105	99.00	3.39	93	101	0.707
L_D / mm	26.50	1.17	25	28	29.20	1.79	28	32	0.002
L_M / mm	22.25	1.71	19	24	23.60	1.67	22	26	0.157
L_P / mm	50.92	3.03	47	58	46.20	2.17	43	49	**0.007**
D_D / mm	15.78	1.02	14.3	17.45	18.28	1.69	15.87	19.91	**0.002**
P_D / mm	20.58	1.08	19.5	22.69	21.12	0.92	20.32	22.69	0.341
IF_D/ mm	18.18	1.01	17.105	20.07	19.70	1.20	18.10	21.30	**0.016**
IV_D / mm³	5216	857.66	4019	6693	7697.33	1310.48	5535.81	8713.05	**0.000**
IV_P / mm³	17021	2601.58	14029	23440	16223.45	1837.50	13937.52	18994.88	0.545
IV_{IF} / mm³	25974	3579.27	22812	33201	30337.34	4482.11	23903.96	35970.81	**0.050**
HGC / mm	151.83	8.83	136.00	164.00	153.20	4.66	148	159	0.751
HGS_Average	394.85	90.61	215.82	555.90	468.92	36.01	438.18	526.47	0.102
IFGS_Average	130.8	23.87	94.83	179.85	126.88	29.19	101.37	170.04	0.776
R0_D	1.68	0.87	0.71	2.78	1.74	0.82	0.762	2.509	0.900
R1_D	1.18	0.82	0.33	2.15	1.23	0.81	0.33	1.97	0.905
R2_D	0.38	0.17	0.17	0.57	0.37	0.20	0.2164	0.608	0.931
R5_D	0.23	0.17	0.07	0.47	0.21	0.19	0.0674	0.4571	0.839
R7_D	0.10	0.05	0.05	0.21	0.10	0.05	0.0591	0.1862	0.937
R0_P	1.22	0.46	0.88	2.62	1.07	0.10	0.923	1.187	0.474
R1_P	0.58	0.49	0.31	2.12	0.47	0.05	0.42	0.54	0.650
R2_ P	0.57	0.13	0.19	0.65	0.56	0.04	0.5117	0.6049	0.854
R5_ P	0.31	0.09	0.09	0.41	0.30	0.08	0.2126	0.4322	0.902
R7_ P	0.14	0.03	0.07	0.18	0.14	0.04	0.1036	0.1975	0.933
Hyd_D	53.10	16.13	25.38	77.08	50.25	14.45	35.22	69	0.738
Hyd_P	30.16	13.93	16.42	66.14	26.49	9.56	14.1	37.66	0.601
STD_AV	29.65	3.62	22.48	33.96	29.61	1.94	27.22	32.48	0.982
STP_AV	30.02	3.31	23.92	33.88	30.19	2.50	28.1	34.4	0.917
STD_BV	31.54	4.32	21.60	34.92	32.25	1.59	30.54	34.52	0.730
STP_BV	31.67	3.31	23.60	34.70	31.88	2.29	29.06	35.22	0.896
MGF_G15N	16.23	1.21	14.31	18.87	15.81	1.26	14.07	17.35	0.529
MGF_15N	15.52	1.32	13.50	17.50	16.37	0.77	15.17	17.01	0.203
MGF_G30N	29.56	1.85	27.37	33.20	30.62	1.12	28.93	31.53	0.256
MGF_30N	29.30	1.78	26.49	33.25	30.64	1.19	28.71	31.70	0.144
MGF_G50N	48.41	2.05	44.85	52.15	48.79	1.43	47.55	51.13	0.712
MGF_50N	48.07	1.92	45.32	51.65	49.21	1.64	48.02	52.05	0.264

Non- technicians (n=12)					Technicians (n =5)				
	Mean	SD	Min.	Max.	Mean	SD	Min.	Max.	Sig.
RF_G15N	103.44	44.69	51.03	209.87	139.41	47.74	76	193.4	0.158
RF_15N	111.92	28.42	84.70	166.57	170.87	29.96	130.53	209.93	**0.002**
RF_G30N	97.53	44.56	14.37	175.97	92.60	61.37	11.31	183.90	0.854
RF_30N	103.56	48.57	50.07	184.30	97.99	67.09	24.30	208.13	0.849
RF_G50	95.92	52.74	29.07	209.67	99.18	35.45	63.08	157.47	0.902
RF_50N	109.93	44.88	42.53	194.87	116.44	45.30	83.00	168.11	0.789
RF_GT15N	90.88	52.26	22.70	202.78	87.73	24.78	62.50	122.33	0.900
RF_GT30N	126.41	40.57	81.80	206.90	175.52	40.81	126.30	215.92	**0.038**
RF_GT50N	90.77	32.45	51.40	136.27	92.64	9.39	85.10	105.87	0.903
RP_G15N	1.68	0.34	1.26	2.55	1.75	0.50	1.38	2.60	0.719
RP_15N	2.68	1.45	1.34	5.95	1.68	0.35	1.15	2.03	0.156
RP_G30N	2.06	0.72	1.29	3.55	1.67	0.19	1.39	1.91	0.252
RP_30N	2.02	0.97	1.13	4.23	1.46	0.18	1.33	1.76	0.232
RP_G50N	1.66	0.25	1.26	2.02	1.58	0.27	1.14	1.82	0.575
RP_50N	2.11	0.78	1.36	4.05	1.55	0.19	1.27	1.79	0.140
RP_GT15N	1.45	0.36	1.03	2.19	1.94	0.37	1.48	2.38	**0.024**
RP_GT30N	1.80	0.35	1.33	2.51	1.52	0.28	1.23	1.97	0.138
RP_GT50N	1.70	0.58	1.13	3.20	1.44	0.18	1.18	1.62	0.342
SD_5N	6.157	1.1355	3.31	7.61	5.4758	1.02527	3.87	6.36	0.266
SD_10N	15.07	2.4358	9.76	17.67	13.4654	2.72732	9.53	16.91	0.251
SP_5N	4.07	0.76	2.65	5.45	3.31	0.69	2.24	3.99	0.075
SP_10N	16.60	24.78	5.52	91.00	7.69	1.59	5.31	9.50	0.444
Sensitivity $\_D$	0.94	0.07	0.75	1.00	0.87	0.10	0.75	1.00	0.112
Sensitivity $\_M$	0.85	0.09	0.75	1.00	0.75	0.18	0.50	0.92	0.152
Sensitivity $\_P$	0.86	0.10	0.75	1.00	0.58	0.32	0.08	0.92	**0.012**
Tempdrop$_D$	1.92	1.78	-1.64	4.72	2.64	1.08	1.8	4.38	0.418
Tempdrop$_P$	1.57	1.66	-0.32	4.6	1.69	1.22	0.52	3.36	0.880

Appendix – G: Pearson correlation for anthropometric measurements including hand and finger grip strength

	Age	Height	Weight	WC	PW	Hand size	L_{IF}	L_D	L_M
Age / years	1								
Height / m	-0.238	1							
Weight / kg	-0.116	.505*	1						
WC / mm	0.312	0.022	0.474	1					
PW / mm	0.324	0.058	0.333	.508*	1				
Hand size / inch	0.301	-0.163	0.209	0.335	.840**	1			
L_{IF} / mm	0.208	0.46	.499*	.641**	0.128	0.022	1		
L_D / mm	0.431	-0.098	-0.076	0.384	0.219	0.163	0.232	1	
L_M / mm	0.199	0.393	0.291	0.122	0.233	0.37	0.276	0.247	1
L_P / mm	-0.136	0.27	0.345	0.319	-0.114	-0.25	.646**	-0.433	-0.38
D_D / mm	.666**	-0.126	0.11	.721**	0.421	0.407	0.373	.622**	0.438
P_D / mm	.519*	-0.196	0.478	.831**	.567*	.527*	.560*	0.357	0.208
IF_D/ mm	.662**	-0.166	0.272	.828**	.518*	.491*	.482*	.565*	0.38
IV_D / mm³	.675**	-0.119	0.05	.678**	0.405	0.373	0.365	.758**	0.43
IV_P / mm³	0.304	-0.026	.533*	.780**	0.336	0.236	.743**	0.034	-0.067
IV_{IF} / mm³	.627**	-0.058	0.344	.866**	.492*	0.445	.627**	.530*	0.392
HGC	-0.048	0.441	0.023	0.1	0.067	-0.205	0.352	0.199	-0.026
HGS_Average	0.32	-0.041	-0.049	0.292	0.227	0.176	0.329	.657**	0.4
IFGS_Average	-0.013	0.032	0.124	0.213	-0.094	-0.101	0.374	0.366	0.15

** Correlation is significant at the 0.01 level (2-tailed).
* Correlation is significant at the 0.05 level (2-tailed).

	L_P	D_D	P_D	IF_D	IV_D	IV_P	IV_{IF}	HGC	HGS Aver.	IFGS Aver.
L_P / mm	1									
D_D / mm	-0.205	1								
P_D / mm	0.216	.681**	1							
IF_D/ mm	-0.048	.953**	.871**	1						
IV_D / mm³	-0.28	.980**	.634**	.920**	1					
IV_P / mm³	.689**	0.39	.854**	.616**	0.314	1				
IV_{IF} / mm³	0.095	.918**	.889**	.984**	.884**	.703**	1			
HGC	0.228	-0.063	0	-0.042	-0.003	0.107	0.026	1		
HGS_Average	-0.244	0.389	0.435	0.441	.484*	0.186	0.448	0.155	1	
IFGS_Average	0.073	0.164	0.272	0.223	0.223	0.244	0.267	-0.224	.678**	1

Appendix – H: Pearson correlation anthropometric measurements including hand and finger grip strength with vibration measurements

	MGF_15N	MGF_30N	MGF_50N	RF_15N	RF_30N	RF_50N	RP_15N	RP_30N	RP_50N

Age / years	.593*	.593*	0.415	.529*	0.058	-0.064	-0.482	-0.059	-0.424
Height / m	-.560*	-.561*	-0.335	-0.124	-0.289	-0.019	0.14	-0.022	0.064
Weight / kg	-0.064	-0.1	0.168	-0.164	-0.233	-0.174	0.109	0.157	-0.006
WC / mm	0.015	-0.137	0.14	0.32	0.316	0.089	0.298	0.361	0.144
PW / mm	0.256	0.187	0.252	0.357	0.058	-0.35	0.029	0.04	-0.052
Hand size / inch	0.412	0.262	0.398	0.316	0.139	-0.311	0.022	0.036	-0.125
L_{IF} / mm	-0.2	-0.412	-0.162	-0.004	0.104	0.052	0.162	0.373	0.025
L_D / mm	0.14	0.112	-0.06	.578*	0.136	0.005	-0.065	-0.056	-0.252
L_M / mm	-0.005	-0.157	0.264	0.095	-0.19	-0.181	-0.322	-0.437	-.523*
L_P / mm	-0.251	-0.352	-0.248	-0.352	0.118	0.135	0.342	.586*	0.416
D_D / mm	0.22	0.129	0.265	.589*	0.43	0.094	-0.085	-0.007	-0.216
P_D / mm	0.402	0.219	0.319	0.191	0.254	-0.093	-0.048	0.235	-0.164
IF_D/ mm	0.314	0.177	0.309	0.474	0.394	0.024	-0.077	0.093	-0.213
IV_D / mm³	0.212	0.14	0.222	.642**	0.379	0.065	-0.112	-0.044	-0.25
IV_P / mm³	0.176	-0.01	0.098	-0.062	0.249	0.01	0.142	.506*	0.083
IV_{IF} / mm³	0.242	0.079	0.254	0.411	0.369	0.027	-0.042	0.16	-0.188
HGC	-0.315	-0.424	-.685**	0.178	0.025	0.302	0.266	0.227	0.306
HGS_Average	0.16	-0.027	0.034	0.066	0.02	-0.207	-0.305	-0.302	-0.462
IFGS_Average	-0.108	-0.137	0.014	-0.385	0.133	-0.271	-0.216	-0.231	-0.359

* Correlation is significant at the 0.05 level (2-tailed).
** Correlation is significant at the 0.01 level (2-tailed).

Appendix – I: Strain sweep test obtained for Siliskin 10 silicone at two different manufacturing protocols

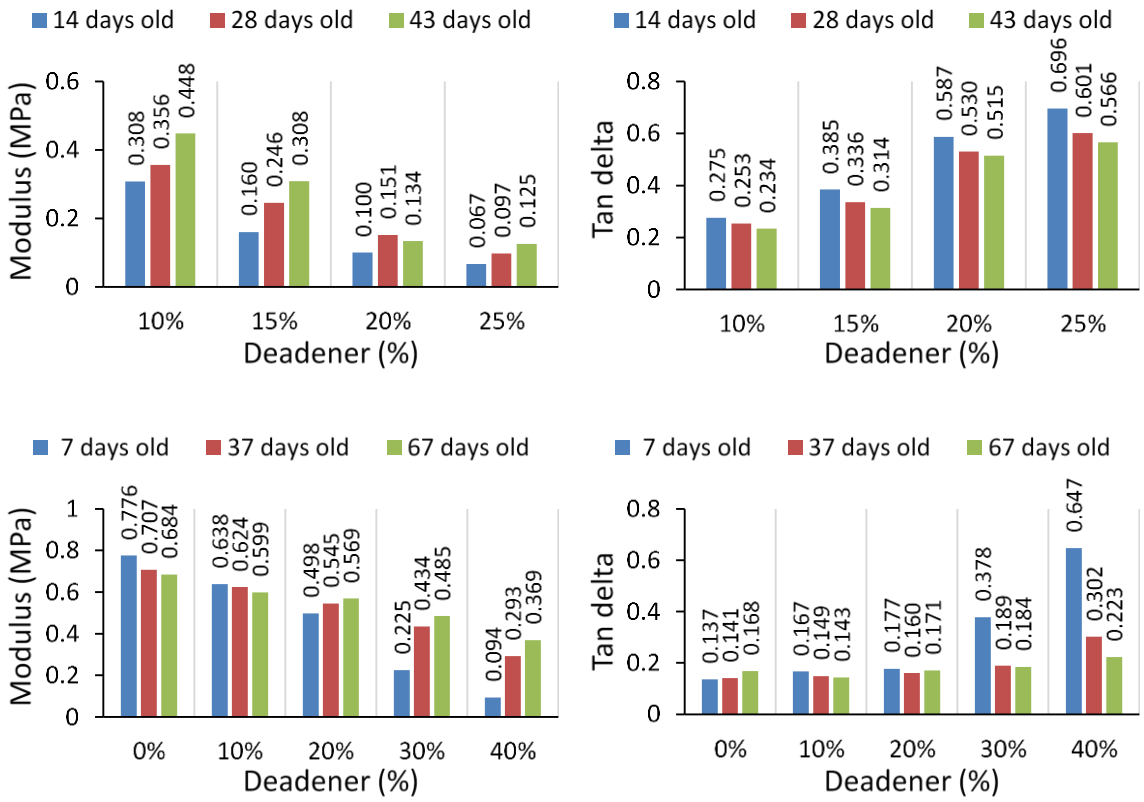

Appendix – J: Results obtained from temperature sweep test for the initial protocol used and over time

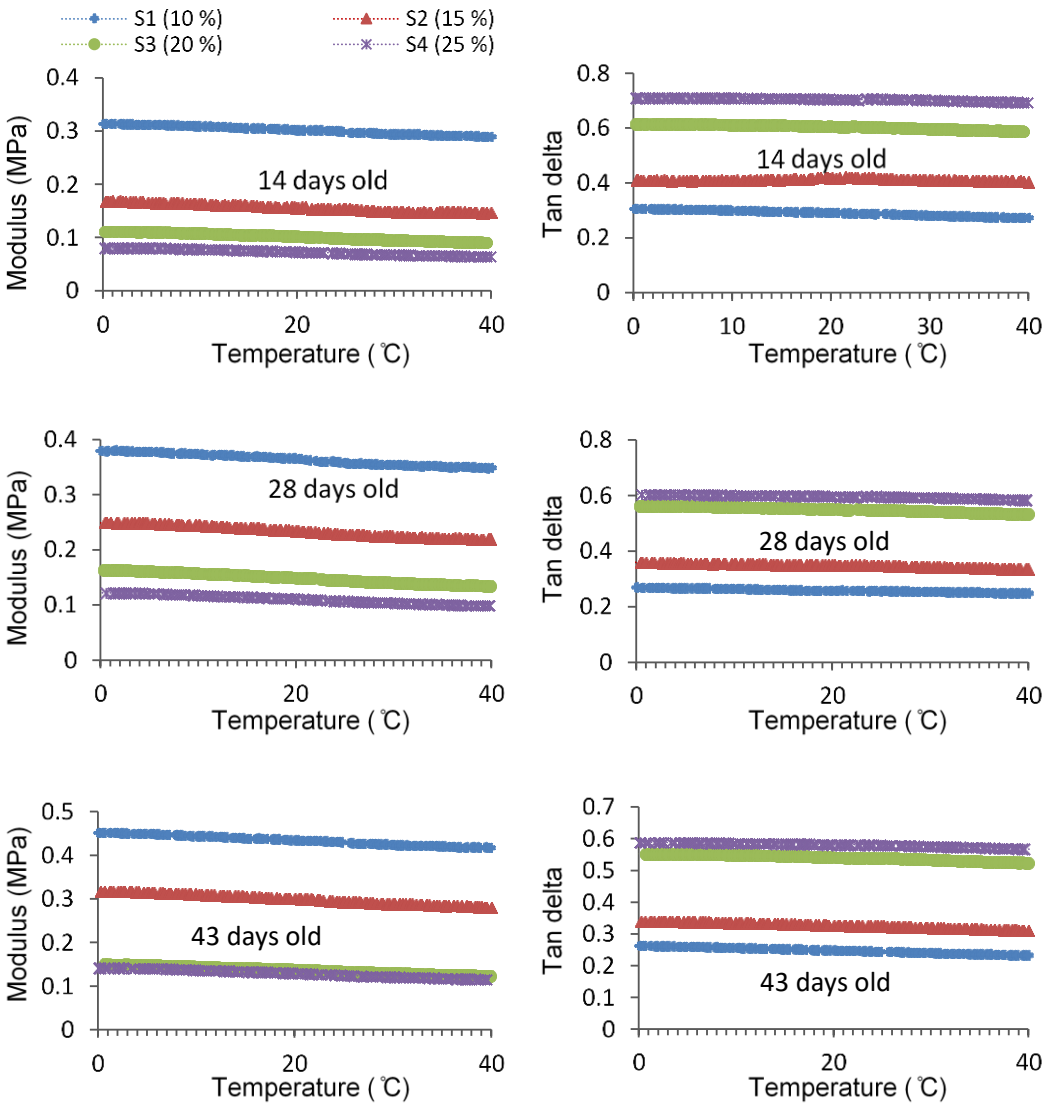

Appendix – K: Results obtained from temperature sweep test for the second protocol used and over time

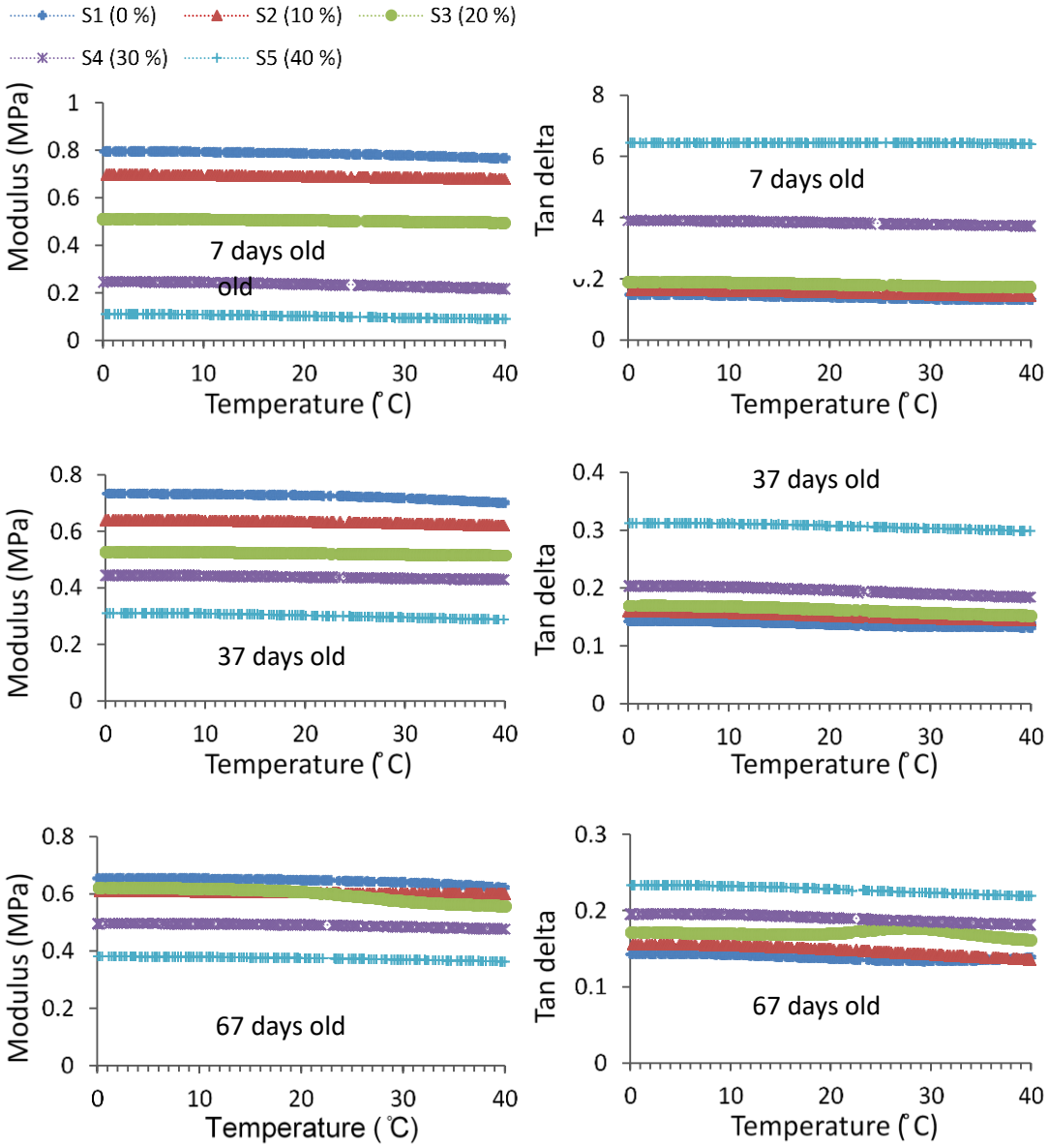

Appendix – L: Stiffness measured for the five models of finger at loading of 5 and 10 N

	c_0	c_1	c_2	c_3	c_4	k, N/mm at 5 N	k, N/mm at 10 N
Right index proximal finger							
AF1	-0.69702	0.42494	-0.04143	0.00144	0.00003	1.32	2.72
AF2	-0.72369	0.53980	-0.07524	0.00486	-0.00008	1.18	2.77
AF3	-0.82332	0.29317	0.01466	-0.00588	0.00035	1.38	3.27
AF4	-0.69217	0.46174	-0.04956	0.00226	0.00001	1.51	2.61
AF5	-0.62218	0.64023	-0.08756	0.00577	-0.00011	2.82	3.50

Appendix – M: measurement of mean grip force, frequency and transmissibility peaks measured for all artificial models of finger